



Universiteit
Leiden
The Netherlands

Chemical biology studies on retaining α -glucosidases

Su, Q.

Citation

Su, Q. (2024, November 6). *Chemical biology studies on retaining α -glucosidases*. Retrieved from <https://hdl.handle.net/1887/4107652>

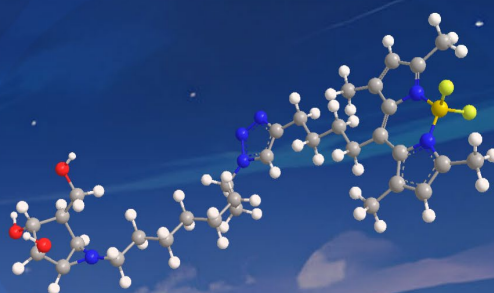
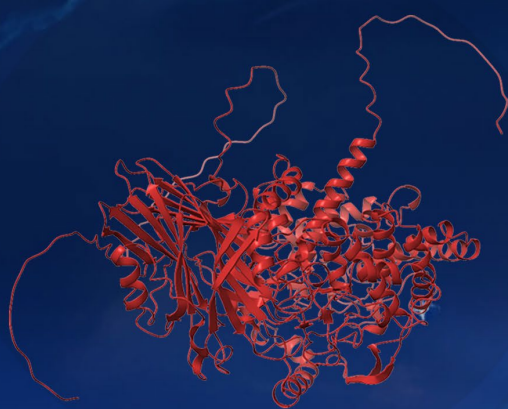
Version: Publisher's Version

License: [Licence agreement concerning inclusion of doctoral thesis in the Institutional Repository of the University of Leiden](#)

Downloaded from: <https://hdl.handle.net/1887/4107652>

Note: To cite this publication please use the final published version (if applicable).

Chemical biological studies on retaining exo- β -glucosidases



Qin Su



Chemical biology studies on retaining exo- β -glucosidases

Proefschrift

ter verkrijging van
de graad van doctor aan de Universiteit Leiden,
op gezag van rector magnificus prof.dr.ir. H. Bijl,
volgens besluit van het college voor promoties
te verdedigen op woensdag 6 november 2024
klokke 11:30 uur

door

Qin Su
geboren te Laibin, China
in 1993

Promotores

Prof. dr. J. M. F. G. Aerts

Prof. dr. H. S. Overkleeft

Co-promotor

Dr. R. G. Boot

Promotiecommissie

Prof. dr. M. Ubbink

Prof. dr. M. van der Stelt

Prof. dr. L. P. W. J. van den Heuvel (Radboud University Medical Center)

Prof. dr. S. I. van Kasteren

Dr. T. Wennekes (Utrecht University)

Dr. M. E. Artola Perez de Azanza

Table of Contents

Chapter 1	1
General introduction	
Chapter 2	15
Xylose-configured cyclophellitols as selective inhibitors for glucocerebrosidase	
Chapter 3	41
Selective labelling of GBA2 in cells with fluorescent β -D-arabinofuranosyl cyclitol aziridines	
Chapter 4	73
Reactivity of cytosolic retaining β -glucosidase towards retaining glycosidase ABPs	
Chapter 5	91
Characterization of <i>C. elegans</i> retaining β -glucosidases	
Chapter 6	115
Expression and analysis of <i>Nicotiana tabacum</i> β -glucosidase B56 in mammalian cells	
Chapter 7	135
Summary and future prospects	
Appendices	143
Nederlandse samenvatting	
Summary in Chinese	
List of publications	
<i>Curriculum vitae</i>	
Acknowledgements	

Chapter 1

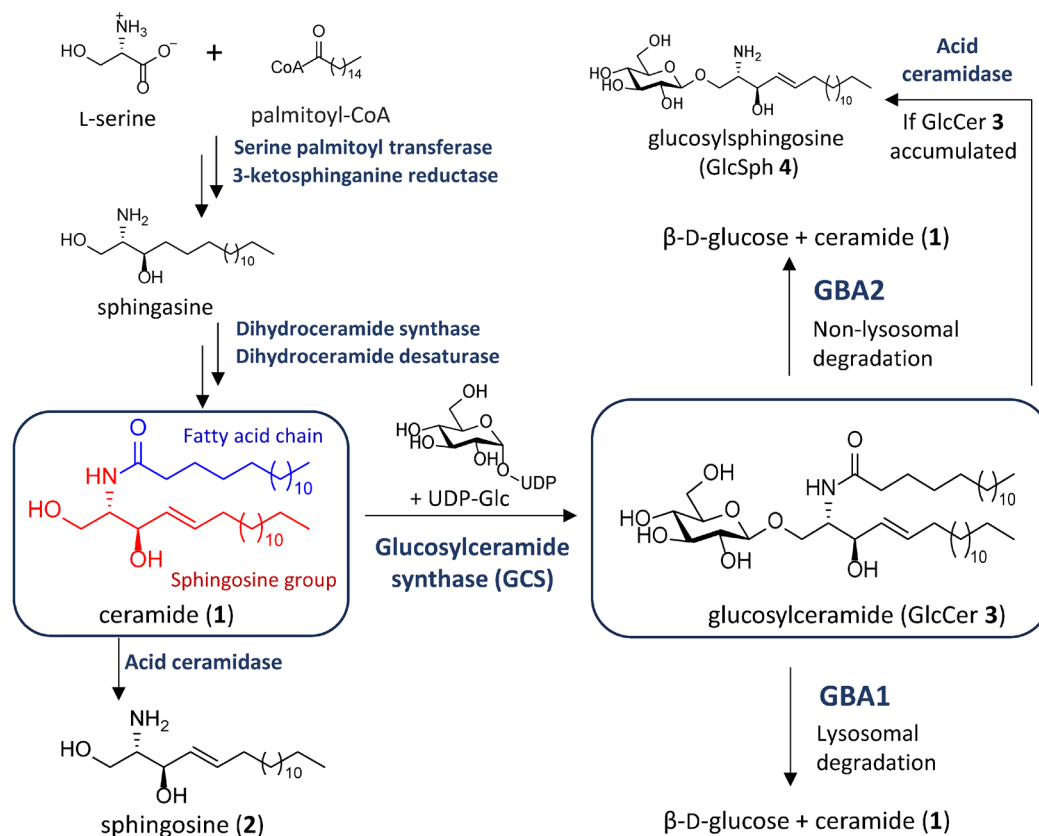
General introduction

Glycosphingolipids

Glycosphingolipids (GSLs) are essential structural components of mammalian cell membranes and play a role in many (patho)physiological processes including cellular signaling, cell adhesion/recognition processes, and modulation of signal transduction processes.¹ Glycosphingolipids are composed of carbohydrates linked to the 1-hydroxyl group of ceramide (**1**) which itself consists of a sphingoid base which is *N*-acylated with a fatty acid (see Scheme 1). The most abundant sphingoid base in mammals is sphingosine (**2**) containing 18 carbons and one double bond (d18:1), while sphingoid bases encompassing 12 to 26 carbons also exist.¹ Of all mammalian GSLs, over 90% are derived from glucosylceramide (GlcCer, **3**, also known as glucocerebroside), while the remainder is derived from galactosylceramide (GalCer).^{2,3}

The first step in the biosynthesis of ceramide (**1**), the precursor from which GlcCer is formed, comprises^{1,3} (Scheme 1) condensation of the amino acid L-serine and an acyl-CoA thioester (usually palmitoyl-CoA) into 3-ketosphinganine. The resultant 3-ketosphinganine is then reduced into sphinganine, acylation of which gives dihydroceramide, and desaturation then gives ceramide. After completing its synthesis at the cytosolic side of the ER membrane, ceramide **1** is transported to the cytosolic side of the cis-Golgi apparatus membrane where it is transformed into GlcCer **3** by the membrane bound glucosylceramide synthase⁴ (GCS) using UDP-glucose as the donor glycoside. The synthesized GlcCer **3** is then transported to the luminal side of the Golgi membrane, where it is galactosylated to form lactosylceramide (LacCer). LacCer is an important branching point from which a series of complex glycosphingolipids such as the gangliosides, neolactosides, and lactosides are synthesized by stepwise elongation with various monosaccharides.

In humans, the catabolism of GlcCer (**3**) is mainly mediated by the lysosomal retaining exo- β -glucosidase, GBA1. The resultant ceramide **1** is further processed into sphingosine **2** and a free fatty acid by acid ceramidase (ASAH1) inside the lysosome. The generated sphingosine is exported from lysosomes and can be reused in the cytosol for regenerating ceramide via the salvage pathway.



Scheme 1. A brief schematic representation of GSLs biosynthesis and catabolism. Metabolic enzymes in blue.

Mammalian cells may contain several retaining exo- β -glucosidases. All cells express the lysosomal GBA1, many cell types express the cytosol-facing membrane-associated GBA2 and specific cells express the cytosolic GBA3. These retaining β -glucosidases all hydrolyze GlcCer **3** through a Koshland double displacement mechanism, which involves the formation of a covalent glucosyl enzyme intermediate.⁵ The hydrolysis process (Figure 1) commences with attack of the nucleophilic carboxylic acid residue towards the substrate anomeric center, while simultaneously the catalytic acid/base protonates the aglycon, thereby making it a better leaving group. As the result, an intermediate of covalent glycosyl-enzyme adduct is formed with inversion of the anomeric configuration of the substrate glycoside. The aglycon then leaves the enzyme active site, generating space for a water molecule to enter. In a reversal of steps, the covalent enzyme-substrate intermediate is then hydrolyzed, during which the water molecule is deprotonated by the catalytic acid-base residue. The stereochemistry at the anomeric position of the glucose moiety is again inverted, resulting in a net retention of anomeric stereochemistry.⁶⁻⁸ In this process, the substrate β -glucopyranoside adopts a 1S_3 skew-boat conformation in the initial Michaelis complex with the enzyme active site, placing the aglycon in an axial position allowing for ensuing nucleophilic displacement. During this first S_N2 displacement, the sugar is distorted to a 4H_3 half-chair transition state (TS) conformation from which after formation of the covalent enzyme-substrate acylal adduct the pyranose conformation turns to 4C_1 .^{9,10} Notably, retaining β -glucosidases have the intrinsic capacity to transfer glucose from their substrate to water (giving hydrolysis process A of Figure 1), but also to other acceptor alcohols, leading to an overall transglycosylation event. For instance, GBA1 as well as GBA2 has been shown to be able to transfer glucose from GlcCer to cholesterol (see Figure 1 process B) to give, also with net retention of anomeric configuration, cholesterol β -glucoside as the transglycosylation product.¹¹

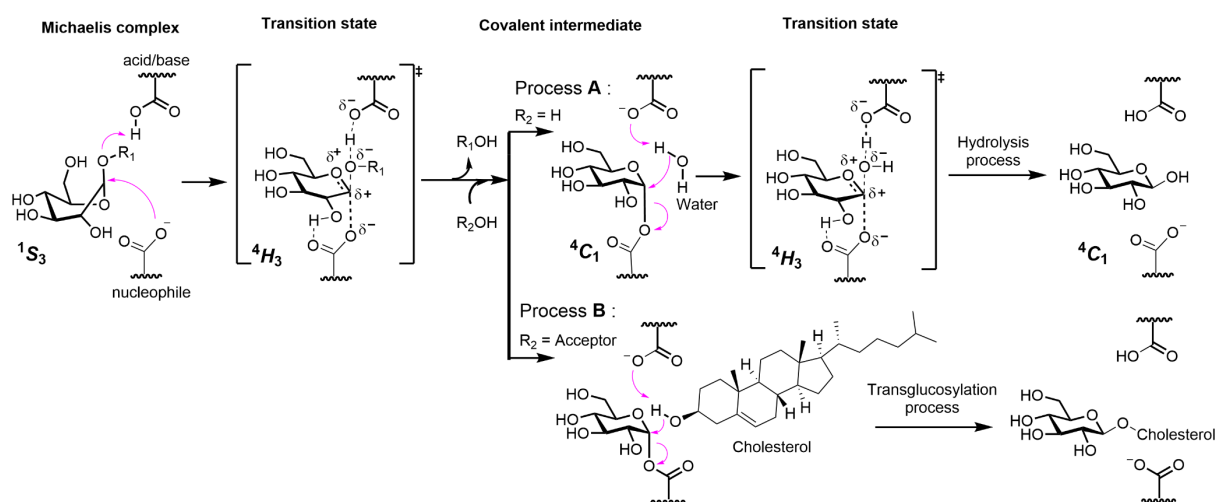


Figure 1. Koshland double-replacement catalytic mechanism of retaining β -glucosidases. Process A: hydrolysis, process B: transglycosylation.

Gaucher disease, a common lysosomal storage disorder caused by genetic deficiency in GBA1

Lysosomal storage disorders (LSDs) are rare inherited metabolic disorders that are caused by dysfunction of specific lysosomal metabolic processes.¹²⁻¹⁵ Lysosome dysfunction may result from defects in the formation or stability of lysosomes, export of degradation products or defects in specific enzymatic activities. Often, dysfunction of lysosomes is caused by the mutation of a gene encoding a specific glycosidase that is responsible for the hydrolysis of substrates inside lysosomes, or that of related lysosomal activator proteins, lysosomal transporters, or integral membrane proteins.

Gaucher disease (GD) is the most common LSD,¹⁶ and was first described by Phillippe C. E. Gaucher, who in his doctoral thesis described a patient with an unexplained hepatosplenomegaly in 1882. GD is caused by genetic deficiency in lysosomal acid β -glucosidase GBA1 (Enzyme Commission (EC) number 3.2.1.45), resulting in accumulation of GlcCer (**3**) in lysosomes of tissue macrophages that then transform into lipid-laden Gaucher cells. As a consequence of accumulating GlcCer, also

glucosylsphingosine (GlcSph **4**) levels increase through the action of acid ceramidase (Scheme 1),^{16,17} and GlcSph, which is present in very low levels in healthy individuals, is now viewed as a valuable GD biomarker.¹⁸ GD storage macrophages are thought to underlie characteristic symptoms of GD patients such as hepatosplenomegaly and pancytopenia (shortage of red blood cells and platelets). GD has an average frequency of 1 in 50,000–200,000 births and occurs at a much higher frequency among the Ashkenazi Jewish population (1:1,000).¹²

The clinical phenotype of GD patients is heterogenous, even in some cases of homozygotic twins.¹⁹ The common visceral symptoms include hepatosplenomegaly, thrombocytopenia, abnormalities in coagulation, anemia, and skeletal manifestations (for instance, bone pain and bone fractures). Three different clinical types of this disorder are generally discerned. Type I GD is the most common form. This chronic non-neurological phenotype is characterized by organomegaly, bone disease (for instance, avascular necrosis, bone pain) and cytopenia. Type II GD patients show acute neurological manifestations already in the first year of life, while type III GD patients develop sub-acute, progressive neurological symptoms at a later age. The distinction of GD in these three phenotypes is not very strict and nowadays the existence of a continuum of phenotypes is proposed.²⁰

Therapeutic strategies to treat GD

There has been considerable progress in the development of therapeutic strategies to treat GD in the past decades, making GD perhaps the best-studied LSD from a clinical perspective. Yet, no curative treatment for this disease exist and as well neuropathological (type II , III) manifestations of the disease are difficult to treat by any of the developed therapies.^{12,14,21,22} Two therapeutic strategies are clinical practice and comprise enzyme replacement therapy (ERT) and substrate reduction therapy (SRT). Besides these, several alternative strategies are in (pre)clinical experimental phases, including pharmacological chaperone therapy (PCT). The concept of ERT is to complement endogenous, defective enzyme with a functional, recombinant one.¹⁶ Macrophages, including GD cells, express mannose receptors on the surface, which can be utilized to bind high-mannose type N-glycans in recombinant GBA1 which are then delivered to lysosomes. ERT has been approved for GD by the U.S. Food and Drug Administration (FDA) and the European Medicines Agency (EMA). The available therapeutic enzymes include Imiglucerase²³, Velaglucerase alfa²⁴, and Taliglucerase alfa.²⁵ ERT is however effective only for the non-neuronopathic phenotype (type I) and does not prevent neurological symptoms in patients with types II and III, this because recombinant enzyme is unable to penetrate into the brain. The concept of SRT is to use small molecules to inhibit the build-up of storage molecules in lysosomes by (partially) blocking their biosynthesis.¹⁶ In the context of GD, the registered small-molecule drugs imiglustat and eliglustat, both glucosylceramide synthase (GCS) inhibitors, have been approved for the treatment of type I Gaucher disease.²⁶ SRT drugs have the advantage over recombinant enzymes (which are administered intravenously) that they are oral medications. However, small compound SRT drugs have a slower onset of efficacy than ERT. The concept of PCT is to use small molecules to improve the folding of misfolded protein in patients.²⁷ These small molecules (named pharmacological chaperones) can favorably interact with mutant proteins by assisting folding in the ER. In an alternative version merging PCT with ERT, small molecule pharmacological chaperones are used to stabilize recombinant enzyme in circulation, thereby elevating protein levels that end up in disease tissue.¹⁶ Migalastat as a competitive inhibitor of α -galactosidase A is the first approved PCT drug by the FDA,²⁸ but there is no approved PCT drug for GD at present. Other therapies in development include gene therapy, both *in vivo* transduction (termed AAV therapy) and *ex vivo* transduction (termed lentiviral gene therapy).^{12,21,22}

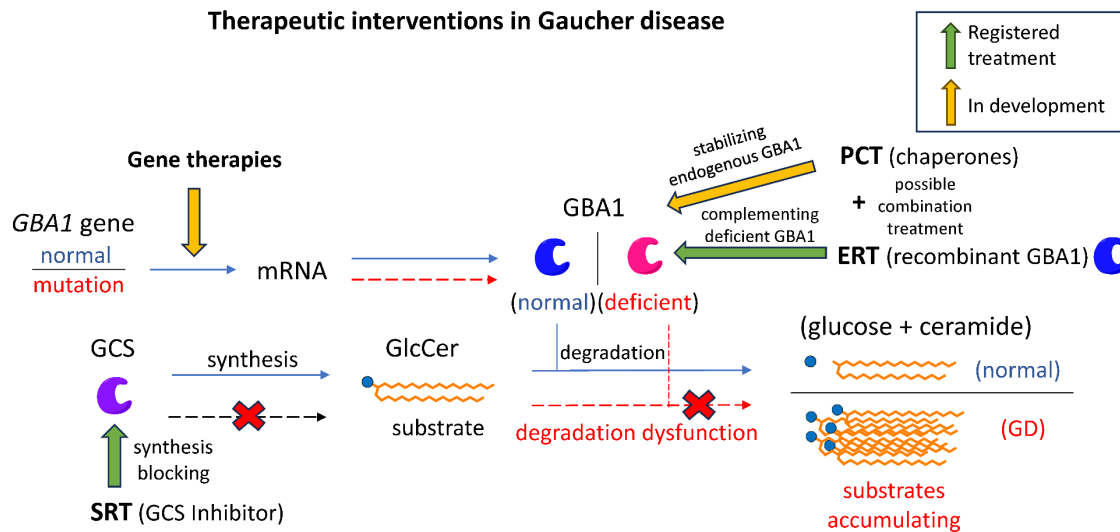


Figure 2. Therapeutic strategies to treat GD.

Properties of retaining exo- β -glucosidases in human cells

Human cells contain four reported retaining exo- β -glucosidases. The lysosomal acid β -glucosidase GBA1 (glucosylceramidase; glucocerebrosidase; GCase, EC. 3.2.1.45, GH30), is encoded by the *GBA1* gene located on locus 1q21 of the human chromosome 1. GBA1 is a 497 amino acid glycoprotein with four N-linked glycans and has a characteristic $(\alpha/\beta)_8$ TIM barrel catalytic domain.³⁰ In this domain, Glu 340 and Glu 235 are employed as catalytic nucleophile and acid/base residues.³¹ Nascent GBA1 that emerges from ER-associated ribosomal protein synthesis undergoes N-glycosylation to yield, within the ER lumen, newly formed glycoprotein featuring three to four high mannose-type N-glycans. After proceeding through the ER quality control system (the calnexin-calreticulin cycle) and the Golgi apparatus, at which stage three of the high-mannose-type N-glycans are trimmed and reglycosylated to yield complex N-glycans, the GBA1 protein is shuttled to lysosomes by means of the mannose 6-phosphate independent receptor. During this process, GBA1 associates with the lysosomal integral membrane protein 2 (LIMP2) chaperone, from which it detaches once in the acidic environment of lysosomes.³² GBA1 has an optimal catalytic activity at around pH 5.2 *ex vivo*³³ and requires the sphingolipid activator protein, saposin C, to hydrolyze GlcCer located in the lysosomal membrane.³⁴ As described above, deficiency of GBA1 as caused by inherited mutations of the *GBA1* gene are at the basis of GD. Of note, clinical and genetic evidence has shown that GBA1 mutations are also a risk factor for the development of Parkinson Disease.^{35,36}

The non-lysosomal β -glucosidase GBA2 (EC 3.2.1.45, GH116) is thought to locate closely to the cell plasma membrane³⁷ and on the cytosolic surface of the ER and Golgi apparatus.³⁸ It is a protein encompassing 927 amino acids and is encoded by the *GBA2* gene located on human chromosome 9 at position p13.3.³⁹ The enzyme employs E527 as catalytic nucleophile and D677 as acid/base and a retaining mechanism in catalyzing β -glucoside hydrolysis.³¹ *Ex vivo*, GBA2 shows an optimal hydrolysis ability at around pH 5.8.⁴⁰ In humans, GBA2 is mainly expressed in brain, heart, skeletal muscle, kidney and placenta and at lower levels also in liver, spleen, small intestine and lung. GBA2 has been considered to play a compensatory role in GD through hydrolysis of accumulating GlcCer. GBA1 deficient mice and cells from GD patients show elevated GBA2 levels as well as an increase in *in vitro* GBA2 activity.^{41,42} The action of GBA2 in GBA1 deficient GD patients may actually be harmful and inhibition of GBA2 may be beneficial. GBA2 deletion in type I GD mice has been reported to rescue the disease phenotype, despite an increase in GlcCer and GlcSph levels.⁴³ The mechanism for the observed beneficial action of GBA2 deletion in GD mice is not fully understood yet. Mutations in GBA2 have furthermore been associated with spastic paraplegia and cerebellar ataxia.⁴⁴⁻⁴⁶

The cytosolic β -glucosidase GBA3 (EC 3.2.1.21, GH1), also referred as non-specific β -glucosidase, broad-specificity β -glycosidase, and Klotho related protein (KLrP), is a retaining β -glucosidase composed of 469 amino acid and having a broad substrate specificity.⁴⁷ GBA3 is encoded by the *GBA3* gene located in locus 4p15.2, and is expressed as cytosolic protein in human liver, kidney, intestine, and spleen. GBA3 employs E373 as catalytic nucleophile and E165 as catalytic acid/base^{31,48} and has an optimum pH at around 6 to 7. It has been reported that GBA3 can efficiently hydrolyze the artificial C6-NBD-GlcCer but natural GlcCer only at a very low rate.⁴⁹ Besides β -glucosides, GBA3 is also able to hydrolyze β -D-galactosides, β -D-fucosides, α -L-arabinosides and β -D-xylosides. However, the endogenous substrates of GBA3 in human are not known. Beyond GBA1, GBA2 and GBA3, intestinal lactase-phlorizin hydrolase (LPH, EC 3.2.1.23/62, GH1) exclusively found on the brush border of the mammalian small intestine, features retaining β -glucosidase activity.⁵⁰⁻⁵² This enzyme was not subject of the research described in this Thesis.

Table 1. General overview of the human retaining exo- β -glucosidases, GBA1, GBA2 and GBA3.

Enzyme	GBA1	GBA2	GBA3
GH family	30	116	1
Sub-cellular localization	lysosome	plasma membrane ³⁷ / cytosolic surface of ER, Golgi ³⁸	cytosol
Tissue distribution	ubiquitous	brain, heart, skeletal muscle, kidney and placenta	liver, kidney, intestine, and spleen
Optimum pH	5.2	5.8	6.0 - 7.0
Additives for activity	additives needed ³³	no additives ⁴⁰	no additives
Gene mutant consequence	Gaucher Disease	Associated with spastic paraplegia and cerebellar ataxia	unknown

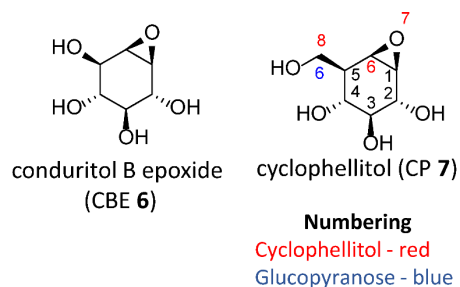
Chemical tools for studying retaining exo- β -glucosidases

Over the past decades, a series of chemical tools have been developed for retaining exo- β -glucosidase (activity) detection, inhibition, and visualization, including fluorogenic substrates, inhibitors, and activity-based probes (ABPs).⁵³⁻⁵⁵ The artificial substrate, 4-methylumbelliferyl- β -D-glucopyranoside **5** (4-MU- β -D-Glc) is composed of a glucose and a 4-methylumbelliferone (4-MU)⁵⁶ group (which is non-fluorescent when attached to the sugar). It can be employed to reflect the β -glycosidic bond hydrolysis activity of retaining exo- β -glucosidases through detecting the released, fluorescent 4-MU.

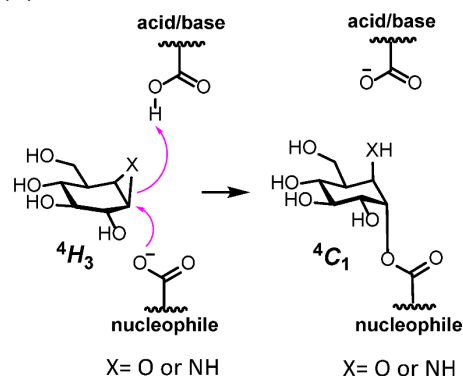
Small molecule β -glucosidase inhibitors have received considerable attention in studying the mechanism and active site residues of retaining β -glucosidases, as well as their potential value for therapeutic application. Conduritol B epoxide (CBE **6**) and cyclophellitol (CP **7**) have been reported as retaining β -glucosidase-selective inhibitors decades ago (see for their chemical structures Figure 4). CBE **6** and CP **7** both are cyclitol epoxides that covalently and irreversibly reacts with the catalytic nucleophile of retaining β -glucosidases.^{57,58} CBE **6** and cyclophellitol **7** are close structural homologues and their mode of action in inhibiting retaining β -glucosidases is very similar. The inactivation involves attack of the catalytic nucleophile at the pseudo-anomeric position, resulting in opening of the epoxide and the formation of a stable and irreversible enzyme-inhibitor ester adduct. This process is facilitated by protonation of the epoxide by the general acid/base residue (Figure 4B). Compared to CBE **6**, CP **7** has an extra methylene, breaking the symmetry inherent to CBE **6**. As a result, and in contrast to CBE **6**, CP **7** has considerable selectivity for retaining β -glucosidases (note that rotation of CBE over the axis bisecting C3-C4 and C1-C6 yields a close α -glucoside analogue, explaining the inhibitory effect of CBE also on retaining α -glucosidases). An important class of competitive GBA1-3 inhibitors are the *N*-alkylated deoxynojirimycins such as *N*-butyl-1-deoxynojirimycin (NB-DNJ, Miglustat, **8**) and *N*-adamantanemethyloxypentyl-deoxynojirimycin (AMP-DNM, **9**), both originally developed as GCS inhibitors that were subsequently shown to be effective GBA2 inhibitors as well.^{61,62} Activity-based probes (ABPs) finally are powerful chemical tools⁶³⁻⁶⁶ to investigate, retaining β -glucosidases *in vitro* (also in cellular extracts), in cells and in living organisms (see Figure 4).⁶⁴⁻⁶⁹ They are composed of a reactive chemical warhead (to react within the enzyme active site to form a covalent and irreversible enzyme-inhibitor adduct), a recognition element (here a glucopyranose-like structural element) and a reporter tag (fluorescent tag or affinity tag for visualization or purification). The design of β -glucosidase ABPs exploits the scaffold of cyclophellitol **7**^{70,71} onto which a reporter (fluorescent or affinity tag) at C8 of cyclophellitol (for GBA1 selectivity) or at the nitrogen atom of cyclophellitol aziridine (for broad-spectrum reactivity towards retaining β -glucosidases) is grafted. C8-modified cyclophellitol ABPs **10** and **11** potently and selectively label GBA1 over the other two human retaining β -glucosidases, GBA2 and GBA3.^{60,72} Selective labelling of GBA1 by these ABPs was observed in all tested lysates, except in those of the small intestine, in which LPH, and fragments thereof, were also found to be modified.⁷² Vocadlo and co-workers designed fluorogenic substrates equipped with a fluorophore at C6 of a β -glucoside, the aglycon of which carried a fluorescence quencher, compounds that proved to be efficient GBA1-selective substrates able to image GBA1 activity *in situ*.⁵⁹ Artola and co-workers generated cyclophellitol-C8-modified inhibitors (**12**, **13**) that proved to be potent and selective GBA1 inhibitors both *in vitro* and *in vivo*.⁶⁰ Considering that the other two retaining β -glucosidases did only accept C8-modified cyclophellitols, cyclophellitol aziridine scaffolds were developed in which the nitrogen atom of the aziridine was utilized to introduce a fluorescent reporter group (Cy5, BODIPY).⁷³ Cyclophellitol aziridine ABPs **14** and **15** proved to be broad-spectrum retaining β -glucosidase ABPs that label, besides GBA1, also GBA2, GBA3, and LPH.^{73,74} These ABPs report on retaining β -glucosidases irrespective of their origin, this due to the result of conservation of the catalytic pockets. This has allowed the study of retaining β -glucosidases in plants,^{75,76} zebrafish (*Danio rerio*),⁶⁰ and mice.^{72,73} At the onset of the

studies presented in this Thesis, however, no mechanism-based, covalent and irreversible inhibitors, and ABPs derived thereof, selective for either GBA2 or GBA3 were known.

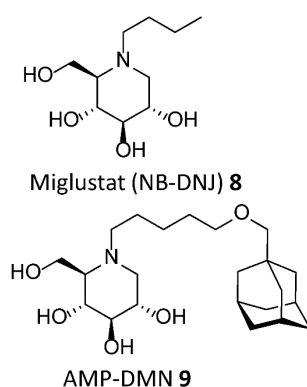
(A) CBE and CP



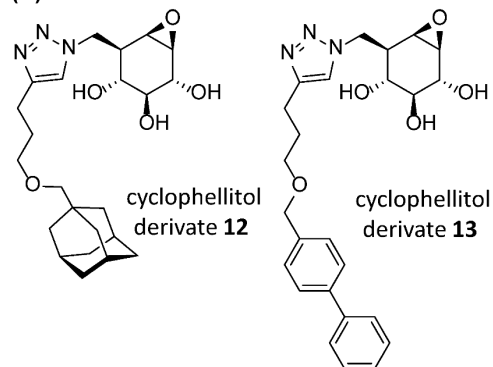
(B) mechanism of inhibition



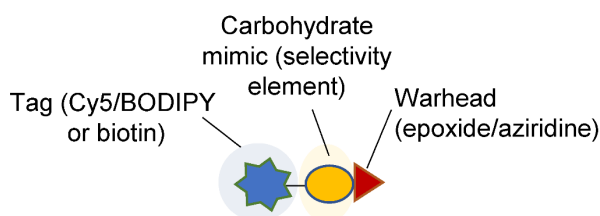
(C) iminosugar inhibitor



(E) GBA1-selective inhibitor

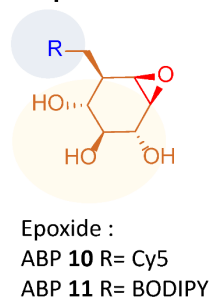


(D) β -glucosidase ABP:



R (Tags): Cy5, BODIPY, Biotin etc.

Cyclophellitol epoxide ABPs



Cyclophellitol aziridine ABPs

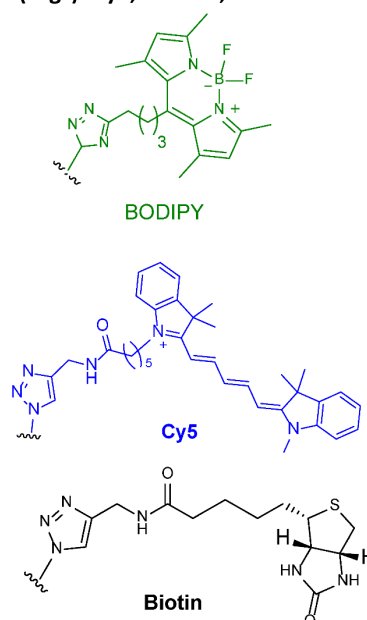
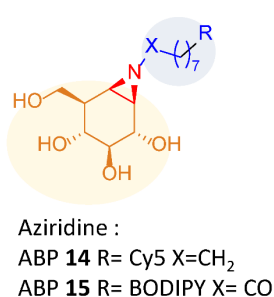


Figure 4. Retaining β -glucosidase inhibitors and ABPs. (A) Structure of CBE 6 and CP 7. (B) Mechanism by means of which cyclophellitol and cyclophellitol aziridine inhibit retaining β -glucosidases. (C) The competitive GBA1-3 inhibitors Miglustat 8 and AMP-DNM 9. (D) Structure of β -glucosidase ABPs. (E) Cyclophellitol-C8-modified GBA1-selective inhibitors 12 and 13.

Thesis outline

The overall aim of the research described in this Thesis was to employ activity-based protein profiling (ABPP) to study retaining β -glucosidases. Part of the research comprises the discovery and application of inhibitors and activity-based probes (ABPs) for each of the three human retaining β -glucosidases, GBA1, GBA2 and GBA3. These studies are complemented by research in which the inhibitors and probes are used to study homologous retaining β -glucosidase activities from other species. **Chapter 2** comprises a study in which three structurally and configurationally closely related cyclitol epoxides and aziridines, namely those derived from conduritol B epoxide, β -D-xylo-cyclophellitol and cyclophellitol, are compared for their activity and selectivity as GBA1 inhibitors and activity-based probes. **Chapter 3** studies β -D-arabinofuranose-configured cyclophellitol aziridine ABPs as selective reporters of mammalian GBA2 activities *in vitro* and *in situ*. **Chapter 4** concerns the exploration of potential GBA3-selective fluorogenic substrates and fluorescent ABPs. **Chapter 5** reports on the use of the established cyclophellitol-based ABPs to probe *Caenorhabditis elegans* (*C. elegans*) samples for β -glucosidase activities and to establish similarities and differences between these and the mammalian enzymes (GBA1, GBA2). **Chapter 6** utilizes the same set of ABPs to study the activity of a putative β -glucosidase (termed B56) from the tobacco plant *Nicotiana tabacum*. **Chapter 7** discusses the results of the experiments described in **Chapters 2-6** and presents some prospects for future research. This thesis is concluded with **Appendices** that include a **list of publications** and a **Curriculum vitae** of the author.

References

1. T. Wennekes, R. J. van den Berg, R. G. Boot, G. A. van der Marel, H. S. Overkleeft, J. M. Aerts, Glycosphingolipids--nature, function, and pharmacological modulation, *Angew. Chem. Int. Ed.* 2009, **48**, 8848-8869.
2. C. A. Lingwood, Glycosphingolipid functions, *Cold Spring Harb. Perspect. Biol.* 2011, **3**, a004788.
3. C. R. Gault, L. M. Obeid, Y. A. Hannun, An overview of sphingolipid metabolism: from synthesis to breakdown, *Sphingolipids as signaling and regulatory molecules* 2010, 1-23.
4. S. Ichikawa, Y. Hirabayashi, Glucosylceramide synthase and glycosphingolipid synthesis, *Trends Cell Biol.*, 1998, **8**, 198-202.
5. D. E. Koshland, Stereochemistry and the mechanism of enzymatic reactions, *Biol. Rev.* 1953, **28**, 416-436.
6. A. Vasella, G. J. Davies, M. Bohm, Glycosidase mechanisms, *Curr. Opin. Chem. Biol.* 2002, **6**, 619-629.
7. D. L. Zechel, S. G. Withers, Glycosidase mechanisms: anatomy of a finely tuned catalyst, *Acc. Chem. Res.* 2000, **33**, 11-18.
8. C. S. Rye, S. G. Withers, Glycosidase mechanisms, *Curr. Opin. Chem. Biol.* 2000, **4**, 573-580.
9. G. J. Davies, A. Planas, C. Rovira, Conformational analyses of the reaction coordinate of glycosidases, *Acc. Chem. Res.* 2012, **45**, 308-316.
10. M. T. C. Walvoort, G. A. van der Marel, H. S. Overkleeft, J. D. C. Codée, On the reactivity and selectivity of donor glycosides in glycochemistry and glycobiology: trapped covalent intermediates, *Chem. Sci.* 2013, **4**, 897-906.
11. A. R. Marques, M. Mirzaian, H. Akiyama, P. Wisse, M. J. Ferraz, P. Gaspar, K. Ghauharali-van der Vlugt, R. Meijer, P. Giraldo, P. Alfonso, P. Irun, M. Dahl, S. Karlsson, E. V. Pavlova, T. M. Cox, S. Scheij, M. Verhoek, R. Ottenhoff, C. P. van Roomen, N. S. Pannu, M. van Eijk, N. Dekker, R. G. Boot, H. S. Overkleeft, E. Blommaart, Y. Hirabayashi, J. M. Aerts, Glucosylated cholesterol in mammalian cells and tissues: formation and degradation by multiple cellular beta-glucosidases, *J. Lipid Res.* 2016, **57**, 451-463.
12. F. M. Platt, A. d'Azzo, B. L. Davidson, E. F. Neufeld, C. J. Tifft, Lysosomal storage diseases, *Nat. Rev. Dis. Primers* 2018, **4**, 27.
13. A. R. A. Marques, P. Saftig, Lysosomal storage disorders - challenges, concepts and avenues for therapy: beyond rare diseases, *J. Cell Sci.* 2019, **132**.
14. G. Parenti, G. Andria, A. Ballabio, Lysosomal storage diseases: from pathophysiology to therapy, *Annu. Rev. Med.* 2015, **66**, 471-486.
15. B. Breiden, K. Sandhoff, Lysosomal glycosphingolipid storage diseases, *Annu. Rev. Biochem.* 2019, **88**, 461-485.
16. J. M. Aerts, C. L. Kuo, L. T. Lelieveld, D. E. C. Boer, M. J. C. van der Lienden, H. S. Overkleeft, M. Artola, Glycosphingolipids and lysosomal storage disorders as illustrated by Gaucher disease, *Curr. Opin. Chem. Biol.* 2019, **53**, 204-215.
17. J. M. Aerts, M. J. Ferraz, M. Mirzaian, P. Gaspar, S. V. Oussoren, P. Wisse, C. L. Kuo, L. T. Lelieveld, K. Kytidou, M. D. Hazeu, D. E. C. Boer, R. Meijer, M. J. C. van der Lienden, D. H. M. Chao, T. L. Gabriel, J. Aten, H. S. Overkleeft, M. van Eijk, R. G. Boot, A. R. A. Marques, *Encyclopedia of Life Sciences* 2017, DOI: 10.1002/9780470015902.a0027592, pp. 1-13.
18. A. Dardis, H. Michelakakis, P. Rozenfeld, K. Fumic, J. Wagner, E. Pavan, M. Fuller, S. Revel-Vilk, D. Hughes, T. Cox, J. M. Aerts, International Working Group of Gaucher, patient centered guidelines for the laboratory diagnosis of Gaucher disease type 1, *Orphanet J. Rare Dis.* 2022, **17**, 442.
19. R. H. Lachmann, I. R. Grant, D. Halsall, T. M. Cox, Twin pairs showing discordance of phenotype in adult Gaucher's disease, *QJM* 2004, **97**, 199-204.
20. E. Sidransky, Gaucher disease: complexity in a "simple" disorder, *Mol. Genet. Metab.* 2004, **83**, 6-15.

21. R. Sam, E. Ryan, E. Daykin, E. Sidransky, Current and emerging pharmacotherapy for Gaucher disease in pediatric populations, *Expert Opin. Pharmacother.* 2021, **22**, 1489-1503.
22. C. Fernandez-Pereira, B. San Millan-Tejado, M. Gallardo-Gomez, T. Perez-Marquez, M. Alves-Villar, C. Melcon-Crespo, J. Fernandez-Martin, S. Ortolano, Therapeutic approaches in lysosomal storage diseases, *Biomolecules* 2021, **11**.
23. Y. Kacher, B. Brumshtein, S. Boldin-Adamsky, L. Toker, A. Shainskaya, I. Silman, J. L. Sussman, A. H. Futerman, Acid beta-glucosidase: insights from structural analysis and relevance to Gaucher disease therapy, *Biol. Chem.* 2008, **389**, 1361-1369.
24. T. A. Burrow, G. A. Grabowski, Velaglucerase alfa in the treatment of Gaucher disease type 1, *Clin. Investig.* 2011, **1**, 285-293.
25. L. van Dussen, A. Zimran, E. M. Akkerman, J. M. Aerts, M. Petakov, D. Elstein, H. Rosenbaum, D. Aviezer, E. Brill-Almon, R. Chertkoff, M. Maas, C. E. Hollak, Taliglucerase alfa leads to favorable bone marrow responses in patients with type I Gaucher disease, *Blood Cells Mol. Dis.* 2013, **50**, 206-211.
26. M. Pineda, M. Walterfang, M. C. Patterson, Miglustat in Niemann-Pick disease type C patients: a review, *Orphanet J. Rare Dis.* 2018, **13**, 140.
27. J. M. Benito, J. M. Garcia Fernandez, C. Ortiz Mellet, Pharmacological chaperone therapy for Gaucher disease: a patent review, *Expert Opin. Ther. Pat.* 2011, **21**, 885-903.
28. A. Markham, Migalastat: first global approval, *Drugs* 2016, **76**, 1147-1152.
29. V. Lombard, H. Golaconda Ramulu, E. Drula, P. M. Coutinho, B. Henrissat, The carbohydrate-active enzymes database (CAZy) in 2013, *Nucleic Acids Res.* 2014, **42**, D490-495.
30. F. Ben Bdira, M. Artola, H. S. Overkleeft, M. Ubbink, J. M. Aerts, Distinguishing the differences in beta-glycosylceramidase folds, dynamics, and actions informs therapeutic uses, *J. Lipid Res.* 2018, **59**, 2262-2276.
31. W. W. Kallemijn, M. D. Witte, T. M. Voorn-Brouwer, M. T. Walvoort, K. Y. Li, J. D. Codée, G. A. van der Marel, R. G. Boot, H. S. Overkleeft, J. M. Aerts, A sensitive gel-based method combining distinct cyclophellitol-based probes for the identification of acid/base residues in human retaining beta-glucosidases, *J. Biol. Chem.* 2014, **289**, 35351-35362.
32. D. Reczek, M. Schwake, J. Schröder, H. Hughes, J. Blanz, X. Jin, W. Brondyk, S. Van Patten, T. Edmunds, P. Saftig, LIMP-2 is a receptor for lysosomal mannose-6-phosphate-independent targeting of beta-glucocerebrosidase, *Cell* 2007, **131**, 770-783.
33. J. M. Aerts, W. E. Donker-Koopman, M. K. van der Vliet, L. M. Jonsson, E. I. Ginns, G. J. Murray, J. A. Barranger, J. M. Tager, A. W. Schram, The occurrence of two immunologically distinguishable beta-glucocerebrosidases in human spleen, *Eur. J. Biochem.* 1985, **150**, 565-574.
34. R. J. Tamargo, A. Velayati, E. Goldin, E. Sidransky, The role of saposin C in Gaucher disease, *Mol. Genet. Metab.* 2012, **106**, 257-263.
35. E. Aflaki, W. Westbroek, E. Sidransky, The complicated relationship between Gaucher disease and Parkinsonism: insights from a rare disease, *Neuron* 2017, **93**, 737-746.
36. J. Do, C. McKinney, P. Sharma, E. Sidransky, Glucocerebrosidase and its relevance to Parkinson disease, *Mol. Neurodegener.* 2019, **14**, 36.
37. R. G. Boot, M. Verhoek, W. Donker-Koopman, A. Strijland, J. van Marle, H. S. Overkleeft, T. Wennekes, J. M. Aerts, Identification of the non-lysosomal glucosylceramidase as beta-glucosidase 2, *J. Biol. Chem.* 2007, **282**, 1305-1312.
38. H. G. Korschen, Y. Yildiz, D. N. Raju, S. Schonauer, W. Bonigk, V. Jansen, E. Kremmer, U. B. Kaupp, D. Wachten, The non-lysosomal beta-glucosidase GBA2 is a non-integral membrane-associated protein at the endoplasmic reticulum (ER) and Golgi, *J. Biol. Chem.* 2013, **288**, 3381-3393.
39. A. Massimo, S. Maura, L. Nicoletta, M. Giulia, M. Valentina, C. Elena, P. Alessandro, B. Rosaria, S. Sandro, Current and novel aspects on the non-lysosomal beta-glucosylceramidase GBA2, *Neurochem. Res.* 2016, **41**, 210-220.
40. S. van Weely, M. Brandsma, A. Strijland, J. M. Tager, J. M. Aerts, Demonstration of the existence of a second, non-lysosomal glucocerebrosidase that is not deficient in Gaucher disease, *Biochim. Biophys. Acta* 1993, **1181**, 55-62.

41. D. G. Burke, A. A. Rahim, S. N. Waddington, S. Karlsson, I. Enquist, K. Bhatia, A. Mehta, A. Vellodi, S. Heales, Increased glucocerebrosidase (GBA) 2 activity in GBA1 deficient mice brains and in Gaucher leucocytes, *J. Inherit. Metab. Dis.* 2013, **36**, 869-872.
42. Y. Yildiz, P. Hoffmann, S. Vom Dahl, B. Breiden, R. Sandhoff, C. Niederau, M. Horwitz, S. Karlsson, M. Filocamo, D. Elstein, M. Beck, K. Sandhoff, E. Mengel, M. C. Gonzalez, M. M. Nothen, E. Sidransky, A. Zimran, M. Mattheisen, Functional and genetic characterization of the non-lysosomal glucosylceramidase 2 as a modifier for Gaucher disease, *Orphanet J. Rare Dis.* 2013, **8**, 151.
43. P. K. Mistry, J. Liu, L. Sun, W. L. Chuang, T. Yuen, R. Yang, P. Lu, K. Zhang, J. Li, J. Keutzer, A. Stachnik, A. Mennone, J. L. Boyer, D. Jain, R. O. Brady, M. I. New, M. Zaidi, Glucocerebrosidase 2 gene deletion rescues type 1 Gaucher disease, *Proc. Natl. Acad. Sci. U. S. A.* 2014, **111**, 4934-4939.
44. S. Sultana, J. Stewart, A. C. van der Spoel, Truncated mutants of beta-glucosidase 2 (GBA2) are localized in the mitochondrial matrix and cause mitochondrial fragmentation, *PLoS One* 2020, **15**, e0233856.
45. M. B. Hammer, G. Eleuch-Fayache, L. V. Schottlaender, H. Nehdi, J. R. Gibbs, S. K. Arepalli, S. B. Chong, D. G. Hernandez, A. Sailer, G. Liu, P. K. Mistry, H. Cai, G. Shrader, C. Sassi, Y. Bouhlal, H. Houlden, F. Hentati, R. Amouri, A. B. Singleton, Mutations in GBA2 cause autosomal-recessive cerebellar ataxia with spasticity, *Am. J. Hum. Genet.* 2013, **92**, 245-251.
46. E. Martin, R. Schule, K. Smets, A. Rastetter, A. Boukhris, J. L. Loureiro, M. A. Gonzalez, E. Mundwiler, T. Deconinck, M. Wessner, L. Jornea, A. C. Oteyza, A. Durr, J. J. Martin, L. Schols, C. Mhiri, F. Lamari, S. Zuchner, P. De Jonghe, E. Kabashi, A. Brice, G. Stevanin, Loss of function of glucocerebrosidase GBA2 is responsible for motor neuron defects in hereditary spastic paraplegia, *Am. J. Hum. Genet.* 2013, **92**, 238-244.
47. Y. Hayashi and M. Ito, Klotho-related protein KLRP: structure and functions, *Vitam. Horm.* 2016, **101**, 1-16.
48. Y. Hayashi, N. Okino, Y. Kakuta, T. Shikanai, M. Tani, H. Narimatsu, M. Ito, Klotho-related protein is a novel cytosolic neutral beta-glycosylceramidase, *J. Biol. Chem.* 2007, **282**, 30889-30900.
49. N. Dekker, T. Voorn-Brouwer, M. Verhoek, T. Wennekes, R. S. Narayan, D. Speijer, C. E. Hollak, H. S. Overkleeft, R. G. Boot, J. M. Aerts, The cytosolic beta-glucosidase GBA3 does not influence type 1 Gaucher disease manifestation, *Blood Cells Mol. Dis.* 2011, **46**, 19-26.
50. H. Skovbjerg, H. Sjostrom, O. Noren, Purification and characterisation of amphiphilic lactase/phlorizin hydrolase from human small intestine, *Eur. J. Biochem.* 1981, **114**, 653-661.
51. H. Elferink, J. P. J. Bruekers, G. H. Veeneman, T. J. Boltje, A comprehensive overview of substrate specificity of glycoside hydrolases and transporters in the small intestine : "A gut feeling", *Cell Mol. Life Sci.* 2020, **77**, 4799-4826.
52. H. Wacker, P. Keller, R. Falchetto, G. Legler, G. Semenza, Location of the two catalytic sites in intestinal lactase-phlorizin hydrolase. Comparison with sucrase-isomaltase and with other glycosidases, the membrane anchor of lactase-phlorizin hydrolase, *J. Biol. Chem.* 1992, **267**, 18744-18752.
53. H. M. Burke, T. Gunnlaugsson, E. M. Scanlan, Recent advances in the development of synthetic chemical probes for glycosidase enzymes, *Chem. Commun.* 2015, **51**, 10576-10588.
54. L. Wu, Z. Armstrong, S. P. Schröder, C. de Boer, M. Artola, J. M. Aerts, H. S. Overkleeft, G. J. Davies, An overview of activity-based probes for glycosidases, *Curr. Opin. Chem. Biol.* 2019, **53**, 25-36.
55. M. D. Witte, G. A. van der Marel, J. M. Aerts, H. S. Overkleeft, Irreversible inhibitors and activity-based probes as research tools in chemical glycobiology, *Org. Biomol. Chem.* 2011, **9**, 5908-5926.
56. J. Mead, J. Smith, R. Williams, The biosynthesis of the glucuronides of umbelliferone and 4-methylumbelliferone and their use in fluorimetric determination of β -glucuronidase, *Biochem. J.* 1955, **61**, 569-574.

57. C. L. Kuo, W. W. Kallemeyjn, L. T. Lelieveld, M. Mirzaian, I. Zoutendijk, A. Vardi, A. H. Futerman, A. H. Meijer, H. P. Spaink, H. S. Overkleeft, J. M. Aerts, M. Artola, In vivo inactivation of glycosidases by conduritol B epoxide and cyclophellitol as revealed by activity-based protein profiling, *FEBS J.* 2019, **286**, 584-600.
58. S. Atsumi, K. Umezawa, H. Iinuma, H. Naganawa, H. Nakamura, Y. Iitaka, T. Takeuchi, Production, isolation and structure determination of a novel beta-glucosidase inhibitor, cyclophellitol, from *Phellinus* sp, *J. Antibiot.* 1990, **43**, 49-53.
59. A. K. Yadav, D. L. Shen, X. Shan, X. He, A. R. Kermode, D. J. Vocadlo, Fluorescence-quenched substrates for live cell imaging of human glucocerebrosidase activity, *J. Am. Chem. Soc.* 2015, **137**, 1181-1189.
60. M. Artola, C. L. Kuo, L. T. Lelieveld, R. J. Rowland, G. A. van der Marel, J. D. C. Codée, R. G. Boot, G. J. Davies, J. M. Aerts, H. S. Overkleeft, Functionalized cyclophellitols are selective glucocerebrosidase inhibitors and induce a bona fide neuropathic Gaucher model in zebrafish, *J. Am. Chem. Soc.* 2019, **141**, 4214-4218.
61. H. S. Overkleeft, G. H. Renkema, J. Neele, P. Vianello, I. O. Hung, A. Strijland, A. M. van der Burg, G. J. Koomen, U. K. Pandit, J. M. Aerts, Generation of specific deoxynojirimycin-type inhibitors of the non-lysosomal glucosylceramidase, *J. Biol. Chem.* 1998, **273**, 26522-26527.
62. D. Lahav, B. Liu, R. van den Berg, A. van den Nieuwendijk, T. Wennekes, A. T. Ghisaidoobe, I. Breen, M. J. Ferraz, C. L. Kuo, L. Wu, P. P. Geurink, H. Ovaa, G. A. van der Marel, M. van der Stelt, R. G. Boot, G. J. Davies, J. M. Aerts, H. S. Overkleeft, A fluorescence polarization activity-based protein profiling assay in the discovery of potent, selective inhibitors for human nonlysosomal glucosylceramidase, *J. Am. Chem. Soc.* 2017, **139**, 14192-14197.
63. J. M. Punt, D. van der Vliet, M. van der Stelt, Chemical probes to control and visualize lipid metabolism in the brain, *Acc. Chem. Res.* 2022, **55**, 3205-3217.
64. P. Yang, K. Liu, Activity-based protein profiling: recent advances in probe development and applications, *ChemBioChem* 2015, **16**, 712-724.
65. N. Li, H. S. Overkleeft, B. I. Florea, Activity-based protein profiling: an enabling technology in chemical biology research, *Curr. Opin. Chem. Biol.* 2012, **16**, 227-233.
66. M. B. Nodwell, S. A. Sieber, ABPP methodology: introduction and overview, *Top. Curr. Chem.* 2012, **324**, 1-41.
67. D. Hunerdosse, D. K. Nomura, Activity-based proteomic and metabolomic approaches for understanding metabolism, *Curr. Opin. Biotechnol.* 2014, **28**, 116-126.
68. S. Wang, Y. Tian, M. Wang, M. Wang, G. B. Sun, X. B. Sun, Advanced activity-based protein profiling application strategies for drug development, *Front. Pharmacol.* 2018, **9**, 353.
69. J. Krysiak, R. Breinbauer, in *Activity-Based Protein Profiling*, 2011, DOI: 10.1007/128_2011_289, ch. Chapter 289, pp. 43-84.
70. W. W. Kallemeyjn, M. D. Witte, T. Wennekes, J. M. Aerts, Mechanism-based inhibitors of glycosidases: design and applications, *Adv. Carbohydr. Chem. Biochem.* 2014, **71**, 297-338.
71. L. I. Willems, J. Jiang, K. Y. Li, M. D. Witte, W. W. Kallemeyjn, T. J. Beenakker, S. P. Schröder, J. M. Aerts, G. A. van der Marel, J. D. Codée, H. S. Overkleeft, From covalent glycosidase inhibitors to activity-based glycosidase probes, *Chem. Eur. J.* 2014, **20**, 10864-10872.
72. M. D. Witte, W. W. Kallemeyjn, J. Aten, K. Y. Li, A. Strijland, W. E. Donker-Koopman, A. M. van den Nieuwendijk, B. Bleijlevens, G. Kramer, B. I. Florea, B. Hooibrink, C. E. Hollak, R. Ottenhoff, R. G. Boot, G. A. van der Marel, H. S. Overkleeft, J. M. Aerts, Ultrasensitive in situ visualization of active glucocerebrosidase molecules, *Nat. Chem. Biol.* 2010, **6**, 907-913.
73. W. W. Kallemeyjn, K. Y. Li, M. D. Witte, A. R. Marques, J. Aten, S. Scheij, J. Jiang, L. I. Willems, T. M. Voorn-Brouwer, C. P. van Roomen, R. Ottenhoff, R. G. Boot, H. van den Elst, M. T. Walvoort, B. I. Florea, J. D. Codée, G. A. van der Marel, J. M. Aerts, H. S. Overkleeft, Novel activity-based probes for broad-spectrum profiling of retaining beta-exoglucosidases in situ and in vivo, *Angew. Chem. Int. Ed.* 2012, **51**, 12529-12533.
74. S. P. Schröder, J. W. van de Sande, W. W. Kallemeyjn, C. L. Kuo, M. Artola, E. J. van Rooden, J. Jiang, T. J. M. Beenakker, B. I. Florea, W. A. Offen, G. J. Davies, A. J. Minnaard, J. M. Aerts, J. D.

- C. Codée, G. A. van der Marel, H. S. Overkleeft, Towards broad spectrum activity-based glycosidase probes: synthesis and evaluation of deoxygenated cyclophellitol aziridines, *Chem. Commun.* 2017, **53**, 12528-12531.
75. A. M. Husaini, K. Morimoto, B. Chandrasekar, S. Kelly, F. Kaschani, D. Palmero, J. Jiang, M. Kaiser, O. Ahrazem, H. S. Overkleeft, R. A. L. van der Hoorn, Multiplex fluorescent, activity-based protein profiling identifies active alpha-glycosidases and other hydrolases in plants, *Plant Physiol.* 2018, **177**, 24-37.
76. B. Chandrasekar, T. Colby, A. Emran Khan Emon, J. Jiang, T. N. Hong, J. G. Villamor, A. Harzen, H. S. Overkleeft, R. A. van der Hoorn, Broad-range glycosidase activity profiling, *Mol. Cell. Proteomics* 2014, **13**, 2787-2800.

Chapter 2

Xylose-configured cyclophellitols as selective inhibitors for glucocerebrosidase

Taken in part from:

Qin Su, Sybrin P. Schröder, Lindsey T. Lelieveld, Maria J. Ferraz, Marri Verhoek, Rolf G. Boot, Herman S. Overkleeft, Johannes M. F. G. Aerts, Marta Artola, Chi-Lin Kuo, Xylose-configured cyclophellitols as selective inhibitors for glucocerebrosidase, *ChemBioChem*, **2021**, 22, 3090-3098.

Abstract

Glucocerebrosidase (GBA1), a lysosomal retaining β -D-glucosidase, has recently been shown to hydrolyze β -D-xylosides and to transxylosylate cholesterol. Genetic defects in GBA1 cause the lysosomal storage disorder Gaucher disease (GD), and also constitute a risk factor for developing Parkinson's disease. GBA1 and other retaining glycosidases can be selectively visualized by activity-based protein profiling (ABPP) using fluorescent probes composed of a cyclophellitol scaffold having a configuration tailored to the targeted glycosidase family. GBA1 processes β -D-xylosides in addition to β -D-glucosides, this in contrast to the other two mammalian cellular retaining β -D-glucosidases, GBA2 and GBA3. Here it is shown that the xylopyranose preference also holds up for covalent inhibitors: xylose-configured cyclophellitol and cyclophellitol aziridines selectively react with GBA1 over GBA2 and GBA3 *in vitro* and *in vivo*. As well, it is shown that the xylose-configured cyclophellitol is more potent and more selective for GBA1 than the classical GBA1 inhibitor, conduritol B epoxide (CBE). Both xylose-configured cyclophellitol and cyclophellitol aziridine cause accumulation of glucosylsphingosine in zebrafish embryo, a characteristic hallmark of GD, and it can be concluded that these compounds are well suited for creating such chemically induced GD models.

Introduction

The lysosomal retaining β -D-glucosidase, glucocerebrosidase (GBA1) receives considerable interest given its role in several pathologies.¹ Gaucher disease (GD), an autosomal recessive lysosomal storage disorder, is caused by mutations in the *GBA1* gene that result in reduced lysosomal GBA1 activity. In GD patients, tissue macrophages excessively store in their lysosomes glucosylceramide (GlcCer), an ubiquitous glycosphingolipid.² Part of the accumulating GlcCer is converted into glucosylsphingosine (GlcSph) by lysosomal acid ceramidase.³ The water-soluble GlcSph is able to leave cells and is prominently elevated in plasma and tissues of GD patients.⁴ This striking abnormality is exploited for diagnosis.⁵⁻⁷ Recently, it has been recognized that carriers of mutations in the *GBA1* gene are at an increased risk for developing Parkinson's disease (PD)⁸, in which excessive GlcSph is speculated to promote harmful α -synuclein aggregation.^{9,10}

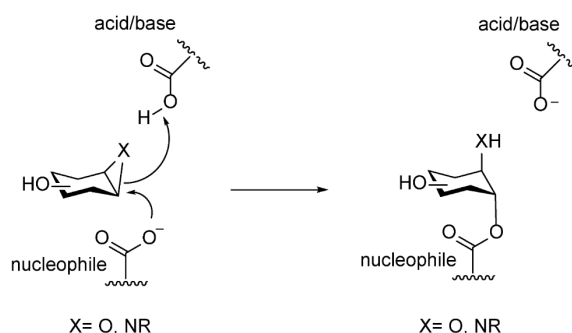
The current therapies for the treatment of GD are enzyme supplementation based on chronic intravenous administration of macrophage-targeted human recombinant GBA1, also known as "enzyme replacement therapy", and "substrate reduction therapy" founded on the inhibition of GlcCer synthesis.¹¹ Gene therapy approaches are presently actively studied in pre-clinical and clinical settings.^{12,13} GBA1 has been extensively examined and its life cycle and structural features have been elucidated by various techniques.¹ The catalytic mechanism of GBA1 involves a Koshland double-displacement mechanism in which E340 and E325 serve as nucleophile and acid/base catalytic residues, respectively.¹⁴ Conduritol B epoxide (CBE)¹⁵ reacts with the catalytic nucleophile of GBA1 to form a covalent and irreversible bond, thereby irreversibly inactivating the enzyme,^{16,17} and is used extensively in GD¹⁷⁻²⁰ and PD research.²¹⁻²³ Cyclophellitol and its analogues react in the same manner (Figure 1A), but are much more potent GBA1 inhibitors.^{16,24} Based on the cyclophellitol scaffold two classes of GBA1-reactive activity-based probes (ABPs) were recently developed: one with the reporter group (fluorophore or biotin) connected via the cyclophellitol O8 and one with the reporter group grafted onto the nitrogen of cyclophellitol aziridine.^{25,26} The cyclophellitol-based ABPs react in a highly specific manner with GBA1 and allow its selective and sensitive visualization in organisms and intact cells, even in individual lysosomes.^{27,28} The cyclophellitol aziridine-based ABPs on the other hand react with all the cellular retaining β -D-glucosidases: lysosomal GBA1, cytosol-facing, membrane bound GBA2 and cytosolic GBA3.²⁹

Recent investigations have revealed that GBA1 is catalytically more versatile than previously considered. Besides hydrolysis of β -D-glucosides, the enzyme catalyses transglucosylation, a process in which glucose is transferred, with retention of anomeric configuration, from GlcCer to an acceptor hydroxyl such as the one in cholesterol.^{30,31} In addition, GBA1 hydrolyses β -D-xylosides, including 4-methylumbelliferyl- β -D-xylopyranoside and plant derived β -xylosides like cyanidin- β -xyloside from plums and berries, as well as xylosylceramide.³² GBA1 is also able to use β -xylosides as donors in transglycosylation reactions, generating xylosylcholesterol and di-xylosylcholesterol, again with retention of configuration with respect to the anomeric centre of the transferred xylose residues.³³ In contrast to GBA1, GBA2 is not active towards β -xylosides and the activity of GBA3 towards these substrates is very low.³³ It thus appears that the presence of the pendant CH₂OH group that distinguishes β -glucosides from β -xylosides is a prerequisite for affinity for GBA2 and GBA3. The flexibility of GBA1 for substrates with a modification at the glucose-C6 is also

reflected by its selective reactivity towards O8-modified cyclophellitol-based inhibitors and ABPs and with those of glucose-C6 modified substrates.³⁴⁻³⁷

In the study described in this chapter, it was examined whether xylose-configured cyclophellitol and cyclophellitol aziridines can react with GBA1, GBA2 and/or GBA3 *in vitro* and *in vivo*, by applying activity-based protein profiling (ABPP) and fluorogenic substrate hydrolysis readouts. These studies reveal that *xylo*-cyclophellitol is a highly effective GBA1 inhibitor that is both more potent and more selective than the widely applied GBA1 inhibitor, CBE.

(A)



(B)

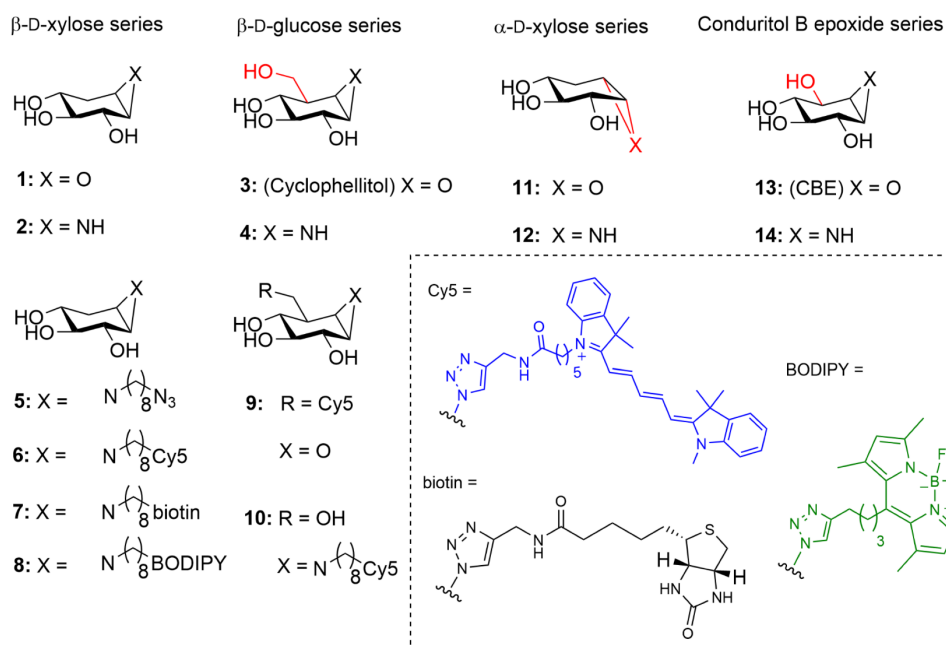


Figure 1. (A) Irreversible inhibition by cyclophellitol and cyclophellitol-aziridine configured compounds. (B) Structures of cyclophellitol configured epoxide and aziridines subject of the research described in this chapter.

Results

In vitro affinity and selectivity of cyclophellitol- and xylo-cyclophellitol-based inhibitors and ABPs towards human β -glucosidases

The synthesis of β -xylo-cyclophellitol **1**, β -xylo-cyclophellitol aziridines **2** and **5** and ABPs **6** and **7**^{38,39}, cyclophellitol aziridine **4**⁴⁰, conduritol B aziridine **14**⁴⁰, α -D-xylose-configured cyclophellitol **11** and cyclophellitol aziridine **12** was published previously³⁸, whereas that of ABP **8** can be found in the appendix and is based on synthetic procedures reported previously.⁴¹

In the first instance, the inhibitory potency of **1** and **2** for GBA1, GBA2, and GBA3 was assessed by competitive activity-based protein profiling (cABPP). For this, HEK293T cells were generated that contain endogenous GBA1 and overexpressed GBA2 and GBA3. Cell lysates were incubated with **1** or **2** at different concentrations before treatment with the broad-spectrum retaining β -glucosidase ABP **10**.⁴² As can be seen in Figure 2, β -xylo-cyclophellitol **1** is able to compete ABP labelling of GBA1 but not that of GBA2 or GBA3 at 10-100 μ M. β -Xylo-cyclophellitol aziridine **2** similarly competes labelling of GBA1 with **10** at lower concentrations (1-10 μ M), and also competes ABP labelling of GBA2 at a higher concentration (100 μ M). GBA3 was found to be very insensitive towards both compounds, **1** and **2**. GBA1-selectivity was not observed for cyclophellitol **3** nor cyclophellitol aziridine **4** when assessed in the same cABPP assay: both inhibitors block ABP labelling of GBA1 and GBA2 at equal concentrations (0.1-1 μ M) (Figure 2) and, though with less potency, also that of GBA3. Compound **5** comprises an extended version of compound **2** bearing an azido-octyl moiety at the aziridine, and it appeared that this hydrophobic extension greatly enhances inhibitory potency against GBA1 and GBA3, but not against GBA2. Conduritol B epoxide **13** (CBE), which is often used to block GBA1 *in situ* or *in vivo*,^{18,37,43} showed less GBA1 selectivity: both GBA1 and GBA2 were shown to be inhibited at close concentrations.

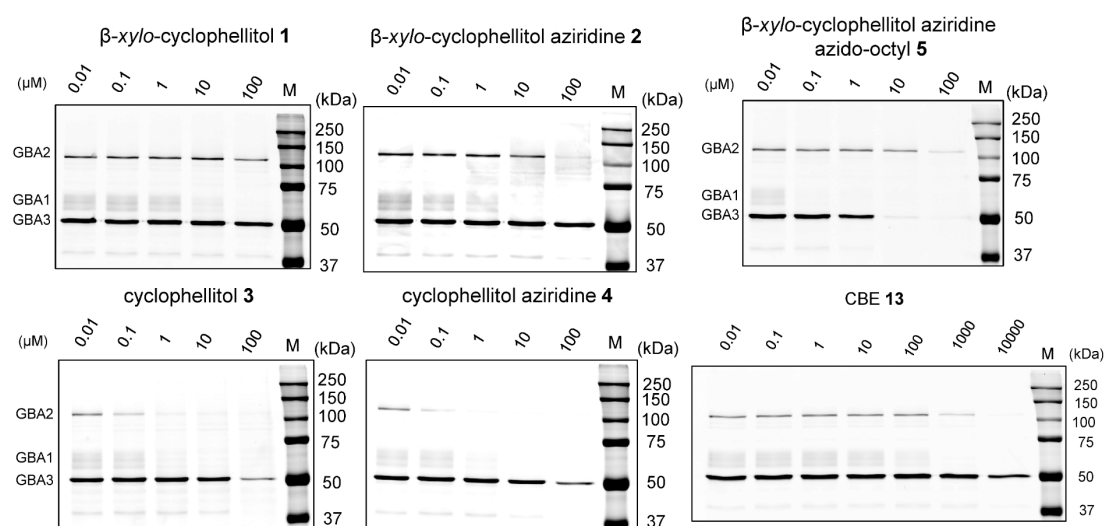


Figure 2. Selectivity of compounds **1-5** towards GBA1, GBA2 and GBA3 as visualized by competitive ABPP. Lysates of HEK293T cells expressing human GBA1, GBA2 and GBA3 were incubated with compounds **1-5** at indicated concentrations for 30 min, following by treatment with ABP **10**, separation of the denatured protein content by SDS-PAGE and fluorescence scanning of the wet gel slabs.

ABPP was next used to assess the GBA1/GBA2/GBA3 activity and selectivity of β -*xylo*-cyclophellitol aziridine ABPs **6** and **8** in comparison to those of GBA1-selective ABP **9** and ABP **10**. Surprisingly, the labelling pattern of GBA1 and GBA2 with *xylo*-cyclophellitol ABP **6** was very similar to that of the broad-spectrum retaining β -glucosidase ABP **10** (Figure 3): both probes label the two enzymes equally well, while ABP **6** labels GBA3 tenfold less efficiently than ABP **10**. ABP **8** gives a similar labelling pattern of GBA1 and GBA2 but has a higher affinity for GBA3, similar to that of ABP **10** (Figure S4). Cyclophellitol ABP **9** proved to be the most selective ABP towards GBA1 over GBA2 and GBA3, in line with previous results.³⁶ The unexpected reaction of GBA2 with **6** happens at the catalytic nucleophile (E527) and not at other sites of GBA2, since the GBA2 E527G mutant and the E527G/D677G double mutant did not yield a fluorescent band upon treatment with **6** (Figure 3B). This result is consistent with the observed labelling pattern from the glucose-configured cyclophellitol aziridine ABP **10** (Figure S5).

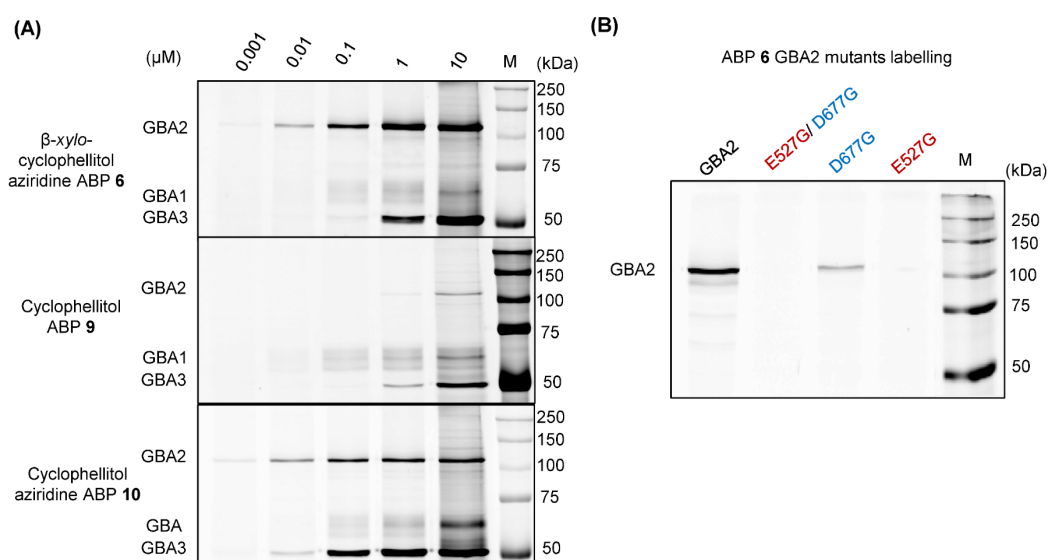


Figure 3. (A) Lysate of HEK293T cells expressing human GBA1, GBA2 and GBA3 was incubated with indicated ABPs (**6**, **9** or **10**) for 30 min at pH 6.0. ABP-reacted proteins were visualized after SDS-PAGE by fluorescence scanning of the wet gel slabs. (B) Labelling with ABP **6** of wild type, catalytic nucleophile mutant (E527G), catalytic acid/base mutant (D677G) or double (E527G/D677G) mutant GBA2 in HEK293T cell extracts.

Apparent IC_{50} values for *xylo*-cyclophellitols (**1**, **2**, **5-8**), in comparison with *Glc*-cyclophellitols (**3**, **4**), as inhibitors of GBA1, GBA2 and GBA3 were next determined in fluorogenic substrate assays as follows. Either recombinant, isolated GBA1 (imiglucerase), lysate of GBA1/GBA2 knockout (KO) HEK293T cells overexpressing GBA2, or lysate of GBA1/GBA2 KO cells overexpressing GBA3 were incubated for 30 min with varying concentrations of each of the inhibitors **1-14** followed by treatment with the fluorogenic substrate, 4-methylumbelliferyl- β -D-glucopyranoside (4-MU- β -D-Glc) and fluorescence readout. In agreement with the cABPP results, compounds **1** and **2** proved to be potent inhibitors of GBA1 (apparent IC_{50} of 2671 nM and 719 nM respectively) while only modestly inhibiting GBA2 and GBA3 (apparent $IC_{50} > 25 \mu$ M), whereas cyclophellitol **3** and aziridine **4** are

equally potent against GBA1 and GBA2.⁴⁴ A somewhat decreased potency against GBA3 was also noted from **1** and **2** over **3** and **4**, consistent with the cABPP results. *N*-octyl *xylo*-cyclophellitol aziridine **5** proved to be a much more potent GBA1 and GBA3 inhibitor with 600-fold increased potency for GBA1 and over 40-fold increased potency for GBA3, when compared to the unsubstituted *xylo*-cyclophellitol aziridine **2**. In contrast, its potency as GBA2 inhibitor proved to be only five-fold higher than that of **2** (Table 1). Compound **5** is therefore an even more GBA1-selective inhibitor *in vitro* when compared to **2** (IC₅₀ ratio GBA2/GBA1 = 5317, GBA3/GBA1 = 486). The *xylo*-cyclophellitol aziridine ABPs **6-8** also selectively inhibit GBA1 over GBA2 and GBA3, but their selectivity window between GBA1 and GBA2 is less than that of **5**.⁴⁵ Neither α -D-*xylo*-configured epoxide **11** nor aziridine **12** show significant inhibition of either of the three retaining β -glucosidases (Table S1), in contrast to the observed affinity of α -glucose configured cyclophellitol aziridines, both of which have been shown to react with GBA1 and GBA2.³⁹

Table 1. *In vitro* apparent IC₅₀ values (nM) of compounds **1-8** and **13** towards β -glucosidases rhGBA1, GBA2 and GBA3. Apparent IC₅₀ values were derived from the average of three individual experiments as measured by enzymatic assays using 4-MU- β -D-Glc as the fluorogenic substrate. Inhibitors were incubated with enzymes for 30 min, following addition of 4-MU- β -D-Glc for 30 min incubation. Error ranges = \pm SD, n = 3 replicates.

inhibitors	rhGBA1 ^[a]	GBA2 ^[b]	GBA3 ^[c]	(Ratio) GBA2/ GBA1	(Ratio) GBA3/ GBA1
1	2671 \pm 94.5	> 5 \times 10 ⁴	> 5 \times 10 ⁴	> 19	> 19
2	719 \pm 196	31587 \pm 926	> 2.5 \times 10 ⁴	44	> 35
3 (CP)	400 \pm 12.4	148 \pm 7.51	51499 \pm 4013	0.4	129
4	341 \pm 5.82	279 \pm 44.5	33817 \pm 2428	0.8	99
5	1.20 \pm 0.06	6380 \pm 1155	583 \pm 202	5317	486
6	6.44 \pm 0.49	544 \pm 110	10055 \pm 1003	84	1561
7	164 \pm 22.1	48270 \pm 9014	25267 \pm 5007	295	155
8	2.70 \pm 0.45	61.2 \pm 12.0	522 \pm 209	23	193
13 (CBE)	34902 \pm 1668	> 5 \times 10 ⁵	> 5 \times 10 ⁵	> 14	> 14

^[a]rhGBA1 = isolated, recombinant human GBA1 (Imiglucerase). ^[b]GBA2 = lysate of GBA1/GBA2 KO HEK293T cells with GBA2 overexpression. ^[c]GBA3 = lysate of GBA1/GBA2 KO HEK293T cells with GBA3 overexpression.

Affinity and selectivity of xylose-configured cyclophellitol epoxide **1** and aziridine **2** towards human β -glucosidases *in vivo*

The activity of **1** and **2** towards the three human β -glucosidases in intact HEK293T cells was investigated next. For this experiment, HEK293T cells expressing endogenous GBA1, and overexpressing GBA2 and GBA3 were treated with varying concentrations of **1** or **2** for 24 h, after which lysates were subjected to ABPP using the broad-spectrum β -glucosidase ABP **10**,

followed by SDS-PAGE, fluorescence scanning of the gels and quantification of the fluorescent bands. Compounds **1** and **2** show low IC₅₀ values (5.7 nM and 42.2 nM, respectively) for GBA1 and good selectivity for this enzyme relative to GBA2 and GBA3 (Figure 4).

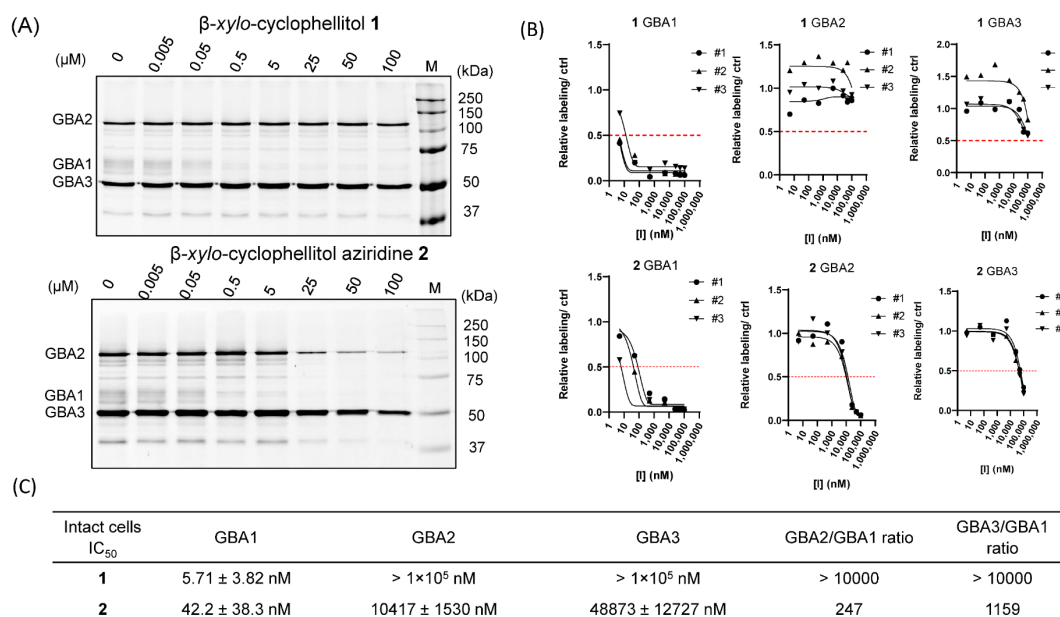


Figure 4. Inhibitory effect of β -D-xylo-cyclophellitol **1** and β -D-xylo-cyclophellitol aziridine **2** on β -glucosidases in intact HEK293T cells expressing endogenous GBA1, and overexpressing GBA2 and GBA3. (A) Representative gel images of cABPP where cells were treated for 24 h with varying concentrations of the indicated inhibitor. Lysates were then prepared and labelled with fluorescent ABP **10**. Fluorescently labelled proteins were visualized after SDS-PAGE (1 set from n = 3 replicates), and IC₅₀ values were determined by quantification of fluorescence intensity of the bands. (B) IC₅₀ curves (C) IC₅₀ values for compounds **1** and **2** as GBA1, GBA2 and GBA3 inhibitors as derived from this cABPP assay.

The affinity of xylo-configured cyclophellitols **1** and **2** for retaining β -glucosidases in living animals was then investigated using zebrafish (*Danio rerio*) embryos, which express homologues of both human GBA1 and GBA2. Following exposure for 5 days, fish larvae were sacrificed and lysed, and treatment with ABP **10** was used to detect residual active β -glucosidase molecules in the lysates and for IC₅₀ determination. Epoxide **1** selectively abrogates ABP labelling of GBA1 without targeting GBA2 at 150 μ M (Figure 5A). Aziridine **2** is also selective against GBA1 over GBA2, albeit with a narrower selectivity window (Figure 5A-C). The apparent IC₅₀ in zebrafish embryo is much lower than that observed in intact cells despite the longer incubation time, which could be a result of poor bioavailability of the cyclophellitol-related structures in whole animal, as noted earlier.³⁷ It was also observed that xylo-cyclophellitol **1** has a better GBA1:GBA2 selectivity window over CBE **13** in zebrafish embryo using the same experimental setup, but still do not outperform the previously reported novel GBA1-selective inhibitors based on cyclophellitol functionalized with hydrophobic moieties at C8 (cyclophellitol numbering, the primary carbon corresponding to C6 in glucose).³⁶ Finally, as revealed by quantification of LC-MS/MS, treatment of zebrafish embryos with compound **1** or **2** in zebrafish embryos led to increased levels of GlcSph (Figure 5D) when compared to non-treated embryos, reflecting functional inactivation of GBA1.

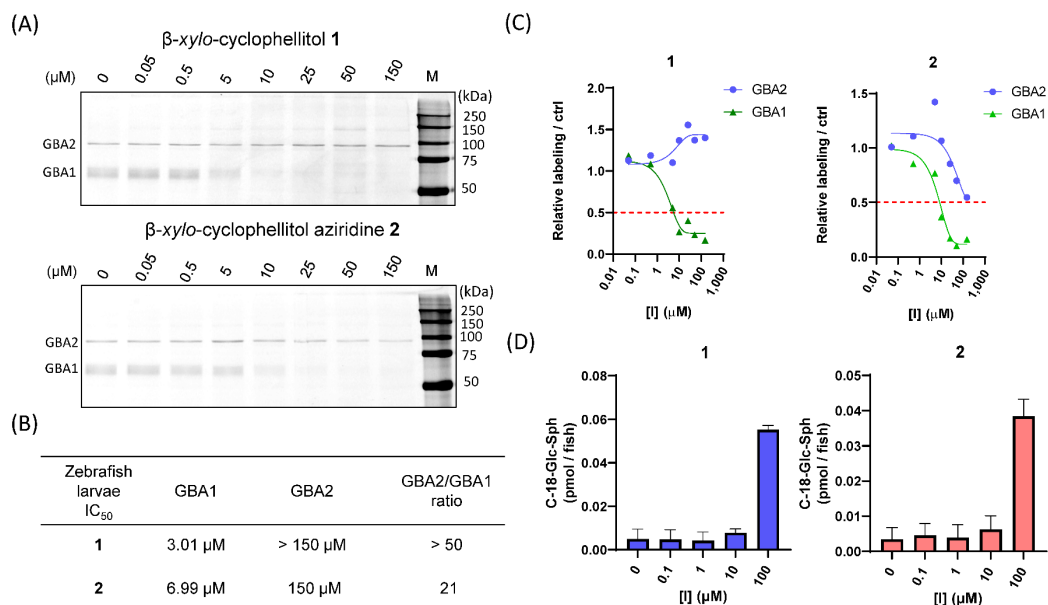


Figure 5. *In vivo* inhibitory activity of β -D-xylo-cyclophellitol **1** and β -D-xylo-cyclophellitol aziridine **2** towards GBA1 and GBA2 in zebrafish (*Danio rerio*) larvae. (A) Larvae were exposed to the indicated inhibitor for 5 days. Larvae were harvested, lysed and incubated with fluorescent ABP **10**. Fluorescently labelled proteins were visualized after SDS-PAGE. (B) Apparent IC₅₀ values towards β -glucosidases (GBA1 and GBA2) were determined by fluorescence quantification. (C) *In vivo* inhibition curves. (D) Glucosylsphingosine (GlcSph) levels in zebrafish larvae were determined by quantification of LC-MS/MS, n = 2 replicates.

Comparison of β -D-xylo-cyclophellitol (aziridine) and conduritol B epoxide (aziridine)

Prompted by the observation that β -D-xylo-cyclophellitol **1** has a better *in vivo* GBA1:GBA2 selectivity profile than CBE (compound **13**), these compounds were compared head-to-head as inhibitors of GBA1 and GBA2 in an *in vitro* setting. For comparison, recombinant, isolated GBA1 (imiglucerase), or lysate of GBA1/GBA2 KO HEK293T cells overexpressing GBA2 were used to incubated with compound **1**, **2**, or **13** for 3 h. In addition, CBE-aziridine **14** was synthesized³⁸ to allow comparison with β -D-xylo-cyclophellitol aziridine **2** in this setting. Using a fluorogenic substrate assay (hydrolysis of 4-MU- β -D-Glc) as readout, a marked increase of potency was observed towards GBA1 for **1** compared to CBE **13**, leading to a seven-fold increase in GBA1:GBA2 selectivity window (as calculated by IC₅₀ ratio of GBA2/GBA1, Table 2). Xylo-cyclophellitol aziridine **2** also has a slightly larger (three-fold increase) GBA1:GBA2 selectivity window when compared to that of conduritol B aziridine **14** (Table 2), however it is apparent that aziridines **2** and **14** are not as selective towards GBA1 as their epoxide analogues **1** and **13**. In addition, the cABPP assays reveal the poor reactivity of all these compounds towards GBA3 (Figure S3).

Table 2. Inhibition of GBA1 and GBA2 by conduritol B epoxide **13** and aziridine **14** in comparison with β -D-xylo-cyclophellitol **1** and aziridine **2**. *In vitro* apparent IC₅₀ of **1**, **2**, **13** and **14** as determined by using recombinant GBA1 or lysates of GBA1/GBA2 KO HEK293T cells expressing GBA2. Enzymatic assays were performed for 3 h incubation, n = 3 replicates.

Apparent IC ₅₀	Inhibitors	rhGBA1 ^[a]	GBA2 ^[b]	GBA2/GBA1 ratio
<i>In vitro</i> (3 h)	13	2.63 ± 0.34 μ M	105.3 ± 5.85 μ M	40
	14	1.63 ± 0.07 μ M	10.79 ± 3.30 μ M	6.6
	1	0.45 ± 0.02 μ M	122.3 ± 30.20 μ M	272
	2	0.24 ± 0.03 μ M	5.31 ± 0.12 μ M	22

^[a] rhGBA1 = recombinant human GBA1, Imiglucerase. ^[b] GBA2 = lysate of GBA1/GBA2 KO HEK293T cells with GBA2 overexpression.

Discussion

Following the observation that GBA1 is able to hydrolyze β -D-xylosides³³, the question arose whether xylose-configured cyclophellitols can be exploited as GBA1 selective inhibitors. The here-described study reveals that xylo-configured cyclophellitol **1** is indeed a potent GBA1 inhibitor that poorly reacts with GBA2 and GBA3 *in vitro*, in intact cells, and in zebrafish larvae. In zebrafish larvae, it functionally inhibits GBA1 as demonstrated by elevated levels of glucosylsphingosine (GlcSph). These data highlight that compound **1** has the required features for the generation of GBA1 chemical knockouts in cells and animals in the context of Gaucher and Parkinson disease research.

The xylo-configured cyclophellitol aziridine **2** and its *N*-octyl derivatives **5-8** are also all potent GBA1 inhibitors, however their concomitant increase in potency towards GBA2 renders them less GBA1:GBA2 selective compared to xylo-cyclophellitol **1**. The labelling of GBA2 by a xylo-configured cyclophellitol aziridine **2** is somewhat surprising given the finding that GBA2 does not hydrolyze 4-methylumbelliferyl- β -D-xylopyranoside.³³ Neither the catalytic nucleophile mutant (E527G) nor a combined substitution of catalytic nucleophile and acid/base residue (E527G/D677G) were shown to react, suggesting that the labelling proceeds via the catalytic nucleophile, identical to that of the broad-spectrum β -glucosidase cyclophellitol aziridine ABP **10**.

Finally, it was demonstrated in a head-to-head comparison that xylose-configured cyclophellitol **1** is more potent and selective against GBA1 than conduritol B epoxide (CBE, **13**), which is the compound commonly used to generate chemical knockdown GD models in cells and even organisms such as mice.^{18,37,43} Xylo-cyclophellitol aziridine **2** is similarly more potent and selective against GBA1 than conduritol aziridine **14**, again demonstrating the superiority of the xylo-configuration over the CBE configuration in terms of GBA1 selectivity. Xylo-cyclophellitol **1** may therefore be a suitable compound for generating improved chemical GBA1 knockout cells and animal models for the study of Gaucher disease and Parkinson's disease.

Experimental procedures

Materials

Recombinant human GBA1 (rhGBA1, Imiglucerase) was obtained from Sanofi Genzyme (Cambridge, MA, USA). 4-Methylumbelliferyl- β -D-glucopyranoside was purchased from Glycosynth (Warrington Cheshire, UK). HEK293T (CRL-3216™) cells were purchased from ATCC (Manassas, VA, USA), and cultured in DMEM medium (Sigma-Aldrich), supplied with 10% (v/v) FCS, 0.1% (w/v) penicillin/streptomycin and 1% (v/v) Glutamax, at 37°C under 7% CO₂. Zebrafish (strain AB/TL) were housed at Leiden University, The Netherlands, and maintained and handled in compliance with the directives of the local animal welfare committee (Instantie voor Dierwelzijn, Leiden) and guidelines specified by the EU Animal Protection Directive 2010/63/EU. Polytron PT 1300D sonicator (Kinematica, Luzern, Switzerland) and potassium phosphate buffer (25 mM KH₂PO₄-K₂HPO₄, pH 6.5, supplemented with protease inhibitor cocktail (EDTA-free, Roche, Basel, Switzerland) and 0.1% (v/v) Triton X-100) were used for lysing cells and homogenizing zebrafish larvae. Protein concentration was measured using the Pierce BCA assay kit (Thermo Fisher Scientific, Waltham, MA, USA). Harvested cells (cell pellets) and cell lysates not used directly were stored at -80 °C.

Cyclophellitol and xylose-configured inhibitors and ABPs **1**, **2**, **11** and **12**³⁸; **4** and **14**²⁶; **5**, **6** and **7**⁴⁶; **3**, **9**, **10** and **13**^{39,47} were synthesized as described in the literature. Synthetic methods and NMR characterization of compound **8** can be found in the appendix (Scheme S1). Chemicals were obtained from Sigma-Aldrich (St. Louis, MO, USA) if not otherwise indicated. Conduritol B epoxide (CBE) was purchased from Enzo Life Sciences (Farmingdale, NY, USA).

Generation of cells genetically modified in β -glucosidase expression

For overexpression of the different β -glucosidases, use was made of HEK293T cells lacking both GBA1 and GBA2. To this end the CRISPR/Cas9 system and the PX330 plasmid were used in order to generate knockout HEK293T cells for both GBA1 and GBA2 genes in these cells.⁴⁸ First the GBA1 knockout cells were generated using the annealed oligonucleotides (top strand: 5'-CACCGCGCTATGAGAGTACACGCAG-3', bottom strand: 5'-AAACCTGCGTGACTCTCATAGCGC-3') after ligation in the BbsI site of the px330 and subsequent transfection into HEK293T cells. Single cells were created and the different clones were analyzed for lack of expression of GBA1 with enzyme activity assays and ABPP and subsequent genomic sequence analysis. GBA1 knockout cells were next used to create the GBA1/GBA2 double knockout cells using the px330 and the following annealed and ligated oligonucleotides (top strand: 5'-CACCGGACGGACTGCTGCAATCCGG-3', bottom strand: 5'-AAACCCGGATTGCAGCAGTCCGTCC-3'). Double GBA1/GBA2 knockout cells were selected using fluorogenic substrate and ABPP assays and used for transfection with either human GBA2 or human GBA3 constructs. The design of cloning primers was based on NCBI reference sequences NM_020944.2 for human GBA2 and NM_020973.3 for human GBA3.

The HEK293T cells with either overexpressed GBA2 or GBA3 (in the GBA1/GBA2 KO background) were generated for 4MU fluorogenic assays as described below. GBA1/2 KO HEK293T cells with GBA2 overexpression were generated by transfecting the double GBA1 and GBA2 gene knockout HEK293T cells with human GBA2 constructs. GBA1/2 KO HEK293T cells

with GBA3 overexpression were generated by transfecting the double GBA1 and GBA2 gene knockout HEK293T cells with human GBA3 constructs.

To generate HEK293T cells expressing all cellular β -glucosidases (GBA1, GBA2, and GBA3) for ABPP assays, wild-type HEK293T cells containing endogenous GBA1 and GBA2 were first transfected with human GBA2 constructs to overexpress GBA2, then the GBA1 endogenous and GBA2 overexpressed cells were transfected with human GBA3 constructs to overexpress GBA3.

HEK293T cells expressing GBA2-E527G, GBA2-D677G, or GBA2-E527G/D677G mutants were generated as described previously for COS-7 cells.⁴⁹

Cell lysis

HEK293T cells were cultured with the method described above to 80-90% confluency, and were detached from the culture dishes by trypsin treatment after which some DMEM medium was added. The cells were collected by pipetting and DMEM medium was removed by centrifuging. The cells were washed 3 times with cold PBS (phosphate-buffered saline), after which they were centrifuged to remove PBS and lysed in potassium phosphate buffer for immediate use by sonication on ice with a sonicator. After sonication, lysed mixtures were centrifuged at 10,000 $\times g$ for 3 min at 4°C, and the supernatants containing the retaining β -glucosidase activities were used for experiments.

Zebrafish maintaining and homogenization

As earlier described⁵⁰, zebrafish embryos and larvae were kept at a constant temperature of 28.5 °C. Embryos and larvae were raised in egg water (60 $\mu\text{g}\cdot\text{L}^{-1}$ sea salt, Sera Marin). Synchronized wild-type ABTL zebrafish embryos were acquired after fertilizing adult female zebrafish (> 3 months old). Larvae were homogenized by using potassium phosphate buffer and a sonicator.

Enzyme activity assays using 4MU fluorogenic substrate

All assays were performed with either recombinant GBA1 or lysates of HEK293T cells or zebrafish larvae in 96-well plates at 37 °C. Samples were diluted with McIlvaine buffer (150 mM citric acid- Na_2HPO_4) to a final volume of 25 μL , at pH appropriate for each enzyme. Assays were performed by incubating the samples with 100 μL 4-methylumbelliferyl- β -D-glucopyranoside substrate diluted in McIlvaine buffer (with 0.1% (w/v) bovine serum albumin (BSA)) for a period of 30 min. The substrate mixtures used for each enzyme were as follows: GBA1: 3.75 mM 4-MU- β -D-glucopyranoside at pH 5.2, supplemented with 0.2% (w/v) sodium taurocholate, 0.1% (v/v) Triton X-100, 0.1% (w/v) bovine serum albumin (BSA); GBA2: 3.75 mM 4 MU- β -D-glucopyranoside at pH 5.8; GBA3: 3.75 mM 4-MU- β -D-glucopyranoside at pH 6.0. After stopping the enzyme reaction with 200 μL 1M NaOH-glycine (pH 10.3), 4-methylumbelliferone fluorescence was measured with a fluorimeter LS55 (Perkin Elmer, Waltham, MA, USA) with λ_{EX} 366 nm and λ_{EM} 445 nm. Enzyme activities were determined by subtraction of the background signal (measured for incubations without enzyme).

The IC_{50} values were determined using fluorogenic substrate assays. For GBA1, 3.16 ng (53 fmol) of rhGBA1 was prepared in 12.5 μL McIlvaine buffer (150 mM, pH 5.2) supplemented

with 0.1 % (v/v) Triton X-100, and 0.2 % (w/v) sodium taurocholate, 0.1% (w/v) bovine serum albumin (BSA). The enzyme was incubated with 12.5 μ L of inhibitors diluted in McIlvaine buffer (150 mM, pH 5.2) at 37 °C for 30 min or 3 h. For GBA2, lysate of GBA1/GBA2 KO HEK293T cells overexpressing GBA2 was prepared in 12.5 μ L McIlvaine buffer (150 mM, pH 5.8) and incubated with 12.5 μ L of inhibitors diluted in McIlvaine buffer (150 mM, pH 5.8) at 37 °C for 30 min or 3 h. For GBA3, lysate of GBA1/GBA2 KO HEK293T cells overexpressing GBA3 was prepared in 12.5 μ L McIlvaine buffer (150 mM, pH 6.0) and incubated with 12.5 μ L of inhibitors diluted in McIlvaine buffer (150 mM, pH 6.0) at 37 °C for 30 min or 3 h. The enzymatic activities of GBA1, GBA2 and GBA3 were measured as described above. The IC₅₀ value was calculated using Graphpad Prism 8.0 with the Nonlinear regression (curve fit) - [Inhibitor] vs. response - Variable slope (four parameters) equation as earlier description.³⁷

Activity-based protein profiling (ABPP) with SDS-PAGE

Samples containing GBA1, GBA2 or GBA3 (see above for the exact constitution of these samples) were incubated with excess fluorescent ABPs at optimized conditions. ABPP assays were performed at 37 °C for 30 min if not otherwise stated, in a total sample volume of 20-40 μ L and 0.5-1 % final concentration of DMSO. For ABPP of recombinant GBA1 (Imiglucerase), samples containing recombinant GBA1 were treated with either 200 nM β -glucose-configured epoxide ABP **9** or aziridine ABP **10** in McIlvaine buffer (150 mM, pH 5.2, 0.1 % (v/v) Triton X-100, 0.2 % (w/v) sodium taurocholate). For ABPP of samples containing GBA1 and GBA2, such as HEK293T cell lysates containing endogenous GBA1 and overexpressed GBA2, or zebrafish larvae homogenates containing endogenous GBA1 and GBA2, samples were treated with 200 nM ABP **10** in McIlvaine buffer (150 mM, pH 5.8). For ABPP of HEK293T cell lysates containing endogenous GBA1 and overexpressed GBA2/GBA3, samples were treated with 200 nM ABP **10** in McIlvaine buffer (150 mM, pH 6.0). For testing reactivity of β -xylo-cyclophellitol aziridine ABP **6** or **8** towards β -glucosidases (GBA1/GBA2/GBA3), ABP **6**, **8** and cyclophellitol configured ABP **9**, **10** (for comparison) with varying concentrations were incubated with HEK293T cell lysates containing endogenous GBA1 and overexpressed GBA2/GBA3 in McIlvaine buffer (150 mM, pH 6.0). For competitive ABPP, HEK293T cell lysates containing endogenous GBA1 and overexpressed GBA2/GBA3 were first treated with inhibitors (**1-5**, **13**, **14**) in McIlvaine buffer (150 mM, pH 6.0), following incubation with ABP **10** to reveal residual active β -glucosidases. After incubation with ABP, samples were boiled in 5 \times Laemmli buffer (50 % (v/v) 1 M Tris-HCl, pH 6.8, 50 % (v/v) 100 % glycerol, 10 % (w/v) DTT, 10 % (w/v) SDS, 0.01 % (w/v) bromophenol blue) for 5 min at 98 °C, and separated by gel electrophoresis on 10 % (w/v) SDS-PAGE gels running continuously at 90V for 1-1.5 h. Wet gel slabs were scanned for fluorescence using the Typhoon FLA 9500 (GE Healthcare) at λ_{EX} 473 nm and $\lambda_{EM} \geq 510$ nm for fluorescent ABP **8**; and at λ_{EX} 635 nm and $\lambda_{EM} \geq 665$ nm for fluorescent ABP **6**, **9** and **10**. ABP-emitted fluorescence was quantified using ImageQuant software (GE Healthcare, Chicago, IL, USA) and curve-fitted using Prism 8.0 (GraphPad Software). After fluorescence scanning, SDS-PAGE gels were stained for loading control of proteins with Coomassie G250 and scanned on a ChemiDoc MP imager (Bio-Rad, Hercules, CA, USA).²⁵

Assessment of inhibitor activity in cultured cells

Confluent HEK293T expressing human GBA1 and overexpressing both GBA2 and GBA3 were cultured in 24-well plates in triplicates with or without inhibitors for 24 h at 37 °C under 7% CO₂. Next, cells were washed three times with PBS, subsequently lysed in potassium phosphate buffer (with 2.5 U/ mL Benzonase® nuclease), the thus obtained samples were incubated for 30 min on ice (for degradation of DNA and RNA by Benzonase® nuclease), aliquoted, and used. After determination of the protein concentration, lysates containing equal protein amount (4–8 µg total protein per measurement) were adjusted to 4 µL with potassium phosphate buffer and subjected to residual activity measurements and/or detection of remaining active enzyme molecules using ABP labelling (n = 3 biological replicates).

Inhibition of enzymes in zebrafish larvae

Experiments were performed with 5 dpf (days post fertilization) larvae. For inhibitor treatment, a single fertilized embryo was seeded in a well of a 96-wells plate and exposed to 200 µL inhibitor with varying concentrations in egg water (60 µg·L⁻¹ sea salt) for 115 hours at 28.5 °C. Per condition, n = 24 embryos were used. At 115 hours, larvae were collected, rinsed three times with egg water, fully aspirated, snap-frozen in liquid nitrogen and homogenized in 96 µL 25 mM potassium phosphate buffer per 24 individuals. Lysis was conducted by sonication on ice with a sonicator at 20% power, three times for three seconds. Samples containing 5-20 µg total protein were used for ABPP assays.

Sphingolipid extraction and analysis by mass spectrometry in inhibitor treated zebrafish larvae

Zebrafish embryos were seeded in 96-well plates (1 fish embryo/well, 200 µL egg water/well) and treated with inhibitors at various concentrations for 103 hours at 28.5 °C. Thereafter, zebrafish larvae were washed three times with egg water, and collected in clean snap-cap Eppendorf tubes. Lipids were extracted and measured according to the methods below which were adapted from the literature.⁵⁰ Briefly, after removing the supernatant, 20 µL of ¹³C-GlcSph (0.1 pmol/ µL⁻¹ in MeOH), 480 µL MeOH, and 250 µL CHCl₃ were added to the sample. The samples were then stirred, left for 30 min at RT, sonicated (5 x 1 min in sonication water bath) and centrifuged for 10 min at 15,700 rpm. Supernatant was collected in a clean tube, and 250 µL CHCl₃ and 450 µL 100 mM formate buffer (pH 3.2) were added. The samples were stirred and centrifuged, after which the upper phase was transferred to a clean tube. The lower phase was extracted with 500 µL MeOH and 450 µL formate buffer. The upper phases were pooled and taken to dryness in a vacuum concentrator at 45 °C. The residue was extracted with 700 µL butanol and 700 µL water, stirred and centrifuged. The upper phase (butanol phase) was dried and the residue dissolved in 100 µL MeOH. 10 µL of this sample was used for LC-MS-mediated lipid detection and identification.⁵¹ Two-tailed unpaired t-test was performed in Prism 8.0 software (GraphPad) to determine statistical significance; *p* value <0.05 was considered significant.

References

1. J. M. Aerts, C. L. Kuo, L. T. Lelieveld, D. E. C. Boer, M. J. C. van der Lienden, H. S. Overkleeft and M. Artola, Glycosphingolipids and lysosomal storage disorders as illustrated by gaucher disease, *Curr. Opin. Chem. Biol.*, 2019, **53**, 204-215.
2. J. M. Aerts, M. Artola, M. van Eijk, M. J. Ferraz and R. G. Boot, Glycosphingolipids and infection: potential new therapeutic avenues, *Front. Cell Dev. Biol.*, 2019, **7**, 324.
3. M. J. Ferraz, A. R. Marques, M. D. Appelman, M. Verhoek, A. Strijland, M. Mirzaian, S. Scheij, C. M. Ouairy, D. Lahav, P. Wisse, H. S. Overkleeft, R. G. Boot and J. M. Aerts, Lysosomal glycosphingolipid catabolism by acid ceramidase: formation of glycosphingoid bases during deficiency of glycosidases, *FEBS Lett.*, 2016, **590**, 716-725.
4. N. Dekker, L. van Dussen, C. E. Hollak, H. Overkleeft, S. Scheij, K. Ghauharali, M. J. van Breemen, M. J. Ferraz, J. E. Groener, M. Maas, F. A. Wijburg, D. Speijer, A. Tytki-Szymanska, P. K. Mistry, R. G. Boot and J. M. Aerts, Elevated plasma glucosylsphingosine in Gaucher disease: relation to phenotype, storage cell markers, and therapeutic response, *Blood*, 2011, **118**, 118-127.
5. V. Murugesan, W. L. Chuang, J. Liu, A. Lischuk, K. Kacena, H. Lin, G. M. Pastores, R. Yang, J. Keutzer, K. Zhang and P. K. Mistry, Glucosylsphingosine is a key biomarker of Gaucher disease, *Am. J. Hematol.*, 2016, **91**, 1082-1089.
6. A. Rolfs, A. K. Giese, U. Grittner, D. Mascher, D. Elstein, A. Zimran, T. Bottcher, J. Lukas, R. Hubner, U. Golnitz, A. Rohle, A. Dudesek, W. Meyer, M. Wittstock and H. Mascher, Glucosylsphingosine is a highly sensitive and specific biomarker for primary diagnostic and follow-up monitoring in Gaucher disease in a non-Jewish, Caucasian cohort of Gaucher disease patients, *PLoS One*, 2013, **8**, e79732.
7. M. van Eijk, M. J. Ferraz, R. G. Boot and J. M. Aerts, Lyso-glycosphingolipids: presence and consequences, *Essays Biochem.*, 2020, **64**, 565-578.
8. E. Sidransky, M. A. Nalls, J. O. Aasly, J. Aharon-Peretz, G. Annesi, E. R. Barbosa, A. Bar-Shira, D. Berg, J. Bras, A. Brice, C. M. Chen, L. N. Clark, C. Condroyer, E. V. De Marco, A. Durr, M. J. Eblan, S. Fahn, M. J. Farrer, H. C. Fung, Z. Gan-Or, T. Gasser, R. Gershoni-Baruch, N. Giladi, A. Griffith, T. Gurevich, C. Januario, P. Kropp, A. E. Lang, G. J. Lee-Chen, S. Lesage, K. Marder, I. F. Mata, A. Mirelman, J. Mitsui, I. Mizuta, G. Nicoletti, C. Oliveira, R. Ottman, A. Orr-Urtreger, L. V. Pereira, A. Quattrone, E. Rogaeva, A. Rolfs, H. Rosenbaum, R. Rozenberg, A. Samii, T. Samaddar, C. Schulte, M. Sharma, A. Singleton, M. Spitz, E. K. Tan, N. Tayebi, T. Toda, A. R. Troiano, S. Tsuji, M. Wittstock, T. G. Wolfsberg, Y. R. Wu, C. P. Zabetian, Y. Zhao and S. G. Ziegler, Multicenter analysis of glucocerebrosidase mutations in Parkinson's disease, *N. Engl. J. Med.*, 2009, **361**, 1651-1661.
9. Y. V. Taguchi, J. Liu, J. Ruan, J. Pacheco, X. Zhang, J. Abbasi, J. Keutzer, P. K. Mistry and S. S. Chandra, Glucosylsphingosine promotes alpha-synuclein pathology in mutant GBA-associated Parkinson's disease, *J. Neurosci.*, 2017, **37**, 9617-9631.
10. M. P. Srikanth, J. W. Jones, M. Kane, O. Awad, T. S. Park, E. T. Zambidis and R. A. Feldman, Elevated glucosylsphingosine in Gaucher disease induced pluripotent stem cell neurons deregulates lysosomal compartment through mammalian target of rapamycin complex 1, *Stem Cells Transl. Med.*, 2021, DOI: 10.1002/sctm.20-0386.

11. J. M. Aerts, C. E. Hollak, R. G. Boot, J. E. Groener and M. Maas, Substrate reduction therapy of glycosphingolipid storage disorders, *J. Inherit. Metab. Dis.*, 2006, **29**, 449-456.
12. Phase 1/2 Lentiviral Vector Gene Therapy - The GuardOne Trial of AVR-RD-02 for Subjects With Type 1 Gaucher Disease, <https://clinicaltrials.gov/ct2/show/NCT04145037>).
13. Phase 1/2 Clinical Trial of PR001 in Infants With Type 2 Gaucher Disease (PROVIDE), <https://clinicaltrials.gov/ct2/show/NCT04411654>).
14. C. L. Kuo, E. van Meel, K. Kytidou, W. W. Kallemeijn, M. Witte, H. S. Overkleeft, M. Artola and J. M. Aerts, Activity-based probes for glycosidases: profiling and other applications, *Methods Enzymol.*, 2018, **598**, 217-235.
15. S. Atsumi, C. Nosaka, H. Iinuma and K. Umezawa, Inhibition of glucocerebrosidase and induction of neural abnormality by cyclophellitol in mice, *Arch. Biochem. Biophys.*, 1992, **297**, 362-367.
16. M. D. Witte, W. W. Kallemeijn, J. Aten, K. Y. Li, A. Strijland, W. E. Donker-Koopman, A. M. van den Nieuwendijk, B. Bleijlevens, G. Kramer, B. I. Florea, B. Hooibrink, C. E. Hollak, R. Ottenhoff, R. G. Boot, G. A. van der Marel, H. S. Overkleeft and J. M. Aerts, Ultrasensitive in situ visualization of active glucocerebrosidase molecules, *Nat. Chem. Biol.*, 2010, **6**, 907-913.
17. L. Premkumar, A. R. Sawkar, S. Boldin-Adamsky, L. Toker, I. Silman, J. W. Kelly, A. H. Futerman and J. L. Sussman, X-ray structure of human acid-beta-glucosidase covalently bound to conduritol-B-epoxide. Implications for Gaucher disease, *J. Biol. Chem.*, 2005, **280**, 23815-23819.
18. A. Vardi, H. Zigdon, A. Meshcheriakova, A. D. Klein, C. Yaacobi, R. Eilam, B. M. Kenwood, A. A. Rahim, G. Massaro, A. H. Merrill, Jr., E. B. Vitner and A. H. Futerman, Delineating pathological pathways in a chemically induced mouse model of Gaucher disease, *J. Pathol.*, 2016, **239**, 496-509.
19. Y. Kacher, B. Brumshtein, S. Boldin-Adamsky, L. Toker, A. Shainskaya, I. Silman, J. L. Sussman and A. H. Futerman, Acid beta-glucosidase: insights from structural analysis and relevance to Gaucher disease therapy, *Biol. Chem.*, 2008, **389**, 1361-1369.
20. L. G. Kanfer, J. Sullivan, S. S. Raghavan and R. A. Mumford, The Gaucher mouse, *Biochem. Biophys. Res. Commun.*, 1975, **67**, 85-90.
21. A. B. Manning-Bog, B. Schule and J. W. Langston, Alpha-synuclein-glucocerebrosidase interactions in pharmacological Gaucher models: a biological link between Gaucher disease and parkinsonism, *Neurotoxicology*, 2009, **30**, 1127-1132.
22. Y. H. Xu, Y. Sun, H. Ran, B. Quinn, D. Witte and G. A. Grabowski, Accumulation and distribution of alpha-synuclein and ubiquitin in the CNS of Gaucher disease mouse models, *Mol. Genet. Metab.*, 2011, **102**, 436-447.
23. E. M. Rocha, G. A. Smith, E. Park, H. Cao, A. R. Graham, E. Brown, J. R. McLean, M. A. Hayes, J. Beagan, S. C. Izen, E. Perez-Torres, P. J. Hallett and O. Isacson, Sustained systemic glucocerebrosidase inhibition induces brain alpha-synuclein aggregation, microglia and complement C1q activation in mice, *Antioxid. Redox Signal.*, 2015, **23**, 550-564.

24. S. G. Withers and K. Umezawa, Cyclophellitols: A naturally occurring mechanism-based inactivator of beta-glucosidases, *Biochem. Biophys. Res. Commun.*, 1991, **177**, 532-537.
25. W. W. Kallemijn, K. Y. Li, M. D. Witte, A. R. Marques, J. Aten, S. Scheij, J. Jiang, L. I. Willems, T. M. Voorn-Brouwer, C. P. van Roomen, R. Ottenhoff, R. G. Boot, H. van den Elst, M. T. Walvoort, B. I. Florea, J. D. Codée, G. A. van der Marel, J. M. Aerts and H. S. Overkleeft, Novel activity-based probes for broad-spectrum profiling of retaining beta-exoglucosidases in situ and in vivo, *Angew. Chem. Int. Ed.*, 2012, **51**, 12529-12533.
26. L. Wu, Z. Armstrong, S. P. Schröder, C. de Boer, M. Artola, J. M. Aerts, H. S. Overkleeft and G. J. Davies, An overview of activity-based probes for glycosidases, *Curr. Opin. Chem. Biol.*, 2019, **53**, 25-36.
27. D. Herrera Moro Chao, W. W. Kallemijn, A. R. Marques, M. Orre, R. Ottenhoff, C. van Roomen, E. Foppen, M. C. Renner, M. Moeton, M. van Eijk, R. G. Boot, W. Kamphuis, E. M. Hol, J. Aten, H. S. Overkleeft, A. Kalsbeek and J. M. Aerts, Visualization of active glucocerebrosidase in rodent brain with high spatial resolution following *in situ* labeling with fluorescent activity based probes, *PLoS One*, 2015, **10**, e0138107.
28. E. van Meel, E. Bos, M. J. C. van der Lienden, H. S. Overkleeft, S. I. van Kasteren, A. J. Koster and J. M. Aerts, Localization of active endogenous and exogenous beta-glucocerebrosidase by correlative light-electron microscopy in human fibroblasts, *Traffic*, 2019, **20**, 346-356.
29. W. W. Kallemijn, K. Y. Li, M. D. Witte, A. R. Marques, J. Aten, S. Scheij, J. Jiang, L. I. Willems, T. M. Voorn-Brouwer, C. P. van Roomen, R. Ottenhoff, R. G. Boot, H. van den Elst, M. T. Walvoort, B. I. Florea, J. D. Codée, G. A. van der Marel, J. M. Aerts and H. S. Overkleeft, Novel activity-based probes for broad-spectrum profiling of retaining beta-exoglucosidases in situ and in vivo, *Angew. Chem. Int. Ed.*, 2012, **51**, 12529-12533.
30. H. Akiyama, S. Kobayashi, Y. Hirabayashi and K. Murakami-Murofushi, Cholesterol glucosylation is catalyzed by transglucosylation reaction of beta-glucosidase 1, *Biochem. Biophys. Res. Commun.*, 2013, **441**, 838-843.
31. A. R. Marques, M. Mirzaian, H. Akiyama, P. Wisse, M. J. Ferraz, P. Gaspar, K. Ghauharali-van der Vlugt, R. Meijer, P. Giraldo, P. Alfonso, P. Irun, M. Dahl, S. Karlsson, E. V. Pavlova, T. M. Cox, S. Scheij, M. Verhoek, R. Ottenhoff, C. P. van Roomen, N. S. Pannu, M. van Eijk, N. Dekker, R. G. Boot, H. S. Overkleeft, E. Blommaart, Y. Hirabayashi and J. M. Aerts, Glucosylated cholesterol in mammalian cells and tissues: formation and degradation by multiple cellular beta-glucosidases, *J. Lipid Res.*, 2016, **57**, 451-463.
32. D. E. C. Boer, M. Mirzaian, M. J. Ferraz, A. Nadaban, A. Schreuder, A. Hovnanian, J. van Smeden, J. A. Bouwstra and J. M. Aerts, Glucosylated cholesterol in skin: synthetic role of extracellular glucocerebrosidase, *Clin. Chim. Acta.*, 2020, **510**, 707-710.
33. D. E. Boer, M. Mirzaian, M. J. Ferraz, K. C. Zwiers, M. V. Baks, M. D. Hazeu, R. Ottenhoff, A. R. A. Marques, R. Meijer, J. C. P. Roos, T. M. Cox, R. G. Boot, N. Pannu, H. S. Overkleeft, M. Artola and J. M. Aerts, Human glucocerebrosidase mediates formation of xylosyl-cholesterol by beta-xylosidase and transxylosidase reactions, *J. Lipid Res.*, 2021, **62**, 100018.
34. R. A. Ashmus, D. L. Shen and D. J. Vocadlo, Fluorescence-quenched substrates for quantitative live cell imaging of glucocerebrosidase activity, *Methods Enzymol.*, 2018, **598**, 199-215.

35. M. C. Deen, C. Proceviat, X. Shan, L. Wu, D. L. Shen, G. J. Davies and D. J. Vocadlo, Selective fluorogenic beta-glucocerebrosidase substrates for convenient analysis of enzyme activity in cell and tissue homogenates, *ACS Chem. Biol.*, 2020, **15**, 824-829.
36. M. Artola, C. L. Kuo, L. T. Lelieveld, R. J. Rowland, G. A. van der Marel, J. D. C. Codée, R. G. Boot, G. J. Davies, J. M. Aerts and H. S. Overkleeft, Functionalized cyclophellitols are selective glucocerebrosidase inhibitors and induce a bona fide neuropathic gaucher model in zebrafish, *J. Am. Chem. Soc.*, 2019, **141**, 4214-4218.
37. C. L. Kuo, W. W. Kallemeyjn, L. T. Lelieveld, M. Mirzaian, I. Zoutendijk, A. Vardi, A. H. Futerman, A. H. Meijer, H. P. Spaink, H. S. Overkleeft, J. M. Aerts and M. Artola, *In vivo* inactivation of glycosidases by conduritol B epoxide and cyclophellitol as revealed by activity-based protein profiling, *FEBS J.*, 2019, **286**, 584-600.
38. S. P. Schröder, R. Petracca, H. Minnee, M. Artola, J. M. F. G. Aerts, J. D. C. Codée, G. A. van der Marel and H. S. Overkleeft, A divergent synthesis of L-arabino- and D-xylo-configured cyclophellitol epoxides and aziridines, *Eur. J. Org. Chem.*, 2016, **2016**, 4787-4794.
39. J. Jiang, C. L. Kuo, L. Wu, C. Franke, W. W. Kallemeyjn, B. I. Florea, E. van Meel, G. A. van der Marel, J. D. C. Codée, R. G. Boot, G. J. Davies, H. S. Overkleeft and J. M. Aerts, Detection of active mammalian GH31 alpha-glucosidases in health and disease using in-class, broad-spectrum activity-based probes, *ACS Cent. Sci.*, 2016, **2**, 351-358.
40. M. Artola, S. Wouters, S. P. Schröder, C. de Boer, Y. Chen, R. Petracca, A. van den Nieuwendijk, J. M. Aerts, G. A. van der Marel, J. D. C. Codée and H. S. Overkleeft, Direct stereoselective aziridination of cyclohexenols with 3-amino-2-(trifluoromethyl)quinazolin-4(3H)-one in the synthesis of cyclitol aziridine glycosidase inhibitors, *Eur. J. Org. Chem.*, 2019, **2019**, 1397-1404.
41. S. P. Schröder, C. de Boer, N. G. S. McGregor, R. J. Rowland, O. Moroz, E. Blagova, J. Reijngoud, M. Arentshorst, D. Osborn, M. D. Morant, E. Abbate, M. A. Stringer, K. Krogh, L. Raich, C. Rovira, J. G. Berrin, G. P. van Wezel, A. F. J. Ram, B. I. Florea, G. A. van der Marel, J. D. C. Codée, K. S. Wilson, L. Wu, G. J. Davies and H. S. Overkleeft, Dynamic and functional profiling of xylan-degrading enzymes in aspergillus secretomes using activity-based probes, *ACS Cent. Sci.*, 2019, **5**, 1067-1078.
42. J. Jiang, W. W. Kallemeyjn, D. W. Wright, A. van den Nieuwendijk, V. C. Rohde, E. C. Folch, H. van den Elst, B. I. Florea, S. Scheij, W. E. Donker-Koopman, M. Verhoek, N. Li, M. Schurmann, D. Mink, R. G. Boot, J. D. C. Codée, G. A. van der Marel, G. J. Davies, J. M. Aerts and H. S. Overkleeft, *In vitro* and *in vivo* comparative and competitive activity-based protein profiling of GH29 alpha-L-fucosidases, *Chem. Sci.*, 2015, **6**, 2782-2789.
43. G. Legler, Studies on the action mechanism of glycoside splitting anzymes, I. Presentation and properties of specific inhibitors, *Hoppe-Seyler's Zeitschrift für Physiologische Chemie*, 1966, **345**, 197-214.
44. M. Artola, L. Wu, M. J. Ferraz, C. L. Kuo, L. Raich, I. Z. Breen, W. A. Offen, J. D. C. Codée, G. A. van der Marel, C. Rovira, J. M. Aerts, G. J. Davies and H. S. Overkleeft, 1,6-Cyclophellitol cyclosulfates: a new class of irreversible glycosidase inhibitor, *ACS Cent. Sci.*, 2017, **3**, 784-793.
45. R. Charoenwattanasatien, S. Pengthaisong, I. Breen, R. Mutoh, S. Sansenya, Y. Hua, A. Tankrathok, L. Wu, C. Songsirithigul, H. Tanaka, S. J. Williams, G. J. Davies, G. Kurisu

- and J. R. Cairns, Bacterial beta-glucosidase reveals the structural and functional basis of genetic defects in human glucocerebrosidase 2 (GBA2), *ACS Chem. Biol.*, 2016, **11**, 1891-1900.
46. S. P. Schröder, C. de Boer, N. G. S. McGregor, R. J. Rowland, O. Moroz, E. Blagova, J. Reijngoud, M. Arentshorst, D. Osborn, M. D. Morant, E. Abbate, M. A. Stringer, K. Krogh, L. Raich, C. Rovira, J. G. Berrin, G. P. van Wezel, A. F. J. Ram, B. I. Florea, G. A. van der Marel, J. D. C. Codée, K. S. Wilson, L. Wu, G. J. Davies and H. S. Overkleeft, Dynamic and functional profiling of xylan-degrading enzymes in aspergillus secretomes using activity-based probes, *ACS Cent. Sci.*, 2019, **5**, 1067-1078.
 47. S. P. Schröder, J. W. van de Sande, W. W. Kallemeijn, C. L. Kuo, M. Artola, E. J. van Rooden, J. Jiang, T. J. M. Beenakker, B. I. Florea, W. A. Offen, G. J. Davies, A. J. Minnaard, J. Aerts, J. D. C. Codée, G. A. van der Marel and H. S. Overkleeft, Towards broad spectrum activity-based glycosidase probes: synthesis and evaluation of deoxygenated cyclophellitol aziridines, *Chem. Commun.*, 2017, **53**, 12528-12531.
 48. F. A. Ran, P. D. Hsu, J. Wright, V. Agarwala, D. A. Scott and F. Zhang, Genome engineering using the CRISPR-Cas9 system, *Nat. Protoc.*, 2013, **8**, 2281-2308.
 49. W. W. Kallemeijn, M. D. Witte, T. M. Voorn-Brouwer, M. T. Walvoort, K. Y. Li, J. D. C. Codée, G. A. van der Marel, R. G. Boot, H. S. Overkleeft and J. M. Aerts, A sensitive gel-based method combining distinct cyclophellitol-based probes for the identification of acid/base residues in human retaining beta-glucosidases, *J. Biol. Chem.*, 2014, **289**, 35351-35362.
 50. L. T. Lelieveld, M. Mirzaian, C. L. Kuo, M. Artola, M. J. Ferraz, R. E. A. Peter, H. Akiyama, P. Greimel, R. van den Berg, H. S. Overkleeft, R. G. Boot, A. H. Meijer and J. Aerts, Role of beta-glucosidase 2 in aberrant glycosphingolipid metabolism: model of glucocerebrosidase deficiency in zebrafish, *J. Lipid Res.*, 2019, **60**, 1851-1867.
 51. M. Artola, C. L. Kuo, L. T. Lelieveld, R. J. Rowland, G. A. van der Marel, J. D. C. Codée, R. G. Boot, G. J. Davies, J. Aerts and H. S. Overkleeft, Functionalized cyclophellitols are selective glucocerebrosidase inhibitors and induce a bona fide neuropathic gaucher model in zebrafish, *J. Am. Chem. Soc.*, 2019, **141**, 4214-4218.

Appendix

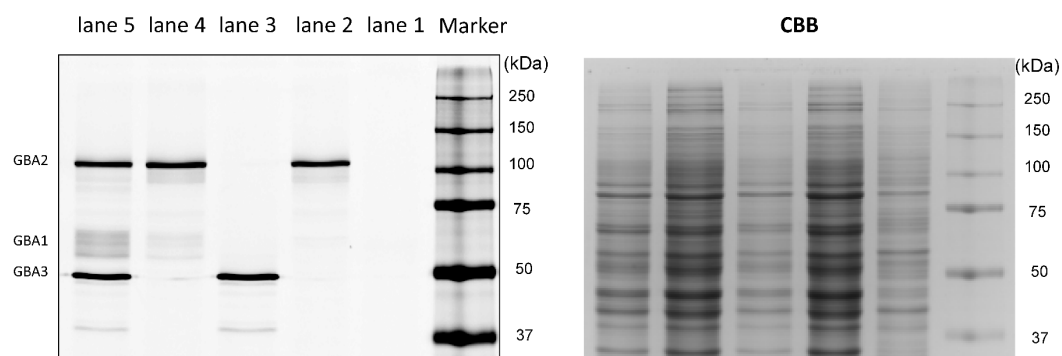


Figure S1. The HEK293T cell line lysates used for experiments. Lane 1, GBA1/GBA2 knock out; Lane 2, GBA1/GBA2 knock out with overexpressed GBA2; Lane 3, GBA1/GBA2 knock out with overexpressed GBA3; Lane 4, GBA1 (endogenous) with overexpressed GBA2; Lane 5, endogenous GBA1 with overexpressed GBA2/GBA3. The cell lysates were incubated with ABP **10** (30 min at pH 6) followed by SDS-PAGE and fluorescent scanning of the gel.

Table S1. *In vitro* apparent IC_{50} of cyclophellitol epoxide ABP **9**, cyclophellitol aziridine ABP **10**, α -xylo-configured epoxide **11** and aziridine **12**. The Inhibition curves are showed in Figure S2. ^[a]rhGBA1 = recombinant human GBA1 (Imiglucerase). ^[b]GBA2 = lysate of GBA1/GBA2 KO HEK293T cells with GBA2 overexpression. ^[c] GBA3 = lysate of GBA1/GBA2 KO HEK293T cells with GBA3 overexpression.

<i>in vitro</i> IC_{50}	rhGBA1 ^[a]	GBA2 ^[b]	GBA3 ^[c]	(Ratio) GBA2/ GBA1	(Ratio) GBA3/ GBA1
9	45.20 \pm 4.54 nM	> 5 μ M	5.78 \pm 0.08 μ M	> 111	128
10	8.10 \pm 1.94 nM	21.5 \pm 0.42 nM	8.54 \pm 1.18 nM	2.6	1
11	> 50 μ M	> 50 μ M	> 50 μ M	/	/
12	> 50 μ M	55.76 \pm 2.34 μ M	> 50 μ M	/	/

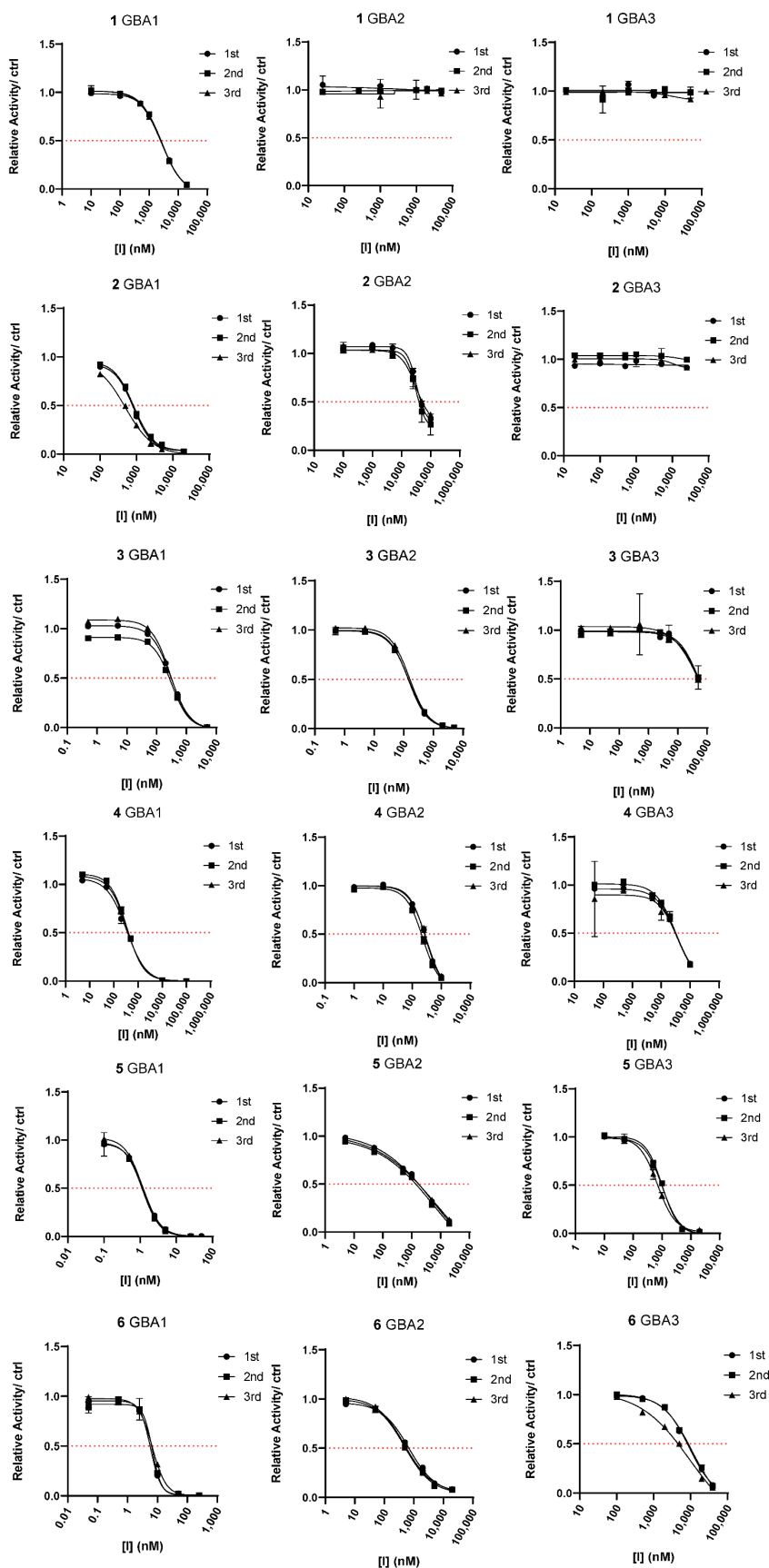


Figure S2 continued (1/3)

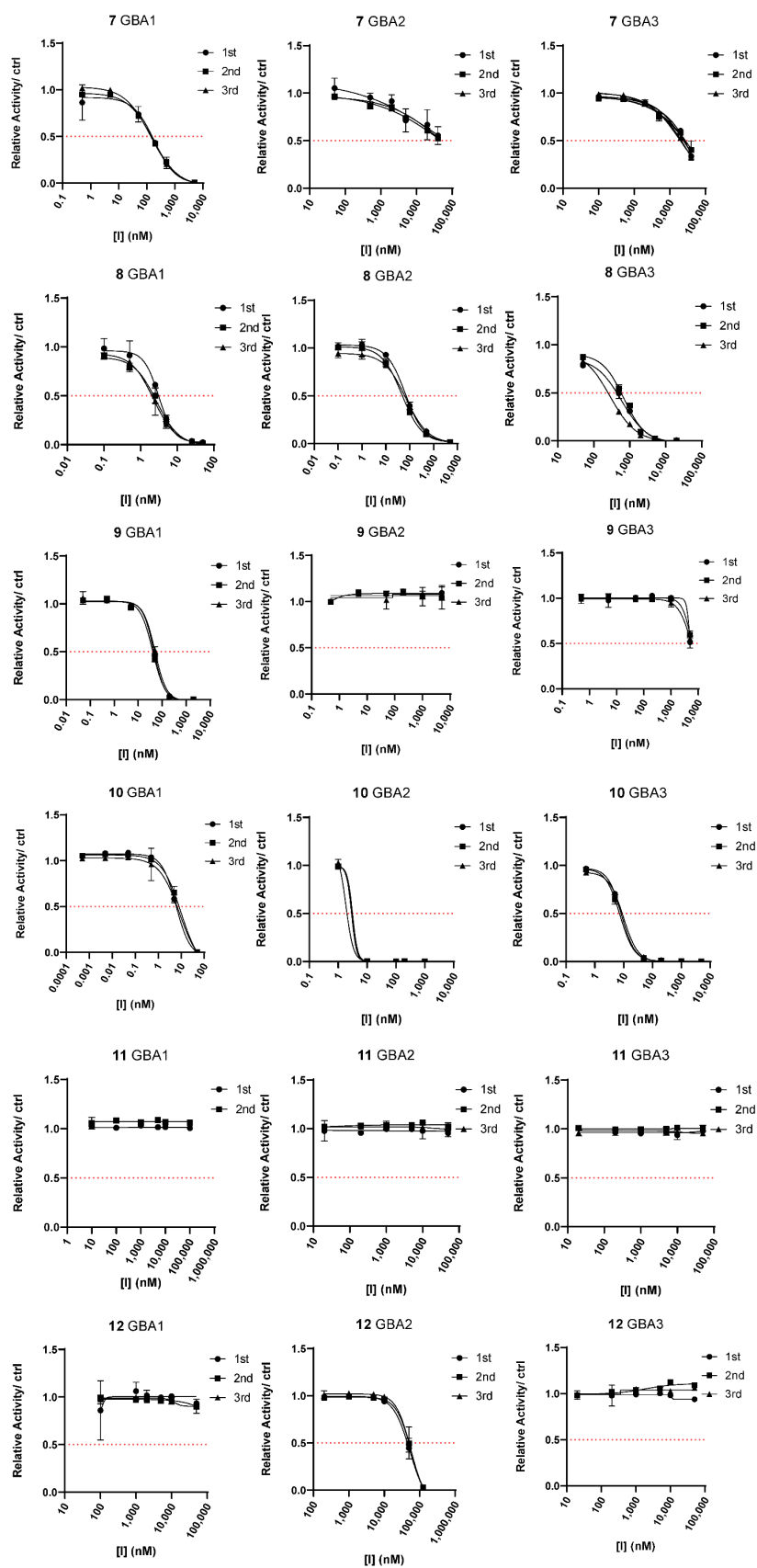


Figure S2 continued (2/3)

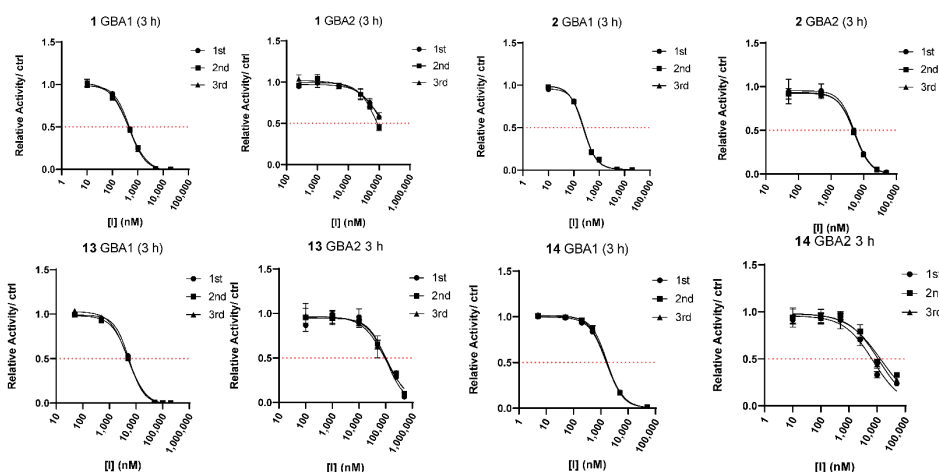


Figure S2. Apparent *In vitro* IC₅₀ curves of the different inhibitors (compounds **1-14**) as determined by activity measurements after incubation with the inhibitors. The enzymes used were recombinant GBA1 (Imiglucerase), lysates of GBA1/GBA2 KO cells with overexpression of either GBA2 or GBA3. Incubation time for enzyme with the inhibitors is 30 min (if not otherwise stated) or 3 h (marked as '3 h' in figure) at the appropriate pH.

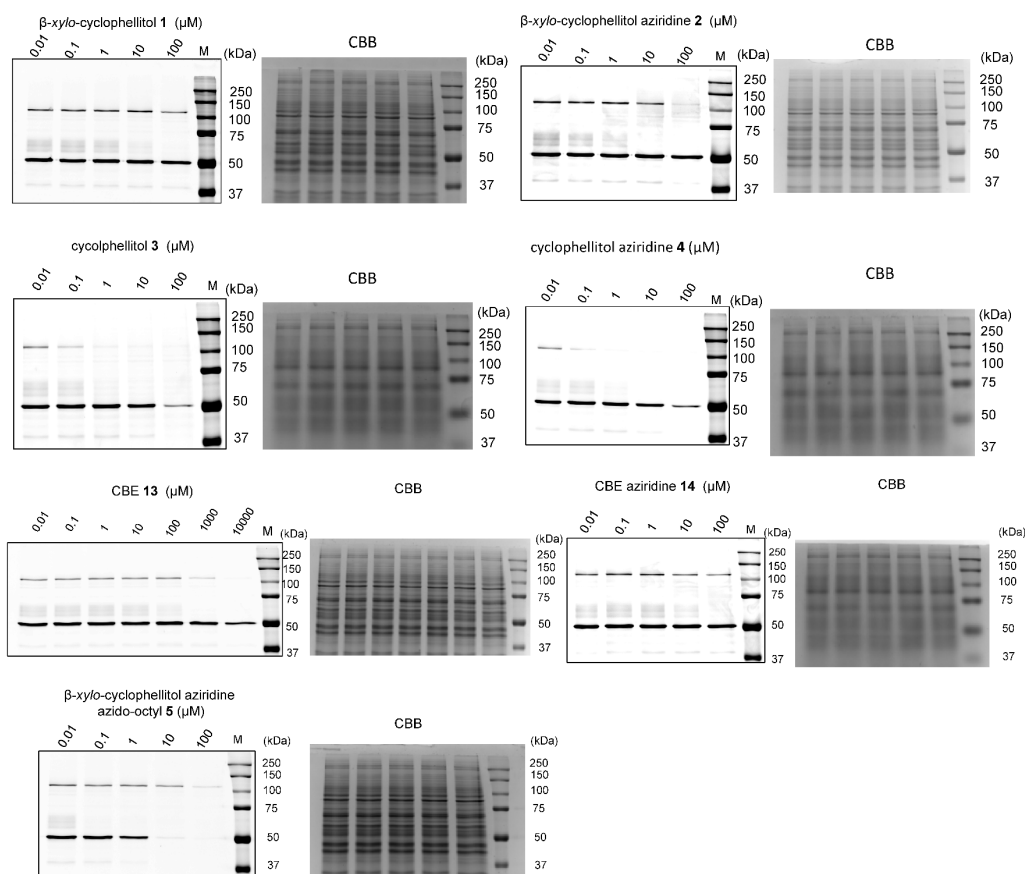


Figure S3. Competitive ABPP assay to visualize the inhibition of compounds (**1-5**, **13**, **14**) on HEK293T cell lysates (endogenous GBA1 with overexpressed GBA2/GBA3). Lysates were incubated with inhibitor for 30 min at 37°C *in vitro*, followed by labelling with ABP **10**, SDS-PAGE and fluorescent scanning of the gels. Coomassie brilliant blue staining (CBB) was performed as a loading control.

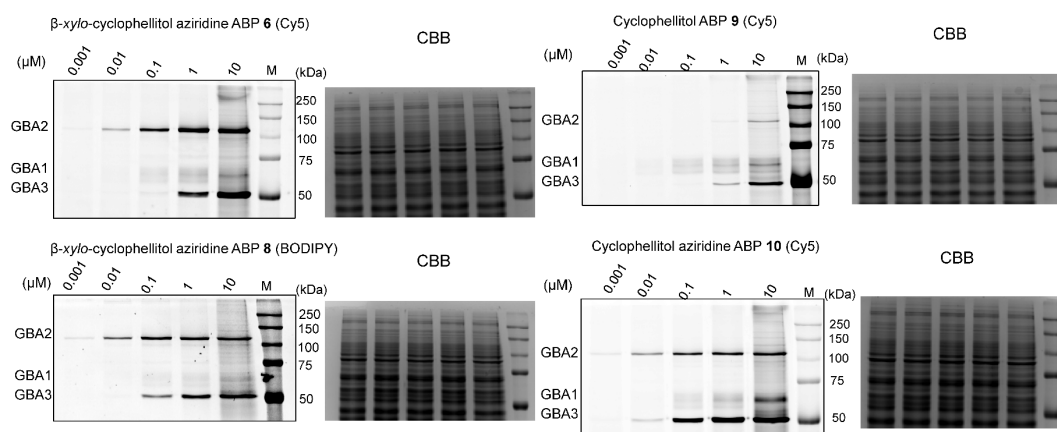


Figure S4. Lysates of HEK293T cells (endogenous GBA1 with overexpressed GBA2/GBA3) were incubated with indicated ABPs (**6**, **8**, **9** or **10**) for 30 min at pH 6.0 *in vitro*. ABP-labelled proteins were visualized after SDS-PAGE by fluorescence scanning of the gels. Coomassie brilliant blue staining (CBB) was performed as a loading control.

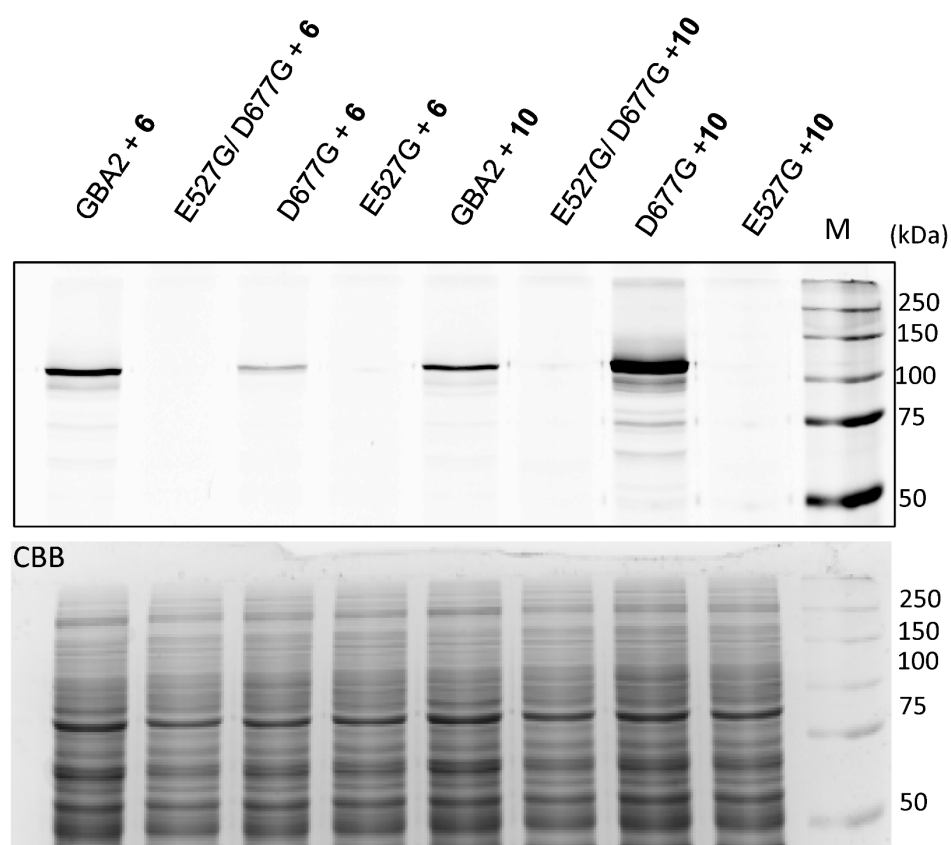


Figure S5. Lysates of HEK293T cells with overexpressed GBA2 variants (either WT, catalytic nucleophile mutant (E527G), catalytic acid/base mutant (D677G) or the double mutant (E527G/D677G)) were incubated with ABP **6** or **10** *in vitro*. ABP-labelled proteins were visualized after SDS-PAGE by fluorescence scanning of the gels. Coomassie brilliant blue staining (CBB) was performed as a loading control.

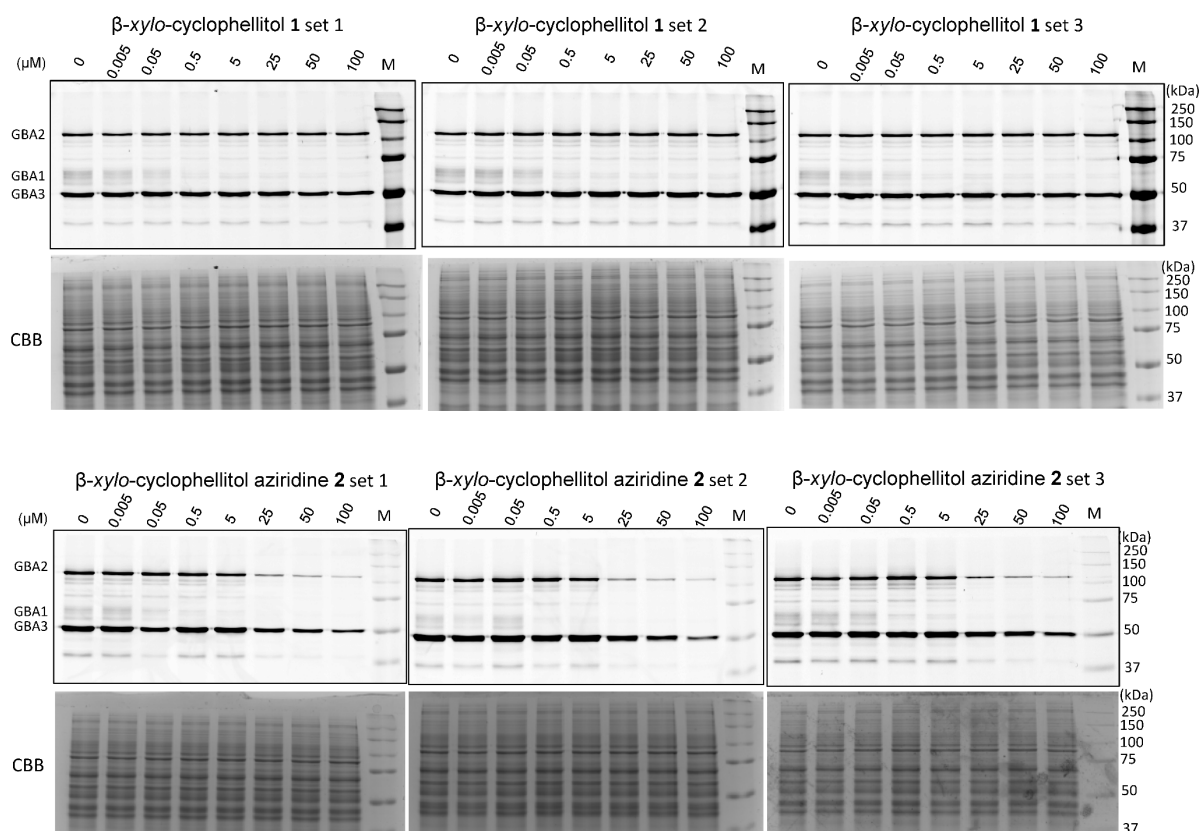


Figure S6. Live cell *in situ* inhibition using β -xylo-cyclophellitol epoxide **1** and aziridine **2** in intact HEK293T cells (expressing endogenous GBA1 with overexpressed GBA2/GBA3) for 24 h. After the incubation the cells were harvested and lysed, followed by labelling with ABP **10** *in vitro*. ABP-labelled proteins were visualized after SDS-PAGE by fluorescence scanning of the gels. Coomassie brilliant blue staining (CBB) was performed as a loading control.

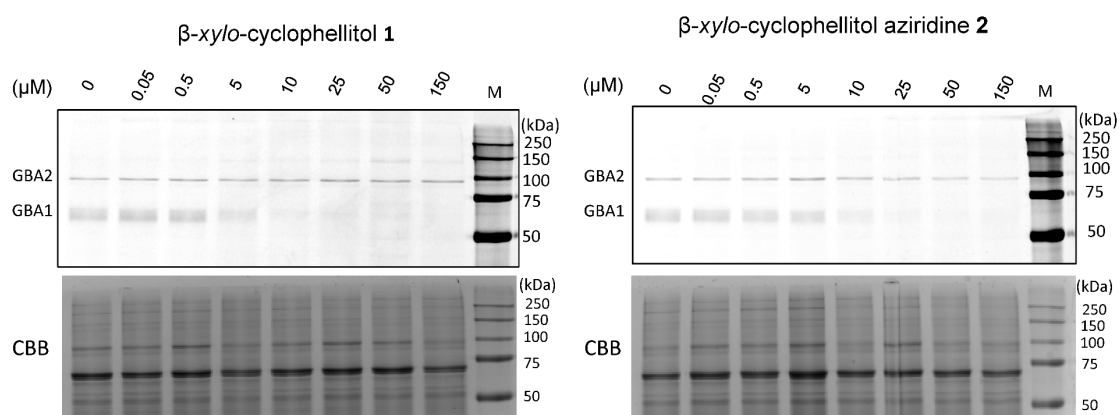
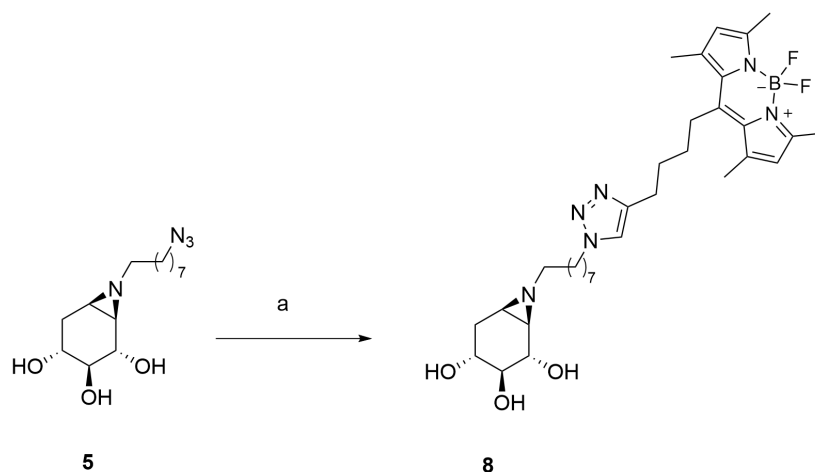


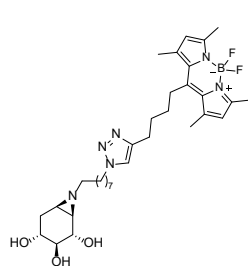
Figure S7. Live zebrafish larvae were incubated with β -xylo-cyclophellitol epoxide **1** or aziridine **2** for 5 days *in vivo*. The larvae were harvested, and the homogenate was labelled with ABP **10** *in vitro*. ABP-labelled proteins were visualized after SDS-PAGE by fluorescence scanning of the gels. Coomassie brilliant blue staining (CBB) was performed as a loading control.



Scheme S1. Synthesis of β -D-xylo-cyclophellitol aziridine BODIPY-FL ABP **8**. Reagents and conditions: a) BODIPY tag-alkyne, CuSO_4 , sodium ascorbate, DMF/ H_2O , rt, 16 h, 58% yield.

β -D-Xylo-cyclophellitol aziridine BODIPY-FL ABP **8**

Compound **5**¹ (4.4 mg, 14.7 μmol) was dissolved in degassed DMF (0.2 mL), then alkyne-BODIPY (1.1 eq), CuSO_4 (0.2 eq) and sodium ascorbate (0.4 eq) were added and the mixture stirred at rt for 16 h. The reaction mixture was concentrated and purified by semi-preparative reversed phase HPLC (linear gradient. Solutions used: A: 50 mM NH_4HCO_3 in H_2O , B: acetonitrile) yielding the desired product as an orange powder (5.4 mg, 58%).



^1H NMR (500 MHz, CD_3OD): δ 7.73 (s, 1H), 6.11 (s, 2H), 4.35 (t, J = 6.9 Hz, 2H), 3.60 (d, J = 8.0 Hz, 1H), 3.38 (m, 1H), 3.05 (dd, J = 9.8, 8.0 Hz, 1H), 3.03 – 2.98 (m, 2H), 2.78 (t, J = 7.2 Hz, 2H), 2.44 (s, 6H), 2.38 (s, 6H), 2.30 (dd, J = 13.1, 5.5 Hz, 1H), 2.20 (t, J = 7.3 Hz, 2H), 1.92 – 1.82 (m, 5H), 1.81 – 1.77 (m, 1H), 1.68 – 1.58 (m, 3H), 1.56 (d, J = 6.3 Hz, 1H), 1.54 – 1.48 (m, 2H), 1.35 – 1.20 (m, 7H) ppm. ^{13}C NMR (125 MHz, CD_3OD): δ 153.6, 147.2, 146.6, 140.8, 131.2, 122.0, 121.3, 77.8, 72.7, 66.8, 60.3, 49.9, 48.5, 44.0, 39.7, 32.1, 30.9, 29.9, 29.5, 29.1, 29.0, 28.5, 27.8, 26.8, 25.9, 24.6, 15.2, 13.1 ppm. HRMS (ESI) m/z : $[\text{M}+\text{H}]^+$ calculated for $\text{C}_{33}\text{H}_{49}\text{BF}_2\text{N}_6\text{O}_3$ 627.4000, found 627.4029.

Supplemental reference

1. S. P. Schröder, C. de Boer, N. G. S. McGregor, R. J. Rowland, O. Moroz, E. Blagova, J. Reijngoud, M. Arentshorst, D. Osborn, M. D. Morant, E. Abbate, M. A. Stringer, K. Krogh, L. Raich, C. Rovira, J. G. Berrin, G. P. van Wezel, A. F. J. Ram, B. I. Florea, G. A. van der Marel, J. D. C. Codée, K. S. Wilson, L. Wu, G. J. Davies and H. S. Overkleeft, Dynamic and functional profiling of xylan-degrading enzymes in aspergillus secretomes using activity-based probes, *ACS Cent. Sci.*, 2019, **5**, 1067-1078.

Chapter 3

Selective labelling of GBA2 in cells with fluorescent β -D-arabinofuranosyl cyclitol aziridines

Taken in part from:

Qin Su, Max Louwerse, Rob F. Lammers, Elmer Maurits, Max Janssen, Rolf G. Boot, Valentina Borlandelli, Wendy A. Offen, Daniël Linzel, Sybrin P. Schröder, Gideon J. Davies, Herman S. Overkleeft, Marta Artola, Johannes M. F. G. Aerts. *Chem. Sci.* doi.org/10.1039/D3SC06146A.

Abstract

GBA2, the non-lysosomal β -glucosylceramidase, is an enzyme involved in glucosylceramide metabolism. Pharmacological inhibition of GBA2 by *N*-alkyl iminosugars is well tolerated and benefits patients suffering from Sandhoff and Niemann-Pick type C diseases, and GBA2 inhibitors have been proposed as candidate-clinical drugs for the treatment of Parkinsonism. With the ultimate goal to unravel the role of GBA2 in (patho)physiology, this chapter describes the development of a GBA2-selective activity-based probe (ABP). A library of probes was tested for activity against GBA2 and the two other cellular retaining β -glucosidases, lysosomal GBA1 and cytosolic GBA3. It is shown that β -D-arabinofuranosyl cyclitol aziridine (β -D-Araf aziridine) reacts with the GBA2 active site nucleophile to form a covalent and irreversible bond. Fluorescent β -D-Araf aziridine probes potently and selectively label GBA2 both *in vitro* and *in situ*, allowing for visualization of subcellular localization of overexpressed GBA2 using fluorescence microscopy. The here-presented ABP technology may be useful for further delineating the role and functioning of GBA2 in disease. As well, the β -D-Araf aziridine scaffold may serve as a good starting point for the development of GBA2-specific inhibitors for clinical development.

Introduction

GBA2 (EC 3.2.1.45, CAZy¹ GH116), a retaining β -glucosidase, was first discovered during the analysis of N-[6-[(7-nitro-2-1,3-benzoxadiazol-4-yl)amino]hexanoyl]- β -D-glucosylceramide (NBD-GlcCer) processing in cultured cells. Ensuing studies demonstrated that GBA2, initially named non-lysosomal glucosylceramidase, is capable of hydrolyzing glucosylceramide (GlcCer), which until that date was thought to be the exclusive activity of the enzyme deficient in Gaucher disease (GD), lysosomal glucocerebrosidase (GBA1, EC 3.2.1.45, GH30).² GBA2 is now implicated in several inherited metabolic disorders.³⁻⁶ As well, companies have announced the development of GBA2 inhibitors for the treatment of Parkinsonism.⁷ Despite this, the physiological role of GBA2, the consequences of cytosolic GlcCer metabolism and the interplay of GBA2 with lysosomal GlcCer breakdown is unclear.

GBA2 is a tightly membrane-bound enzyme whose activity can be assessed in cell and tissue lysates using the artificial fluorogenic substrate, 4-methylumbelliferyl- β -D-glucopyranoside (4MU- β -D-Glc). Compared to GBA1, GBA2 is less sensitive to inactivation by conduritol B epoxide (CBE), but more susceptible to inactivation by various detergents.² The loss of enzymatic activity following its extraction from membranes complicates its purification, and the enzyme's identity was definitively elucidated only after the independent cloning of its cDNA.^{8,9} GBA2 homologues are found in several species, including archaea and bacteria,^{10,11} and GBA2 proteins degrading glucosylceramide are found, besides mammals, in plant and fish.¹²⁻¹⁵ To date mammalian GBA2 has defied resolution of a 3D structure, but structures of bacterial homologs (such as SSO1353 (GH116) in *S. solfataricus* and TxGH116 in *T. xylanolyticum*^{10,11,16}) provide insight in the catalytic machinery of the enzyme.

Human GBA2 is encoded by the *GBA2* gene at locus 9p13.3 and is a 927 amino acid β -glucosidase with E527 as the catalytic nucleophile and D677 as the catalytic acid/base.¹⁷ It is a retaining glycosidase processing its substrate following a classical Koshland double displacement mechanism. GBA2 is initially synthesized as a soluble cytosolic protein that rapidly and tightly associates with membranes by an unknown mechanism. Various subcellular localizations of (overexpressed, tagged) GBA2 have been reported, ranging from endoplasmic reticulum, Golgi apparatus, endosomes and the plasma membrane.^{9,18} The enzyme's localization possibly varies among cells, perhaps reflecting their metabolic status. Unlike GBA1, GBA2 is able to hydrolyze both β -glucoside and β -galactoside substrates.² GBA2 can also act as a transglycosidase, transferring glucose from GlcCer to, for instance, cholesterol, further adding to the mystery of the physiological role of GBA2.^{19,20}

GBA2 is increasingly considered as therapeutic target for the treatment of a variety of diseases. Inhibition of GBA2 is a side effect of *N*-butyl-deoxynojirimycin (Miglustat), a registered treatment for GBA1-deficient type 1 GD and Niemann Pick disease type C (NPC) patients. Miglustat acts by pharmacological inhibition of glucosylceramide synthase (GCS).²¹⁻²³ Individuals under this treatment appear to develop no overt side effects upon long-term therapy. In line with this, inhibition of GBA2 activity with *N*-adamantanemethyloxypentyl-deoxynojirimycin (AMP-DMN) or its genetic ablation has been found to increase the life span of NPC mice.²² Tissues of NPC mice show partial increase in GBA2 and partial reduced GBA1 levels suggesting a compensatory mechanism between these enzymes.¹⁵ In type 1 GD mice generated by knockdown of GBA1 in a hematopoietic stem cell lineage, GBA2 gene deletion was found to exert beneficial effects.²⁴ In addition, increased GBA2 activities have been documented in leukocytes of GBA1-deficient GD patients.²⁵ Finally and importantly, GBA2 knockout (KO) mice develop no overt pathology besides partially reduced fertility, a phenomenon not observed in primates.^{10,26}

Several classes of GBA2 inhibitors have been identified in the past decades. Competitive GBA2 inhibitors include iminosugars such as AMP-DMN, with an IC₅₀ of approximately 1 nM with respect to GBA2, and *N*-butyl-deoxynojirimycin (Miglustat), with an IC₅₀ of 150-300 nM for GBA2.²⁷ Mechanism-based, covalent and irreversible inhibitors, such as cyclophellitol aziridine act on GBA2 but also on GBA1, and activity-based probes (ABPs) derived from these cannot be used for selective GBA2 detection and imaging in cells.²⁸

For this reason the aim was to develop a GBA2-selective activity-based probe for *in cellulo* GBA2 imaging, and the results of studies in this direction are presented here.²⁹ Previous studies showed the

value of cyclophellitols as GBA1-specific probes,^{15,30} however the closely related cyclophellitol aziridine ABPs (ABP **7** and **8**, Figure 1) label both GBA1 and GBA2.^{28,31} Some cell types also express a soluble, cytosolic β -glucosidase with broad substrate specificity, termed GBA3 (EC 3.2.1.21, GH1), which also reacts with these ABPs.²⁸ Since none of these ABPs react selectively with GBA2, cyclophellitol-type compounds with varying configurations were investigated on their reactivity with GBA2 and related cellular retaining β -glucosidases. The findings of these studies, detailed in this chapter, demonstrate that ABPs with a β -D-Araf aziridine configuration (Figure 1) potently and selectively label GBA2 by reacting with its catalytic nucleophile.

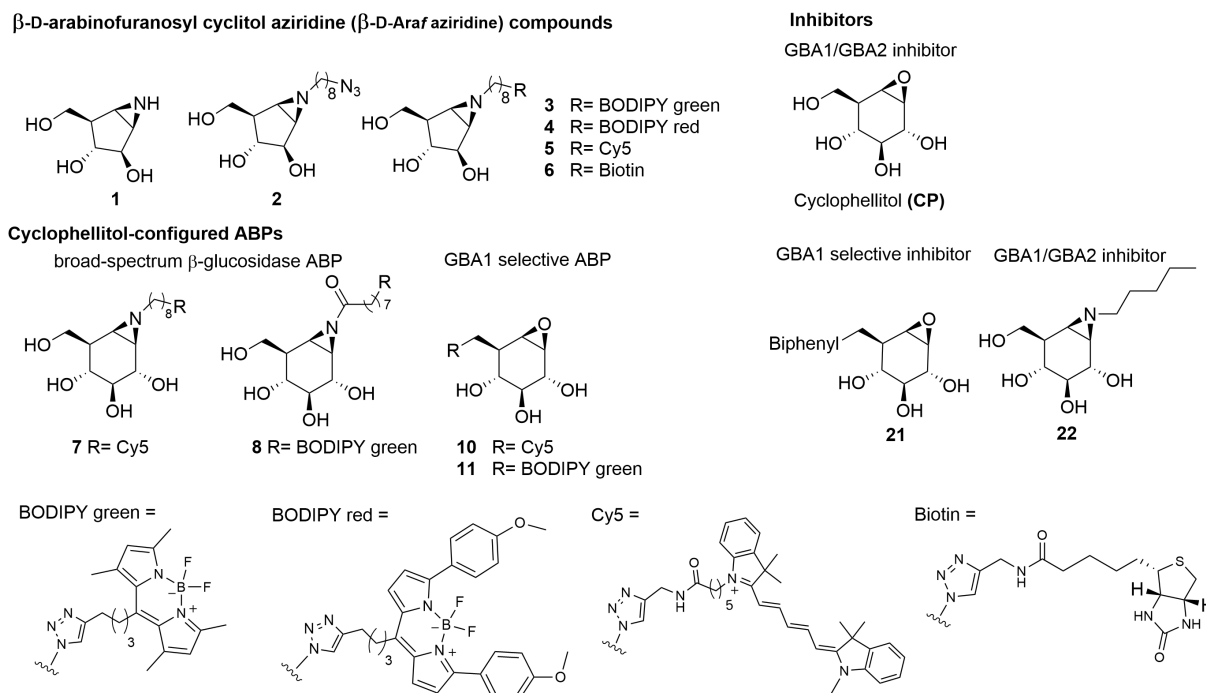


Figure 1. Chemical structures of β -D-arabinofuranosyl cyclitol aziridine **1-6**, cyclophellitol epoxide and aziridine activity-based probes (ABPs) **7-11**, and inhibitors **21** and **22**.

Results

In vitro affinity and selectivity of β -D-Araf cyclitol aziridine ABPs towards human β -glucosidases

To identify an ABP that selectively labels human GBA2 over GBA1 and GBA3, a library of cyclophellitol-based ABPs with varying configurations (Figure S1) was screened for their selectivity towards human retaining β -glucosidases. For this purpose, the inhibition properties of the compounds were first assessed using recombinant human GBA1 (rhGBA1, Imiglucerase), lysates of cells overexpressing GBA2 and lysates overexpressing GBA3, the latter two both in combination with knockout of the other retaining β -glucosidases. In a preliminary screen, enzymes were pre-incubated for 30 min with the tested compounds, followed by the addition of the fluorogenic substrate, 4MU- β -D-Glc, and then quantification of released fluorescent 4MU after 30 minutes. This screening revealed a set of β -D-Araf cyclitol aziridines as potential GBA2 inhibitors. Pre-incubation of the enzymes with β -D-Araf cyclitol aziridine **1** did not show inhibitory effect towards any of the β -glucosidases assayed up to 50 μ M, whereas *N*-azido-octyl aziridine **2** displayed inhibition of all three β -glucosidases (apparent IC_{50} : GBA2 630 nM, GBA1 2730 nM, GBA3 8150 nM) with some selectivity for GBA2 over GBA1 and GBA3 (Table S1). Interestingly, BODIPY green- and BODIPY red-tagged ABPs **3** and **4** exhibited substantial affinity towards GBA2 (apparent IC_{50} : 120-160 nM) with clear selectivity (defined as IC_{50} Enzyme1/ IC_{50} Enzyme2) for GBA2 over GBA1 and GBA3 (Figure 2A). In contrast, β -D-Araf ABP **5** equipped with a Cy5 fluorophore inhibited GBA1 and GBA2 with about equal potency (apparent IC_{50} 250-300 nM). The biotin-tagged β -D-Araf compound **6** is a poor (apparent IC_{50} > 8 μ M) inhibitor of all three glucosidases.

Arabinofuranosyl cyclitol **12-20** with various configurations (α -L-Araf and β -L-Araf) were also evaluated (Figure S1). Most of these proved to be poor GBA2 inhibitors (apparent $IC_{50} > 20 \mu M$), and none matched the selectivity of β -D-Araf cyclitol aziridines **3** and **4** for GBA2 (Table S1).

Armed with ABPs **3** and **4**, both of which displayed high selectivity for GBA2 over GBA1 and GBA3, their activity in cell lysates was analyzed next. To this end, lysates of HEK293T cells containing all three β -glucosidases (endogenous GBA1 with overexpressed GBA2 and GBA3) were treated with ABPs **3**, **4**, **5** and **7**, followed by protein separation by SDS-PAGE and fluorescence scanning of the wet gel slabs. As depicted in Figure 2B, ABP **7** labelled all β -glucosidases as previously reported.³¹ In contrast, the β -D-Araf aziridine ABPs **3** and **4** selectively labelled GBA2 at a concentration of 100 nM, while Cy5 tagged ABP **5** did so at 500 nM. The GBA2 selectivity of β -D-Araf cyclitol aziridines **3**, **4** and **5** was confirmed in a mixture of a lysate of cells overexpressing GBA2 with rhGBA1 (Figure 2C and Figure S3). In this experiment, the enzyme mixture was first incubated with β -D-Araf aziridine ABPs **3**, **4**, or **5** for 30 minutes, after which selective GBA1 ABP **10**³² or **11**³⁰ was added to label the remaining active rhGBA1 molecules. This experiment revealed the ability of β -D-Araf cyclitol aziridine ABPs, and in particular **3** and **4**, to selectively label GBA2 without significant rhGBA1 labelling, with marginal GBA1 labelling occurring at 10 μM .

The pH and incubation time dependent labelling of GBA2 in HEK293T cells containing all three retaining β -glucosidases by β -D-Araf ABPs was next investigated (Figure 2D, E and Figure S4). All ABPs selectively label GBA2 at a pH range of 4.5-7.5. Using 500 nM of ABP **4**, GBA2 labelling occurred within a minute, and maximal labelling was observed after 20-30 minutes. Importantly, no labelling of GBA1 or GBA3 was observed under varying pH and time conditions (Figure S4).

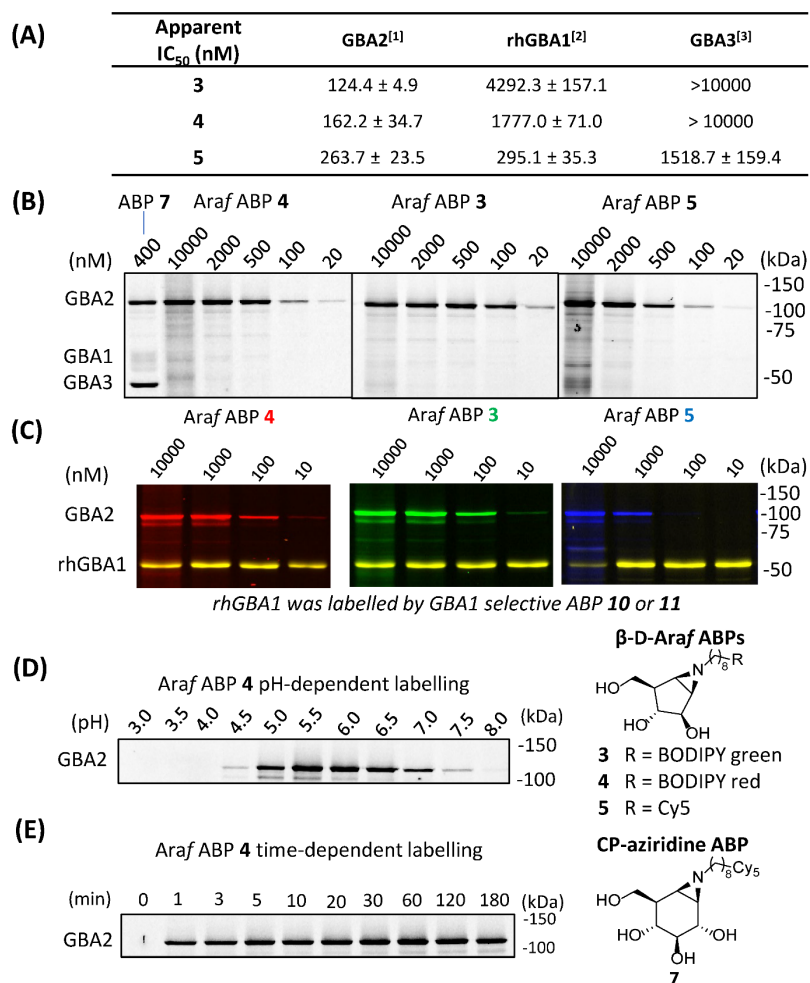


Figure 2. *In vitro* ABPP with β-D-Araf aziridine ABPs **3-5**. (A) Apparent IC₅₀ (nM) of β-D-Araf ABPs, determined by 4MU-β-D-Glc fluorogenic substrate assay, enzyme: [1] GBA2 = GBA1/GBA2 KO HEK293T cell lysates with GBA2 overexpression (OE), [2] rhGBA1 = isolated recombinant Imiglucerase (Cerezyme®). [3] GBA3 = GBA1/GBA2 KO HEK293T cell lysates with GBA3 OE. Error ranges = ± SD, n = 3 replicates. (B) HEK293T cell lysates expressing endogenous GBA1 and overexpressed GBA2/GBA3 were used as enzyme source. Lysates were treated with ABPs **3-5** for 30 min at pH 6.0. (C) Mixture of GBA1/GBA2 KO HEK293T with GBA2 OE lysate and rhGBA1 were incubated with β-D-Araf ABPs (**3-5**) for 30 min at pH 5.8, following addition of 500 nM of ABP **10** (for **3** and **4**) or ABP **11** (for **5**). (D) *In vitro* pH-dependent labelling of ABP **4** (500 nM). (E) *In vitro* time-dependent ABPP assay of ABP **4** (500 nM).

Identification of the catalytic nucleophile of GBA2 reacted with β-D-Araf cyclitol aziridines

GBA2, like TxGH116 (the bacterial homologue of GBA2), induces hydrolysis through a conventional Koshland two-step double-displacement conformational pathway typical of retaining β-glucosidases, progressing from ¹S₃ to ⁴H₃ to ultimately adopt the ⁴C₁ in the covalent complex (Figure 3A).¹¹ In contrast to cyclophellitol aziridines, which mimic the ⁴H₃ transition state, β-D-Araf aziridines adopt an ³E conformation³³ which resembles the ¹S₃ initial Michaelis complex conformation (Figure 3B).³⁴ Previous research had established that E527 (catalytic nucleophile) and D677 (catalytic acid/base) are the catalytic residues in the human GBA2 active site.¹⁷ To investigate whether β-D-Araf aziridine ABPs bind GBA2 in an activity-based manner, firstly mutants of GBA2 were generated by substituting either the E527 nucleophile or the D677 acid/base. Lysates from cells expressing these mutant GBA2 proteins were then incubated with β-D-Araf ABPs **3-5** or cyclophellitol ABP **7** and their labelling pattern was analyzed (Figure 3C). None of the ABPs were found to label the E527G mutant or the E527G/D677G double mutant, demonstrating that these probes require the nucleophile E527 for reaction with GBA2. Notably, β-D-Araf ABPs **3-5** exhibit poor reaction with the acid/base mutant D677G, whereas ABP **7**

modified this mutant in significant amounts. At higher ABP concentrations and/or longer incubation times (Figure 3D) some degree of labelling of the acid/base mutant GBA2 was detected also with ABPs **3-5**.

To firmly establish the mode of action of β -D-Araf cyclitol aziridines as mechanism-based GBA2 inhibitors, the 3D structure of the GH116 bacterial GBA2 homolog, TxGH116 from *Thermoanaerobacterium xylanolyticum* in complex with β -D-Araf compound **2** was solved at 1.9 Å resolution. The -1 subsite of TxGH116 is well conserved relative to human GBA2. The solved structure (Figure 3E) reveals reacted **2** with the catalytic nucleophile of TxGH116, occupying the enzyme active site anchored by several hydrogen bonds. The OH group on C2 interacts with NE2 His507 and OD2 Asp452, and the OH on C3 with OD2 Asp452, NH2 Arg792 and OG1 and the alcohol of Thr591. The OH on C5 is hydrogen-bonded to OE2 Glu777 and to NH1 and NH2 Arg786. In addition, the amine from the ring-opened aziridine group forms a hydrogen bond to OD2 Asp593 and to a water molecule (which also interacts with OD1 Asp593). There is insufficient electron density to allow modelling of the end of the azidoctyl group, which extend into a more open region at the edge of the protein where they are less constrained.

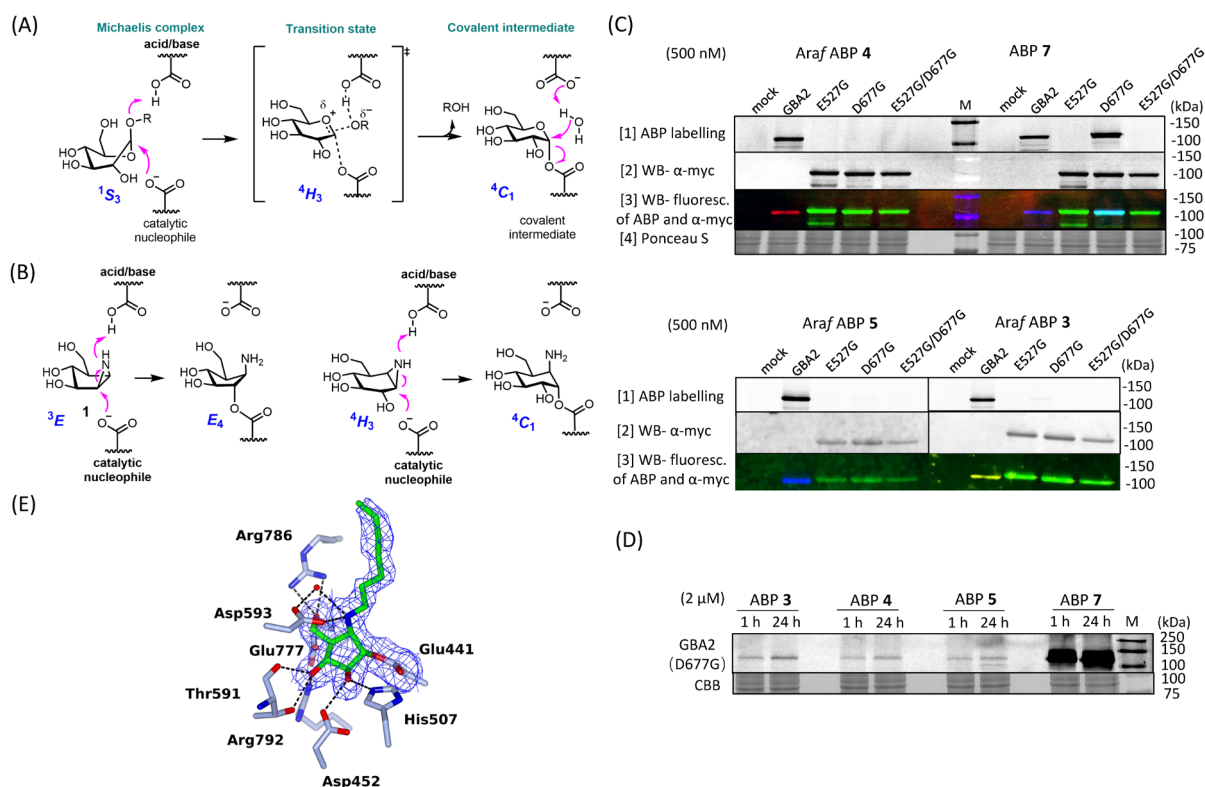


Figure 3. Mechanism of inhibition of GBA2 by β -D-Araf cyclophellitol aziridines. (A) Conformational itinerary of the Koshland double-displacement mechanism employed by retaining β -D-glucosidases. (B) β -D-Araf cyclitol aziridine **1** adopts an envelope-like 3E conformation prior to reaction with the GBA2 active site, whereas cyclophellitol aziridines mimic the 4H_3 transition state conformation. (C) β -D-Araf aziridine ABPs (**3-5**) and cyclophellitol aziridine ABP **7** labelling of lysates of HEK293T cells overexpressing myc-tagged mutant (E527G, D677G or E527G/D677G) or wildtype GBA2. mock = HEK293T GBA1/GBA2 KO cell lysate, GBA2 = HEK293T GBA1/GBA2 KO GBA2 OE cell lysate. Gel images were captured by fluorescence scanning on wet gel slabs (row 1) and Western blot (nitrocellulose membrane) using an anti-myc antibody (row 2). Row 3 represents the Western blot showing fluorescence of both ABPs (**3-5**, **7**) and the anti-myc antibody. row 4 represents Ponceau S stain. (D) 2 μ M β -D-Araf ABPs and ABP **7** incubated with GBA2 D677G mutant for 1 h (at 37 °C) or 24 h (at 4 °C) show the labelling efficiency towards GBA2 D677G mutant. (E) Structure of complex of TxGH116 with **2** showing the electron density difference map calculated for the ligand and side chain of Glu441, contoured at 2.5 σ (0.275 electrons Å⁻³), and showing hydrogen bonds represented as dashed lines.

***In vitro* labelling across species and *in situ* labelling of β -D-Araf cyclitol aziridine ABPs**

GBA2 orthologs are highly conserved among different species. BLAST analysis revealed that human GBA2 shares 87% sequence identity and 93% similarity in the catalytic domain with murine GBA2 and 66% identity and 79% similarity with the zebrafish (*Danio rerio*) enzyme.¹⁴ The reactivity of β -D-Araf aziridine ABPs **3-5** with GBA2 orthologs in these was therefore evaluated. Homogenates of zebrafish larvae or mice brain were incubated with β -D-Araf ABPs **3-5** or broad-spectrum β -glucosidase ABP **7** (Figure 4). As was seen for human cell extracts, β -D-Araf ABPs **3-5** selectively label GBA2 also in these species whereas ABP **7** showed cross-reactivity towards GBA1.

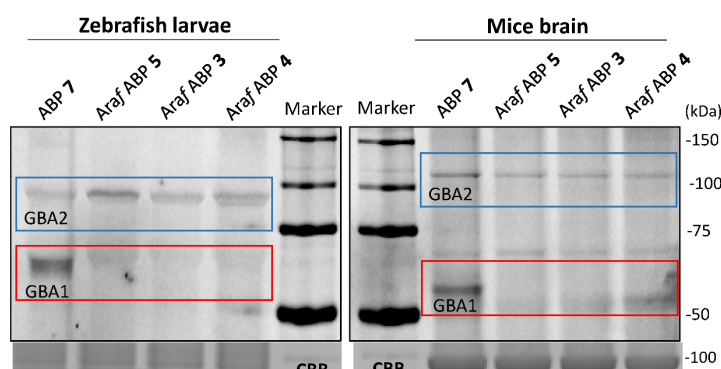


Figure 4. β -D-Araf aziridine ABPs selectively label GBA2 orthologues in different species. Cyclophellitol aziridine ABP **7** (1 μ M) and β -D-Araf ABPs (ABP **3** at 1 μ M and ABP **4** and **5** at 2.5 μ M) were incubated with homogenates of zebrafish larvae and mice brain tissue for 1 h at 37 °C.

As the next research objective, experiments were done to establish whether active GBA2 molecules could be detected and identified in human cells using the β -D-Araf aziridine ABPs. For this purpose, HEK293T cells with endogenous GBA1 and overexpressed GBA2/GBA3 were treated with varying concentrations of β -D-Araf aziridine ABPs **3-5** for 1 h, after which the cells were harvested and washed multiple times prior to lysis. The lysates were then denatured, their protein content separated by SDS-PAGE and the resulting wet gel slabs scanned for fluorescence. In this way it was observed that all three β -D-Araf ABPs **3-5** enter intact cells where they react with endogenous, and given the >24 h lifetime, newly synthesized GBA2 (Figure 5A, Figure S8 A, B). BODIPY tagged ABPs **3** and **4** proved to be the most effective GBA2 probes in these experiments and inactivate GBA2 almost completely at 100 nM final concentration.

To address the concern that the ABPs attach to the cell surface and subsequently *in vitro* label GBA2 following cell lysis, a non-tagged GBA2 inhibitor was added to the lysis buffer. The presence of high concentrations of cyclophellitol (**CP**) or cyclophellitol aziridine ABP **8**, both potent human GBA1 and GBA2 inactivators, did not diminish GBA2 labelling efficiency by ABP **4** (Figure 5B), thus indicating that these ABPs indeed labelled GBA2 *in situ*. Importantly, the GBA2 selectivity of β -D-Araf ABPs **3-5** was maintained during *in situ* labelling of wild-type HEK293T cells (Figure S9). GBA1 labelling only occurred when using a high concentration (500 nM) and longer incubation time (2.5 h) for ABP **5**, while ABP **3** and **4** did not visibly label GBA1 at these conditions (Figure 5B and Figure S9). Even incubation for 24 h gave similar results: ABPs **3** and **4** still selectively labelled GBA2 at 10 nM, and only slight concomitant GBA1 labelling at higher concentrations was observed (Figure S10). Selective GBA2 labelling by ABPs **3** and **4** finally was also observed in human retinal pigment epithelial-1 cells (Figure 5C).

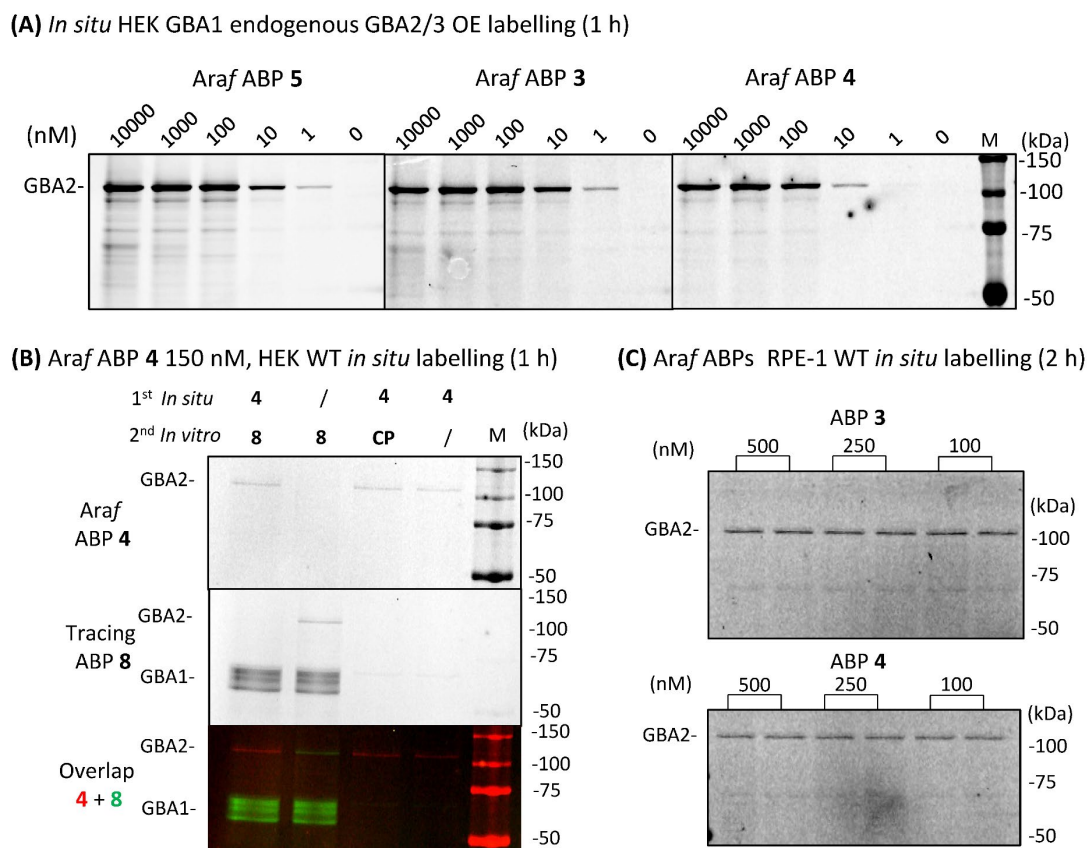


Figure 5. Treating intact cells with β-D-Araf ABPs labels GBA2 *in situ*. (A) Labelling of β-D-Araf ABPs in intact HEK293T cells (GBA1 endogenous and GBA2/3 overexpression) at varying concentrations for 1 h *in situ*. (B) Wild-type HEK293T cells treated with 150 nM ABP 4 *in situ* for 1 h, followed by adding lysis buffer containing ABP 8 (1 μM final concentration with 1% DMSO final concentration), or cyclophellitol (CP, 1 μM final concentration with 1% DMSO final concentration), or the blank (‘/’) 1% DMSO (final concentration) for ABPP analysis. (C) ABP 3 and 4 labelling of GBA2 in intact wild-type human retinal pigment epithelial-1 (RPE-1) cells.

Localization of GBA2 with an β-D-Araf cyclitol aziridine ABP

As the final set of experiments, red fluorescent ABP 4 was used to study the localization of GBA2 in HEK293T cells. After incubation with 50 nM ABP 4 for 2 h, the samples were fixed and also stained with a green-fluorescent anti-GBA1-antibody in order to observe the difference in localization between GBA1 and GBA2. Confocal microscopy of wild-type (WT) HEK293T cells showed an unambiguous staining for GBA1 with a distinct perinuclear lysosomal distribution pattern. However, no clear signals for ABP 4 modified proteins were observed (Figure 6). Attention was therefore redirected to the use of GBA2 overexpression (OE) cells and GBA1/GBA2 knockout (KO) + GBA2 OE cells.^{19,31} These cells did present clear GBA2 staining, which is localized to the cell membrane (Figure 6). As well, no overlap is observed between red fluorescence (localization of GBA2-selective ABP 4) and green fluorescence (localization of GFP-tagged anti-GBA1), indicating that GBA2 resides in subcellular compartments distinct from those in which GBA1 resides. To confirm the selective staining of GBA2, cells overexpressing GBA2 were pre-treated with either the selective GBA1 inhibitor **21**³² or the GBA1/GBA2 inhibitor **22**³⁵. Confocal microscopy showed no change in the staining of GBA2 after pre-treatment with the GBA1 specific inhibitor **21**, however the signal of GBA2 was completely abrogated by prior treatment with the dual target inhibitor **22** (Figure S11B).

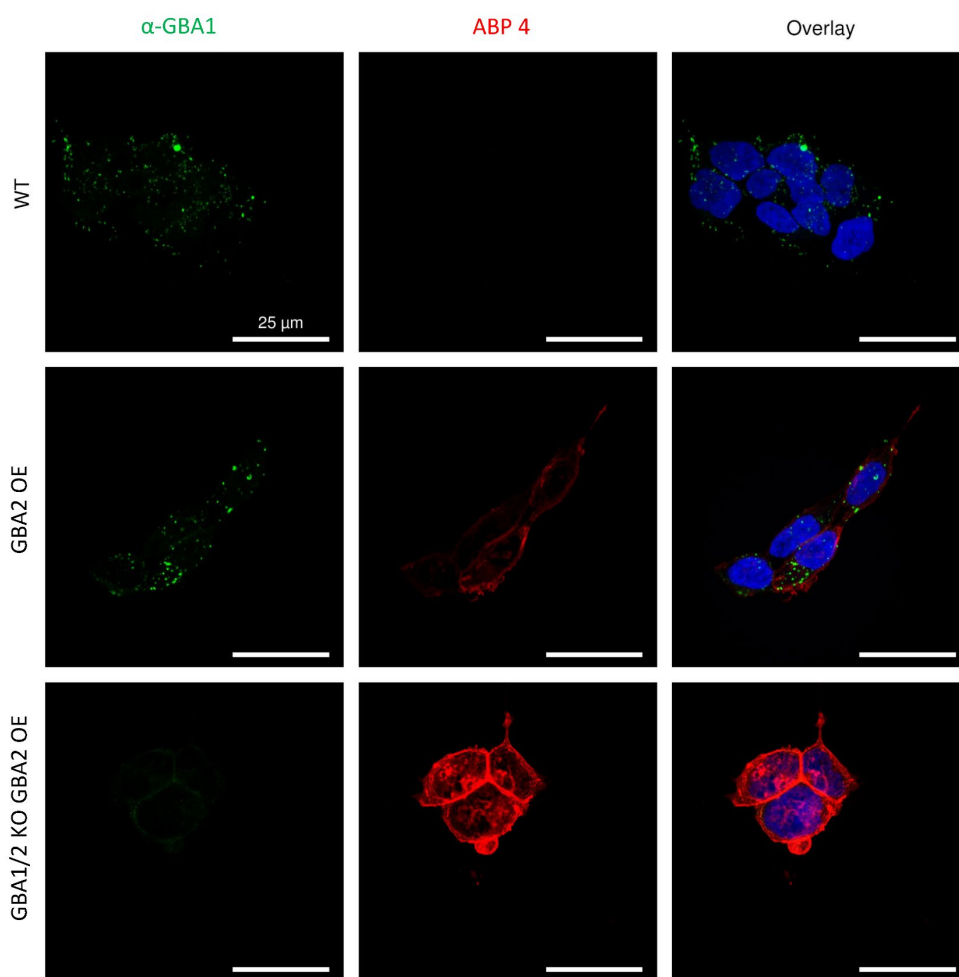


Figure 6. Confocal fluorescence microscopy of GBA1 and GBA2 as detected by red fluorescent β -D-Araf aziridine **4** and green fluorescent anti-GBA1-antibody with Alexa Fluor® 647 conjugation. Used were different HEK293T cells: HEK293T wild-type (WT), GBA2 overexpression (OE), and GBA1/GBA2 knock out (KO) with GBA2 overexpression (OE). Cells were treated with 50 nM β -D-Araf aziridine **4** (red) for 2 h. After fixation all cells were stained for GBA1 using an anti-GBA1-antibody (green) and nuclei were stained with 10 μ g/ml DAPI (blue).

Discussion

GBA2 attracts increasing attention given its potential role in pathophysiological mechanisms in a variety of human diseases. While the catalytic machinery, the mode of action and the substrate specificity of the enzyme has now been firmly established, little is known about its physiological role and even its subcellular localization is a matter of debate. The acquisition of such knowledge is hampered by the absence of cell-permeable, GBA2-selective chemical probes, comparable to the counterpart developed for the selective visualization of active GBA1 in living cells.^{30,36-38} The work described here was aimed to rectify this situation. Screening of a library of activity-based glycosidase probes led to the discovery of fluorescent β -D-Araf cyclitol aziridines that selectively label GBA2 both *in vitro* and in intact cells. The labelling occurs through mechanism-based, covalent and irreversible inhibition of the ABP and is abolished by mutagenesis of the catalytic nucleophile. GBA2 labelling of cells combined with fluorescence microscopy clearly shows that GBA2, in contrast to GBA1, is not located in lysosomes. While labelled GBA2 is easily detected in cells overexpressing the enzyme, intensity of the fluorescent signal is relatively weak in wild type cells, and future use of more advanced fluorescence microscopy (for instance, including spectral imaging and use of a supersensitive camera with higher quantum yield) may improve detection of native GBA2. It should be kept in mind that

disperse distribution of GBA2 among membranes, contrary to the intrinsic concentration of GBA1 molecules in lysosomes, does not favor detection by simple fluorescence microscopy.

The observed high affinity and selectivity of β -D-Araf cyclophellitol aziridines equipped with a hydrophobic fluorescent tag for labelling GBA2 is quite remarkable. A very recent publication by Shimokawa and coworkers³⁹ reports that a GH116 exo- β -D-arabinofuranosidase from *Microbacterium arabinogalactanolyticum* termed ExoMA2 shows similarities in structure to that of the GH116 β -glucosidase from *Thermoanaerobacterium xylanolyticum* (TxGH116). Both enzymes have a two-domain structure consisting of N-terminal β -sandwich and C-terminal (α/α) 6-barrel domains, the latter being the catalytic domain. The two catalytic residues, as well as several other residues in the active site pocket are conserved, but substrate recognition at subsite -1 differs. Given the similarities in the catalytic pocket, the catalytic residues and even the transglycosylation abilities^{19,39,40} of the three enzymes, it is perhaps not surprising that β -D-Araf cyclitol aziridines bind well to the GBA2 active site.

In conclusion, β -D-Araf aziridine ABPs were identified as a new class of GBA2 selective ABPs. The newly described ABPs allow to specifically monitor GBA2 and act as specific GBA2 suicide inhibitors to selectively inactivate GBA2. The β -D-arabinofuranosyl cyclophellitol aziridine ABPs are novel tools for the study of the intriguing enzyme GBA2, and the development of GBA2 selective inhibitors based on the β -D-Araf cyclophellitol scaffold is warranted in the future.

Experimental procedures

Materials

Recombinant human GBA1 (rhGBA1, Imiglucerase) was kindly provided by Sanofi Genzyme (Cambridge, MA, USA). HEK293T (CRL-3216™) cells and RPE-1 (CRL-4000™) cells were purchased from ATCC (Manassas, VA, USA). 4-Methylumbelliferyl- β -D-glucopyranoside was purchased from Glycosynth (Warrington Cheshire, UK). Polytron PT 1300D sonicator (Kinematica, Luzern, Switzerland) and potassium phosphate buffer (K_2HPO_4 - KH_2PO_4 , 25 mM, pH 6.5, supplemented with protease inhibitor cocktail (EDTA-free, Roche, Basel, Switzerland) and 0.1% (v/v) Triton X-100 and) were used for lysing cells and homogenizing zebrafish larvae and mice tissues. Harvested cells (cell pellets), cell lysates and tissue homogenates not used directly were stored at -80 °C. Protein concentration was measured using the Pierce BCA assay kit (Thermo Fisher Scientific, Waltham, MA, USA).

Cell culture

HEK293T cells were cultured in DMEM medium (Sigma-Aldrich), supplied with 10% (v/v) FCS, 0.1% (w/v) penicillin/streptomycin and 1% (v/v) Glutamax, at 37 °C under 7% CO₂. RPE-1 cells were cultured in HAMF12-DMEM medium (Sigma Aldrich), supplied with 10% (v/v) FCS, 0.1% (w/v) penicillin/streptomycin and 1% (v/v) Glutamax, at 37 °C under 5% CO₂.

Generation of cells genetically modified in β -glucosidase expression

GBA1/GBA2 knockout (KO) HEK293T cells, GBA1/GBA2 KO HEK293T cells with either GBA2 overexpression (OE) or GBA3 overexpression, and HEK293T cells expressing all cellular β -glucosidases (containing endogenous GBA1 and overexpressed GBA2 and GBA3) were generated as described in Chapter 2.

Cell lysis

HEK293T and RPE-1 cells were cultured with the method described above to 80-90% confluency, and were isolated, washed with Dulbecco's phosphate buffered saline (PBS), subsequently collected and lysed as the method described in Chapter 2 which were adapted from the literature.⁴¹

4MU fluorogenic substrate assay for determination of enzyme activity and apparent IC₅₀

4MU fluorogenic substrate assays (using isolated recombination human GBA1 or lysates of HEK293T cells) were conducted in 96-well plates at 37 °C. Assay procedures and conditions for measuring enzyme activity and apparent IC₅₀ of each enzyme (rhGBA1, GBA2, or GBA3) are the same as previously described in Chapter 2. In brief, enzymes were diluted with McIlvaine buffer (150 mM citric acid- Na_2HPO_4 , at the appropriate pH for each enzyme), to a final volume of 25 μ L with or without inhibitors. For enzyme activity measurement, samples were incubated with 100 μ L 4-methylumbelliferyl- β -D-glucopyranoside substrates diluted in McIlvaine buffer for 30 min. For apparent IC₅₀ measurement, enzymes were incubated with inhibitor diluted in McIlvaine buffer for 30 min or 3 h, followed by incubation with 100 μ L 4-methylumbelliferyl- β -D-glucopyranoside substrates for 30 min. After stopping the enzyme reaction with 200 μ L 1M NaOH-glycine (pH 10.3), 4-methylumbelliferone fluorescence was measured with a fluorimeter LS55 (Perkin Elmer, Waltham, MA, USA). Enzyme activities and apparent IC₅₀ values were determined by subtraction of the background signal (measured for incubations without enzyme), as previously described.⁴² The IC₅₀ value was calculated using Graphpad Prism 9.0 with the Nonlinear regression (curve fit) - [Inhibitor] vs. response - Variable slope (four parameters) equation.

Activity-based protein profiling (ABPP) with SDS-PAGE

Samples containing GBA1, GBA2 or GBA3 (see the exact constitution of these samples as described in the specific case) were incubated with fluorescent ABPs at optimum conditions at 37 °C for 30 min (if not otherwise stated) as described in Chapter 2. The total sample volume was 20–40 μ L with a 0.5–1% final concentration of DMSO in the appropriate pH Mcllvaine buffer (150 mM). For assessing the reactivity of arabinofuranose-configured cyclitol ABPs towards β -glucosidases, lysates of HEK293T cells expressing endogenous GBA1 and overexpressed GBA2/GBA3 were incubated with varying concentration of ABP in Mcllvaine buffer (150 mM, pH 6.0). After incubation with ABP, samples were subjected to SDS-PAGE and fluorescence scanning as described in Chapter 2. Wet gel slabs were imaged using a Typhoon FLA 9500 scanner (GE Healthcare) at λ_{EX} 473 nm and $\lambda_{\text{EM}} \geq 510$ nm for BODIPY green fluorescence; at λ_{EX} 532 nm and $\lambda_{\text{EM}} \geq 575$ nm for the BODIPY red fluorescence; at λ_{EX} 635 nm and $\lambda_{\text{EM}} \geq 665$ nm for Cy5 fluorescence. Afterwards, the wet gel slab was stained by Coomassie brilliant blue (CBB) G250 or R250 for loading control of proteins.

 β -Glucosidase inactivation visualized by competitive ABPP with SDS-PAGE

In general, samples containing GBA1, GBA2 or GBA3 (see the exact constitution of these samples described below) are first incubated (*in vitro* or *in situ*) with the compounds, subsequently, the fluorescent readout ABPs were added and incubated with mixture to reveal the residual enzymes that were not inactivated by the inhibitor compound.

To Figure S12, lysate of HEK293T cells expressing all cellular β -glucosidases were first incubated with compound **6** for 3 h at 37°C (*in vitro*), after which readout ABP **7** was added and incubated for 30 min at 37 °C (*in vitro*) to reveal the residual active β -glucosidases, following the procedures described above for SDS-PAGE and fluorescence scanning to visualize the outcome. To Figure S8B, intact living HEK293T cells expressing all cellular β -glucosidases were first incubated with fluorescent ABP **3-5** (*in situ*) for 24h at 37°C under 7% CO₂, then cells were harvest and lysed as description in cell lysis. Subsequently, readout ABP (one of **7-9**) was added, and same procedures described above for outcome visualization were conducted to reveal the active β -glucosidases not occupied by ABP **3-5**. Of note, a fluorescent readout ABP (**7-9**) with different scanning wavelength from ABP (**3-5**) should be chosen. For example, if ABP **3** with BODIPY-green tag is first used to inactivate β -glucosidases, the readout ABP should be ABP **7** with Cy5 tag or ABP **9** with BODIPY-red tag.

To obtain competitive ABPP quantified IC₅₀ values, the ABP-emitted fluorescence of the read out ABP was quantified by ImageQuant (GE Healthcare, Chicago, IL, USA) and calculated with Graphpad Prism 9.0 using Analyze – Nonlinear regression (curve fit) – One phase association.

Irreversibility evaluation by competition with irreversible ABP

The irreversibility of enzyme inhibition was evaluated as below (Figure S6A). Lysates of GBA1/GBA2 KO HEK293T with GBA2 OE were used. A total of 60 μ g lysate was incubated with or without 1 μ M β -D-Araf cyclitol aziridines **2-4** for 1 h at 37 °C, a part of the lysates was taken and used for parallel activity measurements using the 4MU- β -D-Glc fluorogenic substrate assay. Subsequently, the lysate mixtures were washed by passing through Zeba™ spin desalting columns with 40k MWCO (Thermo Scientific) to remove excess compounds. The washing was repeated every 2 h, with 3 washes conducted in total, during which the lysate was kept on ice or at 4 °C. After the last washing step, the same volume of lysates was taken and incubated with 1 μ M β -glucosidase ABP **7**, over 30 min at 37 °C, or over 24 h or 48 h at 4 °C. Then the competition results were revealed by SDS-PAGE and in-gel fluorescence scanning as described above. Parallel activity measurement results show GBA2 activity recovery after desalting washing (Figure S6B).

Stability of β -D-Araf aziridine binding towards GBA2

In Figure S6C, A total of 90 μ g GBA2 (lysates of GBA1/GBA2 KO HEK293T with GBA2 OE) in potassium phosphate buffer was diluted with 60 μ L Mcllvaine buffer (150 mM, pH 6.0) and incubated with or without 1 μ M β -D-Araf aziridine compound **2-5** for 1 h at 37 °C. Thereafter, the total 100 μ L sample was passed through a desalting column as described above. To assess the activity of GBA2 bound with the β -D-Araf compound **2-5**, all samples were kept at 4 °C until GBA2 activity was measured by incubation with 4MU- β -D-Glc at time points 0.5 h, 24 h and 96 h and subsequent measurement of emerging fluorescence. The GBA2 activity assays were performed with 10 μ L sample in triplicate, and the activity of GBA2 incubated without inhibitors was used as a control.

Reactivity of β -D-Araf aziridines towards GBA2 mutants

For overexpression of GBA2 mutants, HEK293T GBA1/GBA2 KO cells were used. GBA2-E527G, GBA2-D677G, or GBA2- E527G/D677G double mutants containing a myc tag were generated as described previously for COS-7 cells.¹⁷ Next, 500 nM β -D-Araf cyclitol aziridine ABP **3-5** or cyclophellitol-aziridine ABP **7** were incubated with the corresponding lysates for 30 min at 37 °C, followed by SDS-PAGE and fluorescence scanning as described in ABPP. Subsequently, proteins in the wet gel slabs were transferred to nitrocellulose membranes for Western blotting. Ponceau S staining was used to show loading control of proteins. Primary antibody used was Mouse anti myc (α -myc, Bioke). Secondary antibodies, donkey anti mouse with Alexa 488 (Invitrogen) or goat anti mouse with Alexa 532 (Invitrogen) were used to visualize GBA2 mutants with the myc tag.

Reactivity of β -D-Araf aziridines towards GBA2 orthologue in other species

β -D-Araf aziridine ABP **3-5** or ABP **7** was incubated with homogenates of zebrafish (*Danio rerio*) larvae or mice brain for 1 h at 37 °C. The homogenates were obtained as follows. Zebrafish larvae were kept at a constant temperature of 28.5 °C and raised in egg water (60 μ g L-1 sea salt, Sera Marin) for 5 days, larvae were collected and sacrificed for making homogenates, a total 10-20 μ g larvae homogenates were used for ABPP. Extracts of mouse brain were obtained from existing mice extraction stocks that were stored at -20 °C; a total of 10-20 μ g mouse brain homogenate was used. The zebrafish homogenate was passed through a desalting column (in the same way as described for the irreversibility evaluation above) to remove interference from biological pigments when scanning at λ_{EX} 473 nm and $\lambda_{EM} \geq 510$ nm for BODIPY green fluorescence.

In situ intact cell permeability assays

Confluent HEK293T cells expressing human endogenous GBA1 and overexpressed GBA2/GBA3, wild-type HEK293T cells or wild-type human retinal pigment epithelial-1 (RPE-1) cells were cultured in 12-well plates for duplicates or triplicates with (or without) compounds (**3-5**) for the described incubation times using the conditions as described for the cell culture. The cells were harvested and lysed as described in the cell lysis method. After determination of the protein concentration by BCA assay, the lysates were adjusted to 10 μ L by addition of potassium phosphate buffer in order to normalize the amount of protein loaded (to 10-25 μ g total protein per measurement) and subjected to ABPP as described above.

In situ visualization of GBA2 using confocal microscopy

HEK293T wild-type (WT), GBA1 endogenous and GBA2 overexpression (GBA2 OE), or GBA1/GBA2 knockout (KO) GBA2 overexpression (GBA1/GBA2 KO GBA2 OE) cells were cultured as described in cell culture.^{31,43} Cells were grown to approximately 75% confluency on \varnothing 15 mm glass coverslips coated with 0.1 mg/ml poly-D-Lysine. Samples were pretreated for 16 h with 100 nM of a GBA1 inhibitor (**21**³², 0.5% DMSO), 500 nM of a GBA1 and GBA2 inhibitor (**22**³⁵, 0.5% DMSO) or with 0.5% DMSO alone. GBA2 was

subsequently incubated by the addition of 50 nM ABP **4** (BODIPY-red) to cells for 2 h at 37 °C with 5% CO₂. Unbound probe was washed away with PBS and cells were fixed with 4% paraformaldehyde (Alfa Aesar)/PBS for 15 min at RT. After fixation the cells were washed with PBS and directly permeabilized with 0.1% Tween20 (Sigma-Aldrich)/TBS for 30 min at RT. After gentle washing in PBS, the samples were blocked using 3% (w/v) BSA (Sigma-Aldrich)/PBS for 30 min at RT. Immunofluorescence staining was performed with mouse-anti-GBA1 (8E4, generated as described in the literature⁴⁴ 1:250 in 3% BSA-PBS and visualized with a donkey-anti-mouse-Alexa647 (Molecular Probes) 1:1000 in 3% BSA-PBS. Nuclei were stained with 10 μ g/ml DAPI (Sigma-Aldrich). Afterwards the samples were mounted on ProLong Diamond (Molecular Probes) and imaged on a Nikon Eclipse Ti2 confocal microscope with a 100x/1.49 Numerical Aperture SR HP Apo TIRF oil immersion objective equipped with a PMTs detector.

Expression, purification and crystallization of TxGH116

A construct consisting of TxGH116 Δ 1-18 cloned into pET30a was transformed into *E. coli* BL21(DE3) and used for the expression of TxGH116 and its purification based on the method described.¹⁶ Purified TxGH116 at 1 mg/ml in 20 mM Tris-HCl pH 8.0, 150 mM NaCl was crystalized in a sitting drop plate, in a 2:1 ratio to the well solution, which consisted of 20 % (w/v) polyethylene glycol 3000, 100 mM ammonium sulfate, 0.1 M 2-(*N*-morpholino) ethanesulfonic acid pH 6.0. A crystal was soaked by the addition of a 10 mM solution of 8-azido-octyl- β -D-arabinofuranosyl cyclitol aziridine **2** dissolved in water to a final concentration of 3.3 mM in the drop and fished after 68 hours into liquid nitrogen without additional cryoprotection.

Data collection and refinement

Data were collected at beamline io4 at the Diamond Light Source (UK), processed using DIALS⁴⁵ and scaled with AIMLESS⁴⁶. There are 2 molecules per asymmetric unit and the space group is P2₁2₁2₁. The structure was solved using Phaser⁴⁷ with PDB entry 5BVU as the model, and refined using REFMAC5⁴⁸ interspersed with rounds of model building in Coot⁴⁹. The ligand was built and dictionary restraints generated using AceDRG⁵⁰. The programs were run through the CCP4/2⁵¹ graphical interface. Data collection and refinement statistics are given in Table S2.

References

1. E. Drula, M. L. Garron, S. Dogan, V. Lombard, B. Henrissat and N. Terrapon, The carbohydrate-active enzyme database: functions and literature, *Nucleic Acids Res.*, 2022, **50**, D571-D577.
2. S. van Weely, M. Brandsma, A. Strijland, J. M. Tager and J. M. Aerts, Demonstration of the existence of a second, non-lysosomal glucocerebrosidase that is not deficient in Gaucher disease, *Biochim. Biophys. Acta.*, 1993, **1181**, 55-62.
3. S. Sultana, J. Reichbauer, R. Schule, F. Mochel, M. Synofzik and A. C. van der Spoel, Lack of enzyme activity in GBA2 mutants associated with hereditary spastic paraplegia/cerebellar ataxia (SPG46), *Biochem. Biophys. Res. Commun.*, 2015, **465**, 35-40.
4. E. Martin, R. Schule, K. Smets, A. Rastetter, A. Boukhris, J. L. Loureiro, M. A. Gonzalez, E. Mundwiller, T. Deconinck, M. Wessner, L. Jornea, A. C. Oteyza, A. Durr, J. J. Martin, L. Schols, C. Mhiri, F. Lamari, S. Zuchner, P. De Jonghe, E. Kabashi, A. Brice and G. Stevanin, Loss of function of glucocerebrosidase GBA2 is responsible for motor neuron defects in hereditary spastic paraplegia, *Am. J. Hum. Genet.*, 2013, **92**, 238-244.
5. M. Gatti, S. Magri, D. Di Bella, E. Sarto, F. Taroni, C. Mariotti and L. Nanetti, Spastic paraplegia type 46: novel and recurrent GBA2 gene variants in a compound heterozygous Italian patient with spastic ataxia phenotype, *Neurol. Sci.*, 2021, **42**, 4741-4745.
6. M. A. Woeste, S. Stern, D. N. Raju, E. Grahn, D. Dittmann, K. Gutbrod, P. Dormann, J. N. Hansen, S. Schonauer, C. E. Marx, H. Hamzeh, H. G. Korschen, J. M. Aerts, W. Bonigk, H. Endepols, R. Sandhoff, M. Geyer, T. K. Berger, F. Bradke and D. Wachten, Species-specific differences in nonlysosomal glucosylceramidase GBA2 function underlie locomotor dysfunction arising from loss-of-function mutations, *J. Biol. Chem.*, 2019, **294**, 3853-3871.
7. Biogen, June 6, 2022, "Biogen and Alectos Therapeutics announce license and collaboration agreement for AL01811, a novel GBA2 inhibitor for the potential treatment of Parkinson's disease", <https://investors.biogen.com/news-releases/news-release-details/biogen-and-alectos-therapeutics-announce-license-and>.
8. Y. Yildiz, H. Matern, B. Thompson, J. C. Allegood, R. L. Warren, D. M. Ramirez, R. E. Hammer, F. K. Hamra, S. Matern and D. W. Russell, Mutation of beta-glucosidase 2 causes glycolipid storage disease and impaired male fertility, *J. Clin. Invest.*, 2006, **116**, 2985-2994.
9. R. G. Boot, M. Verhoek, W. Donker-Koopman, A. Strijland, J. van Marle, H. S. Overkleeft, T. Wennekes and J. M. Aerts, Identification of the non-lysosomal glucosylceramidase as beta-glucosidase 2, *J. Biol. Chem.*, 2007, **282**, 1305-1312.
10. B. Cobucci-Ponzano, V. Aurilia, G. Riccio, B. Henrissat, P. M. Coutinho, A. Strazzulli, A. Padula, M. M. Corsaro, G. Pieretti, G. Pocsfalvi, I. Fiume, R. Cannio, M. Rossi and M. Moracci, A new archaeal beta-glycosidase from *Sulfolobus solfataricus*: seeding a novel retaining beta-glycan-specific glycoside hydrolase family along with the human non-lysosomal glucosylceramidase GBA2, *J. Biol. Chem.*, 2010, **285**, 20691-20703.
11. S. Pengthaisong, B. Piniello, G. J. Davies, C. Rovira and J. R. Ketudat Cairns, Reaction mechanism of glycoside hydrolase family 116 utilizes perpendicular protonation, *ACS Catal.*, 2023, **13**, 5850-5863.
12. G. Y. Dai, J. Yin, K. E. Li, D. K. Chen, Z. Liu, F. C. Bi, C. Rong and N. Yao, The Arabidopsis AtGCD3 protein is a glucosylceramidase that preferentially hydrolyzes long-acyl-chain glucosylceramides, *J. Biol. Chem.*, 2020, **295**, 717-728.
13. L. T. Lelieveld, M. Mirzaian, C.-L. Kuo, M. Artola, M. J. Ferraz, R. E. A. Peter, H. Akiyama, P. Greimel, R. J. B. H. N. van den Berg, H. S. Overkleeft, R. G. Boot, A. H. Meijer and J. M. Aerts, Role of μ -glucosidase 2 in aberrant glycosphingolipid metabolism: model of glucocerebrosidase deficiency in zebrafish, *J. Lipid Res.*, 2019, **60**, 1851-1867.
14. S. Sultana, N. Y. Truong, D. B. Vieira, J. G. Wigger, A. M. Forrester, C. J. Veinotte, J. N. Berman and A. C. van der Spoel, Characterization of the zebrafish homolog of beta-glucosidase 2: a target of the drug Miglustat, *Zebrafish*, 2016, **13**, 177-187.

15. A. R. Marques, J. Aten, R. Ottenhoff, C. P. van Roomen, D. Herrera Moro, N. Claessen, M. F. Vinueza Veloz, K. Zhou, Z. Lin, M. Mirzaian, R. G. Boot, C. I. De Zeeuw, H. S. Overkleeft, Y. Yildiz and J. M. Aerts, Reducing GBA2 activity ameliorates neuropathology in Niemann-Pick type C mice, *PLoS One*, 2015, **10**, e0135889.
16. R. Charoenwattanasatien, S. Pengthaisong, I. Breen, R. Mutoh, S. Sansenya, Y. Hua, A. Tankrathok, L. Wu, C. Songsiriritthigul, H. Tanaka, S. J. Williams, G. J. Davies, G. Kurisu and J. R. Cairns, Bacterial beta-glucosidase reveals the structural and functional basis of genetic defects in human glucocerebrosidase 2 (GBA2), *ACS Chem. Biol.*, 2016, **11**, 1891-1900.
17. W. W. Kallemeijn, M. D. Witte, T. M. Voorn-Brouwer, M. T. Walvoort, K. Y. Li, J. D. Codée, G. A. van der Marel, R. G. Boot, H. S. Overkleeft and J. M. Aerts, A sensitive gel-based method combining distinct cyclophellitol-based probes for the identification of acid/base residues in human retaining beta-glucosidases, *J. Biol. Chem.*, 2014, **289**, 35351-35362.
18. H. G. Korschen, Y. Yildiz, D. N. Raju, S. Schonauer, W. Bonigk, V. Jansen, E. Kremmer, U. B. Kaupp and D. Wachten, The non-lysosomal beta-glucosidase GBA2 is a non-integral membrane-associated protein at the endoplasmic reticulum (ER) and Golgi, *J. Biol. Chem.*, 2013, **288**, 3381-3393.
19. A. R. Marques, M. Mirzaian, H. Akiyama, P. Wisse, M. J. Ferraz, P. Gaspar, K. Ghauharali-van der Vlugt, R. Meijer, P. Giraldo, P. Alfonso, P. Irun, M. Dahl, S. Karlsson, E. V. Pavlova, T. M. Cox, S. Scheij, M. Verhoek, R. Ottenhoff, C. P. van Roomen, N. S. Pannu, M. van Eijk, N. Dekker, R. G. Boot, H. S. Overkleeft, E. Blommaart, Y. Hirabayashi and J. M. Aerts, Glucosylated cholesterol in mammalian cells and tissues: formation and degradation by multiple cellular beta-glucosidases, *J. Lipid Res.*, 2016, **57**, 451-463.
20. H. Akiyama, M. Ide, Y. Nagatsuka, T. Sayano, E. Nakanishi, N. Uemura, K. Yuyama, Y. Yamaguchi, H. Kamiguchi, R. Takahashi, J. M. Aerts, P. Greimel and Y. Hirabayashi, Glucocerebrosidases catalyze a transgalactosylation reaction that yields a newly-identified brain sterol metabolite, galactosylated cholesterol, *J. Biol. Chem.*, 2020, **295**, 5257-5277.
21. T. Cox, R. Lachmann, C. Hollak, J. M. Aerts, S. van Weely, M. Hrebicek, F. Platt, T. Butters, R. Dwek, C. Moyses, I. Gow, D. Elstein and A. Zimran, Novel oral treatment of Gaucher's disease with N-butyldeoxynojirimycin (OGT 918) to decrease substrate biosynthesis, *Lancet*, 2000, **355**, 1481-1485.
22. T. M. Cox, J. M. Aerts, G. Andria, M. Beck, N. Belmatoug, B. Bembi, R. Chertkoff, S. Vom Dahl, D. Elstein, A. Erikson, M. Giral, R. Heitner, C. Hollak, M. Hrebicek, S. Lewis, A. Mehta, G. M. Pastores, A. Rolfs, M. C. Miranda, A. Zimran and Advisory Council to the European Working Group on Gaucher, The role of the iminosugar N-butyldeoxynojirimycin (miglustat) in the management of type I (non-neuronopathic) Gaucher disease: a position statement, *J. Inherit Metab. Dis.*, 2003, **26**, 513-526.
23. M. Pineda, M. Walterfang and M. C. Patterson, Miglustat in Niemann-Pick disease type C patients: a review, *Orphanet J. Rare Dis.*, 2018, **13**, 140.
24. P. K. Mistry, J. Liu, L. Sun, W. L. Chuang, T. Yuen, R. Yang, P. Lu, K. Zhang, J. Li, J. Keutzer, A. Stachnik, A. Mennone, J. L. Boyer, D. Jain, R. O. Brady, M. I. New and M. Zaidi, Glucocerebrosidase 2 gene deletion rescues type 1 Gaucher disease, *Proc. Natl. Acad. Sci. U. S. A.*, 2014, **111**, 4934-4939.
25. D. G. Burke, A. A. Rahim, S. N. Waddington, S. Karlsson, I. Enquist, K. Bhatia, A. Mehta, A. Vellodi and S. Heales, Increased glucocerebrosidase (GBA) 2 activity in GBA1 deficient mice brains and in Gaucher leucocytes, *J. Inherit Metab. Dis.*, 2013, **36**, 869-872.
26. J. K. Amory, C. H. Muller, S. T. Page, E. Leifke, E. R. Pagel, A. Bhandari, B. Subramanyam, W. Bone, A. Radlmaier and W. J. Bremner, Miglustat has no apparent effect on spermatogenesis in normal men, *Hum. Reprod.*, 2007, **22**, 702-707.
27. H. S. Overkleeft, G. H. Renkema, J. Neele, P. Vianello, I. O. Hung, A. Strijland, A. M. van der Burg, G. J. Koomen, U. K. Pandit and J. M. Aerts, Generation of specific deoxynojirimycin-type inhibitors of the non-lysosomal glucosylceramidase, *J. Biol. Chem.*, 1998, **273**, 26522-26527.

28. W. W. Kallemeyjn, K. Y. Li, M. D. Witte, A. R. Marques, J. Aten, S. Scheij, J. Jiang, L. I. Willems, T. M. Voorn-Brouwer, C. P. van Roomen, R. Ottenhoff, R. G. Boot, H. van den Elst, M. T. Walvoort, B. I. Florea, J. D. Codée, G. A. van der Marel, J. M. Aerts and H. S. Overkleeft, Novel activity-based probes for broad-spectrum profiling of retaining beta-exoglucosidases in situ and in vivo, *Angew. Chem. Int. Ed.*, 2012, **51**, 12529-12533.
29. L. Wu, Z. Armstrong, S. P. Schröder, C. de Boer, M. Artola, J. M. Aerts, H. S. Overkleeft and G. J. Davies, An overview of activity-based probes for glycosidases, *Curr. Opin. Chem. Biol.*, 2019, **53**, 25-36.
30. M. D. Witte, W. W. Kallemeyjn, J. Aten, K. Y. Li, A. Strijland, W. E. Donker-Koopman, A. M. van den Nieuwendijk, B. Bleijlevens, G. Kramer, B. I. Florea, B. Hooibrink, C. E. Hollak, R. Ottenhoff, R. G. Boot, G. A. van der Marel, H. S. Overkleeft and J. M. Aerts, Ultrasensitive in situ visualization of active glucocerebrosidase molecules, *Nat. Chem. Biol.*, 2010, **6**, 907-913.
31. Q. Su, S. P. Schröder, L. T. Lelieveld, M. J. Ferraz, M. Verhoek, R. G. Boot, H. S. Overkleeft, J. M. Aerts, M. Artola and C. L. Kuo, Xylose-configured cyclophellitols as selective inhibitors for glucocerebrosidase, *Chembiochem*, 2021, **22**, 3090-3098.
32. M. Artola, C. L. Kuo, L. T. Lelieveld, R. J. Rowland, G. A. van der Marel, J. D. C. Codée, R. G. Boot, G. J. Davies, J. M. Aerts and H. S. Overkleeft, Functionalized cyclophellitols are selective glucocerebrosidase inhibitors and induce a bona fide neuropathic Gaucher model in zebrafish, *J. Am. Chem. Soc.*, 2019, **141**, 4214-4218.
33. O. Lopez Lopez, J. G. Fernandez-Bolanos, V. H. Lillelund and M. Bols, Aziridines as a structural motif to conformational restriction of azasugars, *Org. Biomol. Chem.*, 2003, **1**, 478-482.
34. D. E. Koshland, Stereochemistry and the mechanism of enzymatic reactions, *Biol. Rev.*, 1953, **28**, 416-436.
35. K. Y. Li, J. Jiang, M. D. Witte, W. W. Kallemeyjn, W. E. Donker-Koopman, R. G. Boot, J. M. Aerts, J. D. Codée, G. A. van der Marel and H. S. Overkleeft, Exploring functional cyclophellitol analogues as human retaining beta-glucosidase inhibitors, *Org. Biomol. Chem.*, 2014, **12**, 7786-7791.
36. A. K. Yadav, D. L. Shen, X. Shan, X. He, A. R. Kermode and D. J. Vocadlo, Fluorescence-quenched substrates for live cell imaging of human glucocerebrosidase activity, *J. Am. Chem. Soc.*, 2015, **137**, 1181-1189.
37. M. C. Deen, C. Proceviat, X. Shan, L. Wu, D. L. Shen, G. J. Davies and D. J. Vocadlo, Selective fluorogenic beta-glucocerebrosidase substrates for convenient analysis of enzyme activity in cell and tissue homogenates, *ACS Chem. Biol.*, 2020, **15**, 824-829.
38. S. Zhu, M. C. Deen, Y. Zhu, P. A. Gilormini, X. Chen, O. B. Davis, M. Y. Chin, A. G. Henry and D. J. Vocadlo, A fixable fluorescence-quenched substrate for quantitation of lysosomal glucocerebrosidase activity in both live and fixed cells, *Angew. Chem. Int. Ed.*, 2023, DOI: 10.1002/anie.202309306, e202309306.
39. M. Shimokawa, A. Ishiwata, T. Kashima, C. Nakashima, J. Li, R. Fukushima, N. Sawai, M. Nakamori, Y. Tanaka, A. Kudo, S. Morikami, N. Iwanaga, G. Akai, N. Shimizu, T. Arakawa, C. Yamada, K. Kitahara, K. Tanaka, Y. Ito, S. Fushinobu and K. Fujita, Identification and characterization of endo-alpha-, exo-alpha-, and exo-beta-D-arabinofuranosidases degrading lipoarabinomannan and arabinogalactan of mycobacteria, *Nat. Commun.*, 2023, **14**, 5803.
40. S. Pengthaisong, Y. Hua and J. R. Ketudat Cairns, Structural basis for transglycosylation in glycoside hydrolase family GH116 glycosynthases, *Arch. Biochem. Biophys.*, 2021, **706**, 108924.
41. C. L. Kuo, E. van Meel, K. Kytidou, W. W. Kallemeyjn, M. Witte, H. S. Overkleeft, M. Artola and J. M. Aerts, Activity-based probes for glycosidases: profiling and other applications, *Methods Enzymol.*, 2018, **598**, 217-235.
42. C. L. Kuo, W. W. Kallemeyjn, L. T. Lelieveld, M. Mirzaian, I. Zoutendijk, A. Vardi, A. H. Futerman, A. H. Meijer, H. P. Spaink, H. S. Overkleeft, J. M. Aerts and M. Artola, In vivo inactivation of glycosidases by conduritol B epoxide and cyclophellitol as revealed by activity-based protein profiling, *FEBS J.*, 2019, **286**, 584-600.

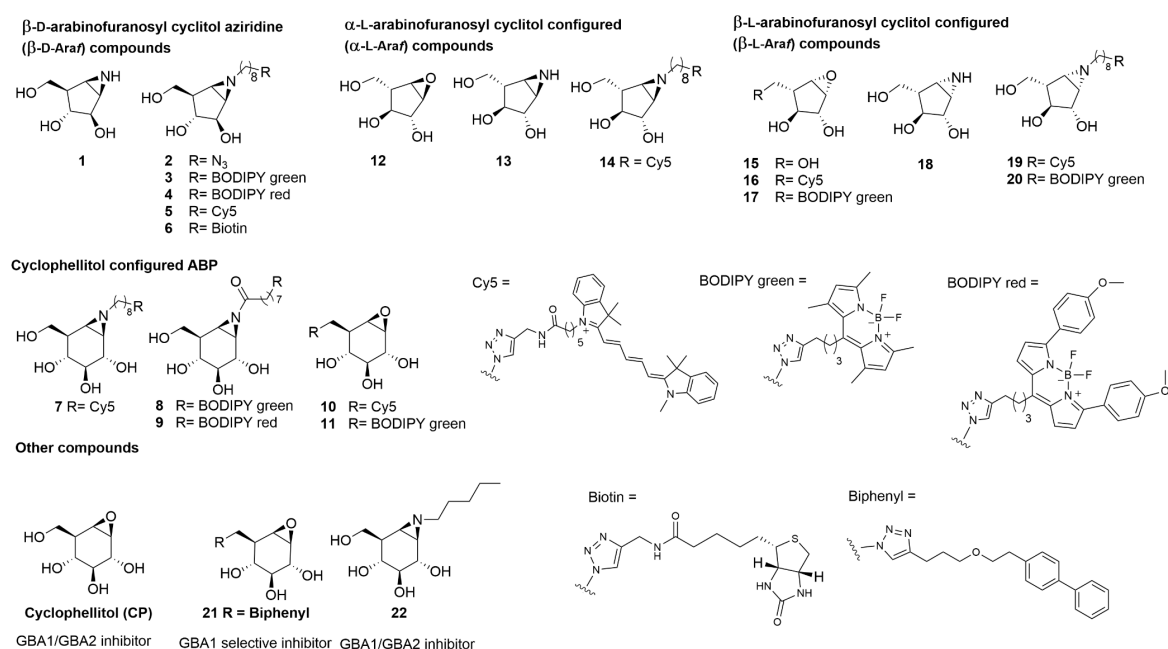
43. D. Lahav, B. Liu, R. van den Berg, A. van den Nieuwendijk, T. Wennekes, A. T. Ghisaidoobe, I. Breen, M. J. Ferraz, C. L. Kuo, L. Wu, P. P. Geurink, H. Ovaa, G. A. van der Marel, M. van der Stelt, R. G. Boot, G. J. Davies, J. M. Aerts and H. S. Overkleeft, A fluorescence polarization activity-based protein profiling assay in the discovery of potent, selective inhibitors for human nonlysosomal glucosylceramidase, *J. Am. Chem. Soc.*, 2017, **139**, 14192-14197.
44. J. M. Aerts, W. E. Donker-Koopman, G. J. Murray, J. A. Barranger, J. M. Tager and A. W. Schram, A procedure for the rapid purification in high yield of human glucocerebrosidase using immunoaffinity chromatography with monoclonal antibodies, *Anal. Biochem.*, 1986, **154**, 655-663.
45. D. G. Waterman, G. Winter, R. J. Gildea, J. M. Parkhurst, A. S. Brewster, N. K. Sauter and G. Evans, Diffraction-geometry refinement in the DIALS framework, *Acta Crystallogr. D*, 2016, **72**, 558-575.
46. P. R. Evans and G. N. Murshudov, How good are my data and what is the resolution?, *Acta Crystallogr. D*, 2013, **69**, 1204-1214.
47. A. J. McCoy, R. W. Grosse-Kunstleve, P. D. Adams, M. D. Winn, L. C. Storoni and R. J. Read, Phaser crystallographic software, *J. Appl. Crystallogr.*, 2007, **40**, 658-674.
48. G. N. Murshudov, P. Skubak, A. A. Lebedev, N. S. Pannu, R. A. Steiner, R. A. Nicholls, M. D. Winn, F. Long and A. A. Vagin, REFMAC5 for the refinement of macromolecular crystal structures, *Acta Crystallogr. D*, 2011, **67**, 355-367.
49. P. Emsley, B. Lohkamp, W. G. Scott and K. Cowtan, Features and development of Coot, *Acta Crystallogr. D*, 2010, **66**, 486-501.
50. F. Long, R. A. Nicholls, P. Emsley, S. Graaeulis, A. Merkys, A. Vaitkus and G. N. Murshudov, AceDRG: a stereochemical description generator for ligands, *Acta Crystallogr. D*, 2017, **73**, 112-122.
51. L. Potterton, J. Agirre, C. Ballard, K. Cowtan, E. Dodson, P. R. Evans, H. T. Jenkins, R. Keegan, E. Krissinel, K. Stevenson, A. Lebedev, S. J. McNicholas, R. A. Nicholls, M. Noble, N. S. Pannu, C. Roth, G. Sheldrick, P. Skubak, J. Turkenburg, V. Uski, F. von Delft, D. Waterman, K. Wilson, M. Winn and M. Wojdyr, CCP4i2: the new graphical user interface to the CCP4 program suite, *Acta Crystallogr. D*, 2018, **74**, 68-84.

Appendix

Table S1. Apparent IC₅₀ values (nM) of arabinofuranosyl cyclitol configured compounds as β -glucosidase inhibitors, determined by 4-MU- β -D-Glc fluorogenic substrate assays.

β-D-Araf	GBA2 ^[a]	rhGBA1 ^[b]	GBA3 ^[c]
1 (aziridine)	> 50000	> 50000	> 50000
2 (octyl-azido)	630.0 \pm 95.6	2730.0 \pm 907.2	8149.6 \pm 1425.8
3 (BODIPY green)	124.4 \pm 4.9	4292.3 \pm 157.1	>10000
4 (BODIPY red)	162.2 \pm 34.7	1777.0 \pm 71.0	> 10000
5 (Cy5)	263.7 \pm 23.5	295.1 \pm 35.3	1518.7 \pm 159.4
6 (Biotin)	8481.0 \pm 762.6	10671.0 \pm 786.5	10281.7 \pm 1896.5
α-L-Araf	GBA2 ^[a]	rhGBA1 ^[b]	GBA3 ^[c]
12 (epoxide)	> 50000	> 50000	> 50000
13 (aziridine)	> 50000	> 50000	> 50000
14 (aziridine Cy5)	1850 (30 min) N.D. (3 h)	> 50000 (30 min) 1340 (3 h)	> 50000 (3 h)
β-L-Araf	GBA2 ^[a]	rhGBA1 ^[b]	GBA3 ^[c]
15 (epoxide)	> 20000	> 20000	> 20000
16 (epoxide Cy5)	> 20000	> 20000	> 20000
17 (epoxide BODIPY green)	> 20000	> 20000	> 20000
18 (aziridine)	> 20000	> 20000	> 20000
19 (aziridine Cy5)	> 20000	> 20000	> 20000
20 (aziridine BODIPY green)	20000	> 20000	> 20000

N.D. = not determined, enzyme: [a] GBA2 = GBA1/GBA2 KO and GBA2 OE HEK293T cell lysate, [b] rhGBA1 = isolated Imiglucerase (Cerezyme®), [c] GBA3 = GBA1/GBA2 KO and GBA3 OE HEK293T cell lysate. Incubation time of compounds and enzymes is 30 min, assays was also conducted for 3 h incubation of compound **14** and marked in the table. Error ranges = \pm SD, n = 3 replicates for β -D-Araf aziridine compounds, n = 1 replicates for α -L-Araf and β -L-Araf compounds.

**Figure S1.** Compound library used in this chapter.

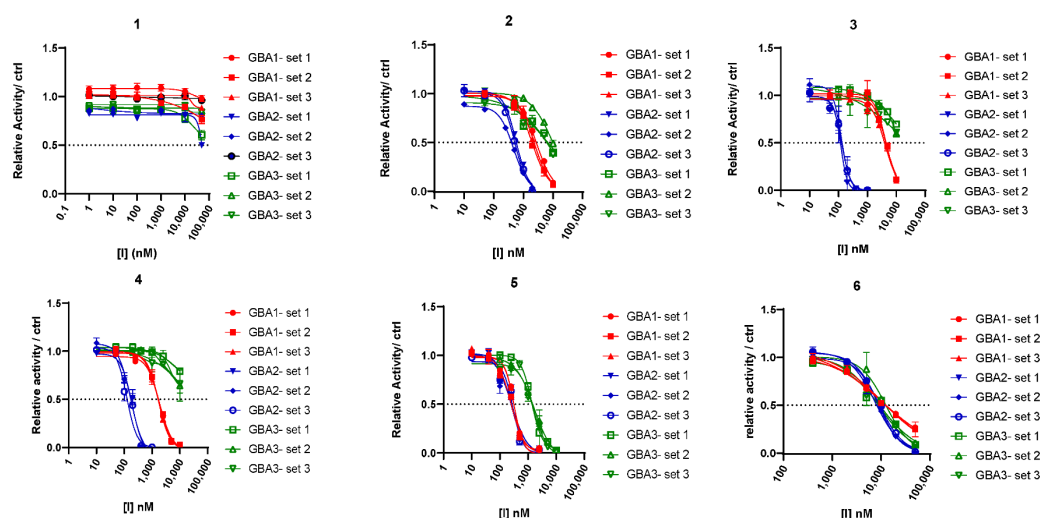
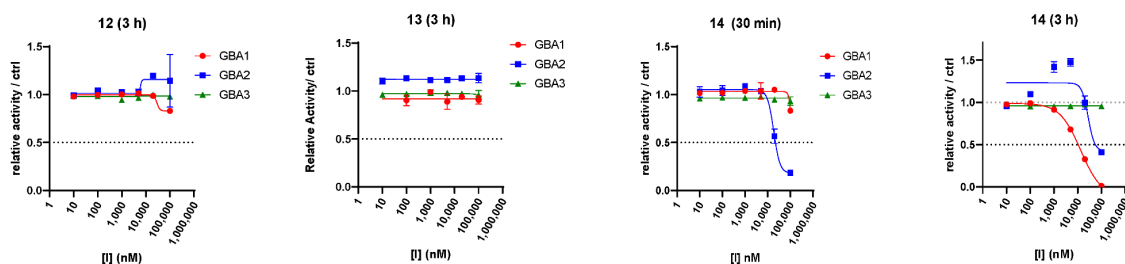
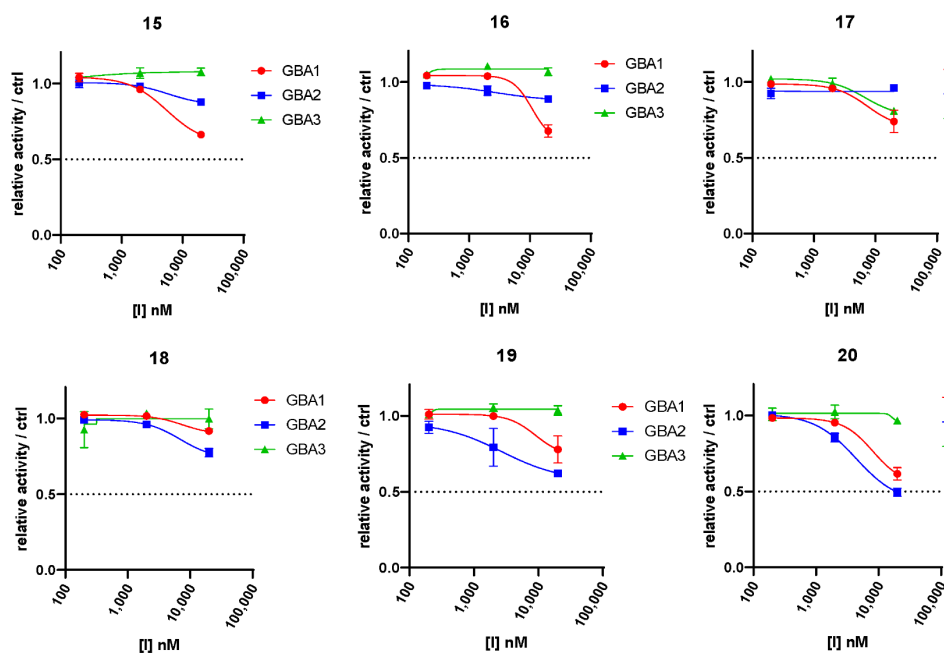
Apparent IC₅₀ curves of β -D-Araf compoundsApparent IC₅₀ curves of α -L-Araf compoundsApparent IC₅₀ curves of β -L-Araf compounds

Figure S2. Apparent IC₅₀ curves of arabinofuranosyl configured compounds (1-6, 12-20) based on 4MU fluorogenic substrate assays using 4MU- β -D-Glc. The enzymes used were recombinant GBA1 (Imiglucrase), lysates of GBA1/GBA2 KO cells with overexpression of either GBA2 or GBA3. Incubation time for enzyme with the inhibitors is 30 min (if not otherwise stated) or 3 h (marked as '3 h' in figures) at the appropriate pH.

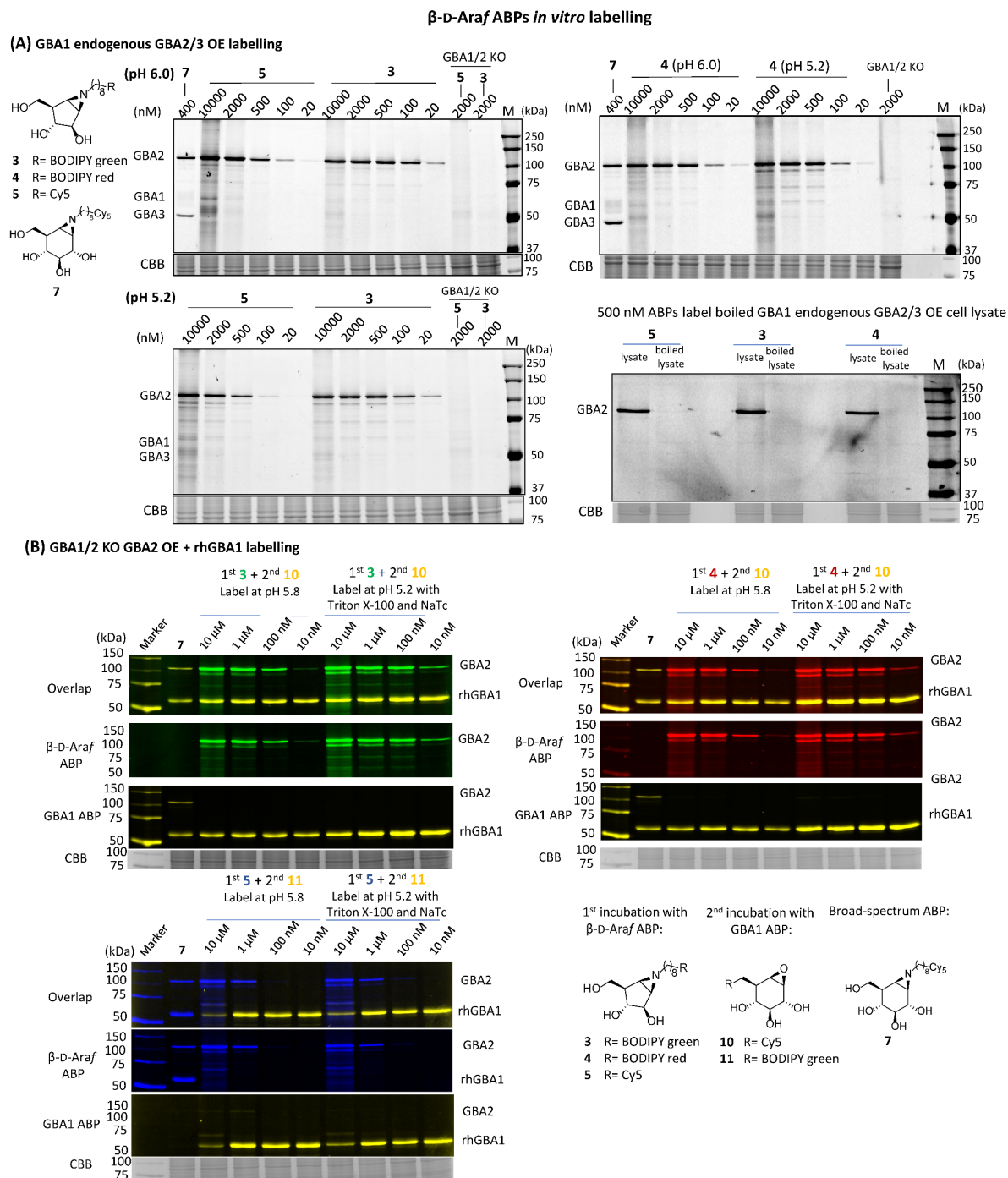


Figure S3-1. *In vitro* reactivity of β -D-Araf aziridine ABPs **3-5** towards β -glucosidases. (A) β -D-Araf ABPs incubated with HEK293T GBA1 endogenous and GBA2/GBA3 OE cell lysate *in vitro* for 30 min at 37 °C. To test the activity of ABP **3-5** towards boiled lysates (boiled for 5 min at 98 °C). The boiled lysates were incubated with ABPs **3-5** for 30 min at 37 °C. Result was read out by SDS-PAGE and fluorescence scanning. (B) β -D-Araf ABPs **3-5** labelled mixture of HEK293T GBA1/GBA2 KO GBA2 OE cell lysates and recombinant human GBA1 (rhGBA1) at optimal conditions of GBA2 (left) or rhGBA1 (right). Lysate mixtures were first incubated with β -D-Araf ABPs **3-5** for 30 min at 37 °C, followed by labeling of rhGBA1 by ABP **10** at 500 nM (for **3** and **4**) or ABP **11** at 500 nM (for **5**). Lane marked as '7', only ABP **7** was added to show the presence of GBA2 and rhGBA1. To label rhGBA1 at its optimal condition, McIlvaine buffer (pH 5.2) with 0.1% (v/v) Triton X-100 and 0.2% (w/v) sodium taurocholate (NaTc) was used.

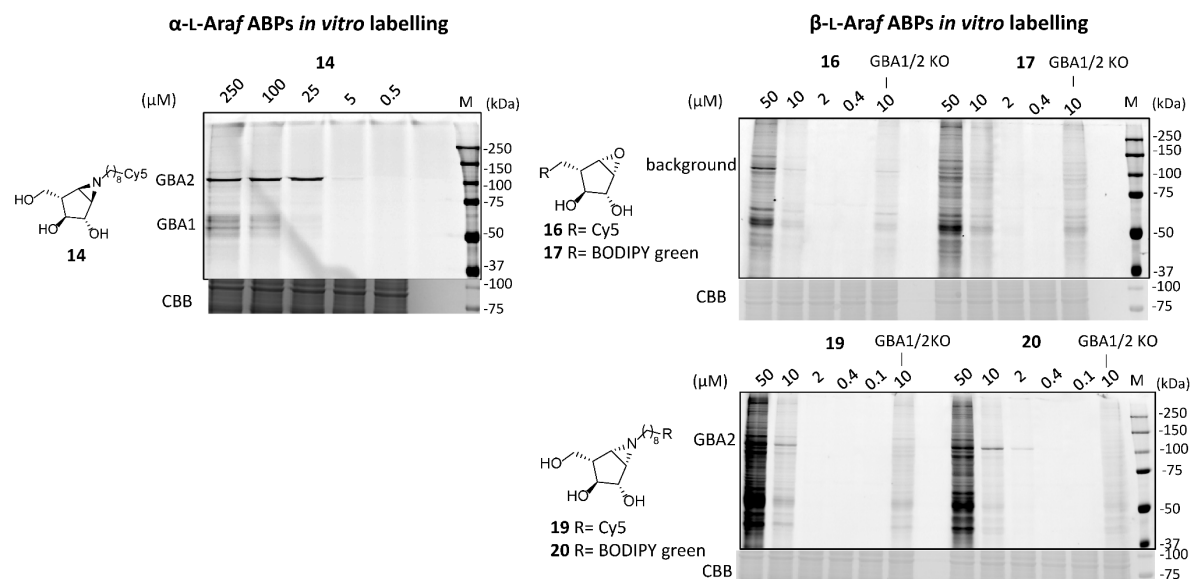


Figure S3-2. Reactivity of α-L-Araf and β-L-Araf ABPs towards β-glucosidases. HEK293T GBA1 endogenous and GBA2/GBA3 OE cell lysates were used and incubated with these ABPs *in vitro* for 30 min at 37 °C, followed by SDS-PAGE and fluorescent scanning of the gels. Coomassie brilliant blue staining (CBB) was performed as a loading control.

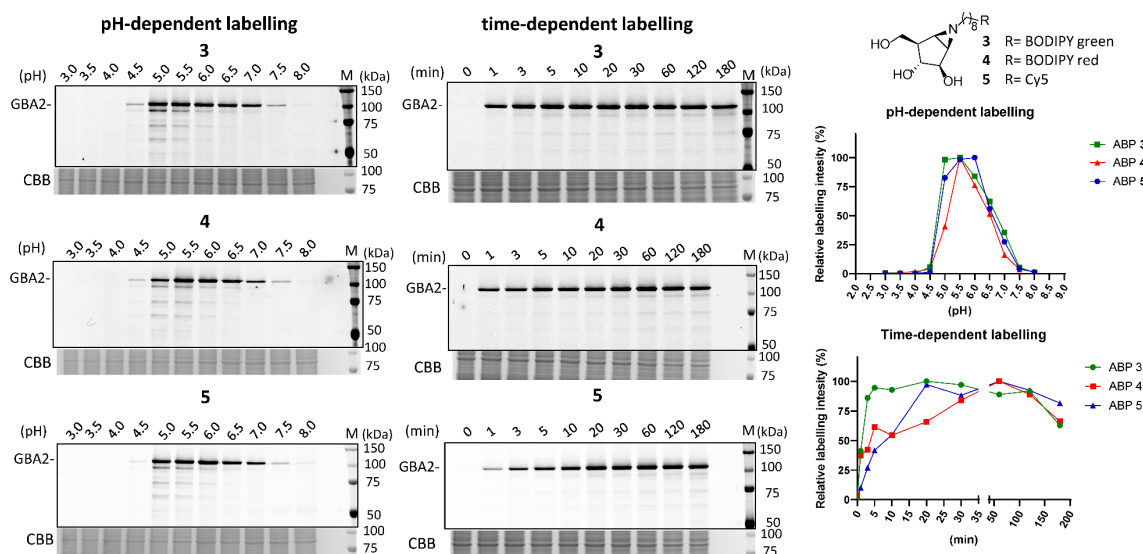


Figure S4. *In vitro* pH- or time-dependent reactivity of β-D-Araf ABPs 3-5 (500 nM) towards β-glucosidases. HEK293T GBA1 endogenous and GBA2/GBA3 OE cell lysates were used and incubated with ABP 3-5 at the indicated conditions. Fluorescence intensity of ABPs 3-5 was quantified and the result was presented as the curve on the right.

The GBA2 interaction efficiency of β -D-Araf aziridine ABPs **3-5** and cyclophellitol-aziridine ABP **7** was compared by simultaneous incubation with GBA2 for competition. The mixture of β -D-Araf aziridine ABP (**3-5**) against cyclophellitol-aziridine ABP (**7** or **8**) in varying ratios was set up for assays. For each ratio, the amount of total molecules is same (final 500 nM concentration). After incubation, result was read out by SDS-PAGE and fluorescence scanning. As shown in Figure S5, ABP **3** and **4** have equal GBA2 labelling efficiency with ABP **7** at 90:10 ratio (nM of β -D-Araf aziridine ABP : cyclophellitol-aziridine ABP) and ABP **5** only able to label GBA2 at 100:1 ratio when competing with ABP **8**.

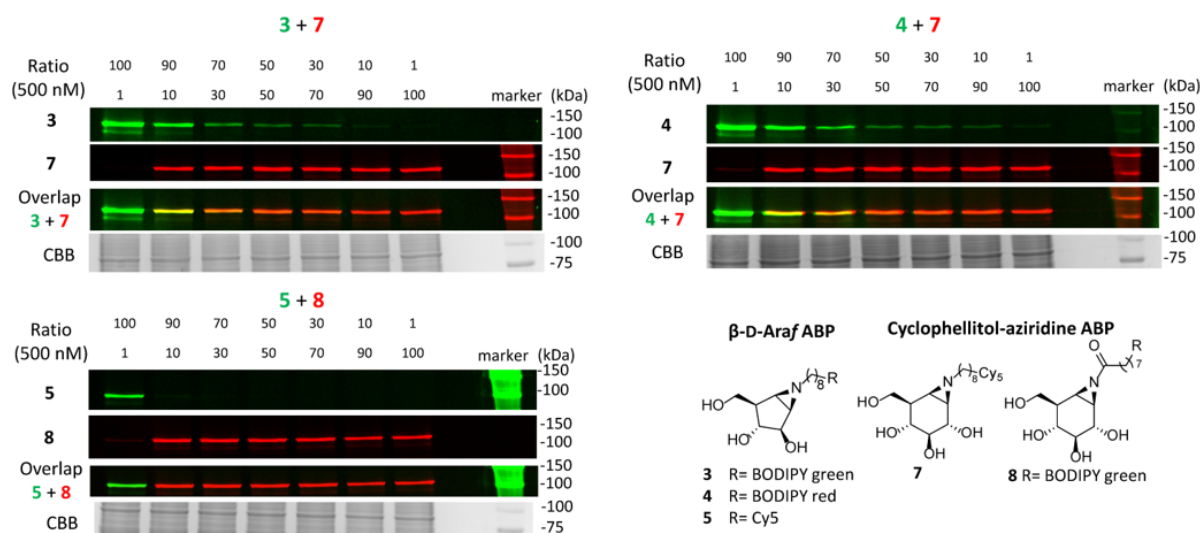


Figure S5. Comparison of the interaction efficiency between β -D-Araf aziridine ABPs (**3-5**) and cyclophellitol-aziridine ABPs (**7** or **8**) towards GBA2 *in vitro*. GBA1/GBA2 KO GBA2 OE HEK293T cell lysates were incubated with a total final amount of 500 nM of β -D-Araf ABP and cyclophellitol aziridine ABP **7** (or **8**) mixture in varying ratio as indicated.

To assess the irreversibility of the GBA2 labelling by β -D-Araf cyclitol aziridines, competitive ABPP experiment was conducted. First, lysates of HEK293T GBA1/GBA2 KO cells with GBA2 OE was preincubated with β -D-Araf compound **2-4**. After employing a desalting column to remove unbound probe with three consecutive washing steps, the lysate was next incubated with fluorescent broad-spectrum β -glucosidase ABP **7**, an ABP irreversibly binds β -glucosidases, for variable time. No further labelling with **7** was observed compared to the control set (first lane of each set), indicating that the GBA2 molecule had formed a covalent and irreversible bond with β -D-Araf compound **2-4**, preventing binding of ABP **7** to GBA2 anymore (Figure S6A). In complementary experiments in which GBA2 lysates were incubated with β -D-Araf compounds **2-5** followed by washing to remove any unbound probe, no recovery of GBA2 activity was observed even after 96 h (Figure S6C).

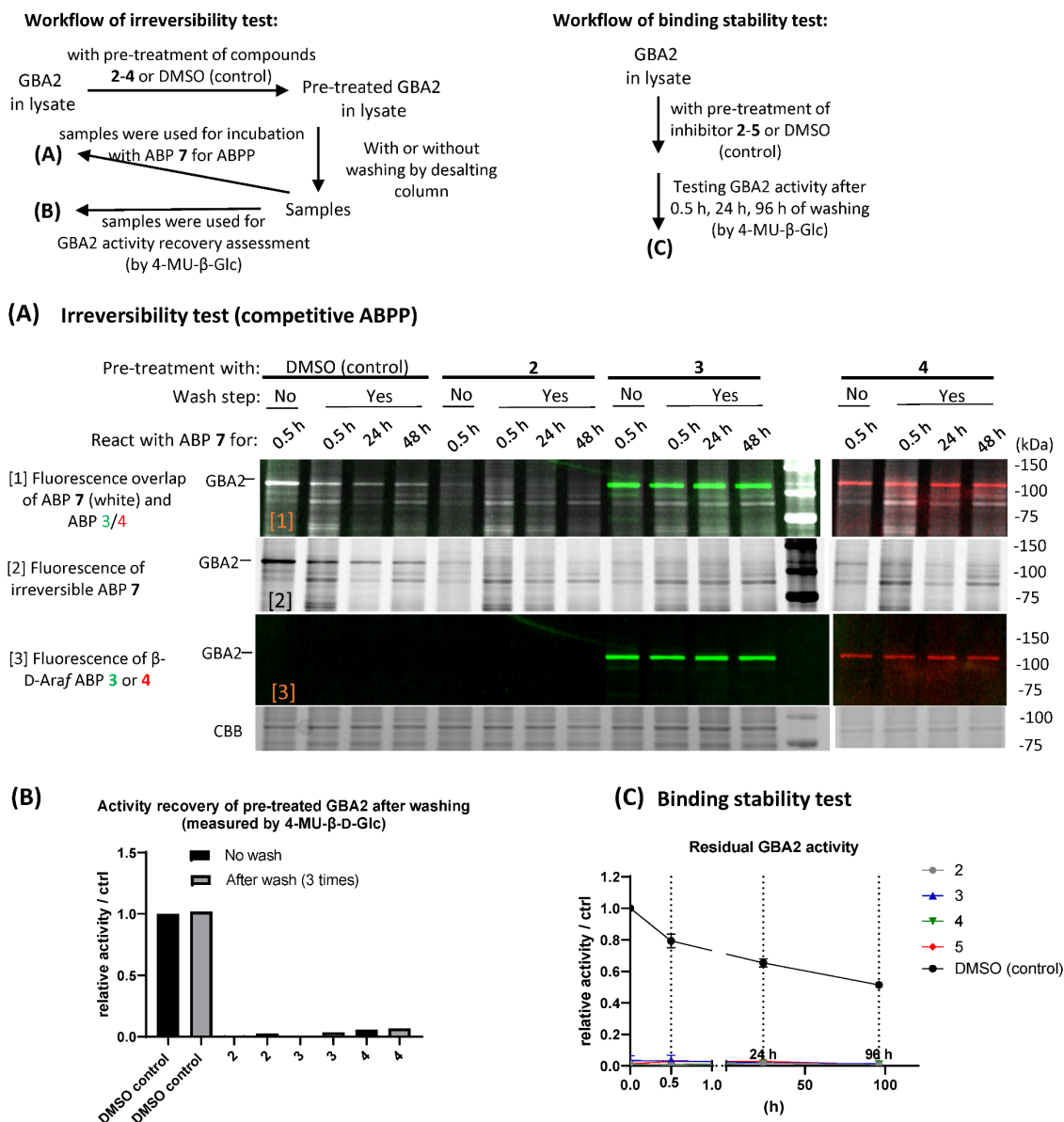


Figure S6. (A) Irreversibility of β -D-Araf aziridine compounds revealed by a competition ABPP assay. Lysates of GBA1/GBA2 KO cells with GBA2 overexpression were first pre-treated with the β -D-Araf compounds **2-4** or an equivalent volume without compound (0.5% DMSO final concentration in this step as control) for 30 min at 37°C, followed by three times of consecutive washing with a desalting column and incubation with 1 μ M irreversible ABP **7** for 30 min (for competition analysis) after the washing step, the final concentration of DMSO in all samples after addition of ABP **7** was maintained at 1%. Lanes: 'No wash, 0.5 h' = GBA2 pre-treated with compounds **2-4** or DMSO, without undergoing the washing steps, followed by incubating with ABP **7** for 0.5 h at 37 °C. The samples that underwent the washing step (lanes marked with 'wash step, yes'), were incubated either with ABP **7** for 24 h or 48 h at 4 °C (for enzyme stability reasons), or with ABP **7** for 0.5 h at 37 °C. Afterwards, samples were subjected to ABPP. (B) A subset of above samples pre-treated with compounds **2-4** or DMSO, were washed three times with a desalting column, subsequently, samples were measured for GBA2 activity by the 4-MU- β -D-Glc fluorogenic substrate assay, to assess whether GBA2, which had reacted with compounds **2-4**, could recover activity after the washing step. (C) Binding stability of compounds **2-5** towards GBA2 revealed by the 4-MU- β -D-Glc fluorogenic substrate assay. Lysates of GBA1/GBA2 KO cells with GBA2 overexpression were pre-treated with compounds **2-5** or an equivalent volume of DMSO (as control) and washed once by a desalting column, then the lysates were stored at 4°C until the time point for activity measurement was reached. 0 h = measured activity of lysates prior to washing by desalting column. '0.5 h, 24 h, or 96 h' = measured activity of lysates at a certain time point after washing steps.

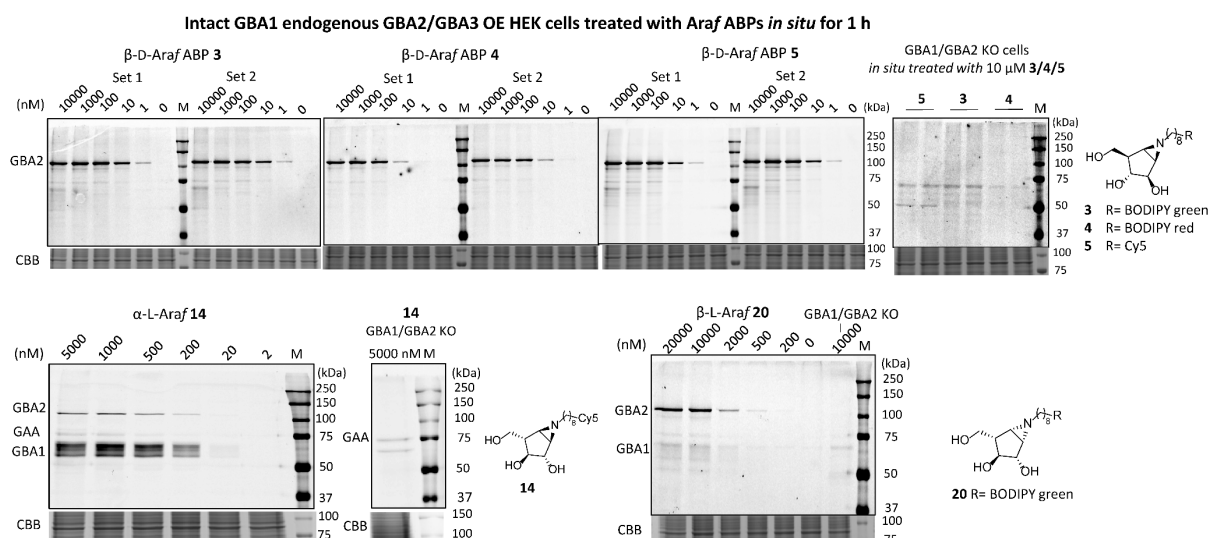


Figure S7. Intact HEK293T cells, either with endogenous GBA1 and GBA2/GBA3 OE, or with GBA1/GBA2 KO, were incubated with arabinofuranosyl cyclitol configured ABPs (**3-5**, **14**, **20**) for 1 h *in situ*, then cells were lysed and subjected to ABPP. GAA = Lysosomal α -glucosidase (EC 3.2.1.20, CAZy GH31).

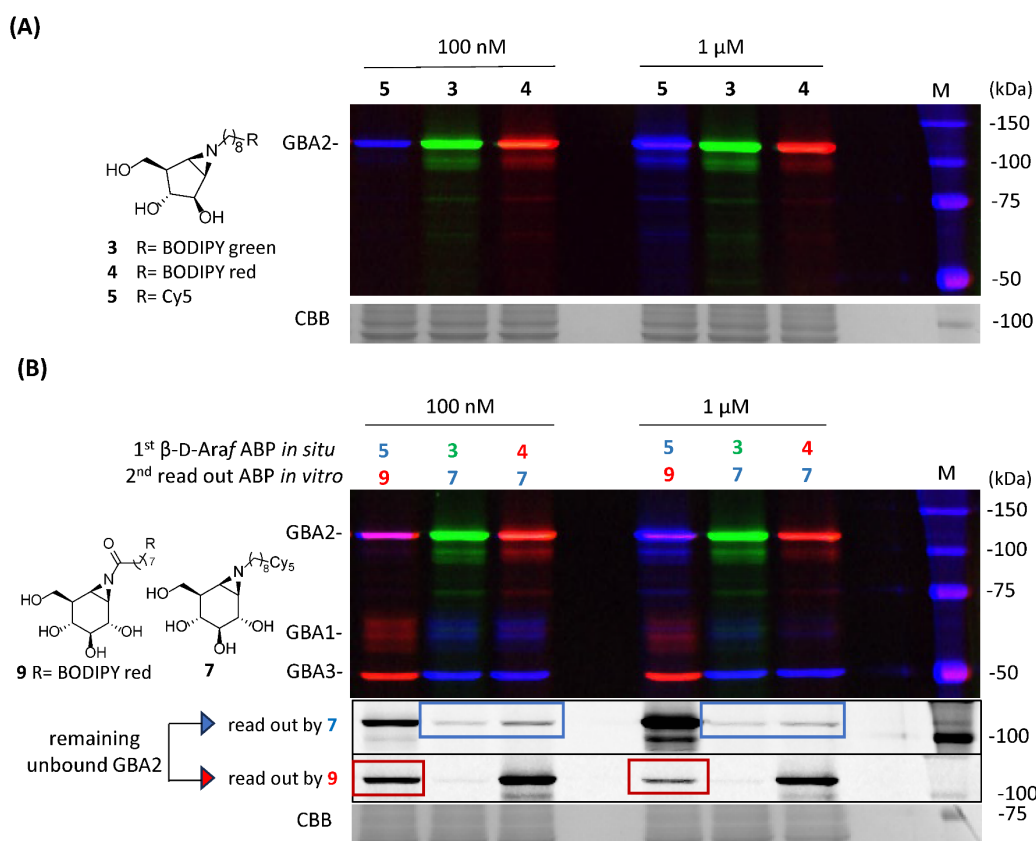


Figure S8. β -D-Araf aziridine ABPs incubated with intact HEK293T cells (endogenous GBA1 and GBA2/GBA3 OE) for 24 h *in situ*. Intact HEK293T cells were treated with β -D-Araf ABPs (**3-5**) for 24 h at 37 $^{\circ}$ C under 7% CO_2 , then cells were collected and lysed, followed by ABPP. (A) ABPP of intact cells labelled by β -D-Araf ABPs (**3-5**) *in situ*. (B) Intact cells labelled by β -D-Araf ABPs (**3-5**) *in situ* were lysed and followed by *in vitro* incubation with 500 nM broad-spectrum β -glucosidase ABP **7** (for **3** and **4**) or **11** (for **5**), to reveal residual active β -glucosidases not bound by ABP **3-5**.

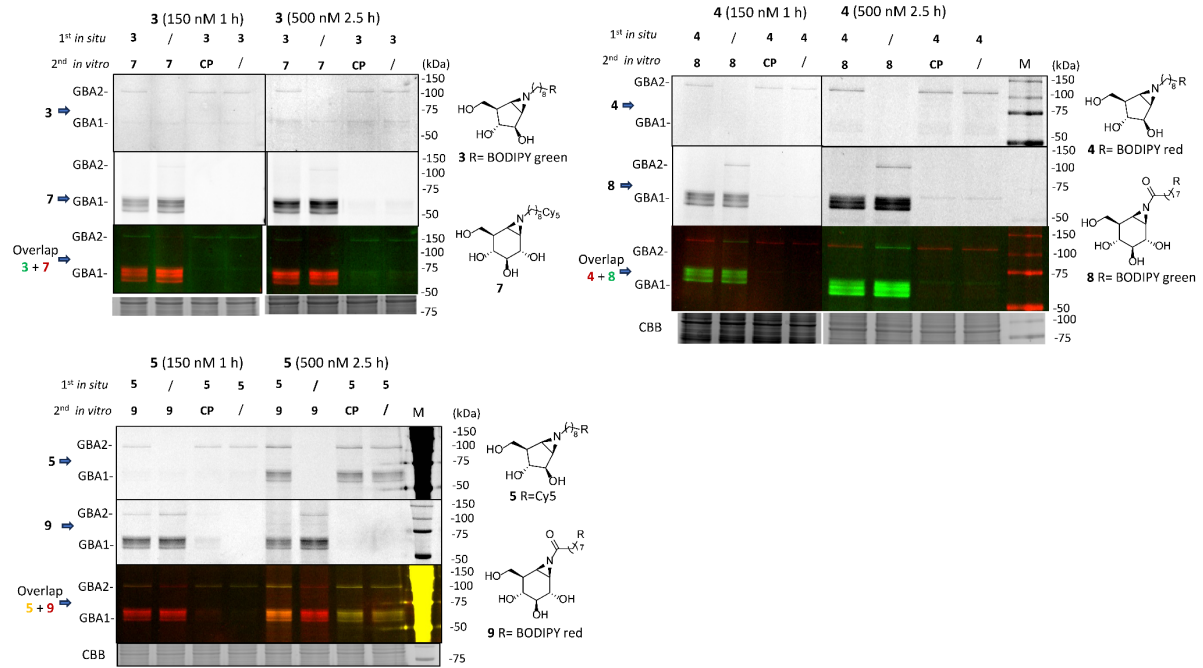


Figure S9. Intact wild-type HEK293T cells treated with β -D-Araf aziridine ABPs (3-5) *in situ*. β -D-Araf ABPs were firstly incubated with intact wild-type HEK293T *in situ* for the indicated incubation time, then cells were harvested, followed by adding lysis buffer (potassium phosphate buffer) containing ABP (7, 8, or 9, 1 μ M final concentration with a 1% DMSO final concentration), or cyclophellitol (CP, 1 μ M final concentration with a 1% DMSO final concentration), or the blank ('/') 1% DMSO (final concentration) for ABPP analysis. Then harvested cells were lysed in lysis buffer and incubated for 30 min on ice and 30 min at 37°C *in vitro* for ABPP.

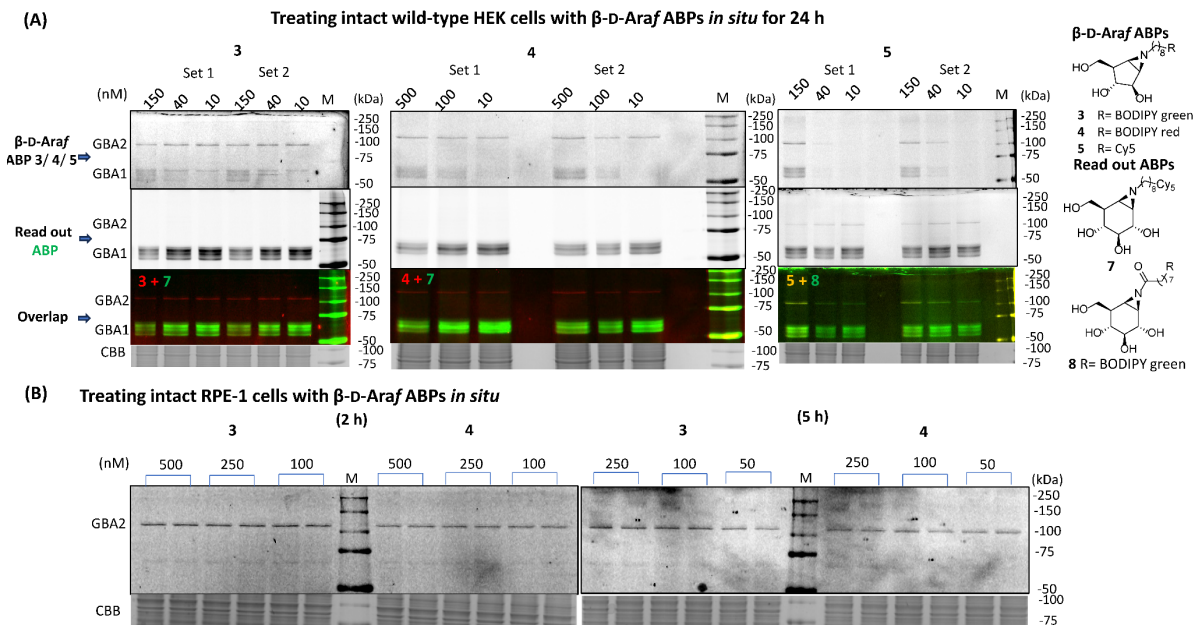


Figure S10. (A) Intact HEK293T wild-type cells treated with β -D-Araf aziridine ABPs 3-5 *in situ* for 24 h. Intact wild-type HEK293T cells were incubated with described concentration of β -D-Araf ABP, after 24 h, cells were collected and lysed, residual GBA2 and GBA1 activity were read out by incubation with 500 nM ABP 7 (for 3 and 4) or ABP 8 (for 5). (B) Wild-type human retinal pigment epithelial-1 (RPE-1) cells were treated with β -D-Araf aziridine ABPs 3-5 for either 2 h or 5 h *in situ*. Then cells were collected, lysed, and subjected to ABPP.

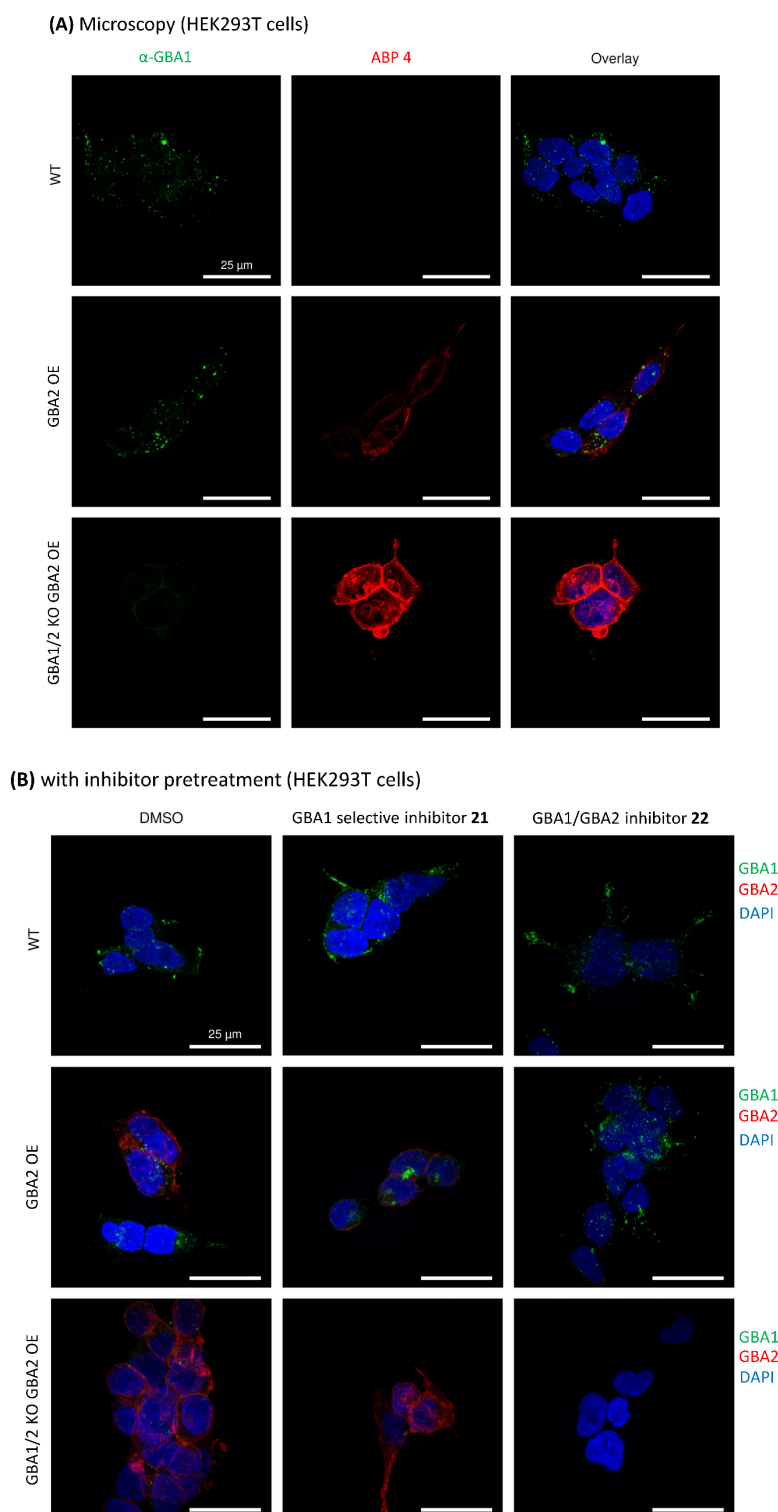


Figure S11. Confocal fluorescence microscopy of GBA1 and GBA2. Applied for incubation were β -D-Araf ABP **4** and anti-GBA1 (α -GBA1) antibody. Used were different HEK293T cells: HEK293T wild-type (WT), GBA2 overexpression (OE), and GBA1/GBA2 knock out (KO) with GBA2 overexpression (OE). Cells were treated with 50 nM β -D-Araf aziridine ABP **4** (Red) for 2 h. After fixation all cells were stained for GBA1 using an anti-GBA1-antibody with Alexa Fluor® 647 conjugation (green) and nuclei were stained with 10 μ g/ml DAPI (Blue). (A) without inhibitor pretreatment. α -GBA1 = immunofluorescent stain of α -GBA1 antibody, GBA2 = fluorescent labelling of ABP **4**, DAPI = nuclei stained by DAPI. (B) microscopy with inhibitor pretreatment. DMSO = same concentration of DMSO (as sets of **21** and **22**) without inhibitor was added (pre-treatment). 100 nM **21** and 500 nM **22** were used for the inhibitor pretreatments.

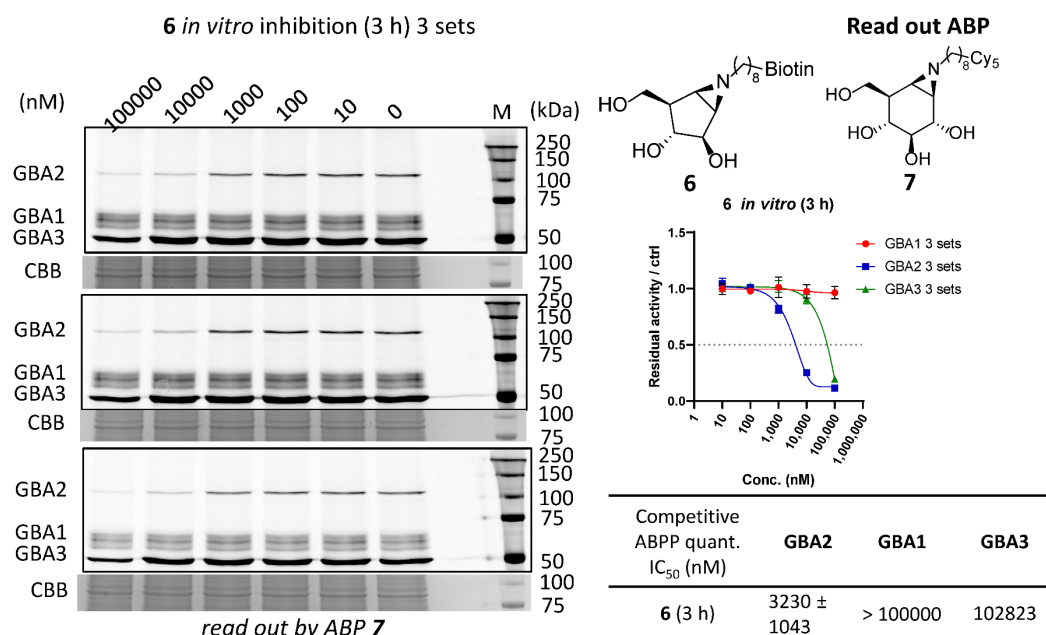


Figure S12. Assessment of the affinity and selectivity of a biotin-tagged compound **6** via *in vitro* competitive ABPP assay. Lysates of HEK293T GBA1 endogenous and GBA2/GBA3 OE cell were pre-treated with **6** for a 3 h incubation at 37 °C, then the residual active β-glucosidases were read out by 500 nM ABP **7** by competitive ABPP quantified IC₅₀ was determined by the fluorescence intensity of ABP **7**.

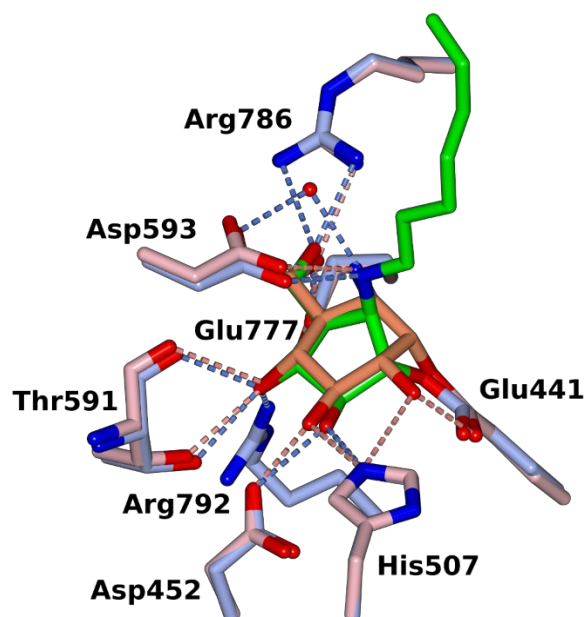


Figure S13. Overlay of structures of TxGH116 complexes with cyclophellitol aziridine (8R06.pdb) and compound **2** (8R1M.pdb). C atoms are shown in orange for cyclophellitol aziridine and light pink for interacting side chains (with hydrogen bonds as coral dashed lines), and in green for **2** and ice blue for interacting side chains (with hydrogen bonds as blue dashed lines).

Table S2. Data collection and refinement statistics for the complex of TxGH116 and β -D-Araf **2**.

TxGH116-2	
Data collection	
Space group	P 21 21 21
Cell dimensions	
<i>a</i> , <i>b</i> , <i>c</i> (Å)	55.0, 165.1, 178.9
α , β , γ (°)	90.0, 90.0, 90.0
Resolution (Å)	56.09 – 1.90 (1.93 - 1.90)*
Total no. reflections	1381158
No. unique reflections	129333 (6302)
<i>R</i> _{sym} Or <i>R</i> _{merge}	0.249 (2.052)
<i>R</i> _{pim}	0.079 (0.643)
<i>CC</i> _{1/2}	0.996 (0.554)
<i>I</i> / σ <i>I</i>	7.1 (1.3)
Completeness (%)	100.0 (100.0)
Redundancy	10.7 (10.9)
Refinement	
No. reflections working set	122902
No. reflections test set	6306
<i>R</i> _{work} / <i>R</i> _{free}	0.18/0.23
No. atoms	
Protein	12592
Ligand/ion	53
Water	880
<i>B</i> -factors	
Protein	24.9
Ligand/ion	31.9
Water	29.9
R.m.s deviations	
Bond lengths (Å)	0.006
Bond angles (°)	1.513
Ramachandran plot residues	
In most favorable regions (%)	95.1
In allowed regions (%)	4.4
PDB code	8R1M

* Figures for highest resolution shell given in parentheses

Compound synthesis

Compounds used in this work were synthesized and obtained at the Bio-organic Synthesis Department, Leiden Institute of Chemistry at Leiden University, according to published methods:

β -D-arabinofuranosyl cyclitol-aziridines : **1**,¹ **2-6**.²

α -L-arabinofuranosyl cyclitol-configured compounds: **12-14**.³

β -L-arabinofuranosyl cyclitol-configured compounds: **15**⁴ and **16-20**.⁵

Cyclophellititol-configured compounds: **7**⁶, **8**⁷, **9**⁸, **10**⁹ and **11**.¹⁰

Other compounds: **21**⁹, **22**.¹¹

Supplementary references

1. O. Lopez Lopez, J. G. Fernandez-Bolanos, V. H. Lillielund and M. Bols, Aziridines as a structural motif to conformational restriction of azasugars, *Org. Biomol. Chem.*, 2003, **1**, 478-482.
2. S. P. Schröder, Cyclophellitol analogues for profiling of exo- and endo-glycosidases, Thesis, Leiden University, 2018, <https://hdl.handle.net/1887/62362>.
3. N. G. S. McGregor, M. Artola, A. Nin-Hill, D. Linzel, M. Haon, J. Reijngoud, A. Ram, M. N. Rosso, G. A. van der Marel, J. D. C. Codée, G. P. van Wezel, J. G. Berrin, C. Rovira, H. S. Overkleeft and G. J. Davies, Rational design of mechanism-based inhibitors and activity-based probes for the identification of retaining α -l-arabinofuranosidases, *J. Am. Chem. Soc.*, 2020, **142**, 4648-4662.
4. N. G. S. McGregor, J. Coines, V. Borlandelli, S. Amaki, M. Artola, A. Nin-Hill, D. Linzel, C. Yamada, T. Arakawa, A. Ishiwata, Y. Ito, G. A. van der Marel, J. D. C. Codée, S. Fushinobu, H. S. Overkleeft, C. Rovira and G. J. Davies, Cysteine nucleophiles in glycosidase catalysis: application of a covalent β -l-arabinofuranosidase inhibitor, *Angew. Chem. Int. Ed.*, 2021, **60**, 5754-5758.
5. V. Borlandelli, W. Offen, O. Moroz, A. Nin-Hill, N. McGregor, L. Binkhorst, A. Ishiwata, Z. Armstrong, M. Artola, C. Rovira, G. J. Davies and H. S. Overkleeft, β -l-Arabinofurano-cyclitol aziridines are covalent broad-spectrum inhibitors and activity-based probes for retaining β -l-arabinofuranosidases, *ACS Chem. Biol.*, 2023, **18**, 2564-2573.
6. S. P. Schröder, J. W. van de Sande, W. W. Kallemeyjn, C. L. Kuo, M. Artola, E. J. van Rooden, J. Jiang, T. J. M. Beenakker, B. I. Florea, W. A. Offen, G. J. Davies, A. J. Minnaard, J. M. Aerts, J. D. C. Codée, G. A. van der Marel and H. S. Overkleeft, Towards broad spectrum activity-based glycosidase probes: synthesis and evaluation of deoxygenated cyclophellitol aziridines, *Chem. Commun.*, 2017, **53**, 12528-12531.
7. W. W. Kallemeyjn, K. Y. Li, M. D. Witte, A. R. Marques, J. Aten, S. Scheij, J. Jiang, L. I. Willems, T. M. Voorn-Brouwer, C. P. van Roomen, R. Ottenhoff, R. G. Boot, H. van den Elst, M. T. Walvoort, B. I. Florea, J. D. Codée, G. A. van der Marel, J. M. Aerts and H. S. Overkleeft, Novel activity-based probes for broad-spectrum profiling of retaining β -exoglucosidases in situ and in vivo, *Angew. Chem. Int. Ed.*, 2012, **51**, 12529-12533.
8. K.-Y. Li, J. Jiang, M. D. Witte, W. W. Kallemeyjn, H. van den Elst, C.-S. Wong, S. D. Chander, S. Hoogendoorn, T. J. M. Beenakker, J. D. C. Codée, J. M. Aerts, G. A. van der Marel and H. S. Overkleeft, Synthesis of cyclophellitol, cyclophellitol aziridine, and their tagged derivatives, *Eur. J. Org. Chem.*, 2014, **2014**, 6030-6043.
9. M. Artola, C. L. Kuo, L. T. Lelieveld, R. J. Rowland, G. A. van der Marel, J. D. C. Codée, R. G. Boot, G. J. Davies, J. M. Aerts and H. S. Overkleeft, Functionalized cyclophellitols are selective glucocerebrosidase inhibitors and induce a bona fide neuropathic Gaucher model in zebrafish, *J. Am. Chem. Soc.*, 2019, **141**, 4214-4218.
10. M. D. Witte, W. W. Kallemeyjn, J. Aten, K. Y. Li, A. Strijland, W. E. Donker-Koopman, A. M. van den Nieuwendijk, B. Bleijlevens, G. Kramer, B. I. Florea, B. Hooibrink, C. E. Hollak, R. Ottenhoff, R. G. Boot, G. A. van der Marel, H. S. Overkleeft and J. M. Aerts, Ultrasensitive in situ visualization of active glucocerebrosidase molecules, *Nat. Chem. Biol.*, 2010, **6**, 907-913.
11. K. Y. Li, J. Jiang, M. D. Witte, W. W. Kallemeyjn, W. E. Donker-Koopman, R. G. Boot, J. M. Aerts, J. D. Codée, G. A. van der Marel and H. S. Overkleeft, Exploring functional cyclophellitol analogues as human retaining β -glucosidase inhibitors, *Org. Biomol. Chem.*, 2014, **12**, 7786-7791.

Chapter 4

Reactivity of cytosolic retaining β -glucosidase towards retaining glycosidase ABPs

Qin Su, Mats Bulterman, Maria Ferraz, Max Janssen, Rita Petracca, Marta Artola, Rolf G. Boot, Herman S. Overkleeft, and Johannes M. F. G. Aerts are acknowledged for their contributions to this chapter.

Abstract

The cytosolic glucosidase GBA3 (EC 3.2.1.21, CAZy GH1) is an enzyme with broad substrate specificity in mammals, where it is thought to partake in the degradation of glycosylated xenobiotics. In humans, inherited deficiency of GBA3 is relatively common but appears not to be accompanied by clinical manifestations. GBA3 is reported to hydrolyze a variety of glycosidic substrates, as is confirmed in this chapter for 4-methylumbelliferyl (4-MU)- β -D-glucopyranoside, 4-MU- β -D-galactopyranoside, 4-MU- β -D-fucopyranoside, 4-MU- β -D-xylopyranoside, and 4-MU- α -L-arabinopyranoside. Moreover, β -D-galactose-configured and α -L-arabinopyranose-configured cyclophellitol-aziridine ABPs were identified that label GBA3 with some selectivity over the other two human retaining glucosidases, GBA1 and GBA2.

Introduction

The cytosolic β -glucosidase, GBA3, also referred to as non-specific β -glucosidase, broad-specificity β -glycosidase, cytosolic β -glucosidase-like protein-1 (cBGL1), and Klotho related protein (KLRP), is a 469 amino acid cytosolic retaining β -exoglucosidase.¹⁻⁶ The human *GBA3* gene is located in locus 4p15.2, and GBA3 is expressed as a cytosolic protein in the liver, kidneys, and intestine, amongst other tissues.⁵ GBA3 (EC 3.2.1.21) is classified as a member of family GH1 of retaining β -glycosidases in the CAZy database (www.cazy.org). The crystal structure of GBA3 reveals structural features of its catalytic pocket.^{5,7,8} GBA3 employs a catalytic nucleophile (E373) and acid/base (E165) in β -glucoside hydrolysis.^{5,7} GBA3 was found to hydrolyze many xenobiotic glycosides including dietary flavonoids and isoflavones and was therefore considered to play a role in xenobiotic metabolism.^{3,9} In addition, it has been reported that GBA3 stabilizes NEU2 (sialidase-2, a cytosolic sialidase), and has a possible role in the catabolism of cytosolic sialic acid-free N-glycans.¹⁰ Besides GBA3, human tissue express two other retaining β -glucosidases, namely, lysosomal GBA1 (EC 3.2.1.45, GH30) and cytosol facing membrane-bound GBA2 (EC 3.2.1.45, GH116).^{7,11,12} Deficiency of GBA1 is at the basis of Gaucher disease (GD), a lysosomal storage disorder characterized by massive accumulation of glucosylceramide (GlcCer) in lysosomes of tissue macrophages.¹³ Patients with the most common GD variant (type 1) do not develop neuropathological complaints, while patients suffering from the rarer variants of GD (type 2 and type 3) eventually develop potentially fatal CNS symptoms.¹⁴ Deficiency of GBA2 in turn is associated with hereditary spastic paraplegia.¹⁴ Dekker *et al.* reported that a common loss-of-function mutation in GBA3 does not correlate with type 1 GD severity.¹⁵ This study corroborates earlier work by Beutler and colleagues, who did not observe a relationship between any of four GBA3 gene polymorphisms with GD manifestation severity.¹⁶ The physiological role of GBA3 remains therefore enigmatic.

GBA3 differs from the other two cellular β -glucosidases (GBA1 and GBA2) in that it has a broad substrate specificity, in particular with respect to the nature of the monosaccharide in its substrate glycosides. GBA3 hydrolyzes, besides β -D-glucopyranosides, also β -D-galactopyranosides (β -D-Gal), β -D-fucopyranosides (β -D-Fuc), β -D-xylopyranosides (β -D-Xyl), and α -L-arabinosides.^{1,2} Besides substrate hydrolysis, GBA3 has also been shown to have transglycosylase activity, producing β -xylosyl-cholesterol (XylChol) from both xylosylceramide and 4-MU- β -D-xylopyranoside as sugar donor and cholesterol as acceptor.¹⁷ Transglycosylation activity is also a feature of GBA1 and GBA2, which transfer β -glucopyranose or β -galactopyranose from GlcCer or GalCer to cholesterol to produce β -glucosyl-cholesterol (GlcChol) or β -galactosyl-cholesterol (GalChol), respectively.^{18,19} GBA3 however, while capable of producing XylChol, does not produce GlcChol, as GBA1 and GBA2 do.¹⁷

The studies described in this chapter were aimed to discover new tools to study GBA3 activity in complex biological milieu. For this purpose, recombinant GBA3 was exposed to a variety of fluorogenic substrates as well as cyclophellitol-based activity-based probes (ABPs) of various nature (configuration, substitution pattern). These studies identify that 4-MU- β -D-Fuc and 4-MU- α -L-Arap are both efficiently and with reasonable selectivity processed by GBA3, and reveal that β -D-galactose configured (β -D-Gal) cyclophellitol ABP **3** and α -L-arabinopyranose configured (α -L-Arap) cyclophellitol aziridine ABP **5** (Figure 1) label GBA3 with some selectivity over GBA1 and GBA2.

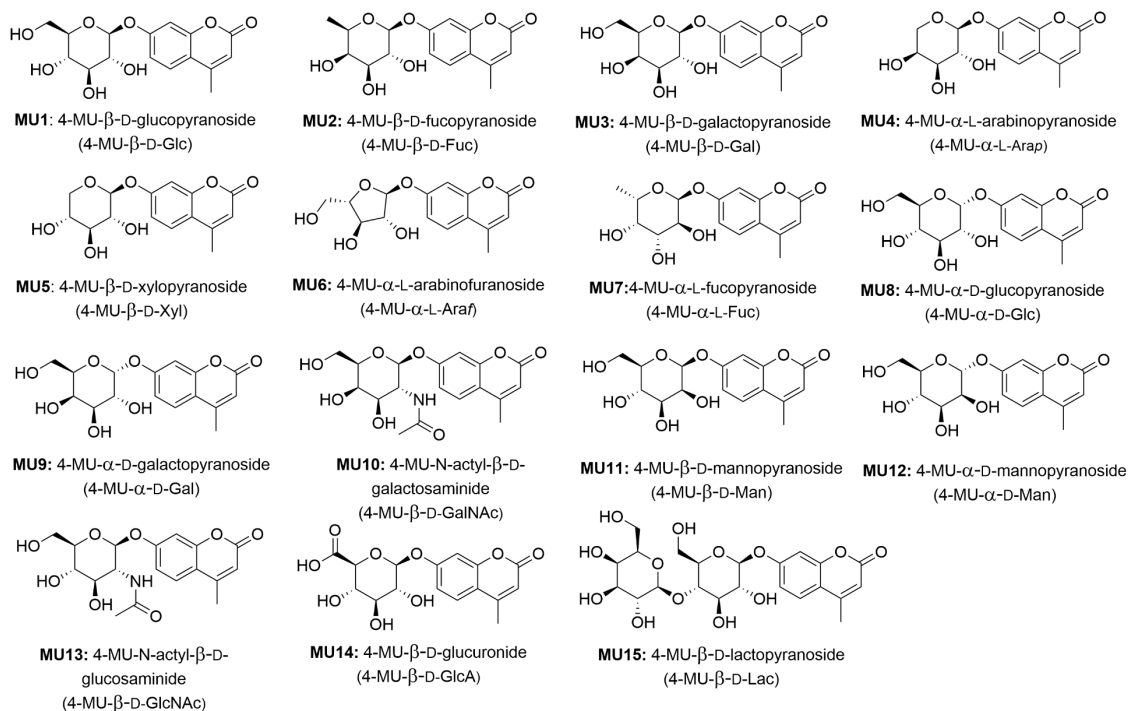
Results

Identification of a GBA3-selective fluorogenic substrate

The first research objective comprised the identification of a reporter substrate for monitoring the activity of GBA3 in biological samples. To this end, the ability of isolated recombinant human GBA3 (rhGBA3) to hydrolyze fifteen 4-methylumbelliferyl (4-MU)-glycosides was investigated first. Corroborating literature studies,^{1,2} rhGBA3 efficiently hydrolyzes 4-MU- β -D-glucopyranoside (β -D-Glc), 4-MU- β -D-galactopyranoside (β -D-Gal), 4-MU- β -D-fucopyranoside (β -D-Fuc), and 4-MU- α -L-arabinopyranoside (α -L-Arap), and to a lesser extent also 4-MU- β -D-xylopyranoside (β -D-Xyl) and 4-MU- α -L-arabinofuranoside (α -L-Araf), but none of the other nine 4-MU-glycosides (Table 1A, see Figure 1 for the structures of the 4-MU-glycosides used). Although their proficiency as reporter substrate

differs, all six GBA3-sensitive substrates can in principle be used to report on GBA3 activity, and the effect of potential inhibitors on this, in settings in which GBA3 is the only retaining β -glucosidase present. Human cells, and extracts thereof, however contain a multitude of glycosidases, including GBA1 and GBA2, and the galactosidases, GLB1 (β -galactosidases, EC 3.2.1.23) and GALC (galactosylceramidase, EC 3.2.1.46).

4-Methylumbelliferyl glycoside (4-MU-glycoside) substrates



ABPs and inhibitors (R_1 = Cy5, R_2 = BODIPY red)

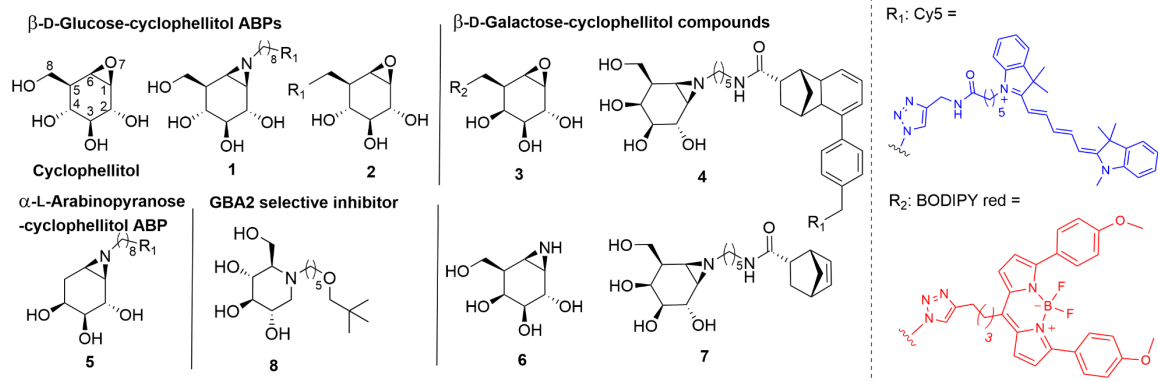


Figure 1. Chemical structure of compounds used in this chapter.

Substrates processed by one or more of these enzymes are not suitable for measuring specifically GBA3 activity in such more complex biological samples. For instance, 4-MU- β -D-Xyl is also hydrolyzed by GBA1, and 4-MU- β -D-Gal by GALC and GLB1. This does not necessarily hold true for 4-MU- β -D-Fuc, 4-MU- α -L-Arap, and 4-MU- α -L-Araf, as the ability of GBA1, GBA2, GALC and GLB1 to process these substrates is not known. To shed light in the possible use of 4-MU- β -D-Fuc, 4-MU- α -L-Arap, or 4-MU- α -L-Araf as selective GBA3 reporters, these three substrates were next exposed to either recombinant human (rh) GBA1 or lysates of GBA1/GBA2 KO HEK293T cells overexpressing GBA2 (hereafter termed GBA2 cells). As shown in Table 1B, neither 4-MU- β -D-Fuc nor 4-MU- α -L-Arap proved to be rhGBA1 substrates, whereas some 4-MU- α -L-Araf processing by rhGBA1 was observed. When exposed to GBA2 cell extract, 4-MU- β -D-Fuc and 4-MU- α -L-Arap were processed with considerable efficiency, while no

discernible hydrolysis of 4-MU- α -L-Araf was observed. GBA2 cell extract-mediated hydrolysis of 4-MU- β -D-Fuc and 4-MU- α -L-Arap could be reduced largely by pretreatment with the potent GLB1 and GALC inhibitor,²⁰ *galacto*-cyclophellitol-aziridine **6**. In contrast, the potent and selective GBA2 inhibitor **8**²¹ had no effect on the GBA2 cell extract-mediated hydrolysis of 4-MU- β -D-Fuc and 4-MU- α -L-Arap. Taken these results together, 4-MU- β -D-Fuc and 4-MU- α -L-Arap emerge as the most GBA3-selective substrates of the series tested and may be useful to report on GBA3 activity in mammalian cell extracts, provided that samples are pretreated with the GLB1/GALC inhibitor **6**.

Table 1. (A) Isolated rhGBA3 hydrolyzes six 4-MU-glycosides. 4-MU-glycosides (2-3.7 mM) in McIlvaine buffer (150 mM, pH 6.0) were incubated with rhGBA3 for 1 h at 37 °C (see Figure 1 for the structures of the fluorogenic substrates). (B) Processing of substrates by recombinant human GBA1 (rhGBA1), lysate of GBA1/GBA2 KO HEK293T cell, and lysate of GBA2 cells. Isolated rhGBA1 was incubated with the indicated substrate for 30 min at 37 °C at pH 5.2. Samples (lysates of either GBA1/GBA2 KO cells or GBA2 cells) were pre-incubated with vehicle (DMSO) or 500 nM inhibitor **6** (to selectively inhibit GLB1/GALC) or 500 nM inhibitor **8** (to selectively inhibit GBA2) for 30 min at 37 °C at pH 5.8, followed by incubation with indicated substrates for 30 min.

A			B				
4-MU-glycosides (2-3.7 mM, at pH 6.0)		rhGBA3 activity (μmol/h/mg)	Activity		4-MU-β- D-Fuc (MU2)	4-MU-α- L-Arap (MU4)	4-MU-α- L-Araf (MU6)
MU1	(β-D-Glc)	1441.7 ± 110.5	Isolated rhGBA1 (μmol/h/mg)		<1	<1	3.6
MU2	(β-D-Fuc)	1353.4 ± 14.7					
MU3	(β-D-Gal)	700.3 ± 19.5	Lysate of GBA1/ GBA2 KO cells (nmol/ h/mg)	No inhibitor (vehicle)	27.0	23.1	< 0.1
MU4	(α-L-Arap)	300.9 ± 106.4					
MU5	(β-D-Xyl)	45.7 ± 15.9		+ GLB1/GALC selective inhibitor 6	0.1	0.4	/
MU6	(α-L-Araf)	14.6 ± 0.8					
MU7	(α-L-Fuc)	<1		No inhibitor (vehicle)	21.4	18.1	0.3
MU8	(α-D-Glc)	<1					
MU9	(α-D-Gal)	<1					
MU10	(β-D-GalNAc)	<1		+ GBA2 selective inhibitor 8	20.5	17.3	/
MU11	(β-D-Man)	<1					
MU12	(α-D-Man)	<1					
MU13	(β-D-GlcNAc)	<1		+ GLB1/GALC selective inhibitor 6	< 0.1	0.3	/
MU14	(β-D-GlcA)	<1					
MU15	(β-D-Lac)	<1					

Towards GBA3-selective activity-based probes

Activity-based protein profiling (ABPP) reports on active enzymes in a manner complementary to that of fluorogenic substrates. Whereas fluorogenic substrates are ideally suited for determining enzyme activity kinetics and enzyme inhibition constants, ABPP is particularly suited to detect and quantify enzymes in complex biological samples. With the aim to uncover a GBA3-selective ABP, lysates of HEK293T cells containing GBA1, GBA2, and GBA3 were incubated with ABPs **3-5**. These three ABPs were selected because they emulate in structure (configuration and substitution pattern) that of the most GBA3-reactive fluorogenic substrates identified in Table 1A, namely β -D-galactopyranoside (for **3** and **4**) and α -L-arabinofuranoside (for **5**). As shown in Figure 2A, β -D-Gal-cyclophellitol (β -D-Gal) ABP **3** gave selective GBA3 labelling above 3 μ M without labelling GBA1 and GBA2. ABP **3** has been reported earlier to selectively label GALC,²² which is however present in low amounts in the HEK293T cells used here,²² and no clear GALC labelling of ABP **3** was observed under these conditions. β -D-Gal-cyclophellitol aziridine ABP **4** at or above 100 nM labels GBA3, but at these concentrations also labels GLB1. ABP **4** is reported²⁰ to react with GBA1 and GBA2, besides the galactosidases, GALC and GLB1, and labelling of GBA2 and GLB1 was observed here as well when treating HEK293T lysate with ABP **4**. α -L-Arap-cyclophellitol (α -L-Arap) aziridine ABP **5** labelled all three retaining β -glucosidases as well as GLB1 with some selectivity for GBA3 over GBA1 and GBA2. To investigate the reactivity of ABP **3** towards GBA1, mixtures of rhGBA1 and rhGBA3 were incubated with ABP **3**. As shown in Figure 2B, ABP **3** clearly labelled rhGBA3, but did not label rhGBA1. ABPs **3** and **5**, exhibiting relatively good selectivity towards GBA3 in ABPP assays, were then measured for their inhibitory potency (apparent IC₅₀ values) towards retaining β -glucosidases in a 4-MU- β -D-Glc fluorogenic substrate assay. Both compounds proved to be somewhat rhGBA3-selective also in these assays.

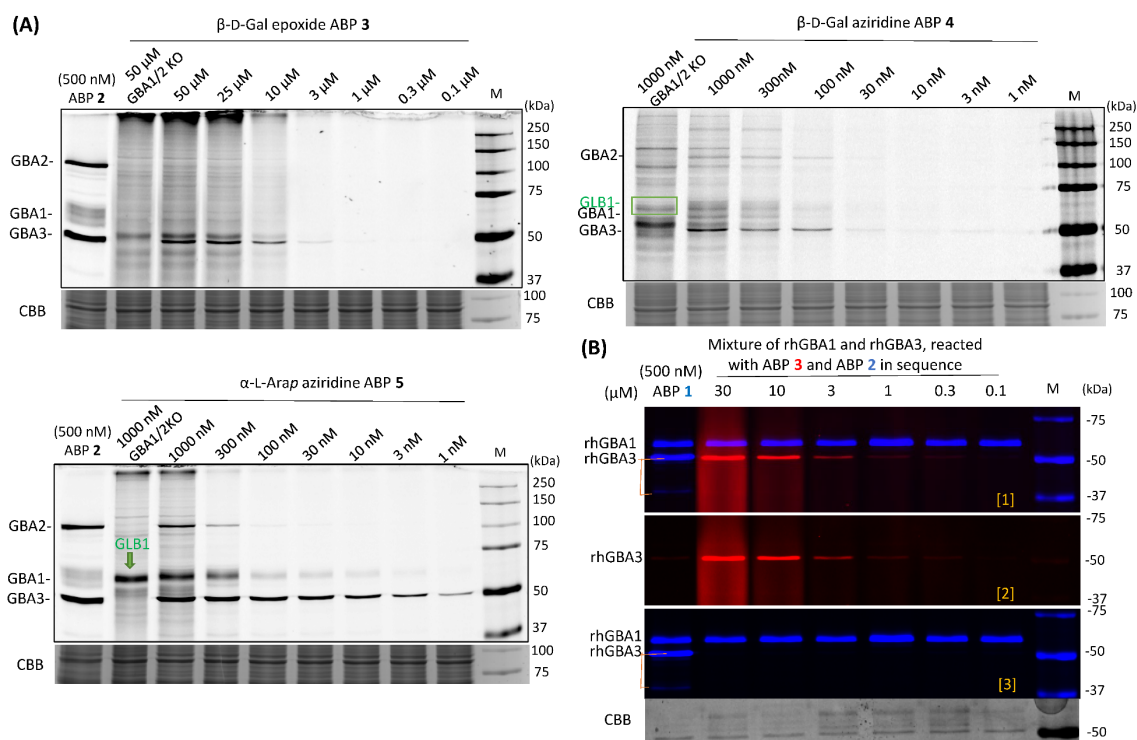
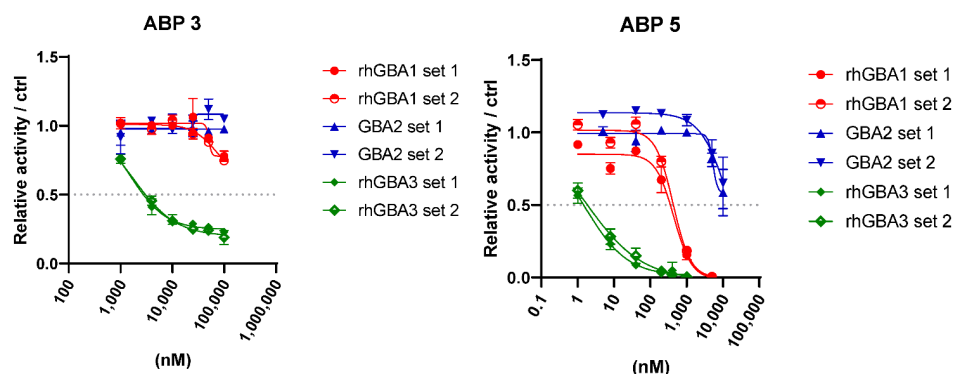


Figure 2. (A) Lysates of HEK293T cells expressing endogenous GBA1 and overexpressed GBA2 and GBA3, or of GBA1/GBA2 knockout (KO) HEK293T cells, were incubated with varying concentrations of ABPs (**3-5**) for 30 min at 37 °C, prior to SDS PAGE and fluorescence scanning of the wet gel slabs. (B) Mixtures of rhGBA1 and rhGBA3 were first treated with varying concentrations of ABP **3** for 30 min at 37 °C. Subsequently, samples were incubated with 250 nM GBA1 selective ABP **2** to show residual active rhGBA1. Labelling of 500 nM broad-spectrum β -glucosidase ABP **1** shows the presence of both rhGBA1 and rhGBA3. [1] Merged fluorescence of ABP **3** (shown as red) and ABP **1**, **2** (shown as blue). [2] Labelling of ABP **3** (red). [3] Labelling of ABP **1** and **2** (blue).

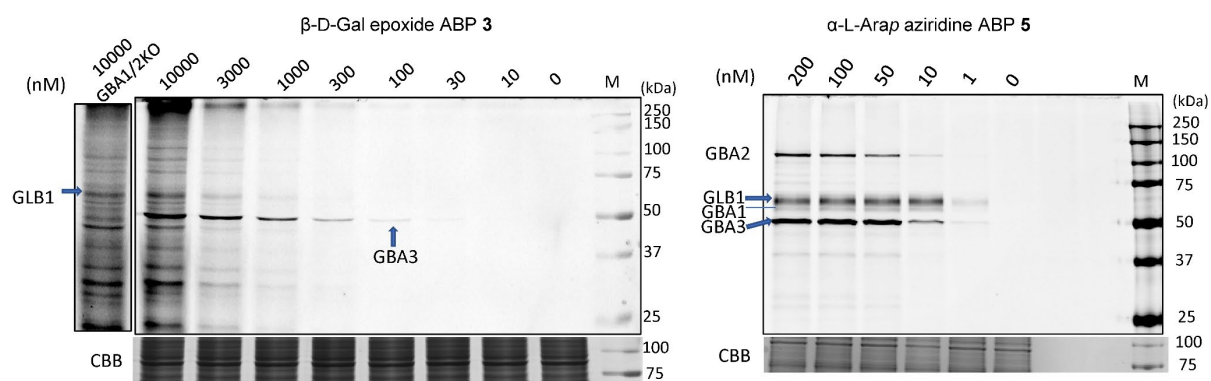
Table 2. Apparent IC₅₀ of ABPs **3** and **5** towards GBA1, GBA2 and GBA3 as determined in a 4-MU-β-D-Glc fluorogenic substrate assay. Error ranges = ± SD, n = 2 replicates.

Apparent IC ₅₀ (nM) of	rhGBA1 ^a	GBA2 ^b	rhGBA3 ^c
β-D-Gal epoxide 3	> 100000	> 100000	1649.0 ± 145.7
α-L-Arap aziridine 5	433.8 ± 11.2	> 10000 ^d	1.60 ± 0.04

^arhGBA1 = Imiglucerase, isolated recombinant human GBA1. ^bGBA2 = lysate of GBA2 cells. ^chGBA3 = isolated recombinant GBA3. The above enzymes were incubated with **3** or **5** for 30 min, following by incubation with 4-MU-β-D-Glc for 30 min. ^dGLB1/GALC in lysates were not inactivated. Error ranges = ± SD, n = 2 (duplicates).

**Figure 3.** Apparent IC₅₀ curve of ABP **3** and **5** as β-glucosidase inhibitors as measured in a 4-MU-β-D-Glc fluorogenic substrate assay.

Next, ABPs **3** and **5** were further examined on their selectivity towards β-glucosidases *in situ* (Figure 4). Intact HEK293T cells endogenously expressing GBA1 and overexpressing GBA2 and GBA3 were treated with varying concentrations of ABP **3** or **5** for 3 h *in situ*. The cells were then harvested and lysed, followed by the ABPP. ABP **3** labelled GBA3 without labelling GBA1 and GBA2, consistent with the *in vitro* ABPP assays. ABP **5** in contrast labelled all β-glucosidases at close concentration with concurrent GLB1 labelling, thus presenting no distinct GBA3 selectivity window *in situ*.

**Figure 4.** Intact HEK293T cells expressing endogenous GBA1 and overexpressing GBA2 and GBA3 were treated with varying concentrations of ABP **3** or **5** *in situ* for 3 h at 37 °C, then lysed, subjected to SDS-PAGE and fluorescence scanning of the wet gel slabs. As a background control intact GBA1/GBA2 KO HEK293T cells were also treated with ABP **3** at the same conditions.

Investigating the reactivity of β -D-Gal epoxide ABP **3** and α -L-Arap aziridine ABP **5** with catalytic residue mutants of GBA3

It was previously demonstrated by site-directed mutagenesis that GBA3 reacts with the β -Glc-cyclophellitol aziridine ABP equipped with a BODIPY fluorophore through covalent linkage to the catalytic nucleophile (E373).¹¹ To establish whether ABPs **3** and **5** react GBA3 via the same catalytic residue, these two ABPs were incubated with either wild-type GBA3, the nucleophile mutant (E373G), the acid/base mutant (E165G), or the double mutant (E373G/E165G). Both probes reacted with the wild-type enzyme, whereas neither reacted with the nucleophile (E373G) and double (E165G/E373G) GBA3 mutants (Figure 5). Of note, the acid/base (E165G) mutant did react with ABP **5** but much less so with ABP **3**. As well, and in line with the results above, labelling of GLB1 with ABP **5** but not with **3** was observed.

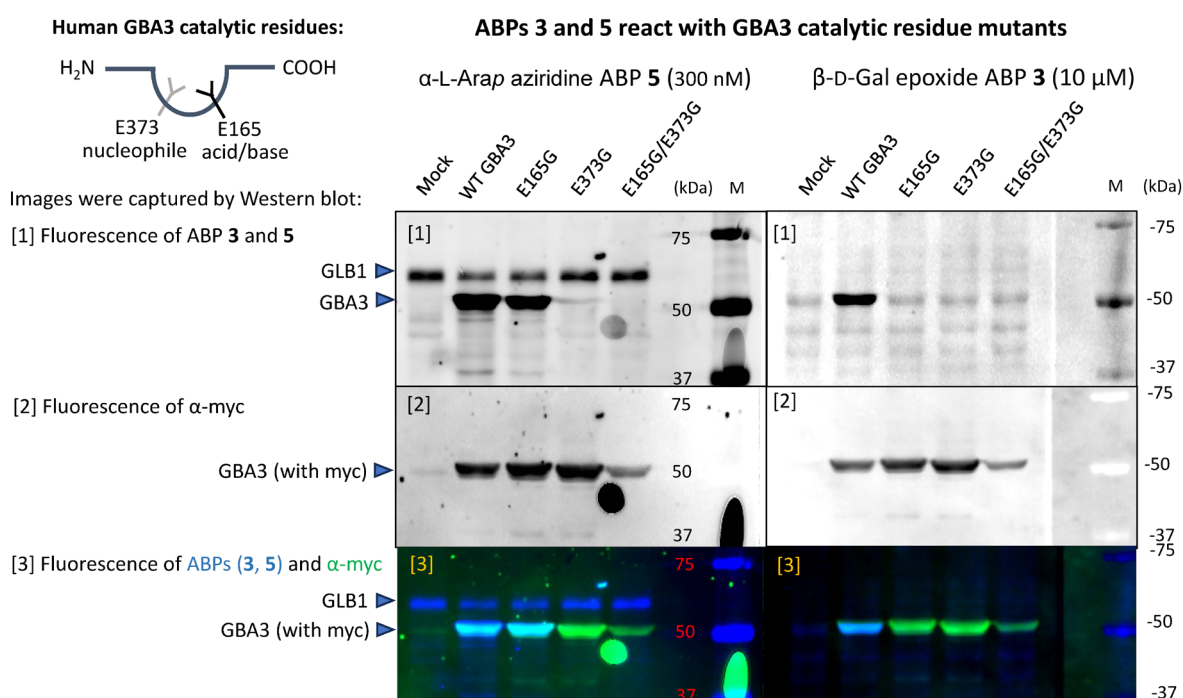


Figure 5. Reactivity of ABPs **3** and **5** towards wild-type GBA3 and GBA3 catalytic residue mutants (all enzymes used contain a myc tag). Lysates of GBA1/GBA2 KO HEK293T cells expressing either wild-type GBA3, or mutant GBA3 were incubated with ABP **3** or **5** for 30 min at 37 °C. After separating proteins with SDS-PAGE, proteins in the wet gel slabs were transferred to a nitrocellulose membrane. The nitrocellulose membrane was then subjected to anti-myc Western blotting. [1] Scanning fluorescence of Cy5 reporter of ABP **3** and **5**. [2] Scanning fluorescence of anti-myc (α -myc) antibody with Alexa Fluor™ 488 conjugation. [3] Merged fluorescence of both ABP **3**, **5** (blue) and anti-myc (green).

Discussion

The cytosolic β -glucosidase GBA3 was already identified in the early 1980s, but its physiological role remains elusive. Arguably, the lack of understanding on GBA3 is in part rooted in the scarcity of suitable reagents: fluorogenic substrates and activity-based probes able to selectively report on GBA3 activity. Indeed, such reagents have helped unraveling the role and activities of the two human retaining glucosidases most closely related to GBA3: GBA1 and GBA2 (see also Chapters 2 and 3). With this reasoning in mind, research was executed, as detailed in this chapter, aimed at identifying both a GBA3 selective fluorogenic substrate and an activity-based probe. From a panel of fifteen differently configured 4-MU-glycoside substrates, 4-MU- β -D-Fuc and 4-MU- α -L-Arap were found as potentially suitable GBA3 selective substrates that can be used in mammalian cell extracts. When the retaining β -galactosidases, GALC and GLB1 (both of process 4-MU- β -D-Gal efficiently), are inactivated by the β -

galactosidase-selective inhibitor **6**, hydrolysis of 4-MU- β -D-Fuc and 4-MU- α -L-Arap in human cell extracts can only be mediated by GBA3 and therefore selectively reflects the activity of GBA3. In the next set of experiments and based on the configurations identified in the fluorogenic substrate assays as accepted by GBA3, ABPs **3-5** were examined on their GBA3-reactivity and selectivity. Despite concurrent β -galactosidase (GLB1/GALC) labelling, both β -D-Gal epoxide ABP **3** and α -L-Arap aziridine ABP **5** labelled GBA3 with relatively good selectivity over GBA1 and GBA2 *in vitro*. When intact HEK293T cells containing all cellular β -glucosidases were treated with ABP **3** or ABP **5** *in situ*, it was observed that ABP **5** did not maintain its GBA3 selectivity it exerts *in vitro*, while ABP **3** did. As well, the lack of reactivity of ABP **3** and **5** towards GBA3 catalytic nucleophile mutants supports the notion that both ABPs **3** and **5** react with GBA3 in an activity-based manner, forming a covalent and irreversible linkage with the GBA3 catalytic nucleophile (E373). Altogether, the results described in this chapter may help in unraveling the role of GBA3 in biology, by offering GBA3 reactive fluorogenic substrates and activity-based probes for detecting GBA3.

Experimental procedures

Materials

Imiglucerase (Cerezyme®), the isolated recombinant human GBA1 (rhGBA1), was kindly provided by Genzyme (Genzyme Nederland, Naarden, The Netherlands). Isolated recombinant human GBA3 (rhGBA3) was purchased from Bio-Techne R&D Systems (Catalog#: 5969-GH-010). 4-Methylumbelliferyl-glycoside substrates were bought from Glycosynth™ (UK), Sigma-Aldrich, or Biosynth Carbosynth. 4-Methylumbelliferone fluorescence was measured with a fluorimeter LS55 (Perkin Elmer, Waltham, MA, USA) with λ_{EX} 366 nm and λ_{EM} 445 nm. Polytron PT 1300D sonicator (Kinematica, Luzern, Switzerland) and potassium phosphate buffer (25 mM KH_2PO_4 - K_2HPO_4 , pH 6.5, supplemented with protease inhibitor cocktail (EDTA-free, Roche, Basel, Switzerland) and 0.1% (v/v) Triton X-100) were used for cell lysis. Protein concentrations were measured using Pierce BCA assay kit (Thermo Fisher Scientific, Waltham, MA, USA). Harvested cells (cell pellets) and cell lysates not used directly were stored at -80 °C. Wet gel slabs for ABPP and nitrocellulose membrane for Western blotting were imaged using a Typhoon FLA 9500 scanner (GE Healthcare) at λ_{EX} 532 nm and $\lambda_{\text{EM}} \geq 575$ nm for the BODIPY red fluorescence and at λ_{EX} 635 nm and $\lambda_{\text{EM}} \geq 665$ nm for Cy5 fluorescence. SDS-PAGE gels were stained for loading control of proteins with Coomassie G250 and scanned on a ChemiDoc MP imager (Bio-Rad, Hercules, CA, USA). The syntheses of the chemical compounds used in this study were previously reported in: **1**²³, **2**²⁴, **3** and **9**,²² **4**, **6**, **7**,²⁰ and **8**.²¹ Compound **5** was synthesized as described in the appendix. Cell lines of GBA1/GBA2 KO HEK293T, GBA1/GBA2 KO HEK293T with GBA2 OE (GBA2 cells), and HEK293T expressing endogenous GBA1 and overexpressed GBA2 and GBA3, were generated as described in Chapter 2.²⁵ Culture and lysis of HEK293T cells was conducted as described in Chapter 2.

4-MU-glycoside fluorogenic substrate assays for enzyme activity and apparent IC_{50} determination

4-MU-glycoside fluorogenic substrate assays for enzyme activity and apparent IC_{50} determination were conducted as described in Chapter 2 with the exception that isolated rhGBA3 was used instead of GBA3 in GBA1/GBA2 KO cell lysate for GBA3 activity measurement. For this, rhGBA3 was diluted in McIlvaine buffer (150 mM, pH 6.0, supplemented with 0.1% bovine serum albumin (BSA)) and was incubated with 2-3.7 mM of the indicated 4-MU-glycoside substrates dissolved in McIlvaine buffer (150 mM, pH 6.0, 0.1% (w/v) BSA) for 1 h at 37 °C.

In vitro ABPP

ABPP experiments were conducted as described in Chapter 2. In brief, samples containing GBA1, GBA2 or GBA3 (see for the exact constitution of these samples below) were incubated with the ABPs for 30 min (if not otherwise stated) at optimized conditions, followed by protein denaturing, SDS-PAGE and fluorescence scanning of the wet gel slabs. The incubation conditions for each enzyme were as follows: isolated rhGBA1 was incubated with the ABPs in McIlvaine buffer (150 mM, pH 5.2) supplemented with 0.1% (v/v) Triton X-100 and 0.2% (w/v) sodium taurocholate. Isolated rhGBA3 was incubated with the ABPs in McIlvaine buffer (150 mM, pH 6.0). In the case of incubating rhGBA3 with ABP for 1-3 h, 0.1% (w/v) BSA was added to the McIlvaine buffer. Lysates of HEK293T containing GBA1, GBA2 and GBA3, as well as GBA1/GBA2 KO HEK293T lysates were incubated with the ABPs in McIlvaine buffer (150 mM, pH 6.0).

In situ ABPP

Confluent GBA1/GBA2 KO HEK293T cells, or HEK293T cells expressing human endogenous GBA1 and overexpressing GBA2/GBA3, were cultured in 12-well dishes with (or without) the indicated ABPs for 3 h at 37 °C under 7% CO_2 atmosphere. After the incubation, cells were harvested and lysed as described in Chapter 2. After determination of the protein concentration by BCA assay, the lysates were adjusted to 10 μL by adding potassium phosphate buffer in order to normalize the amount of proteins

(10-25 µg total protein), after which the samples were subjected to SDS PAGE and in-gel fluorescence scanning.

GBA3 catalytic mutant labelling

For overexpression of GBA3 mutants, GBA1/GBA2 KO HEK293T were used for transfection. Wild-type GBA3, GBA3-E165G, GBA3-E373G, or GBA3- E165G/ E373G double mutants (all containing a myc tag) were generated as described previously for COS-7 cells.¹¹ Extracts of these were then incubated with ABP **3** or **5** for 30 min at 37 °C, and the samples were then subjected to SDS-PAGE and in-gel fluorescence scanning. Subsequently, proteins in the wet slab gels were transferred to a nitrocellulose membrane for Western blotting. Mouse anti-myc (α -myc) primary antibody (Bioke) and a secondary antibody (donkey anti-mouse IgG with an Alexa 488 fluorescent group, Invitrogen) were used to visualize myc-tagged, GBA3 wild-type and GBA3 mutants.

References

1. R. H. Glew, S. P. Peters and A. R. Christopher, Isolation and characterization of beta-glucosidase from the cytosol of rat kidney cortex, *Biochim. Biophys. Acta.*, 1976, **422**, 179-199.
2. L. B. Daniels, P. J. Coyle, Y. B. Chiao, R. H. Glew and R. S. Labow, Purification and characterization of a cytosolic broad specificity beta-glucosidase from human liver, *J. Biol. Chem.*, 1981, **256**, 13004-13013.
3. V. Gopalan, A. Pastuszyn, W. R. Galey and R. H. Glew, Exolytic hydrolysis of toxic plant glucosides by guinea pig liver cytosolic beta-glucosidase, *J. Biol. Chem.*, 1992, **267**, 14027-14032.
4. K. Yahata, K. Mori, H. Arai, S. Koide, Y. Ogawa, M. Mukoyama, A. Sugawara, S. Ozaki, I. Tanaka, Y. Nabeshima and K. Nakao, Molecular cloning and expression of a novel klotho-related protein, *J. Mol. Med.*, 2000, **78**, 389-394.
5. Y. Hayashi, N. Okino, Y. Kakuta, T. Shikanai, M. Tani, H. Narimatsu and M. Ito, Klotho-related protein is a novel cytosolic neutral beta-glycosylceramidase, *J. Biol. Chem.*, 2007, **282**, 30889-30900.
6. Y. Hayashi and M. Ito, Klotho-related protein KLRP: structure and functions, *Vitam. Horm.*, 2016, **101**, 1-16.
7. S. Tribolo, J. G. Berrin, P. A. Kroon, M. Czjzek and N. Juge, The crystal structure of human cytosolic beta-glucosidase unravels the substrate aglycone specificity of a family 1 glycoside hydrolase, *J. Mol. Biol.*, 2007, **370**, 964-975.
8. F. Ben Bdira, M. Artola, H. S. Overkleeft, M. Ubbink and J. M. Aerts, Distinguishing the differences in beta-glycosylceramidase folds, dynamics, and actions informs therapeutic uses, *J. Lipid. Res.*, 2018, **59**, 2262-2276.
9. J. G. Berrin, W. R. McLauchlan, P. Needs, G. Williamson, A. Puigserver, P. A. Kroon and N. Juge, Functional expression of human liver cytosolic beta-glucosidase in *Pichia pastoris*. Insights into its role in the metabolism of dietary glucosides, *Eur. J. Biochem.*, 2002, **269**, 249-258.
10. L. Wang, J. Seino, H. Tomotake, Y. Funakoshi, H. Hirayama and T. Suzuki, Co-expression of NEU2 and GBA3 causes a drastic reduction in cytosolic sialyl free N-glycans in human MKN45 stomach cancer cells-evidence for the physical interaction of NEU2 and GBA3, *Biomolecules*, 2015, **5**, 1499-1514.
11. W. W. Kallemijn, M. D. Witte, T. M. Voorn-Brouwer, M. T. Walvoort, K. Y. Li, J. D. Codée, G. A. van der Marel, R. G. Boot, H. S. Overkleeft and J. M. Aerts, A sensitive gel-based method combining distinct cyclophellitol-based probes for the identification of acid/base residues in human retaining beta-glucosidases, *J. Biol. Chem.*, 2014, **289**, 35351-35362.
12. C. L. Kuo, W. W. Kallemijn, L. T. Lelieveld, M. Mirzaian, I. Zoutendijk, A. Vardi, A. H. Futerman, A. H. Meijer, H. P. Spaik, H. S. Overkleeft, J. M. Aerts and M. Artola, In vivo inactivation of glycosidases by conduritol B epoxide and cyclophellitol as revealed by activity-based protein profiling, *FEBS J.*, 2019, **286**, 584-600.
13. J. Stirnemann, N. Belmatoug, F. Camou, C. Serratrice, R. Froissart, C. Caillaud, T. Levade, L. Astudillo, J. Serratrice, A. Brassier, C. Rose, T. Billette de Villemeur and M. G. Berger, A review of Gaucher disease pathophysiology, clinical presentation and treatments, *Int. J. Mol. Sci.*, 2017, **18**, 441.
14. J. M. Aerts, C. L. Kuo, L. T. Lelieveld, D. E. C. Boer, M. J. C. van der Lienden, H. S. Overkleeft and M. Artola, Glycosphingolipids and lysosomal storage disorders as illustrated by Gaucher disease, *Curr. Opin. Chem. Biol.*, 2019, **53**, 204-215.
15. N. Dekker, T. Voorn-Brouwer, M. Verhoek, T. Wennekes, R. S. Narayan, D. Speijer, C. E. Hollak, H. S. Overkleeft, R. G. Boot and J. M. Aerts, The cytosolic beta-glucosidase GBA3 does not influence type 1 Gaucher disease manifestation, *Blood Cells Mol. Dis.*, 2011, **46**, 19-26.
16. E. Beutler, L. Beutler and C. West, Mutations in the gene encoding cytosolic beta-glucosidase in Gaucher disease, *J. Lab. Clin. Med.*, 2004, **144**, 65-68.
17. D. E. Boer, M. Mirzaian, M. J. Ferraz, K. C. Zwiers, M. V. Baks, M. D. Hazeu, R. Ottenhoff, A. R. A. Marques, R. Meijer, J. C. P. Roos, T. M. Cox, R. G. Boot, N. Pannu, H. S. Overkleeft, M. Artola and

- J. M. Aerts, Human glucocerebrosidase mediates formation of xylosyl-cholesterol by beta-xylosidase and transxylosidase reactions, *J. Lipid. Res.*, 2021, **62**, 100018.
18. A. R. Marques, M. Mirzaian, H. Akiyama, P. Wisse, M. J. Ferraz, P. Gaspar, K. Ghauharali-van der Vlugt, R. Meijer, P. Giraldo, P. Alfonso, P. Irun, M. Dahl, S. Karlsson, E. V. Pavlova, T. M. Cox, S. Scheij, M. Verhoek, R. Ottenhoff, C. P. van Roomen, N. S. Pannu, M. van Eijk, N. Dekker, R. G. Boot, H. S. Overkleeft, E. Blommaart, Y. Hirabayashi and J. M. Aerts, Glucosylated cholesterol in mammalian cells and tissues: formation and degradation by multiple cellular beta-glucosidases, *J. Lipid. Res.*, 2016, **57**, 451-463.
 19. H. Akiyama, M. Ide, Y. Nagatsuka, T. Sayano, E. Nakanishi, N. Uemura, K. Yuyama, Y. Yamaguchi, H. Kamiguchi, R. Takahashi, J. M. Aerts, P. Greimel and Y. Hirabayashi, Glucocerebrosidases catalyze a transgalactosylation reaction that yields a newly-identified brain sterol metabolite, galactosylated cholesterol, *J. Biol. Chem.*, 2020, **295**, 5257-5277.
 20. C. L. Kuo, Q. Su, A. van den Nieuwendijk, T. J. M. Beenakker, W. A. Offen, L. I. Willems, R. G. Boot, A. J. Sarris, A. R. A. Marques, J. D. C. Codée, G. A. van der Marel, B. I. Florea, G. J. Davies, H. S. Overkleeft and J. M. Aerts, The development of a broad-spectrum retaining beta-exo-galactosidase activity-based probe, *Org. Biomol. Chem.*, 2023, **21**, 7813-7820.
 21. D. Lahav, B. Liu, R. van den Berg, A. van den Nieuwendijk, T. Wennekes, A. T. Ghisaidoobe, I. Breen, M. J. Ferraz, C. L. Kuo, L. Wu, P. P. Geurink, H. Ova, G. A. van der Marel, M. van der Stelt, R. G. Boot, G. J. Davies, J. M. Aerts and H. S. Overkleeft, A Fluorescence Polarization Activity-Based Protein Profiling assay in the discovery of potent, selective inhibitors for human nonlysosomal glucosylceramidase, *J. Am. Chem. Soc.*, 2017, **139**, 14192-14197.
 22. A. R. Marques, L. I. Willems, D. Herrera Moro, B. I. Florea, S. Scheij, R. Ottenhoff, C. P. van Roomen, M. Verhoek, J. K. Nelson, W. W. Kallemeyn, A. Biela-Banas, O. R. Martin, M. B. Cachon-Gonzalez, N. N. Kim, T. M. Cox, R. G. Boot, H. S. Overkleeft and J. M. Aerts, A specific activity-based probe to monitor family GH59 galactosylceramidase, the enzyme deficient in Krabbe disease, *ChemBioChem*, 2017, **18**, 402-412.
 23. S. P. Schröder, J. W. van de Sande, W. W. Kallemeyn, C. L. Kuo, M. Artola, E. J. van Rooden, J. Jiang, T. J. M. Beenakker, B. I. Florea, W. A. Offen, G. J. Davies, A. J. Minnaard, J. M. Aerts, J. D. C. Codée, G. A. van der Marel and H. S. Overkleeft, Towards broad spectrum activity-based glycosidase probes: synthesis and evaluation of deoxygenated cyclophellitol aziridines, *Chem. Commun.*, 2017, **53**, 12528-12531.
 24. M. Artola, C. L. Kuo, L. T. Lelieveld, R. J. Rowland, G. A. van der Marel, J. D. C. Codée, R. G. Boot, G. J. Davies, J. M. Aerts and H. S. Overkleeft, Functionalized cyclophellitols are selective glucocerebrosidase inhibitors and induce a bona fide neuropathic Gaucher model in zebrafish, *J. Am. Chem. Soc.*, 2019, **141**, 4214-4218.
 25. Q. Su, S. P. Schröder, L. T. Lelieveld, M. J. Ferraz, M. Verhoek, R. G. Boot, H. S. Overkleeft, J. M. Aerts, M. Artola and C. L. Kuo, Xylose-configured cyclophellitols as selective inhibitors for glucocerebrosidase, *ChemBioChem*, 2021, **22**, 3090-3098.

Appendix

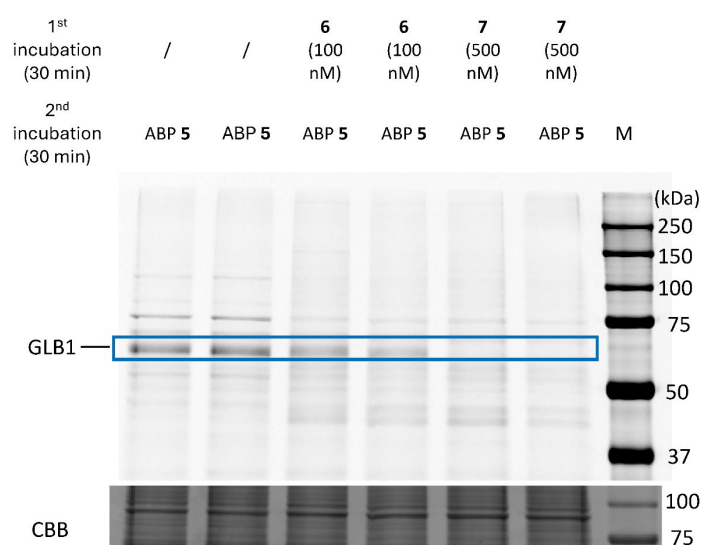


Figure S1. Reaction of α -L-Arap aziridine ABP 5 towards GLB1 in cell lysate was inhibited by pre-treatment of GLB1/GALC selective inhibitor **6** or **7**. Lysates of GBA1/GBA2 KO HEK293T were treated with **6** (100 nM) or **7** (500 nM) for 30 min at 37 °C *in vitro*, followed by incubation with ABP 5 (200 nM) for 30 min, then samples were subjected to SDS-PAGE followed by in-gel fluorescence scanning.

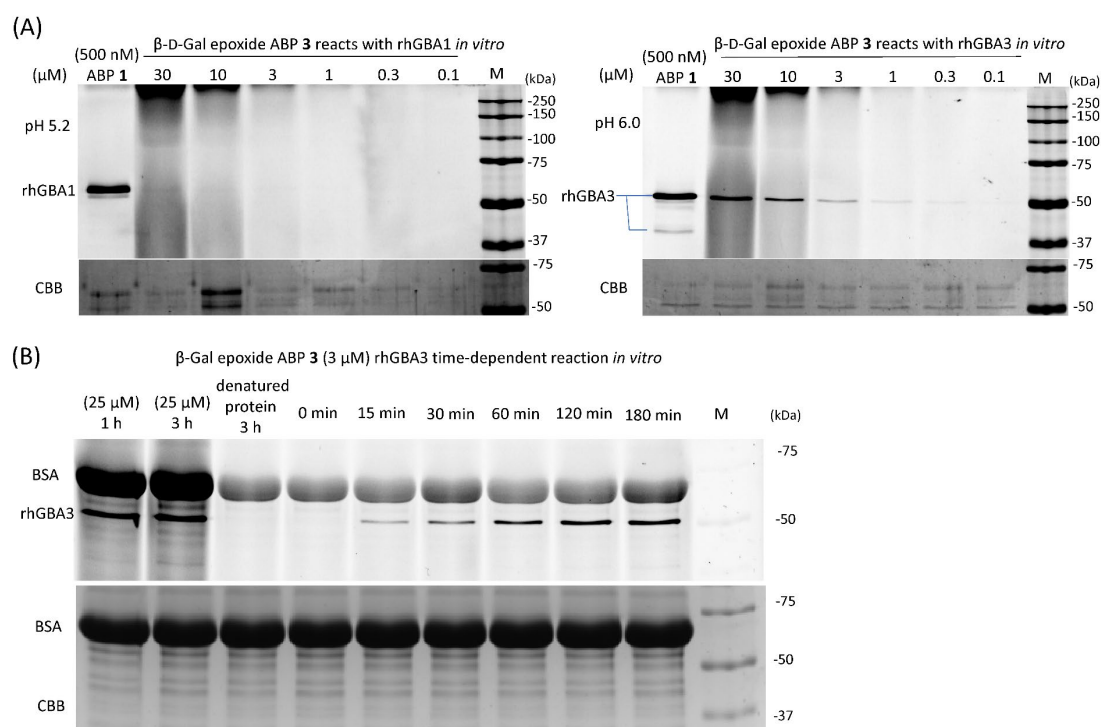


Figure S2. (A) Reactivity of β -D-Gal ABP 3 towards isolated rhGBA1 and rhGBA3 *in vitro*, isolated rhGBA1 or rhGBA3 was incubated with ABP 3 at the indicated pH for 30 min at 37 °C, then samples were subjected to SDS-PAGE and in-gel fluorescence scanning. (B) time-dependent interaction of ABP 3 towards rhGBA3, isolated rhGBA3 was incubated with ABP 3 at pH 6.0 at 37 °C for varying incubation times and subsequently subjected to SDS-PAGE and fluorescence scanning of the wet gel slabs. Bovine serum albumin (BSA) visible at around 65 kDa was added for stabilizing the isolated rhGBA3. Reactivity of ABP 3 towards denatured rhGBA3: rhGBA3 sample was first boiled at 98 °C for 5 min, followed by incubation with ABP 3 for 3 h at pH 6.

Table S1. Comparing hydrolysis activity of GBA1/GBA2 KO HEK293T cell lysates (containing GLB1 and GALC) towards 4-MU- β -D-Gal, 4-MU- β -D-Fuc and 4-MU- α -L-Arap. Lysates were first incubated at 37 °C with or without 500 nM **6** (GALC/GLB1 inhibitor) for 30 min at pH 5 or pH 6, following incubation with indicated 4-MU-glycoside for 30 min. Hydrolysis activity of lysate towards these 4-MU-glycosides is shown as nmol per hour per mg (nmol/h/mg).

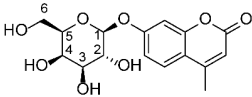
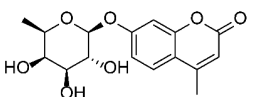
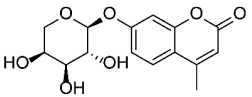
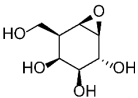
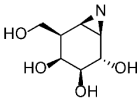
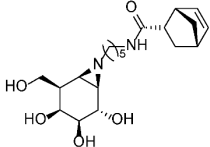
<div style="display: flex; justify-content: space-around; align-items: center;"> <div style="text-align: center;">  <p>4-MU-β-D-Gal</p> </div> <div style="text-align: center;">  <p>4-MU-β-D-Fuc</p> </div> <div style="text-align: center;">  <p>4-MU-α-L-Arap</p> </div> </div>				
Activity (nmol/h/mg) of HEK293T GBA1/2 KO lysate				
Substrates	At pH 5.0		At pH 6.0	
	No inhibitor	+ GLB1/GALC inhibitor 6 (500 nM)	No inhibitor	+ GLB1/GALC inhibitor 6 (500 nM)
4-MU- β -D-Gal	222.2	0.9	71.8	< 0.1
4-MU- β -D-Fuc	23.5	< 0.1	8.2	< 0.1
4-MU- α -L-Arap	17.0	< 0.1	4.6	< 0.1

Table S2. (A) Activity of β -D-galactose configured aziridine inhibitor (**6**, **7**), and β -D-galactose configured epoxide inhibitor **9** towards rhGBA3. (B) Activity of β -L-Arap inhibitors (**10**, **11**)¹, α -L-Arap inhibitors (**12**, **13**)¹ towards β -glucosidases, examined by 4-MU- β -D-Glc fluorogenic substrate assays for 30 min incubation at 37 °C.

<div style="display: flex; justify-content: space-around; align-items: center;"> <div style="text-align: center;">  <p>β-D-Gal epoxide 9</p> </div> <div style="text-align: center;">  <p>β-D-Gal aziridine 6</p> </div> <div style="text-align: center;">  <p>β-D-Gal aziridine 7</p> </div> </div>			
Remaining rhGBA3 activity (%)	β -D-Gal epoxide 9	β -D-Gal aziridine 6	β -D-Gal aziridine 7
+ Inhibitor 10,000 nM	96%	30%	23%
+ Inhibitor 1,000 nM	97%	57%	50%
+ Inhibitor 100 nM	95%	83%	84%
+ Inhibitor 0 nM	100%	100%	100%

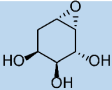
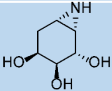
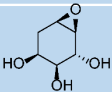
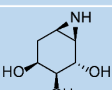
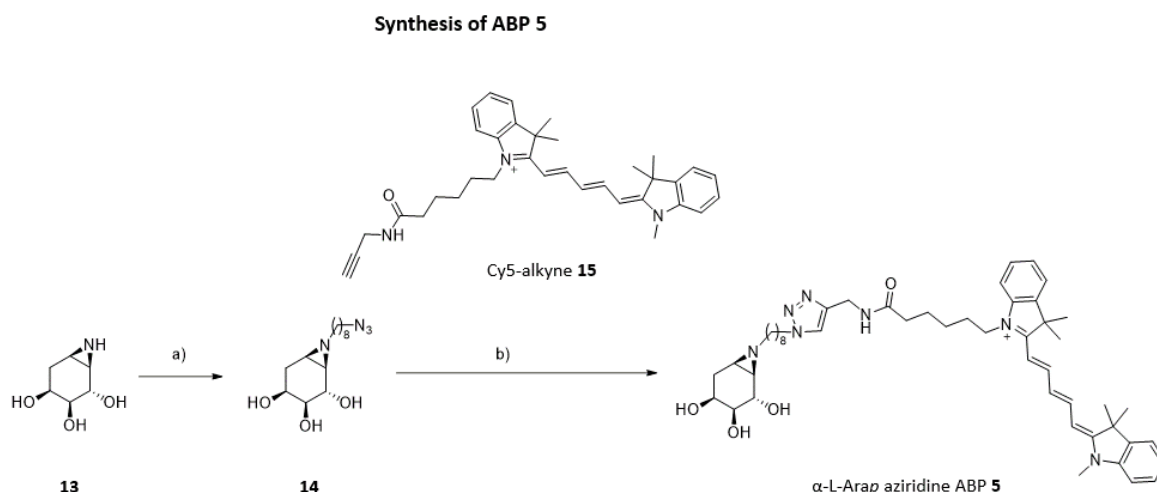
Remaining enzyme activity (%) with 50 μ M inhibitors	rhGBA1	GBA2	rhGBA3
β -L-Arap epoxide 10 	100%	100%	100%
β -L-Arap aziridine 11 	91%	100%	91%
α -L-Arap epoxide 12 	99%	100%	99%
α -L-Arap aziridine 13 	90%	97%	100%

Table S3. An overview of the reactivity of ABPs and inhibitors towards β -glucosidases and other glycosidases. '/' = no available data.

substrates	Inhibitors and ABPs	Apparent IC ₅₀ (nM)				Apparent IC ₅₀ values derived from
		GBA1	GBA2	GBA3	Other enzymes	
4-MU- β -D-Glc	β -D-Glc-cyclophellitol ABP 2 ²	(1) 3.2 ± 0.17 ; (2) 45.20 ± 4.54	(1) $412,000 \pm 10,100$; (2) > 5000	(2) 5784 ± 79	/	(1) Ref ² ; (2) Ref ³
	β -D-Glc-cyclophellitol aziridine ABP 1 ⁴	8.10 ± 1.94	21.5 ± 0.42	8.54 ± 1.18	/	Ref ³
4-MU- β -D-Fuc	Available ABP is not reported at present	/	/	/	/	/
4-MU- β -D-Gal	β -D-Gal-cyclophellitol ABP 3 ⁵	$> 1 \times 10^5$	$> 1 \times 10^5$	1649.0 ± 145.7	GALC: 2800	Ref ⁵
	β -D-Gal-cyclophellitol aziridine ABP 4 ⁶	85.8	752	/	GLB1: 14.6 ± 0.98 ; GALC: 61.0 ± 6.89	Ref ⁶ ; Chapter 4
	β -D-Gal-cyclophellitol aziridine inhibitor 6 ⁶	1560	3290	~ 1000	GLB1 : 2.55 ± 0.59 ; GALC: 5.57 ± 0.36	
	β -D-Gal-cyclophellitol aziridine inhibitor 7 ⁶	5370	$> 10^4$	~ 1000	GLB1 : 57.8 ± 3.05 ; GALC: 98.6 ± 20.8	
4-MU- α -L-Arap	α -L-Arap-cyclophellitol aziridine ABP 5	433.8 ± 11.2	$> 10^4$	1.60 ± 0.04	/	Chapter 4
4-MU- β -D-Xyl	β -D-Xyl-cyclophellitol aziridine ABP ³	6.4 ± 0.5	544 ± 110	$10,055 \pm 1,003$	/	Chapter 2
4-MU- α -L-Araf	α -L-Araf-cyclophellitol aziridine ABP ⁷	$> 5 \times 10^4$	1,850	$> 5 \times 10^4$	/	Chapter 3



Scheme S1. Synthesis route of ABP 5. Reagents and conditions: (a) 1-azido-8-iodo-octane, K_2CO_3 , DMF, 60 °C. (b) CuSO_4 , sodium ascorbate, Cy5-alkyne, DMF, rt.

To a solution of (1*R*,3*S*,4*S*,5*S*,6*R*)-7-azabicyclo[4.1.0]heptane-3,4,5-triol (**13**)¹ (0.010 g, 0.07 mmol) in dry DMF (3.0 mL), 1-azido-8-iodo-octane (0.039 g, 0.14 mmol) and K_2CO_3 (0.029 g, 0.21 mmol) were added. The reaction was left to stir at 60 °C under nitrogen atmosphere. After 15 hours, DMF was evaporated and the crude product purified by silica gel chromatography using a mixture of DCM/MeOH (from 100:0 to 90:10). The thus obtained product **14**, which was obtained together with minor impurities (0.008 g, 0.027 mmol) was dissolved in dry DMF (1.0 mL), to which a degassed solution of $\text{CuSO}_4 \cdot 5\text{H}_2\text{O}$ (40 mL, 0.018 mmol) and sodium ascorbate (0.004 g, 0.020 mmol) were added. After 10 min of stirring Cy5-alkyne **15** was added and the blue solution was stirred at room temperature for 15 hours. HPLC purification (C18 semipreparative column, solvent A: $\text{H}_2\text{O}/\text{NH}_4\text{OH}$, solvent B: CH_3CN) afforded compound **7** (0.009 g, 40%). ^1H NMR (400 MHz, CDCl_3): δ 8.24 (ddd, J = 14.5, 12.6, 2.7 Hz, 2H), 7.84 (s, 1H), 7.49 (dd, J = 7.5, 1.2 Hz, 2H), 7.41 (tdd, J = 7.4, 6.1, 1.2 Hz, 2H), 7.33 – 7.18 (m, 4H), 6.61 (t, J = 12.4 Hz, 1H), 6.34 – 6.16 (m, 2H), 4.40 (s, 2H), 4.36 (s, 2H), 4.08 (t, J = 7.6 Hz, 2H), 3.99 (d, J = 6.2 Hz, 1H), 3.73 (td, J = 2.3, 5.8 Hz, 1H), 3.62 (s, 4H), 3.34 (s, 4H), 2.32 – 2.17 (m, 4H), 2.05 – 1.99 (m, 2H), 1.90 – 1.84 (m, 6H), 1.84 – 1.76 (m, 2H), 1.72 (s, 17H), 1.53 – 1.42 (m, 4H), 1.41 – 1.21 (m, 13H) ppm. ^{13}C NMR (101 MHz, CDCl_3): δ 176.6, 176.3, 175.5, 145.1, 144.4, 143.5, 143.4, 130.6, 130.6, 127.5, 127.1, 125.0, 124.3, 112.7, 105.1, 77.5, 71.8, 69.8, 61.2, 52.2, 45.1, 37.3, 36.4, 32.1, 29.1, 28.1, 28.6, 28.2, 28.2, 27.3 ppm.

Supplemental references

1. S. P. Schröder, R. Petracca, H. Minnee, M. Artola, J. M. Aerts, J. D. C. Codée, G. A. van der Marel and H. S. Overkleeft, A divergent synthesis of L-arabino- and D-xylo-configured cyclophellitol epoxides and aziridines, *Eur. J. Org. Chem.*, 2016, 4787-4794.
2. M. Artola, C. L. Kuo, L. T. Lelieveld, R. J. Rowland, G. A. van der Marel, J. D. C. Codée, R. G. Boot, G. J. Davies, J. M. Aerts and H. S. Overkleeft, Functionalized cyclophellitols are selective glucocerebrosidase inhibitors and induce a bona fide neuropathic Gaucher model in zebrafish, *J. Am. Chem. Soc.*, 2019, **141**, 4214-4218.
3. Q. Su, S. P. Schröder, L. T. Lelieveld, M. J. Ferraz, M. Verhoek, R. G. Boot, H. S. Overkleeft, J. M. Aerts, M. Artola and C. L. Kuo, Xylose-configured cyclophellitols as selective inhibitors for glucocerebrosidase, *ChemBioChem*, 2021, **22**, 3090-3098.
4. S. P. Schröder, J. W. van de Sande, W. W. Kallemeijn, C. L. Kuo, M. Artola, E. J. van Rooden, J. Jiang, T. J. M. Beenakker, B. I. Florea, W. A. Offen, G. J. Davies, A. J. Minnaard, J. M. Aerts, J. D. C. Codée, G. A. van der Marel and H. S. Overkleeft, Towards broad spectrum activity-based

- glycosidase probes: synthesis and evaluation of deoxygenated cyclophellitol aziridines, *Chem. Commun.*, 2017, **53**, 12528-12531.
5. A. R. Marques, L. I. Willems, D. Herrera Moro, B. I. Florea, S. Scheij, R. Ottenhoff, C. P. van Roomen, M. Verhoek, J. K. Nelson, W. W. Kallemeijn, A. Biela-Banas, O. R. Martin, M. B. Cachon-Gonzalez, N. N. Kim, T. M. Cox, R. G. Boot, H. S. Overkleeft and J. M. Aerts, A specific activity-based probe to monitor family GH59 galactosylceramidase, the enzyme deficient in Krabbe disease, *ChemBioChem*, 2017, **18**, 402-412.
 6. C. L. Kuo, Q. Su, A. van den Nieuwendijk, T. J. M. Beenakker, W. A. Offen, L. I. Willems, R. G. Boot, A. J. Sarris, A. R. A. Marques, J. D. C. Codée, G. A. van der Marel, B. I. Florea, G. J. Davies, H. S. Overkleeft and J. M. Aerts, The development of a broad-spectrum retaining beta-exo-galactosidase activity-based probe, *Org. Biomol. Chem.*, 2023, **21**, 7813-7820.
 7. N. G. S. McGregor, M. Artola, A. Nin-Hill, D. Linzel, M. Haon, J. Reijngoud, A. Ram, M. N. Rosso, G. A. van der Marel, J. D. C. Codée, G. P. van Wezel, J. G. Berrin, C. Rovira, H. S. Overkleeft and G. J. Davies, Rational design of mechanism-based inhibitors and activity-based probes for the identification of retaining alpha-L-arabinofuranosidases, *J. Am. Chem. Soc.*, 2020, **142**, 4648-4662.

Chapter 5

Characterization of *C. elegans* retaining β -glucosidases

Qin Su, Mats Bulterman, Tjebbe Boersma, Maria Ferraz, Laura van Vliet, Rolf G. Boot, Bogdan I. Florea, Precious Sadhoe, Herman S. Overkleeft, Marta Artola, and Johannes M. F. G. Aerts are acknowledged for their contributions to this chapter.

Abstract

The human lysosomal β -glucosidase (hGBA1) degrades the glycosphingolipid (GSL) glucosylceramide (GlcCer). Inherited deficiency in hGBA1 causes Gaucher disease (GD). Like mammals, the nematode *C. elegans* contains glycosphingolipids, but with a C17iso sphingoid base instead of the mammalian C18 one (d17iso-GlcCer). Information on β -glucosidase activities of *C. elegans* that may be involved in d17iso-GlcCer metabolism is limited. Substrates, inhibitors, and activity-based probes (ABPs) that report on hGBA1 and the non-lysosomal hGBA2 were used to identify and characterize β -glucosidase activities in *C. elegans*. Candidate genes for the GBA1-like and GBA2-like proteins in *C. elegans*, as well as characteristics of one candidate orthologue of hGBA1 in *C. elegans* encoded by the *gba3*-gene are described in this Chapter.

Introduction

Humans express three cellular β -glucosidases, all employing a retaining reaction mechanism,¹ termed (h)GBA1 (lysosomal glucosylceramidase), (h)GBA2 (non-lysosomal glucosylceramidase) and (h)GBA3 (a broad-spectrum cytosolic β -glucosidase). Whereas the role of hGBA3 is enigmatic (see also Chapter 4), hGBA1 and hGBA2 have in common that both enzymes process the same substrate, namely, glucosylceramide (GlcCer, **1**, Figure 1) into glucose (**2**) and ceramide (**3**). Inherited defects in the hGBA1 gene are linked to the lysosomal storage disorder Gaucher disease (GD),²⁻⁴ and heteroallelic mutations in the hGBA1 gene are a risk factor for Parkinson's disease (PD).^{5,6} Treatment of non-neuronopathic symptoms of type 1/3 GD patients with recombinant hGBA1 (enzyme replacement therapy – ERT) comprises the most successful of the enzyme replacement therapies (ERTs) to date.⁷⁻⁹ hGBA2 in turn is a cytosol-facing membrane-associated glucosylceramidase and while processing the same substrate as hGBA1, it does so in a different cellular compartment.¹⁰ Therapeutic co-inhibition of hGBA2, jointly with the GlcCer-synthesising enzyme, glucosylceramide synthase (GCS), has recently come to the fore as a potentially improved substrate reduction therapy (SRT) for the treatment of neuropathological (type 3) GD patients that cannot be treated by recombinant hGBA1 and neither by selective inhibition of GCS alone (SRT with Zavesca, as is now practice in the clinic as an alternative for ERT).^{11,12}

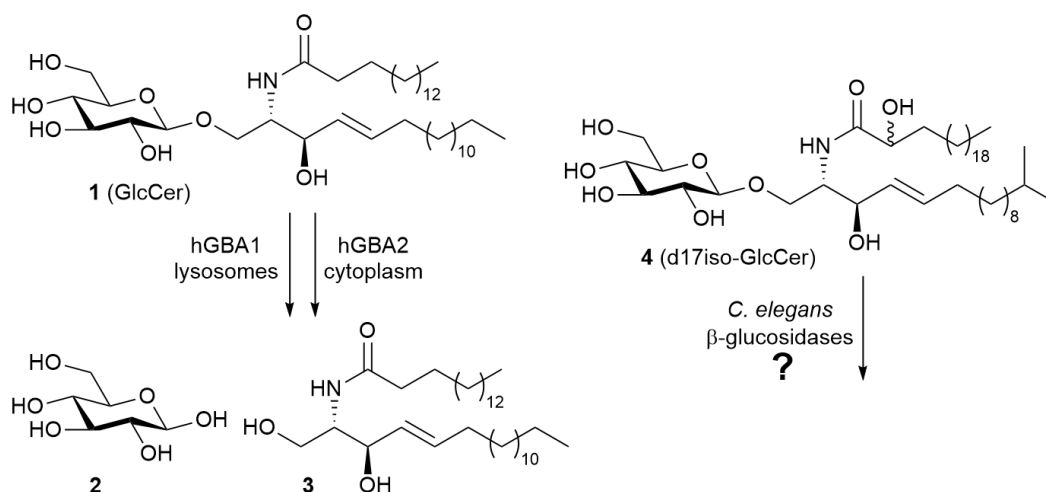


Figure 1. Metabolism of glucosylceramide (GlcCer, **1**) in humans and the closely related *C. elegans* glycosphingolipid, d17iso-GlcCer (**4**, d17iso-GlcCer) a GSL with high abundance in compositions of *C. elegans* GSL. Of note, the side chain fatty acid of d17iso-GlcCer can vary from C12 to C26, with or without the presence of a hydroxyl group¹³. *C. elegans* β -glucosidase activities potentially able to process d17iso-GlcCer are poorly described and subject to the studies presented in this Chapter.

Beyond its key role in these various human pathologies, the importance of GlcCer and its metabolites in nature is reflected by their wide occurrence across the various kingdoms of life. Structural elements in species-specific GlcCer may differ subtly, both in the fatty acid appended to the sphingoid base and the sphingoid base itself (length, branching, saturation, hydroxylation pattern) but the general structure appears conserved. The same appears to be true for the function of GlcCer, which is often utilized as a common starting point in the biosynthesis of a wide array of oligosaccharidic glycosphingolipids (in humans for instance the gangliosides and globosides) that are an integral part of cell membranes where they partake in signalling events.¹⁴ A case in point and subject of the studies described in this Chapter comprises the transparent nematode, *C. elegans* synthesizes d17iso-glucosylceramide (d17iso-GlcCer, **4**, Figure 1),^{13,15,16} which differs from the

mammalian GlcCer by the nature of the sphingoid base: C17iso monomethyl branched-chain sphingosine, as opposed to linear C18-sphingosine in humans. *C. elegans* thus produces a close homologue of the primary storage material in GD (GlcCer). Moreover, it does so in a highly conserved biochemical pathway, starting from serine and a fatty acid, and proceeding through sphinganine which is then acylated, dehydrogenated and glucosylated.^{15,17} The presence of d17iso-GlcCer (**4**) as the central glycosphingolipid in *C. elegans* raises the question whether this species, like humans and other mammals, express d17iso-GlcCer-processing β -glucosidases and if so, whether they possess similar characteristics (cytosolic/acting at neutral pH; lysosomal/acting at acidic pH). Although not studied in detail in biochemical and cell biological experiments, orthologues of human genes encoding lysosomal and cytosolic glucosidases have been identified in *C. elegans* as part of the *C. elegans* Genome Project (see Table 1).¹⁸

Table 1. *C. elegans* genes orthologous to the human genes encoding GBA1 and GBA2. Predicted (BLAST search) homology of proteins and molecular masses. ^aUniprot code, ^bputative description, ^camino acid homology to hGBA1/hGBA2, ^dnumber of amino acids.

Genes			Predicted proteins			
Accession ^a	Description ^b (<i>C. elegans</i>)	Gene	Homology ^c	Size ^d	MW (kDa)	Aligned with
Q9UB00	glucosylceramidase 4	<i>gba-4</i>	42.28%	519	58.24	Human GBA1 (UniProt code: P04062)
G5ECR8	glucosylceramidase 3	<i>gba-3</i>	41.92%	522	59.08	
O16580	glucosylceramidase 1	<i>gba-1</i>	40.00%	523	58.17	
O16581	glucosylceramidase 2	<i>gba-2</i>	38.16%	516	57.78	
Q8WQB2	non-lysosomal glucosylceramidase	<i>hpo-13</i>	40.26%	959	110.85	Human GBA2 (UniProt code: Q9HCG7)
Q6EUT3	non-lysosomal glucosylceramidase	<i>hpo-13</i>	40.26%	922	106.27	
Q6EUT4	non-lysosomal glucosylceramidase	<i>hpo-13</i>	40.26%	930	107.13	
O01893	non-lysosomal glucosylceramidase	<i>R08F11.1</i>	38.77%	819	94.50	

These include the *gba-1*, *2*, *3*, and *4* genes, which have 38-42% sequence homology with hGBA1, and the *hpo-13* and *R08F11.1* genes, with around 40% sequence homology to hGBA2. hGBA1 and hGBA2 possess little sequence homology, if at all, and the presence of *C. elegans* genes with considerable homology to either suggests a similar biochemistry to exist in both species. Information on the catalytic activity and substrate selectivity of these potential hGBA1/hGBA2 analogues however is lacking. With the aim to shed some first light in this, selected fluorogenic and fluorescent substrates, inhibitors, and activity-based probes (ABPs) as also described in the previous experimental chapters that report on, or interfere with, hGBA1/hGBA2 activity were applied to *C. elegans* cell extracts in a variety of biochemical assays to identify and characterize retaining β -glucosidase activities. In this way, as is described below, two candidate-genes were identified with homology for hGBA1 and hGBA2 respectively. The hGBA1-like protein was furthermore cloned and expressed and revealed by competitive activity-based protein profiling (ABPP) to indeed possess characteristics also featured by hGBA1. Altogether the here-presented studies provide circumstantial, but strong evidence of the existence of conserved GlcCer metabolism pathways existing between humans and *C. elegans*, and provide the blueprint and reagents to delve deeper into this matter, possibly also in the context of GD and PD.

Results

The list of reagents used in the biochemical studies presented in this Chapter are depicted in Figure 1 and comprises a set of fluorescent substrates, fluorogenic substrates, competitive inhibitors, mechanism-based covalent and irreversible inhibitors and ABPs that have previously shown their merit in monitoring and modulating the activity of hGBA1 and/or hGBA2 in *in vitro*, *in situ* and sometimes also in *in vivo* settings (see also the preceding Chapters). These substrates, inhibitors and probes are applied to *C. elegans* extracts in a variety of experiments (see below) with the aim to address the questions whether such extracts contain β -glucosidase activity; whether this activity is (in part) effected by hGBA1/hGBA2-like retaining β -glucosidases; and whether this activity processes GlcCer derivatives. 4-Methylumbelliferyl- β -D-glucopyranoside **5** (4-MU- β -D-Glc) is the standard fluorogenic substrate that is processed by many β -exo-glucosidases including hGBA1/2/3. C12-NBD-GlcCer **6** comprises a fluorogenic GlcCer derivative that acts as an efficient substrate for both hGBA1 and hGBA2. Cyclophellitol **7** and conduritol B epoxide (CBE) **8** are broad-spectrum retaining β -glucosidase inhibitors that block both hGBA1 and hGBA2 in a covalent and irreversible manner.¹⁹ Cyclophellitol derivative **9** with a bulky hydrophobic group appended to C6 (glucopyranose numbering) is selective for hGBA1 over hGBA2,²⁰ whereas the competitive inhibitors **10**²¹ and **11**²² comprise *N*-alkyl deoxynojirimycins with some preference for hGBA2. Cyclophellitol-based ABPs **12**²⁰ and **13**²³, with the reporter moiety (Cy5 in **12**, biotin in **13**) grafted to C6 are selective hGBA1 probes, whereas cyclophellitol aziridines ABPs **14**–**17** (with the reporter moiety attached via the aziridine nitrogen) report on hGBA1 and hGBA2 alike.²⁴ Cy5-modified xylose-configured cyclophellitol aziridine **18** as described in Chapter 2 modifies both hGBA1 and hGBA2, whereas β -D-arabinofuranose-configured (β -D-Araf) cyclophellitol aziridines **19** and **20** report, as described in Chapter 3, with some selectivity on the action of hGBA2.

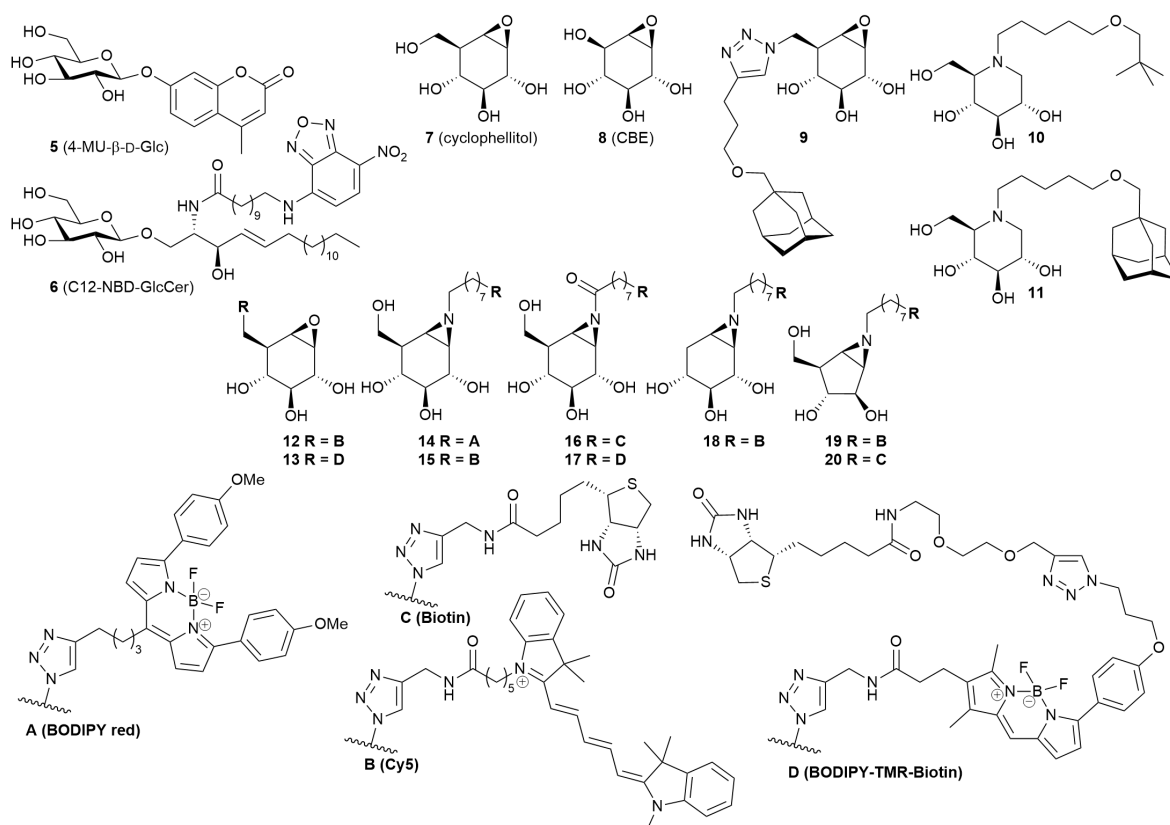


Figure 2. Substrates, inhibitors, and probes used in the here-presented studies.

Fluorogenic and fluorescent β -glucoside processing by *C. elegans* extracts

As the first experiment (Figure 3A), β -glucosidase activity in *C. elegans* homogenate was assessed by incubating *C. elegans* homogenates with 4-MU- β -D-Glc **5** at various pH values (3-7.5). Fluorescence was detected between pH 3 and pH 7.5, with a rather broad area (between pH 4 and pH 6) at which fluorescence is at least 50% of the maximal fluorescence as generated at pH 4.5-5. Next the ability of nematode homogenates to degrade C12-NBD-GlcCer was examined. *C. elegans* homogenate or recombinant hGBA1 (rhGBA1) at pH 5 was incubated for four hours with C12-NBD-GlcCer, after which the lipids were extracted and subjected to high-performance thin layer chromatography (HPTLC). Fluorescence scanning of the TLC plate revealed the formation of NBD-ceramide (NBD-Cer) in both samples.

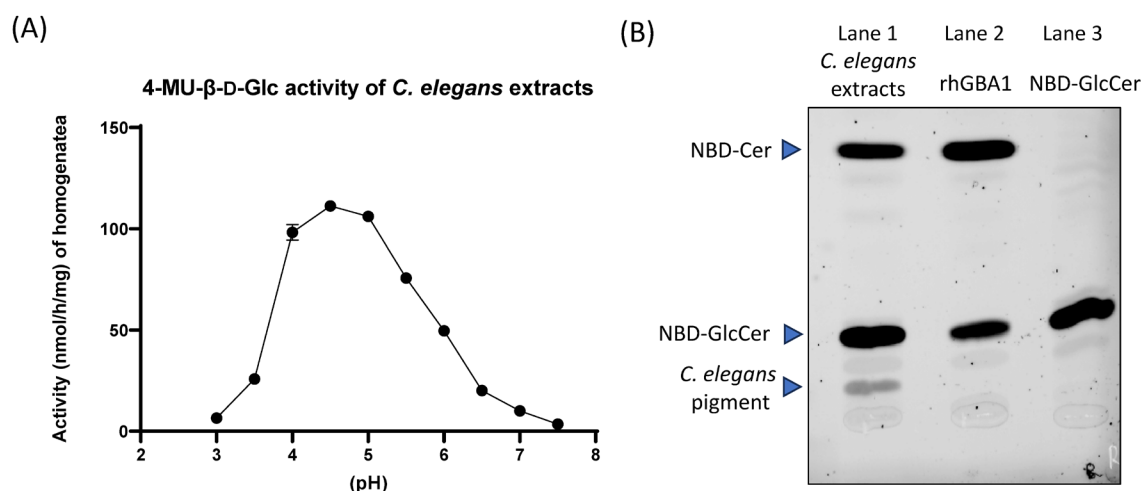


Figure 3. *C. elegans* extracts process 4-MU- β -D-glucopyranoside (A) and C12-NBD-GlcCer (B). (A) *C. elegans* homogenates were incubated with 4-MU- β -D-Glc at various pH values (3-7.5) for 30 min at 37 °C. (B) Lane 1: *C. elegans* homogenates (40-50 μ g) were incubated with 2 μ M C12-NBD-GlcCer in Mcllvaine buffer (150 mM, pH 5.0) for 4 h at 37 °C, followed by lipid extraction and HPTLC separation and fluorescence scanning of the silica gel layers. Lane 2: Around 20 ng isolated recombinant human GBA1 (rhGBA1, Imiglucrase) was used for processing C12-NBD-GlcCer as described above, but now the Mcllvaine buffer (150 mM, pH 5.2) was supplemented with 0.1% (v/v) Trion X-100 and 0.2% (w/v) sodium taurocholate. Lane 3: As the control, 2 μ M C12-NBD-GlcCer in Mcllvaine buffer (150 mM, pH 5.0) was incubated under the conditions described above.

Comparative and competitive ABPP in *C. elegans* extracts

Having established that *C. elegans* extracts contain β -glucosidase activity (Figure 3A) capable of processing the artificial GlcCer derivative **6** (Figure 3B), these extracts were then treated with the panel of retaining glucosidase ABPs **12-20** in a series of comparative and competitive (inclusion of inhibitors **7-11**) ABPP experiments. To this end, *C. elegans* homogenates were first incubated with the ABPs at a pH range of 4 to 7 (Figure 4A) for 30 minutes at 37 °C, after which the homogenates were denatured, the protein content separated by SDS-PAGE and the wet gel slabs scanned for in-gel fluorescence. The two cyclophellitol aziridine probes **14** and **15** as well as the β -xylose-configured one (**18**) return, at pH 5, three distinct fluorescent signals, of which the middle one disappears at elevated pH. These bands indicate modified proteins (or protein mixtures) with molecular weight (MW) of about 52 kDa (Band-1⁺), 95 kDa (Band-2[±]), and 55 kDa (Band-3[•]). Cyclophellitol ABP **12** in contrast predominantly elicits the 52 kDa band together with a faint signal reflecting a higher MW (60 kDa) protein (mixture). β -D-Araf cyclophellitol aziridine **19** also returned one major signal, but now at around 95 kDa. To address the concern that a contamination with *E. coli* may cause some of the

observed labelling is (in part) due to *E. coli* contaminants in the samples (*E. coli* is used to culture *C. elegans*, see experimental procedures), *E. coli* extracts were treated with ABP **14** at pH 4-7. Just one signal at around 70 kDa MW emerged after in-gel fluorescence scanning of the SDS PAGE-separated sample that was treated with probe **14** at pH 5-7 (Figure 4A rightmost lanes). This signal does not overlap with the position of the signals derived from the *C. elegans* homogenates. N-glycanase treatment of probe **14**-treated *C. elegans* extract resolved some, but not all signals, indicating that the different signals do not translate to the same protein present in varying glycoforms (Figure 4B). Finally, inclusion of inhibitors **8-11** in ABP **14**-treated extracts at pH 6 (a pH at which the three predominant signals elicited by **14** are at a maximum signal, see Figure 4A) indicates the presence of at least two distinct retaining β -glucosidases (Figure 4C). It should be noted here that the higher final concentrations of various inhibitors were chosen because these inhibitors did not inhibit the *C. elegans* retaining β -glucosidases at a potency they block human retaining β -glucosidases (the same holds true in selecting the final concentrations of the probes in the comparative ABPP experiments as depicted in Figure 4A). Drawing conclusions should therefore be done with care. Still, the competitive ABPP experiments reveal selective to complete competition of ABP **14**-generated signals, strongly suggesting these signals to relate to distinct retaining β -glucosidases. Iminosugars **10** and **11**, for instance, selectively and almost completely abolish the highest molecular weight signal at 95 kDa. C6-modified cyclophellitol **9** in turn very cleanly block the lower signal at 52 kDa whereas CBE **8** at the applied concentration appears to have little effect. Cyclophellitol **7** finally affects both the high and the low signal while leaving the middle one largely intact at the applied concentration.

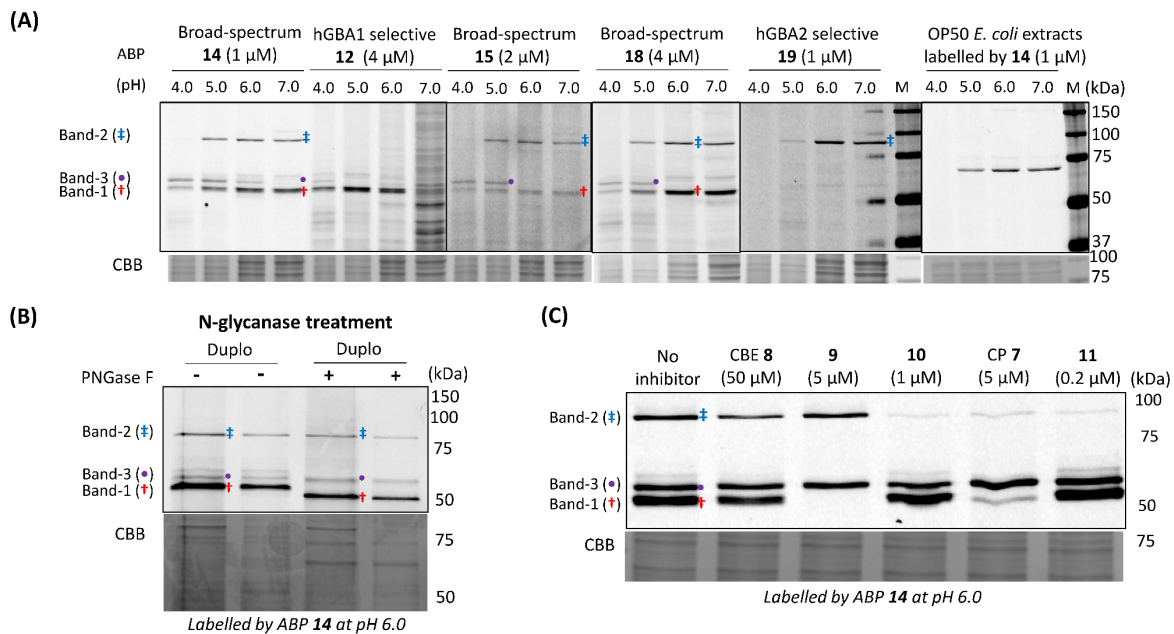
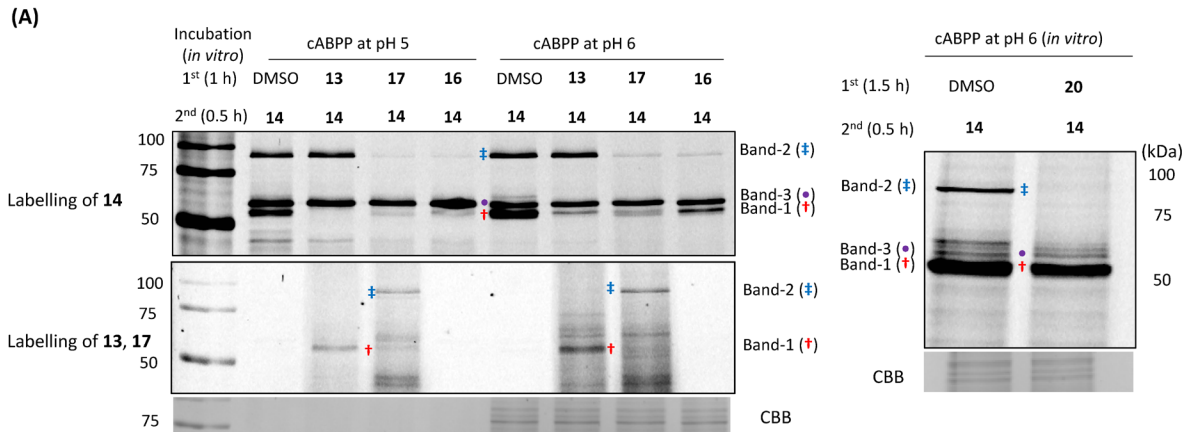


Figure 4. Comparative and competitive ABPP on *C. elegans* extracts. (A) Comparative ABPP. *C. elegans* homogenates were incubated with β -glucosidase ABPs **12**, **14**, **15**, **18**, or **19**, or OP50 *E. coli* homogenates with ABP **14**, for 30 minutes at 37 °C and at various pH values (4-7) *in vitro*, followed by SDS-PAGE, and fluorescence scanning of the wet gel slabs. (B) N-glycanase (PNGase F) treatment. *C. elegans* homogenates were first incubated with ABP **14** at pH 6.0 for 30 min at 37 °C *in vitro*, followed by denaturing of the samples by a 5 min incubation at 98 °C, and subsequent incubation with PNGase F for 2 h, then the samples were subjected to SDS-PAGE and fluorescence scanning. (C) Competitive ABPP. *C. elegans* homogenates were first treated with indicated inhibitor (**7-11**) at pH 6.0 for 30 min *in vitro*, and subsequently incubated with ABP **14** for 30 min, followed by SDS-PAGE and fluorescence scanning.

Chemical proteomics reveals putative hGBA1 and hGBA2 homologues in *C. elegans* extracts

Encouraged by the comparative and competitive ABPP experiments, which indicate the presence of multiple retaining β -glucosidases that moreover show different sensitivities both to pH and selected inhibitors in reacting with the panel of fluorescent probes applied, the biotin ABPs **13**, **16**, **17** and **20** were then investigated on their versatility to isolate and identify these activities (Figure 5 A, B) using a chemical proteomics workflow. In the first instance (Figure 5A) the propensity of the biotin-ABPs to block ABP **14**-mediated generation of the three major fluorescent bands at pH 5 and 6 in *C. elegans* extracts was investigated. As can be seen, neither of the probes were able to block emergence of the middle band. Fluorescent labelling of the upper signal at 95 kDa (by ABPs **16**, **17**, **20**) and the lower signal at 52 kDa (by ABPs **13**, **16**, **17**) in contrast can be competed for, indicating that the protein(s) that are behind these signals may be identified through the biotinylated probes. Probes **13** and **17** moreover besides carrying a biotin are also fluorescent, at a complementary wavelength (both excitation and emission) to that of ABP **14**, allowing to fluorescence-scan the competitive ABPP gel also at the BODIPY-TMR wavelength. As can be seen, the lower signal (now tagged with **13**) and specifically the upper one (with **17**) reemerge at both pH's, indicating that these signals now correspond to proteins that are also biotinylated.

After evaluating the propensity of biotin-ABPs for isolating ABP **14** labelled proteins, *C. elegans* homogenates were then treated with 10 μ M biotin ABPs **13**, **16** or 20 μ M **20** as final concentration for one hour at 37 °C and at pH 5 (for **13**, **16**) or at pH 6 (for **20**). Then the samples were denatured and treated with streptavidin beads. After washing several times to remove unbound proteins, the proteins remaining on the streptavidin beads were digested by trypsin, and the tryptic peptides were analyzed and identified by LC-MS/MS. Usage of ABP **13** yielded the candidate-retaining β -glucosidase gene product encoded by the *gba-3* gene (UniProt code: G5ECR8), and ABP **20** significantly enriched the protein encoded by the *R08F11.1* gene (UniProt code: O01893), while ABP **16** enriched both gene products (see SI Table S1). The *gba-3*-encoded protein has a predicted MW of 59 kDa and the *R08F11.1*-encoded protein a predicted MW of 95 kDa. These predicted protein sizes coincide with the signals as obtained with the comparative ABPP experiments (Figure 4A) with fluorescent ABPs **14** and **15**, and also reflect the MW of hGBA1 and hGBA2.



(B)

Accession	Description	Peptide counts	Sequence coverage	Predicted MW	Score
GSECR8	Putative glucosylceramidase 3 OS=Caenorhabditis elegans OX=6239 GN=gba-3 PE=3 SV=1	22	37.5	59.088	265.07
O01893; A0A168H9S8	Non-lysosomal glucosylceramidase OS=Caenorhabditis elegans OX=6239 GN=CELE_R08F11.1 PE=1 SV=3	28;10	33.5	94.498	216.76

Figure 5. (A) Reactivity of biotin-ABPs (**13**, **16**, **17**, **20**) towards three major fluorescent bands in *C. elegans* extracts as revealed by competitive ABPP. *C. elegans* homogenates were treated with 10 μ M biotin-ABP **13**, **16**, **17**, or 20 μ M **20**, or vehicle alone (DMSO, the final concentration = 0.5%) for 1 h (or 1.5 h for **20**) at 37 °C at the indicated pH, followed by incubation with 1 μ M ABP **14** for 30 min, then samples were subjected to SDS-PAGE and fluorescence scanning of the wet gel slabs. (B) Putative β -glucosidases in *C. elegans* as identified by chemical proteomics.

As the final set of experiments, the *gba-3* protein (cGBA1-3) was brought to expression in both GBA1 KO and GBA1/GBA2 KO HEK293T cell lines. As shown in Figure 6, extracts of *gba-3* cDNA-transfected GBA1/GBA2 KO HEK293T cells give a strong fluorescence signal when treated with 4-MU- β -D-Glc, with maximal fluorescence at pH 4.4 (Figure 6B). This signal is absent in extracts from non-transfected GBA1/GBA2 KO HEK293T cells, indicating that 4MU- β -D-Glc processing in the sample derived from the *gba-3*-transfected cells is caused by the introduced *C. elegans* gene product. The fluorescence signal can be suppressed by inclusion of hGBA1-selective inhibitor **9**, but not by hGBA2-selective inhibitor **10**. Treatment of extracts of the *gba-3*-transfected GBA1 KO and GBA1/GBA2 KO cells with ABP **14** yielded, after SDS-PAGE and fluorescence scanning, two bands at around 54 kDa and 65 kDa MW that are not visible in the samples derived from the non-transfected cell lines (Figure 6C). As in the fluorogenic substrate hydrolysis assay, these signals can be competed for by treatment with hGBA1-selective inhibitor **9** (prior to incubation with ABP **14**), but not with hGBA2-selective inhibitor **10** (Figure 6D). The two labelled bands of recombinant cGBA1-3 can both be reduced molecular weight by N-glycanase (PNGase F) treatment (see SI Figure S4B), but this does not lead to a single signal. Finally, extracts of both transfected cell lines were incubated with C12-NBD-GlcCer, and the lipids extracted and resolved by HPTLC. Fluorescence scanning (Figure 6E) of the TLC plates showed no processing of this artificial GlcCer derivative, this in contrast to rhGBA1-mediated C12-NBD-GlcCer turnover in the control experiment. Altogether these results demonstrate that the *C. elegans gba-3* gene encodes for a retaining β -glucosidase with similarities to hGBA1 in pH optimum and sensitivity to hGBA1-selective inhibitors and ABPs, yet one that is not able to process the artificial substrate, C12-

NBD-GlcCer. Whether it is a *C. elegans* β -glucosidase that processes d17iso-GlcCer remains to be established.

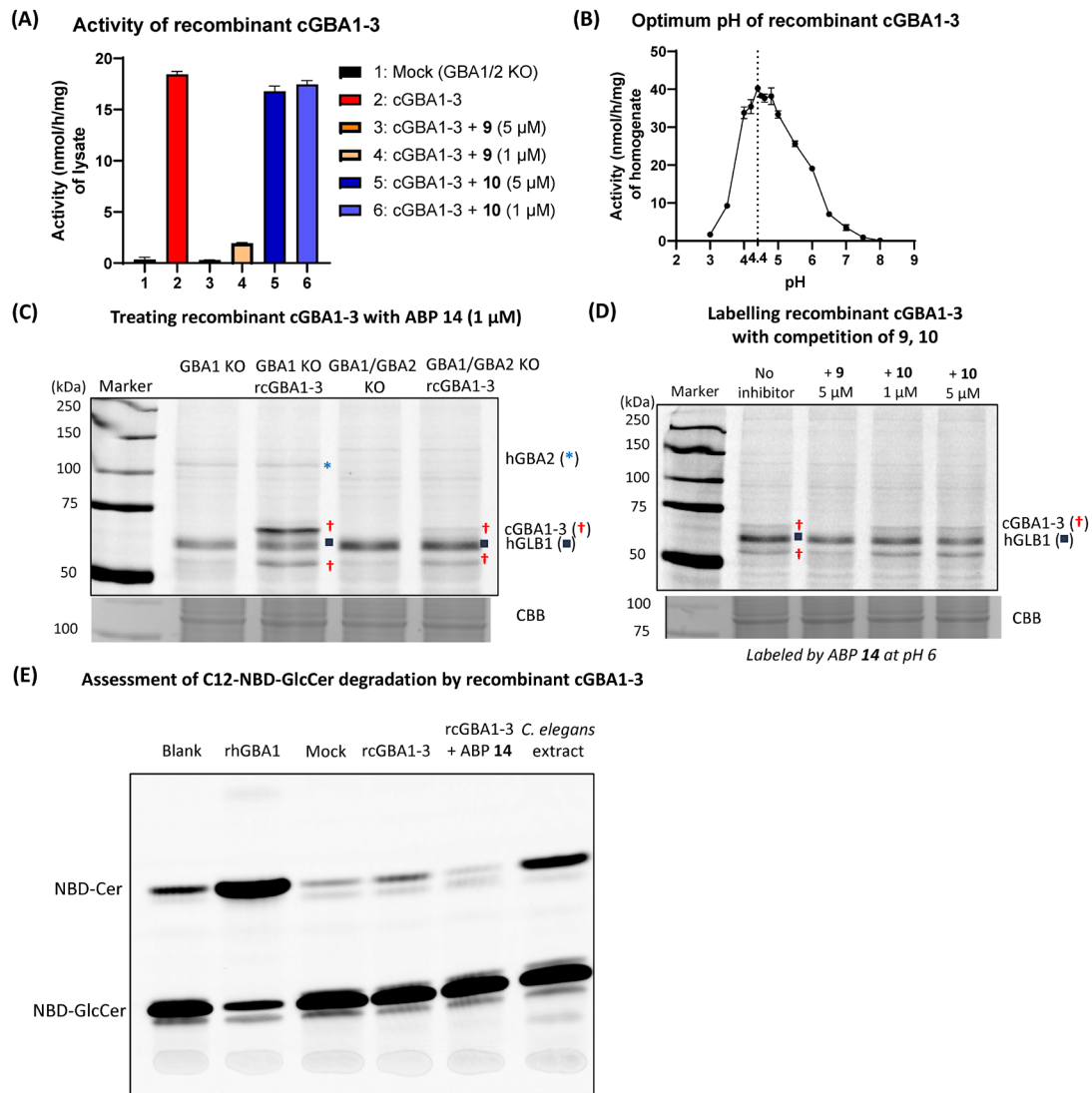


Figure 6. Expression and characterization of cGBA1-3. (A) Enzyme activity of lysates of hGBA1/GBA2 KO HEK293T cells expressing recombinant cGBA1-3 (termed as cGBA1-3 cells), determined by incubation with 4-MU- β -D-Glc for 1 h at pH 5.0 at 37 °C, with or without inhibitor (hGBA1-selective **9** or hGBA2-selective **10**) pre-treatment. Mock = lysate of hGBA1/GBA2 KO HEK293T cells. (B) Optimum pH of rcGBA1-3 for 4-MU- β -D-Glc hydrolysis activity. Lysates of cGBA1-3 cells were incubated with 4-MU- β -D-Glc for 1 h at 37 °C at various pH values (3-8). (C) Lysate of HEK293T cells expressing cGBA-1 (in either hGBA1 KO or hGBA1/GBA2 KO background) were incubated with 1 μ M ABP **14** at pH 6 for 30 min, followed by to SDS-PAGE and fluorescence scanning of the wet gel slabs. hGLB1 = human β -galactosidase (EC 3.2.1.23). (D) lysate of cGBA1-3 cells with or without pre-treatment of inhibitor **9** or **10**, were incubated with 1 μ M ABP **14** at pH 6 for 30 min at 37 °C, followed by SDS-PAGE and fluorescence scanning. (E) Lysates of cGBA1-3 cells was incubated with NBD-GlcCer at pH 4.5 for 4 h at 37 °C. Blank = NBD-GlcCer alone, no enzyme addition. rhGBA1 = 20 ng Imiglucerase (incubated at pH 5.2, supplemented with 0.1% (v/v) Triton X-100 and 0.2% (w/v) sodium taurocholate). Mock = 200 μ g lysates of hGBA1/GBA2 KO HEK293T cells. rcGBA1-3 = 200 μ g lysates of GBA1/GBA2 KO HEK293T cells expressing recombinant cGBA1-3, rcGBA1-3 + ABP **14** = 200 μ g rcGBA1-3 in hGBA1/GBA2 KO HEK293T cell lysates was pre-treated with ABP **14** for 30 min at 37 °C, followed by incubation with NBD-GlcCer. *C. elegans* extracts = 40 μ g *C. elegans* homogenates.

Discussion

Cells of *C. elegans* contain lysosomes with comparable morphology to the ones in vertebrate cells. The here-presented studies comprising measurement of activities in fluorogenic substrate and ABPP assays reveal the presence in *C. elegans* of two putative β -glucosidases with similarities to the human GBA1 and GBA2. Specifically, using biotin-ABPs **13**, **16** and **20** in pull-down chemical proteomics experiments allowed enrichment of a hGBA1-like protein (cGBA1-3) as well as GBA2-like protein (cGBA2). The cGBA1-3 (UniProt code: G5ECR8) encoded by the *gba-3* gene was recombinantly expressed in human HEK293T cells with a hGBA1 as well as a hGBA1/GBA2 KO background. cGBA1-3 shows considerable similarities to human GBA1, in predicted protein structure and polypeptide molecular weight, the presence of N-glycans, and acid pH optimum of enzymatic activity. In addition, the cGBA1-3 resembles hGBA1 in reactivity towards various selective inhibitors and probes. It however does not process (at least in the initial experiments performed) the artificial GlcCer analogue, NBD-GlcCer. This may be an intrinsic property, or the result of the conditions applied, and it is not excluded that cGBA1-3, while inactive towards the artificial substrate (which would set it apart from hGBA1), it does process the *C. elegans* form of GlcCer, d17iso-GlcCer. Alternatively, an endogenous accessory activator protein or lipid activator might be required to allow cGBA1-3, or its orthologs, to be active towards lipid substrates. Future research is needed to address these issues, as indeed glycolipidomics experiments on *C. elegans* extracts need to be done to shed further light into d17iso-GlcCer metabolism and its similarities to human GlcCer metabolism. As well, the enzyme products of the other orthologous genes *gba-1*, *gba-2* and *gba-4* require careful further examination. The identified cGBA2 by biotin-ABP pull down (UniProt code: O01893, encoded by the *R08F11.1* gene) in turn shows similarities to hGBA2 in molecular weight and reactivity with ABPs and inhibitors. More in-depth research, including cloning and expression of this gene, is required to fully comprehend similarities and differences of this *C. elegans* retaining β -glucosidase with hGBA2, as well as its involvement in d17iso-GlcCer metabolism. Such studies may also be geared towards another recent finding regarding human GlcCer metabolism: the ability of hGBA1 and hGBA2 to, besides GlcCer hydrolysis, also perform transglycosylation reactions.²⁵ In this process, GlcCer serves as glucose donor from which glucose is transferred to, instead of water, an acceptor alcohol. In particular, cholesterol was identified as an effective acceptor and β -glucosylcholesterol (GlcChol) has emerged as a natural metabolite in humans that moreover is produced in elevated levels in GD patients.²⁵ In an initial experiment, the presence of GlcChol in *C. elegans* extracts was also established (see SI Figure S5). Further research on d17iso-GlcCer metabolism in *C. elegans*, focusing on the enzymes involved (as initiated by the here-presented studies), but also on the glycosphingolipid pools present under given conditions (inhibitors, genetic manipulations) are needed to establish species-specific events, and whether *C. elegans* would serve as a good model to study cell biological events in the context of GD and PD.

Experimental procedures

Materials

Imiglucerase (Cerezyme®), a recombinant human GBA1 (rhGBA1), was kindly provided by Genzyme (Genzyme Nederland, Naarden, The Netherlands). 4-Methylumbelliferyl-glucopyranoside was bought from Glycosynth (Warrington, UK). HEK293T (CRL-3216™) cells were purchased from ATCC (Manassas, VA, USA), and cultured in DMEM medium (Sigma-Aldrich), supplied with 10% (v/v) FCS, 0.1% (w/v) penicillin/streptomycin and 1% (v/v) Glutamax, at 37°C under 5% CO₂. Polytron PT 1300D sonicator (Kinematica, Luzern, Switzerland) and potassium phosphate buffer (25 mM KH₂PO₄-K₂HPO₄, pH 6.5, supplemented with protease inhibitor cocktail (EDTA-free, Roche, Basel, Switzerland) and 0.1% (v/v) Triton X-100) were used for lysing cell and homogenizing *C. elegans* and *E. coli*. Protein concentration was measured using the Pierce BCA assay kit (Thermo Fisher Scientific, Waltham, MA, USA). Harvested cells (cell pellets), cell lysates, and *C. elegans* homogenates not used directly were stored at -80 °C.

Compounds (in Figure 1) were chemically synthesized and obtained in the department of Bio-organic Synthesis at the Leiden Institute of Chemistry, University of Leiden (Leiden, The Netherlands), based on previous reports: **12**²⁶, **15**²⁷, **14**²⁸, **16**²⁴, **18**²⁹, **19** and **20** (Chapter 3), cyclophellitol **7**³⁰, **10**²⁰, **10**²¹, **11**²², and **13**²³. Compound **17** was synthesized as described in the appendix (Scheme S1). Conduritol B epoxide (CBE) **8** was bought from Enzo Life Sciences Inc. (Farmingdale, NY).

C. elegans: cultivation, collection, and homogenizing

C. elegans (wild type, N2 Bristol) and *E. coli* (OP50 and HB101 strains) used in this work were obtained from the Caenorhabditis Genetics Center (CGC). The culture of *C. elegans* and *E. coli* and the preparation of buffers and media for *C. elegans* cultivation were handled as the described in WormBook.³¹ Influences of using either OP50 or HB101 *E. coli* as food for *C. elegans* cultivation have been reported, and no major differences on lipid composition were described.³² Labelling of ABP **14** towards HB101 fed *C. elegans* homogenates showed the same result with OP50 fed *C. elegans* homogenates (data not shown). *C. elegans* was raised on 10 cm plates which contain nematode growth media (NGM) seeded with OP50 or HB101 *E. coli* at 20 °C. For bacteria used as food for seeding worm plates, *E. coli* strains were grown overnight in LB medium at 37 °C with 220 rpm shaking. NGM plates were seeded with 0.1-0.2 ml *E. coli* of overnight bacterial culture and plates were allowed to dry at 37 °C overnight.

To harvest large quantity of *C. elegans*, the nematodes were cultured in liquid medium as described in WormBook.³¹ Briefly, 6-8 plates of *C. elegans* maintained for 4 days after chunking to new plates, were transferred to a 0.5 L or 1 L flask inoculated with S Medium. The flasks were supplemented with OP50 or HB101 *E. coli* and maintained at 20 °C with vigorously shaking for 4-5 days. For harvesting, the flasks were put on ice for 15 min to allow the *C. elegans* to settle at the bottom and subsequently most of the liquid from the flask was aspirated. After removing clumping of *E. coli* bacteria in liquid as much as possible, the remaining liquid was transferred to a 50 mL conical centrifuge tube and spun down to pellet the worms. Subsequently, the remaining liquid was aspirated, and the pellet washed 2 times with M9 buffer and 1 time with ultrapure water by repeated centrifuge and aspiration steps. After aspirating, the pelleted *C. elegans* were stored at -80 °C.

To generate *C. elegans* homogenates, nematodes were taken from -80 °C and thawed on ice, then nematodes were homogenized in potassium phosphate buffer by sonication on ice with a sonicator (40-50 seconds sonication with 3 second pulse on and a 17 second pulse off cycle at a 40-45% amplitude). Afterwards, the homogenized sample was spun down at 15000 rpm for 3 min at 4 °C, and

the supernatant collected. Homogenate of OP50 *E. coli* was prepared with the same method as described above.

Generation of hGBA1 KO and hGBA1/GBA2 KO HEK293T cells

hGBA1 KO and hGBA1/GBA2 KO HEK293T cell line were generated as described in Chapter 2.²⁹ cGBA1-3 (encoded by *gba-3* gene, UniProt code: G5ECR8) was expressed in either hGBA1 KO or hGBA1/GBA2 KO HEK293T by PEI transfection,³³ followed by Zeocin screening to generate HEK293T cell line stably expressing the recombinant cGBA1-3.

cGBA1-3 cDNA construct

cDNA constructs were ordered from GenScript for *C. elegans* cGBA1-3 encoded by the *gba-3* gene. The construct contains the Genbank sequence NM_070718.4 with a C-terminal DYK tag. The signal peptide was predicted by SignalP 5.0.³⁴ The *gba-3* sequence in a zeocin resistance gene containing plasmid was obtained using the Gateway system (Invitrogen). To perform the PCR for the insert with the attB sites, Phusion polymerase (Fisher Scientific) was used. The fragments were isolated from a 1% agarose gel using the Nucleospin gel extraction kit (Machery-Nagel). All plasmids were sent for Sanger sequencing (LGTC) to confirm the sequences of the inserts.

Tabel 2. Primers for Gateway system.

Reaction	Forward	Reverse
Recombination cGBA1-3	5'- GGGGACAAGTTTGTACAAAAAAGCAGGC TCCGCCACCATGTCAAGATGGAAGGTCGT T -3'	5'- GGGGACCACTTTGTACAAGAAAGCTGG GTCTTATTTCTTTTCTTCCAAATCACT -3'

Measurement of enzymatic activities

Enzyme activities were measured by 4-methylumbelliferyl (MU)- β -D-glucopyranoside fluorogenic substrate assays, conducted in 96-well plates as described in Chapter 2 with adaptations as described below. Briefly, *C. elegans* homogenates, *E. coli* homogenates, or lysates of hGBA1/GBA2 KO HEK293T expressing recombinant cGBA1-3 were prepared in 12.5 μ L potassium phosphate buffer, and mixed with 12.5 μ L McIlvaine buffer (150 mM, at the appropriate pH) and incubated with 100 μ L 3.75 mM 4-MU- β -D-Glc dissolved in McIlvaine buffer (150 mM, at the appropriate pH) for 30 min or 60 min at 37 °C. To assess inhibitory effect of inhibitor, above 12.5 μ L hGBA1/GBA2 KO HEK293T cell lysates containing recombinant cGBA1-3 were mixed with 12.5 μ L inhibitor (**9** or **10**) diluted in McIlvaine buffer (150 mM, at the appropriate pH) and incubated for 30 min at 37 °C, then the 25 μ L samples were incubated with 100 μ L 3.75 mM 4-MU- β -D-Glc dissolved in McIlvaine (150 mM, pH 5.0) at 37 °C for 60 min. After stopping the enzyme reaction with 200 μ L 1 M NaOH-glycine (pH 10.3), 4-methylumbelliferone fluorescence was measured with a fluorimeter LS55 (Perkin Elmer, Waltham, MA, USA) with λ_{EX} 366 nm and λ_{EM} 445 nm. Enzyme activities were determined by subtraction of the background signal (measured for incubations without enzyme).

Activity-based protein profiling (ABPP) with SDS-PAGE

ABPP assays were conducted as described in Chapter 2. Briefly, *C. elegans* homogenates were incubated with a fluorescent ABP under the indicated conditions (at the appropriate pH at 37 °C for 30-60 min). The total sample volume was 20–40 µL with a 0.5–1% DMSO (the vehicle) final concentration in Mcllvaine buffer (150 mM, at the appropriate pH). After incubation with the ABP, samples were boiled the using 5× Laemmli buffer and separated by electrophoresis on 10% (w/v) SDS-PAGE gels. Wet gel slabs were scanned on fluorescence using the Typhoon FLA 9500 (GE Healthcare) at λ_{EX} 532 nm and $\lambda_{\text{EM}} \geq 575$ nm for BODIPY-red mediated fluorescence; and at λ_{EX} 635 nm and $\lambda_{\text{EM}} \geq 665$ nm for Cy5 mediated fluorescence. Afterwards, the gels were stained by Coomassie brilliant blue (CBB) G250 or R250 for protein loading control.

Competitive ABPP with SDS-PAGE

Competitive ABPP assays are conducted as described in Chapter 2 with adaptations as described below. Generally, *C. elegans* homogenates or lysates of hGBA1/GBA2 KO HEK293T expressing recombinant cGBA1-3 were first treated with inhibitors (**7-11**) or the vehicle (DMSO) in Mcllvaine buffer (150 mM, pH 6.0) for 30 min incubation at 37 °C. Subsequently, fluorescent ABP **14** was added to samples and incubated for 30 min at 37 °C to reveal residual active enzymes. Afterwards, samples were subjected to SDS-PAGE and fluorescence scanning as described above. Final concentration of DMSO for all samples is 0.5-1%.

Biotinylated ABP, pull down and proteomics

For pull-down with biotin-ABPs (**13**, **16**, **20**), 500 µg total protein from *C. elegans* homogenates (nematodes were fed with HB101 *E. coli* in liquid NGM) were diluted with Mcllvaine buffer (750 mM, pH 5.0 for ABP **13**, **16**, or pH 6.0 for ABP **20**) to a total volume of 240 µL for each sample and incubated with biotin-tagged ABP (10 µM for **13** and **16**, 20 µM for **20**) at 37 °C for 2 h. For controls, the same volume of DMSO without ABPs was used and all samples have the same final DMSO concentration (0.5-1%). For competition with ABP **14**, the *C. elegans* homogenates were first treated with 5 µM ABP **14** for 1 h incubation at 37 °C, following by incubation with biotin-ABPs (**13**, **16**, **20**) for 2 h at 37 °C. Afterwards, samples were denatured with 10% (w/v) SDS, subjected to chloroform/ methanol precipitation (C/M), reduction/alkylation, C/M precipitation, and pull-down with 75 µL Pierce™ avidin agarose beads (Thermo Scientific) in a volume of 3400 µL pull-down buffer (50 mM Tris-HCl, pH 7.4 with 150 mM NaCl) at 4 °C overnight with a tumbling shaker, as previously described.^{35,36} Afterwards, the samples were subjected to on-bead trypsin digestion and desalted using stage-tips. Desalted peptide samples were reconstituted in 30 µL LC-MS solution (97:3:0.1 H₂O, ACN, FA) containing 10 fmol/µL yeast enolase digest (cat. 186002325, Waters) as injection control. Raw files were analyzed with MaxQuant (Version 2.0.1.0). The following changes were made to the standard settings of MaxQuant: label-free quantification was enabled with an LFQ minimal ratio count of 1. Matches between runs and iBAQ quantification were enabled. Searches were performed against a UniProt database of the *Caenorhabditis elegans* proteome (UP000001940) including yeast enolase (P00924).

N-glycanase treatment

For N-glycans removal, total 20 µg proteins (from *C. elegans* homogenate or lysate of HEK293T hGBA1/GBA2 KO cell expressing recombinant cGBA1-3) in Mcllvaine buffer (150 mM, pH 6.0) were incubated with 1 µM ABP **14** for 30 min at 37 °C. Afterwards, an aliquot of the samples was treated with PNGase F according to the manufacturer's protocol (New England BioLabs). For samples as control

(without incubation with PNGase F), samples with a normalized protein amount were incubated with 1 μ M ABP **14** for 30 min at 37°C in McIlvaine buffer (150 mM, pH 6.0). Subsequently, both the control and PNGase F-treated samples were subjected to SDS PAGE and fluorescence scanning as described above.

Analysis of C12-NBD-Glc degradation using HPTLC

40-50 μ g *C. elegans* homogenates were incubated with 2 μ M C12-NBD-GlcCer in McIlvaine buffer (150 mM) at pH 5.0 for 3-4 h at 37 °C. In the case using lysates of GBA1/GBA2 KO HEK293T expressing rcGBA1-3, a total of 200 μ g lysates were incubated with 2 μ M C12-NBD-GlcCer in McIlvaine buffer (150 mM) at pH 4.5 for 3-4 h at 37 °C. Next, lipids were extracted according to the method of Bligh and Dyer³⁷ by addition of methanol, chloroform, and water (1:1:0.9, v/v/v) and the lower phase was dried under a stream of nitrogen. lipids were separated by HPTLC on silica gel 60 plates (Merck, Darmstadt, Germany) using chloroform/methanol (85:15, v/v) as developing solution followed by detection of NBD-labelled lipids using a Typhoon variable mode imager (GE Healthcare Bio-Science Corp., Piscataway, NJ).³⁸

Analysis of GlcChol by LC-MS/MS

Lipids in *C. elegans* homogenates were extracted and measured according to methods described previously.²⁵ Briefly, 20 μ L of ¹³C-GlcChol (0.1 pmol/ μ L) in MeOH, 480 μ L MeOH, and 250 μ L CHCl₃ were added to the *C. elegans* homogenate samples, stirred, incubated for 30 min at room temperature and sonicated (5 \times 1 min in sonication water bath), followed by centrifugation for 10 min at 15,000 rpm. Supernatants were collected in a clean tube, where 250 μ L CHCl₃ and 450 μ L 100 mM formate buffer (pH 3.2) was added. The samples were stirred and centrifuged, the upper phase was removed. The lower phase was pipetted into a clean tube, to which was added 400 μ L MeOH, 360 μ L formate buffer, and 400 μ L CHCl₃ after which the lower phase was transferred to a clean tube. The lower phase was dried, after which 700 μ L H₂O and BuOH was added and upper phase transferred to a new tube and dried. The residue was dissolved in 100 μ L MeOH. 10 μ L Of these samples were injected into the LC-MS/MS for lipid measurement as previous described.²⁵

References

1. D. E. Koshland, Stereochemistry and the mechanism of enzymatic reactions, *Biol. Rev.* 1953, **28**, 416-436.
2. M. Horowitz, S. Wilder, Z. Horowitz, O. Reiner, T. Gelbart, E. Beutler, The human glucocerebrosidase gene and pseudogene: structure and evolution, *Genomics* 1989, **4**, 87-96.
3. J. Aerts, C. L. Kuo, L. T. Lelieveld, D. E. C. Boer, M. J. C. van der Lienden, H. S. Overkleeft, M. Artola, Glycosphingolipids and lysosomal storage disorders as illustrated by Gaucher disease, *Curr. Opin. Chem. Biol.* 2019, **53**, 204-215.
4. J. Stirnemann, N. Belmatoug, F. Camou, C. Serratrice, R. Froissart, C. Caillaud, T. Levade, L. Astudillo, J. Serratrice, A. Brassier, C. Rose, T. Billette de Villemeur, M. G. Berger, A review of Gaucher disease pathophysiology, clinical presentation and treatments, *Int. J. Mol. Sci.* 2017, **18**.
5. J. Mitsui, I. Mizuta, A. Toyoda, R. Ashida, Y. Takahashi, J. Goto, Y. Fukuda, H. Date, A. Iwata, M. Yamamoto, N. Hattori, M. Murata, T. Toda, S. Tsuji, Mutations for Gaucher disease confer high susceptibility to Parkinson disease, *Arch. Neurol.* 2009, **66**, 571-576.
6. E. Sidransky, G. Lopez, The link between the *GBA* gene and parkinsonism, *Lancet Neurol.* 2012, **11**, 986-998.
7. R. Sam, E. Ryan, E. Daykin, E. Sidransky, Current and emerging pharmacotherapy for Gaucher disease in pediatric populations, *Expert Opin. Pharmacother.* 2021, **22**, 1489-1503.
8. C. Fernandez-Pereira, B. San Millan-Tejado, M. Gallardo-Gomez, T. Perez-Marquez, M. Alves-Villar, C. Melcon-Crespo, J. Fernandez-Martin, S. Ortolano, Therapeutic approaches in lysosomal storage diseases, *Biomolecules* 2021, **11**.
9. G. Parenti, G. Andria, A. Ballabio, Lysosomal storage diseases: from pathophysiology to therapy, *Annu. Rev. Med.* 2015, **66**, 471-486.
10. A. Massimo, S. Maura, L. Nicoletta, M. Giulia, M. Valentina, C. Elena, P. Alessandro, B. Rosaria, S. Sandro, Current and novel aspects on the Non-lysosomal beta-glucosylceramidase *GBA2*, *Neurochem. Res.* 2016, **41**, 210-220.
11. T. Cox, R. Lachmann, C. Hollak, J. Aerts, S. van Weely, M. Hrebicek, F. Platt, T. Butters, R. Dwek, C. Moyses, I. Gow, D. Elstein, A. Zimran, Novel oral treatment of Gaucher's disease with N-butyldeoxynojirimycin (OGT 918) to decrease substrate biosynthesis, *Lancet* 2000, **355**, 1481-1485.
12. T. M. Cox, J. M. Aerts, G. Andria, M. Beck, N. Belmatoug, B. Bembi, R. Chertkoff, S. Vom Dahl, D. Elstein, A. Erikson, M. Giral, R. Heitner, C. Hollak, M. Hrebicek, S. Lewis, A. Mehta, G. M. Pastores, A. Rolfs, M. C. Miranda, A. Zimran, D. Advisory Council to the European Working Group on Gaucher, the role of the iminosugar N-butyldeoxynojirimycin (miglustat) in the management of type I (non-neuronopathic) Gaucher disease: a position statement, *J. Inherit. Metab. Dis.* 2003, **26**, 513-526.
13. X. Cheng, X. Jiang, K. Y. Tam, G. Li, J. Zheng, H. Zhang, Sphingolipidomic analysis of *C. elegans* reveals development- and environment-dependent metabolic features, *Int. J. Biol. Sci.* 2019, **15**, 2897-2910.
14. T. Wennekes, R. J. van den Berg, R. G. Boot, G. A. van der Marel, H. S. Overkleeft, J. M. Aerts, Glycosphingolipids - nature, function, and pharmacological modulation, *Angew. Chem. Int. Ed.* 2009, **48**, 8848-8869.
15. J. L. Watts, M. Ristow, Lipid and carbohydrate metabolism in *Caenorhabditis elegans*, *Genetics* 2017, **207**, 413-446.
16. M. A. Xatse, A. F. C. Vieira, C. Byrne, C. P. Olsen, Targeted lipidomics reveals a novel role for glucosylceramides in glucose response, *J. Lipid Res.* 2023, **64**, 100394.
17. M. A. Xatse, C. P. Olsen, Defining the glucosylceramide population of *C. elegans*, *Front. Physiol.* 2023, **14**, 1244158.
18. C. e. S. Consortium, Genome sequence of the nematode *C. elegans*: a platform for investigating biology, *Science* 1998, **282**, 2012-2018.

19. C. L. Kuo, W. W. Kallemeyjn, L. T. Lelieveld, M. Mirzaian, I. Zoutendijk, A. Vardi, A. H. Futerman, A. H. Meijer, H. P. Spaink, H. S. Overkleeft, J. Aerts, M. Artola, In vivo inactivation of glycosidases by conduritol B epoxide and cyclophellitol as revealed by activity-based protein profiling, *FEBS J.* 2019, **286**, 584-600.
20. M. Artola, C. L. Kuo, L. T. Lelieveld, R. J. Rowland, G. A. van der Marel, J. D. C. Codée, R. G. Boot, G. J. Davies, J. Aerts, H. S. Overkleeft, Functionalized cyclophellitols are selective glucocerebrosidase inhibitors and induce a bona fide neuropathic Gaucher model in zebrafish, *J. Am. Chem. Soc.* 2019, **141**, 4214-4218.
21. D. Lahav, B. Liu, R. van den Berg, A. van den Nieuwendijk, T. Wennekes, A. T. Ghisaidoobe, I. Breen, M. J. Ferraz, C. L. Kuo, L. Wu, P. P. Geurink, H. Ovaa, G. A. van der Marel, M. van der Stelt, R. G. Boot, G. J. Davies, J. Aerts, H. S. Overkleeft, A fluorescence polarization activity-based protein profiling assay in the discovery of potent, selective inhibitors for human nonlysosomal glucosylceramidase, *J. Am. Chem. Soc.* 2017, **139**, 14192-14197.
22. H. S. Overkleeft, G. H. Renkema, J. Neele, P. Vianello, I. O. Hung, A. Strijland, A. M. van der Burg, G. J. Koomen, U. K. Pandit, J. M. Aerts, Generation of specific deoxynojirimycin-type inhibitors of the non-lysosomal glucosylceramidase, *J. Biol. Chem.* 1998, **273**, 26522-26527.
23. N. E. Trenkler, Photocleavable activity-based acid glucosylceramidase probes, Thesis, Leiden University, 2023, <https://hdl.handle.net/1887/3665361>.
24. W. W. Kallemeyjn, K. Y. Li, M. D. Witte, A. R. Marques, J. Aten, S. Scheij, J. Jiang, L. I. Willems, T. M. Voorn-Brouwer, C. P. van Roomen, R. Ottenhoff, R. G. Boot, H. van den Elst, M. T. Walvoort, B. I. Florea, J. D. Codée, G. A. van der Marel, J. M. Aerts, H. S. Overkleeft, Novel activity-based probes for broad-spectrum profiling of retaining beta-exoglucosidases in situ and in vivo, *Angew. Chem. Int. Ed.* 2012, **51**, 12529-12533.
25. A. R. Marques, M. Mirzaian, H. Akiyama, P. Wisse, M. J. Ferraz, P. Gaspar, K. Ghauharali-van der Vlugt, R. Meijer, P. Giraldo, P. Alfonso, P. Irun, M. Dahl, S. Karlsson, E. V. Pavlova, T. M. Cox, S. Scheij, M. Verhoek, R. Ottenhoff, C. P. van Roomen, N. S. Pannu, M. van Eijk, N. Dekker, R. G. Boot, H. S. Overkleeft, E. Blommaart, Y. Hirabayashi, J. M. Aerts, Glucosylated cholesterol in mammalian cells and tissues: formation and degradation by multiple cellular beta-glucosidases, *J. Lipid Res.* 2016, **57**, 451-463.
26. M. D. Witte, W. W. Kallemeyjn, J. Aten, K. Y. Li, A. Strijland, W. E. Donker-Koopman, A. M. van den Nieuwendijk, B. Bleijlevens, G. Kramer, B. I. Florea, B. Hooibrink, C. E. Hollak, R. Ottenhoff, R. G. Boot, G. A. van der Marel, H. S. Overkleeft, J. M. Aerts, Ultrasensitive in situ visualization of active glucocerebrosidase molecules, *Nat. Chem. Biol.* 2010, **6**, 907-913.
27. S. P. Schröder, J. W. van de Sande, W. W. Kallemeyjn, C. L. Kuo, M. Artola, E. J. van Rooden, J. Jiang, T. J. M. Beenakker, B. I. Florea, W. A. Offen, G. J. Davies, A. J. Minnaard, J. Aerts, J. D. C. Codée, G. A. van der Marel, H. S. Overkleeft, Towards broad spectrum activity-based glycosidase probes: synthesis and evaluation of deoxygenated cyclophellitol aziridines, *Chem. Commun.* 2017, **53**, 12528-12531.
28. J. Jiang, T. J. Beenakker, W. W. Kallemeyjn, G. A. van der Marel, H. van den Elst, J. D. Codée, J. M. Aerts, H. S. Overkleeft, Comparing cyclophellitol N-alkyl and N-acyl cyclophellitol aziridines as activity-based glycosidase probes, *Chem. Eur. J.* 2015, **21**, 10861-10869.
29. Q. Su, S. P. Schröder, L. T. Lelieveld, M. J. Ferraz, M. Verhoek, R. G. Boot, H. S. Overkleeft, J. Aerts, M. Artola, C. L. Kuo, Xylose-configured cyclophellitols as selective inhibitors for glucocerebrosidase, *ChemBioChem* 2021, **22**, 3090-3098.
30. K. Y. Li, J. Jiang, M. D. Witte, W. W. Kallemeyjn, H. van den Elst, C. S. Wong, S. D. Chander, S. Hoogendoorn, T. J. M. Beenakker, J. D. C. Codée, J. M. F. G. Aerts, G. A. van der Marel, H. S. Overkleeft, Synthesis of cyclophellitol, cyclophellitol aziridine, and their tagged derivatives, *Eur. J. Org. Chem.* 2014, 6030-6043.
31. T. Stiernagle, Maintenance of *C. elegans*, *WormBook*, 2006, DOI: 10.1895/wormbook.1.101.1, 1-11.

32. S. Melov, K. K. Brooks, B. Liang, J. L. Watts, The influence of bacterial diet on fat storage in *C. elegans*, *PLoS ONE* 2009, **4**.
33. P. A. Longo, J. M. Kavran, M. S. Kim, D. J. Leahy, Transient mammalian cell transfection with polyethylenimine (PEI), *Methods Enzymol.* 2013, **529**, 227-240.
34. J. J. Almagro Armenteros, K. D. Tsirigos, C. K. Sønderby, T. N. Petersen, O. Winther, S. Brunak, G. von Heijne, H. Nielsen, SignalP 5.0 improves signal peptide predictions using deep neural networks, *Nat. Biotechnol.* 2019, **37**, 420-423.
35. N. Li, C. L. Kuo, G. Paniagua, H. van den Elst, M. Verdoes, L. I. Willems, W. A. van der Linden, M. Ruben, E. van Genderen, J. Gubbens, G. P. van Wezel, H. S. Overkleeft, B. I. Florea, Relative quantification of proteasome activity by activity-based protein profiling and LC-MS/MS, *Nat. Protoc.* 2013, **8**, 1155-1168.
36. C. L. Kuo, Q. Su, A. van den Nieuwendijk, T. J. M. Beenakker, W. A. Offen, L. I. Willems, R. G. Boot, A. J. Sarris, A. R. A. Marques, J. D. C. Codée, G. A. van der Marel, B. I. Florea, G. J. Davies, H. S. Overkleeft, J. Aerts, The development of a broad-spectrum retaining beta-exo-galactosidase activity-based probe, *Org. Biomol. Chem.* 2023, **21**, 7813-7820.
37. E. G. Bligh, W. J. Dyer, A rapid method of total lipid extraction and purification, *Can. J. Biochem. Physiol.* 1959, **37**, 911-917.
38. S. van Weely, M. Brandsma, A. Strijland, J. M. Tager, J. M. Aerts, Demonstration of the existence of a second, non-lysosomal glucocerebrosidase that is not deficient in Gaucher disease, *Biochim. Biophys. Acta*, 1993 **1181**, 55-62.

Appendix

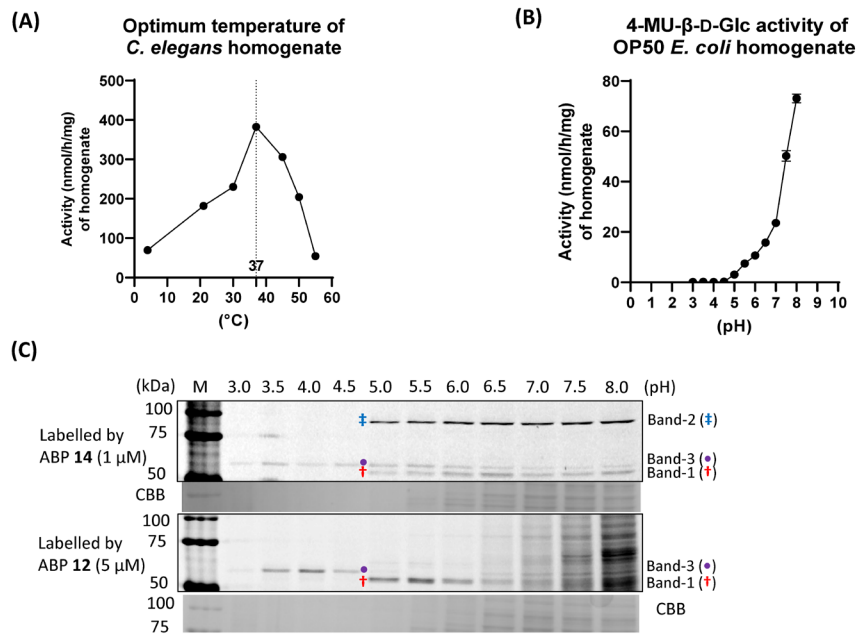


Figure S1. (A) Optimum temperature of *C. elegans* homogenates for hydrolyzing 4-MU- β -D-Glc. *C. elegans* homogenates were incubated with 4-MU- β -D-Glc for 30 min at pH 5.0 under various temperatures (4-55 °C). (B) 4-MU- β -D-Glc hydrolysis activity of OP50 *E. coli* homogenates. OP50 *E. coli* homogenates were incubated with 4-MU- β -D-Glc for 30 min at 37 °C and at various pH values (3-8). (C) *C. elegans* homogenates were incubated with ABP 12 (5 μ M, hGBA1-selective) or 14 (1 μ M, human β -glucosidases broad-spectrum) for 30 min at 37 °C and at various pH values (3-8), subsequently, samples were subjected to SDS-PAGE and fluorescence scanning of the wet gel slabs.

Table S1. Putative β -glucosidases in *C. elegans* homogenates as identified by chemical proteomics, using biotinylated ABP (13, 16, 20). Raw abundance of predicted GBA1-like protein (UniProt code: G5ECR8) and predicted GBA2-like protein (UniProt code: O01893) enriched by ABP 13, 16, 20, indicate by label-free quantification (LFQ) intensity. Higher intensity of LFQ intensity suggests a larger amount of proteins captured and enriched. Samples include the setting groups below. Group 1: Vehicle beads control, pull down (PD) assays only using streptavidin beads, without addition of biotin-ABPs; Group 2-4: PD assays using biotin-ABPs (13, 16, 20); Group 5-6: PD assays with ABP 14 pre-treatment prior to adding biotin-ABPs (16, 20). See detailed conditions in experimental procedures.

		Group 1: Control (without biotin-ABPs)							
Accession	Gene name	Mark	LFQ intensity (3 sets)						
G5ECR8	<i>gba-3</i>	GBA1-like	0	0	0				
O01893; A0A168H9S8	<i>R08F11.1</i>	GBA2-like	0	0	0				
		incubated at	pH 5.0	pH 5.0	pH 6.0				
			Group 2: PD using biotin-ABP 16			Group 5: PD using 16, with ABP 14 pre-treatment			
Accession	Gene name	Mark	LFQ intensity (3 sets)			LFQ intensity (3 sets)			
G5ECR8	<i>gba-3</i>	GBA1-like	2.46E+07	1.68E+07	1.73E+07	6.07E+05	5.18E+05	1.76E+05	
O01893; A0A168H9S8	<i>R08F11.1</i>	GBA2-like	9.98E+06	7.89E+06	5.34E+06	1.87E+04	1.07E+04	0	
		incubated at	pH 5.0						
			Group 3: PD using biotin-ABP 13						
Accession	Gene name	Mark	LFQ intensity (3 sets)						
G5ECR8	<i>gba-3</i>	GBA1-like	1.99E+07	1.41E+07	1.87E+07				
O01893; A0A168H9S8	<i>R08F11.1</i>	GBA2-like	2.76E+03	5.43E+03	3.66E+03				
		incubated at	pH 5.0						
			Group 4: PD using biotin-ABP 20			Group 6: PD using 20, with ABP 14 pre-treatment			
Accession	Gene name	Mark	LFQ intensity (3 sets)			LFQ intensity (2 sets)			
G5ECR8	<i>gba-3</i>	GBA1-like	6.71E+03	3.25E+03	3.69E+03	2.84E+03	0		
O01893; A0A168H9S8	<i>R08F11.1</i>	GBA2-like	1.64E+07	1.03E+07	8.13E+06	0	4.25E+03		
		incubated at	pH 6.0						

(A)	AA number
hGBA1 : MEFFSSPSREECPKPLSRVSIAGSLTGLLLQAVSWASGARPCIPKSF--GYSSVVCVCNATYCDSEFDPPTFPALCTFSRYESTRSCRRM : 89	
cGBA1-3 : -----MSRWKVVLCLLSFMFEIGHASFOCNPKTYDGAFLNIIVCVCNATFCDEIEPIGEIAGEKAIVYRSLDGDRL : 73	
hGBA1 : ---ELSMGPQANHTGTGLLLTLOPEQKFQKVGFGGAWTDAALNIALSPPAONLLLSYFSEEIGYNIIRVPMASCDFSIRTWTYA : 176	
cGBA1-3 : KRMSMKWKEKLRKNESVNVITIDASERFONIFGFGGAFDTSAGDQFVSLSETLQNYIVDSYFGKNCLEYNICRVPTASCDFSITHEISVD : 163	
hGBA1 : DTPDDFOLHNFSLEEDTKLKIPLIHRAQLAORPVSLASPTTSTFWLKTNCVAVNCKGSLKGQPGDIYHOTWARYEVKELDAYAEHLQ : 266	
cGBA1-3 : DVHDDFELKHFALEDEDLKLIKIPKKAIEKTEGNIQLFASPWASAPGWMKVTGRMRGGGAMRNDK--RVYQAYADYEFKEFEAYSSHAIT : 251	
hGBA1 : FWAVTAENFPSACLLSGYPFOCLGFPEHQRDEIARDLGFTIANST-HHNVRLLMLDDORLLLPWAKVVLTDPEAAKYVHGTAVHWYLD : 355	
cGBA1-3 : FWGLTIQNEPSTCADMAWRWQTMNYTAETMRDELKYLGPKLKENKLTETLKVMLDDCRGLLEGWADTIFNDPEATKYADGVAVHWYGN : 341	
hGBA1 : FLAPAKATIGETHRLPENTMLFASACVCSKFEQSVRLCSWDRGMOYSHSITNLLYHVVGWTDWNLAENPEGGPNWVRNFVDSPIIVD : 445	
cGBA1-3 : LYSFAV-LLDITCRHHETKFIFGTACAGY-FGHHGPIMDWFRAESYADDIITDINHHVTGWTDWNLCDEDEGGPNWAVNVDSPPIIVN : 429	
hGBA1 : ITKDTFYKQPMFYHLGHFSKFIPEGSORVGLVASQKNDLDAVALMHPDGSVVVVLNRSKDVPLTIKDPAVGLET-ISPQYSIHTYLW : 534	
cGBA1-3 : RTAQEFYKQPMFYALGHFSKFLPRGSTRVFTKIEGNLAVSATSVVIEGCRRAVILSKASNSLLTRIVDSSTGHSIVLNLPPIHSIHTVIN : 519	
hGBA1 : RRQ-	: 537
cGBA1-3 : KKRK	: 523

(B)

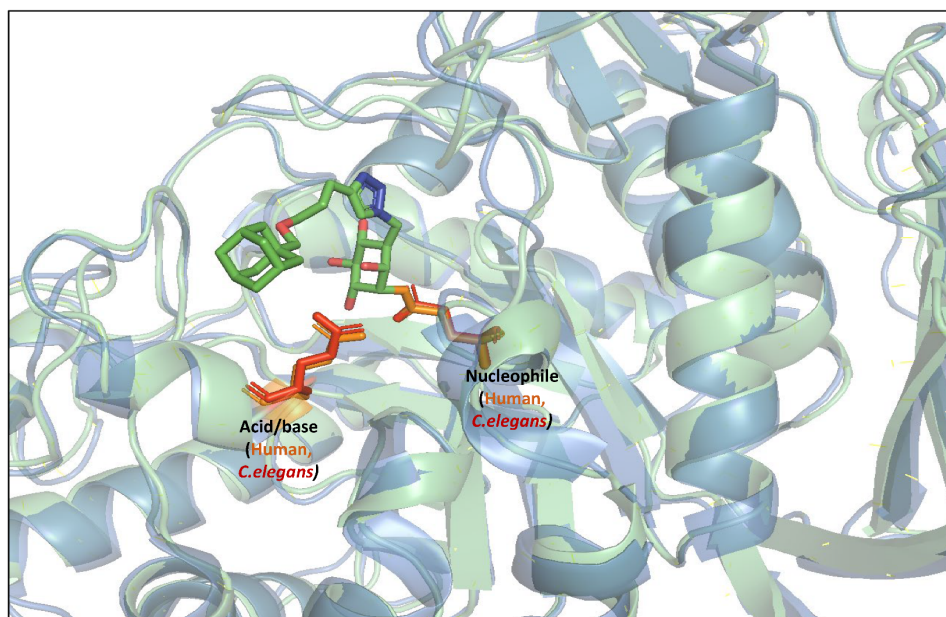


Figure S2. (A) Amino acid (AA) alignment of hGBA1 (UniProt code: P04062) and cGBA1-3 (UniProt code: G5ECR8). Signal peptides predicted by SignalP 5.0 are marked as blue, identical AA are marked with a black box, catalytic active residues are marked as red. (B) Overlap of the AlphaFold¹ predicted protein structure of cGBA1-3 (aqua green) and the complex crystallization of hGBA1 (nattier blue, PDB 6Q6L) with compound **13** (sticks, C = bottle green, O = red, N = blue), processed by PyMOL 2.0. Catalytic active site of (AA numbers without counting signal peptides): hGBA1 (orange sticks), nucleophile = E340, acid/base = E235; cGBA1-3 (red sticks): nucleophile = E343, acid/base = E238.

	AA number
hGBA2 : MGTQDPGNMGTGVPASEQISCAGEDPQVYCPEETGGTKDVQVTDCKSPEDSRPPKETDCCNPEDSGQLMVS Y GKAMGYQVPFFG R ICL :	90
cGBA2 : -----MS F EH R D--RMLEGI G W K ARG :	19
hGBA2 : --AB E TE R K R K P FOANN V LSNM I K H IG M G-LRYLQ W Y R K T HVE K K T P F ID M NS V PL R Q I Y G CP L GG I GG T IT R GW R G O FC R W Q L N F :	177
cGBA2 : DR I P E EP N EP P EP R L K SI K L I PL F VR V AL H T F VE W NG-----RE A F I D I F N VER H F T Y T GV P LG G I G CC S IG T DR E GG N R F SI P :	103
hGBA2 : G M Y Q H R T V -I A D O F T V C L--R R E G Q T V Y Q O V L S L E--R P S V I R S W N W GL C G Y F A F H A L Y P RA W T V Y O PG Q N V LT C R Q IT S IL E HD W Q :	262
cGBA2 : G I KE Q T E T Q K C N O FI V TV H SK K T F E L I Y Q S IL S CA E FP A T V LP K W D TT I PA E D V R G L F PA R W Q E F R I G S SC V TV V EH S L S VI P GD Y S :	193
hGBA2 : D S SL F V G V F V W D V EN E GD F AL D V S IM F SR N CL G GG D D A PG L W N EP F CL R ----S G ET V R G IL L HH P T L NP V TM A VA A R V TA A TT V T :	348
cGBA2 : D S SL F LAN E EF H V F ND S Y E EV S IT M SR N CT N R K W N D E -----N L C S Q S Q I Q K D T M V VR T LA H T V K G M P VT V IA G TE E K--N--G S K V :	275
hGBA2 : H I TA F ED D ST G Q Q V W OD L L Q D F OLD S PT G ST P T Q RG V GI A CV S SK L R E FG Q CR L EF S LA W DM E R I MF G AK G Q V H Y RR Y TR F FG Q D G :	438
cGBA2 : TT C LD P NG T IG G RL N SD L E A Y C HL S SY D HL P ---SR P K E L G TA V CS F FP P ED GA NT O F S LT W Y M P Q V H FG TA ER F Y N R R Y Q R F ENG P D :	362
hGBA2 : D--A A PL S HY A L C RY A E E ER I SA W SP V LD R SL P ANY K S A L F N E LY F LA D CG T V W LE V LD S LP E EL G R N M C HL R PT L R D Y G R F G Y L :	526
cGBA2 : A D EV T A A TC R HL Q N F ST W OK K IED W AP V LD Q KL P W Y K S A I F N ELY I VD G ST V W F E Y DP D W K TE S -L M SE Q TE K Q F K Y G R FG Y M :	451
hGBA2 : G Q E Y RM Y NT Y D V H F Y A S F AL I ML W E K LE L SL O Y D MA L AT L RE D L T RR Y LM S GV M AP V RR R N V IP H DI G DP D EP W LR V NA L I H D T AD :	616
cGBA2 : S W E Y EM I NT Y D V H F Y S W A IL K N W Q I EM S Q L D E AD Q MD R VD N NI A TS I AD G EM T IR S VD R IP H DM G HP MA DP W I H T N A L I L HD T GR :	541
hGBA2 : W K DL N L K F V L Q V R Y Y LT G D Q N---F K DM W P V CL A VM E SE-M K FD K D H D G L I ENG C Y A D Q T Y IG W VT G FS A Y C CG L W L A A V A VM V Q :	701
cGBA2 : W K DL N L K F V IS C Y R Y L EL G SE K G Q V E FF L G K CT K I V D G AL E C W DK D ND G MI EN D GA D Q T Y IV W K M T G FS A Y C CG L W L A A L S SY I E :	631
hGBA2 : M A AL C GA Q DI Q DK F SS I SR G Q E Y E RL W N C RY Y ND S SS R P S RS V MS D CA G W F L K AC G L G EG D TE V FT Q H V VR A L O IT F E L N V Q :	791
cGBA2 : M L K Q SL P T--K H Y E E K EM A Y D AY I G K L W N C TF F K F DEL P E-NS K IV M AD Q LC G FW A MT A MD E ---P V Q I SK D K M K S AL D IT F K Y N V Q :	714
hGBA2 : A F AG C AM G AV N CM Q PH G VP D K S SV Q SD E V W CV V Y G LA T MI Q E L T W EG F OT A EC C Y R TV W ER L CL A F Q TP E AY C Q Q R V FS L AY M R P L :	881
cGBA2 : M Y NN R CA V NG Y LT S ER V D G SS I Q S EE V W A C I T A LS A MM I E K CM D E Q A E KT S E L FS I N H RF L Q Y Q T PE A ITS D GM Y RA L GM Y R P L :	804
hGBA2 : SI W A Q AL Q Q Q HH K AS W PK V K Q GT L RT G PM F GP K E A MAN L SP E :	927
cGBA2 : SI W A Q AL Q DR R Y R E----- :	819

Figure S3. Amino acids (AA) alignment of hGBA2 (UniProt code: Q9HCG7) and cGBA2 (UniProt code: O01893). Identical AA were marked with black box. Catalytic active site of hGBA2 and cGBA2 (predicted) are marked as red: hGBA2, nucleophile = E527, acid/base = D677; cGBA2, nucleophile = E452, acid/base = D607.

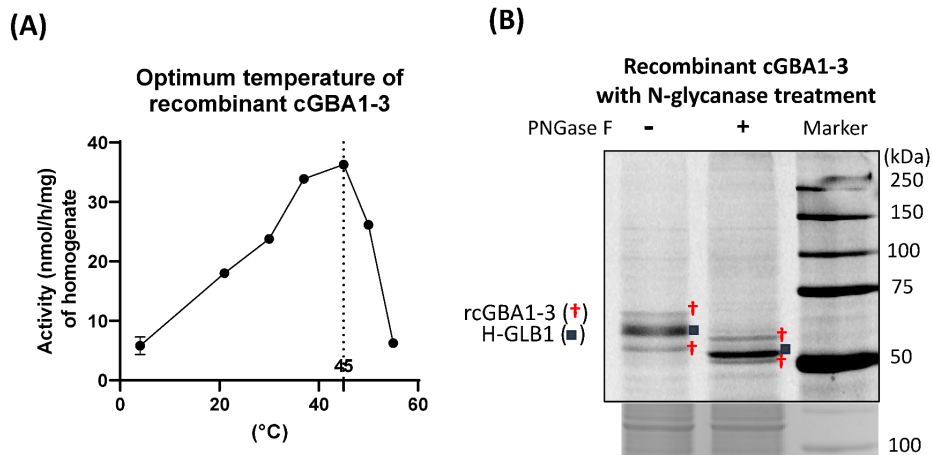


Figure S4. (A) Optimum temperature of recombinant cGBA1-3 for hydrolyzing 4-MU- β -D-Glc. Lysates of hGBA1/GBA2 KO HEK293T cell expressing rcGBA1-3 were incubated with 4-MU- β -D-Glc for 45 min at pH 5.0 under various temperatures (4 °C-55 °C). (B) Treating rc-GBA1-3 with PNGase F. Lysates of hGBA1/GBA2 KO HEK293T cell expressing rcGBA1-3 were incubated with ABP **14** for 30 min at 37 °C at pH 5.0, followed by incubation with PNGase F for 2 h, then samples were subjected to SDS-PAGE and fluorescence scanning of the wet gel slabs.

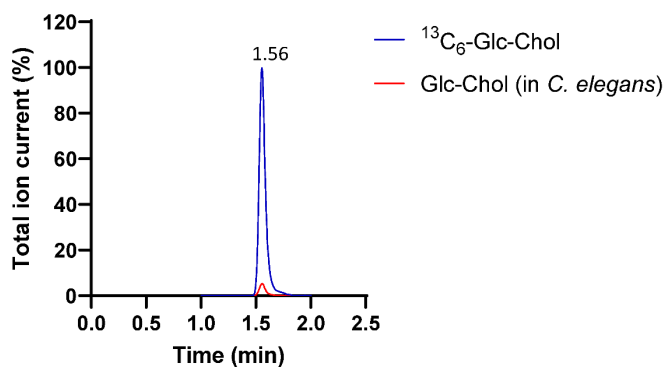
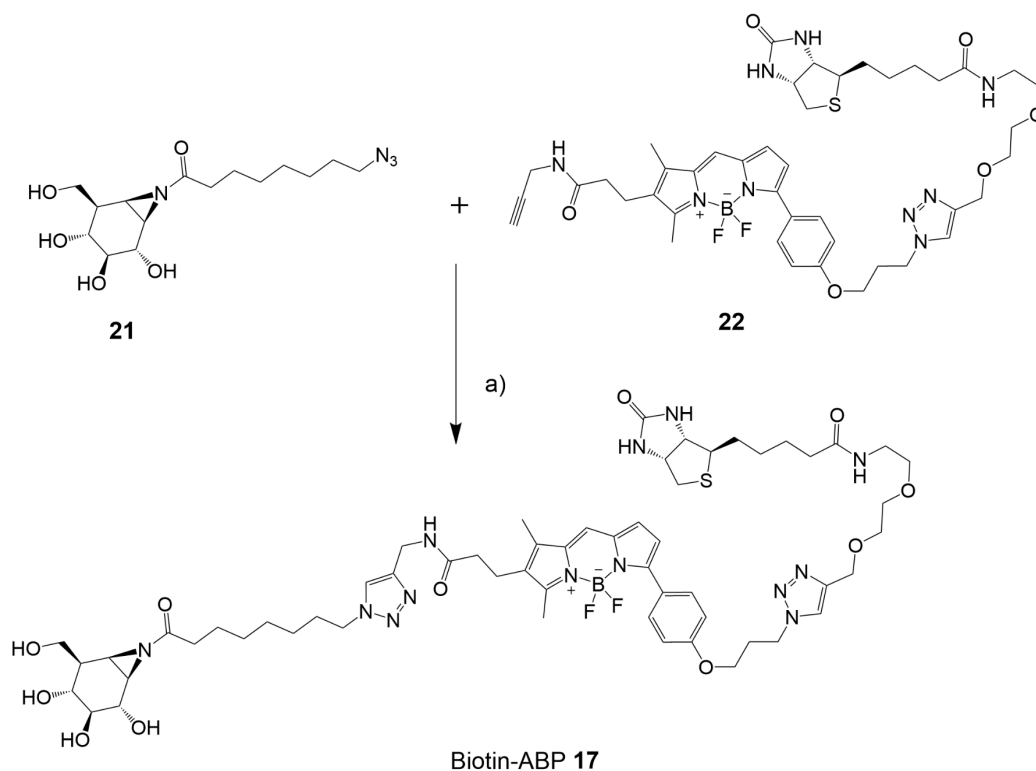
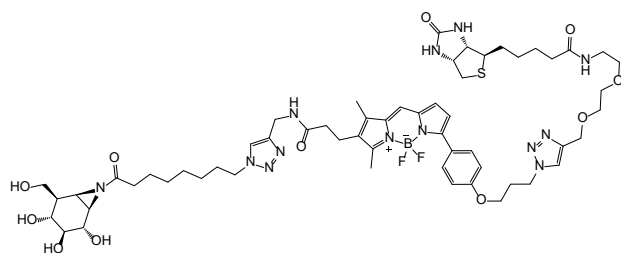
GlcChol of *C. elegans* detected by LC-MS/MS

Figure S5. Presence of GlcChol in *C. elegans* homogenates as detected by LC-MS/MS, using total 2 pmol $^{13}\text{C}_6$ - β -GlcChol as internal standard, $n = 2$ replicates. Quantification reveals the level of GlcChol in *C. elegans* extracts is around 0.1 pmol/ μg .

Synthesis of ABP 17



Scheme S1. Synthesis of ABP 17. (a) CuSO_4 , sodium ascorbate, rt, 15%.



A solution of $\text{CuSO}_4 \cdot 5\text{H}_2\text{O}$ and sodium ascorbate (0.1 M in MilliQ water) was freshly prepared. Cyclophellitol-aziridine azide **21**² (4.71 mg, 14 μmol , 1 eq.) was dissolved in DMF (2 mL), $\text{CuSO}_4 \cdot 5\text{H}_2\text{O}$ (0.1 M, 62 μL , 6.2 μmol , 0.45 eq.) and sodium ascorbate (0.1 M, 62 μL , 6.2 μmol , 0.45 eq.) were added to the solution

under argon atmosphere. Then, a solution of **22**² alkyne biotin (12 mg, 14 μmol , 1 eq.) in 1 mL of DMF was added and the reaction mixture was stirred at rt overnight. The resulting mixture was checked with LC/MS within the elution system of 10% NH_4OAc . Starting material was consumed and the reaction mixture was then concentrated under reduced pressure and purified by semi-preparative reversed HPLC (linear gradient: 32% \rightarrow 35% B in A, 12 min, solutions used A: 50 mM NH_4HCO_3 in H_2O , B: acetonitrile), the fractions were concentrated and lyophilized to the final product (2.52 mg, 14 μmol , 15%) which was freeze-dried and aliquoted in 100 nmol tubes. **¹H NMR** (850 MHz, MeOD) δ 8.02 (s, 1H), 7.93 – 7.89 (m, 2H), 7.45 (d, J = 8.2 Hz, 1H), 7.13 – 7.10 (m, 1H), 6.98 (d, J = 8.4, 1.2 Hz, 2H), 6.68 (dd, J = 6.1, 4.1 Hz, 1H), 4.67 (td, J = 6.8, 1.7 Hz, 2H), 4.65 (d, J = 2.1 Hz, 2H), 4.46 – 4.43 (m, 1H), 4.39 (d, J = 5.5 Hz, 2H), 4.25 (ddd, J = 7.8, 4.3, 1.1 Hz, 1H), 4.11 (t, J = 7.2 Hz, 1H), 4.07 (t, J = 5.6 Hz, 2H), 3.66 – 3.64 (m, 2H), 3.62 – 3.60 (m, 2H), 3.52 – 3.49 (m, 2H), 3.33 (td, J = 5.3, 1.2 Hz, 2H), 3.16 – 3.14 (m, 1H), 2.88 (ddd, J = 12.7, 5.0, 1.0 Hz, 1H), 2.81 (td, J = 7.1, 1.6 Hz, 2H), 2.67 (d, J = 12.7 Hz, 1H), 2.53 – 2.51 (m, 3H), 2.45 – 2.41 (m, 3H), 2.25 – 2.22 (m, 3H), 2.18 (td, J = 7.4, 3.5 Hz, 2H), 2.11 – 2.08 (m, 1H). **¹³C NMR** (214 MHz, MeOD) δ 188.5, 176.1, 174.6, 166.1, 160.9, 156.6, 146.4, 145.8, 142.2, 136.7, 135.6, 131.9, 131.6, 129.6, 127.0, 125.6, 124.8, 123.4, 119.3, 115.3, 115.3, 79.2, 76.0, 74.1, 73.4, 72.2, 71.2, 70.7, 70.6, 69.3, 65.7, 64.9, 63.7, 63.6, 63.3, 61.6, 57.0, 51.3, 51.2, 45.4, 45.3, 42.4, 41.1, 40.3, 35.6, 29.7, 29.5, 27.6, 27.3, 26.9, 25.9, 21.1, 13.3, 9.6.

Supplementary references

1. J. Jumper, R. Evans, A. Pritzel, T. Green, M. Figurnov, O. Ronneberger, K. Tunyasuvunakool, R. Bates, A. Zidek, A. Potapenko, A. Bridgland, C. Meyer, S. A. A. Kohl, A. J. Ballard, A. Cowie, B. Romera-Paredes, S. Nikolov, R. Jain, J. Adler, T. Back, S. Petersen, D. Reiman, E. Clancy, M. Zielinski, M. Steinegger, M. Pacholska, T. Berghammer, S. Bodenstein, D. Silver, O. Vinyals, A. W. Senior, K. Kavukcuoglu, P. Kohli, D. Hassabis, Highly accurate protein structure prediction with AlphaFold, *Nature*, 2021, **596**, 583-589.
2. N. E. Trenkler, Photocleavable activity-based acid glucosylceramidase probes, Thesis, Leiden University, 2023, <https://hdl.handle.net/1887/3665361>.

Chapter 6

Expression and analysis of *Nicotiana tabacum* β -glucosidase B56 in mammalian cells

Qin Su, Rebecca Katzy, Kassiani Kytidou, Yang Lei, Marta Artola, Herman S. Overkleeft, Rolf G. Boot, and Johannes M. F. G. Aerts are acknowledged for their contributions to this chapter.

Abstract

Gaucher disease (GD) is characterized by deficiency in the lysosomal glucosylceramidase, GBA1, with accumulation of glucosylceramide (GlcCer) as the result. Enzyme replacement therapy (ERT), comprising intravenous administration of GD patients with recombinant human (h)GBA1, is an effective, though costly, therapy for type 1/3 GD patients. In principle, β -glucosidases from other species and that are easier to obtain could work as well, provided they reach Gaucher cell lysosomes, act (all or not assisted by endogenous chaperones, as hGBA1 is) on accumulating GlcCer, and do not elicit an immune response. The *Nicotiana tabacum* β -glucosidase B56 features GBA1-like characteristics: it is a retaining β -glucosidase acting at acidic pH. This Chapter reveals that expression of B56 in hGBA1/hGBA2 double knockout HEK293T cells (a human cancer cell line) reintroduces lysosomal β -glucosidase activity: it is *in vitro* active towards retaining β -glucosidase inhibitors and probes and it proceeds through the secretory pathway (as witnessed by its N-glycosylation) to reach lysosomes. It does not process GlcCer-like substrates in extracts of these transgenic cells, though, and neither possesses transglycosylation activity as is one of the characteristics of hGBA1. The study does show that plant glycosidases can be introduced into human cells while retaining activity, inviting further research towards easy-to-access, lysosomal-active retaining β -glucosidases that do act on GlcCer.

Introduction

Glucosylceramide (GlcCer) is the central glycosphingolipid from which all gangliosides and globosides are derived, and aberrations in glycosphingolipid metabolism is a hallmark of several human diseases.^{1,2} Human cells express two retaining β -glucosidases that act on GlcCer in different cellular compartments. Acid glucosylceramidase (GBA1) is the main GlcCer metabolic enzyme, processing GlcCer as the penultimate step in the breakdown of glycosphingolipids within lysosomes.² Glucosylceramidase (GBA2) in turn resides within the inner leaflet of (sub)cellular membranes, where it processes GlcCer to give glucose and ceramide in a different topological compartment (cytosol instead of lysosomes) with possibly different cellular consequences.³ The lysosomal storage disorder, Gaucher disease (GD) is characterized by genetic deficiency in the *GBA1* gene, with different gene mutations leading to different disease states.^{4,5} Some mutations (for instance, N370S) lead to relatively mild manifestations (type 1 GD) which can be treated with considerable success by two distinct therapies: enzyme replacement therapy (ERT) and substrate reduction therapy (SRT).^{5,6} Other mutations exist that lead to less frequent, but more severe (type 2) GD with neuropathological consequences.⁷ Aberrations in GBA1 are moreover also found as a risk factor for Parkinson's disease (PD).^{8,9} In all GD types, GlcCer accumulates as the primary storage material and both ERT and SRT are directed to lower GlcCer concentrations in GD patients. In SRT, this is realised by partial inhibition of the GlcCer synthesising enzyme, glucosylceramide synthase (GCS).⁵ ERT, which is the clinically more successful of the two therapeutic strategies, pertains the intravenous administration of recombinant human (h)GBA1, which is targeted to Gaucher cells through the mannose receptor (for which purpose rhGBA1 is engineered to display high mannose-type N-glycans).^{5,10-12}

Although effective, ERT is a very costly therapy, and costs are in part associated with the production of stable rhGBA1.¹³ Originally harvested (as wild-type enzyme) from human placentas, today rhGBA1 is produced in a variety of production platforms, including cells derived from human fibroblasts¹⁴, Chinese hamster ovary cells (CHOs)^{5,15} and more recently also carrot cells.^{16,17} The non-human production systems are highly engineered to allow the efficient expression of a xenobiotic, human enzyme. On paper, one could also imagine usage of a non-human retaining β -glucosidase in ERT to take over the role of genetically impaired hGBA1 in GD patients. Immune issues aside, such enzymes, which may be harvested from source organisms as wild-type proteins, need to meet several requirements, most predominantly that they are active on GlcCer within lysosomes. The research described in this chapter aimed to establish whether such non-human GBA1 substitutes would be viable *in situ* active retaining β -glucosidases, acting in lysosomes, and attention was turned to the plant world as potentially cheap and easy to manage production vehicles.¹⁸⁻²¹ Earlier research identified the existence of a retaining β -glucosidases in the tobacco plant, *Nicotiana tabacum* with some similarities to hGBA1: it has a similar size (about 57 kD) and more importantly has the highest activity at acidic pH.²² This protein (UniProt code: A0A1S4CL56) classified as a CAZy GH 5 family member, and for the remainder of this chapter termed B56, was putatively classified as a 1,3- β -glucanase.²² Thus, it is not known whether it is involved in processing of plant GlcCer. Still B56 was considered a good starting point to address the question whether it would be a viable lysosomal β -glucosidase in human cells. The research in this chapter reveals this to be true, in part. It withstands lysosomal conditions and reacts with inhibitors and activity-based probes (ABPs) that also react with hGBA1. It does not hydrolyse fluorescent GlcCer derivatives and is thus not a bona fide hGBA1 substitute. Despite this, the work as presented here does reveal that plant retaining β -glucosidases may become targets for new ERT developments. It moreover provides a platform to study such candidates: by overexpressing, in a human GBA1/GBA2 knockout background, of the candidate enzyme, followed by *in vitro* and *in situ* probing of its stability and activity using the set of substrates, inhibitors and probes that also have shown their value in investigating hGBA1 and hGBA2 in the context of GD and PD.

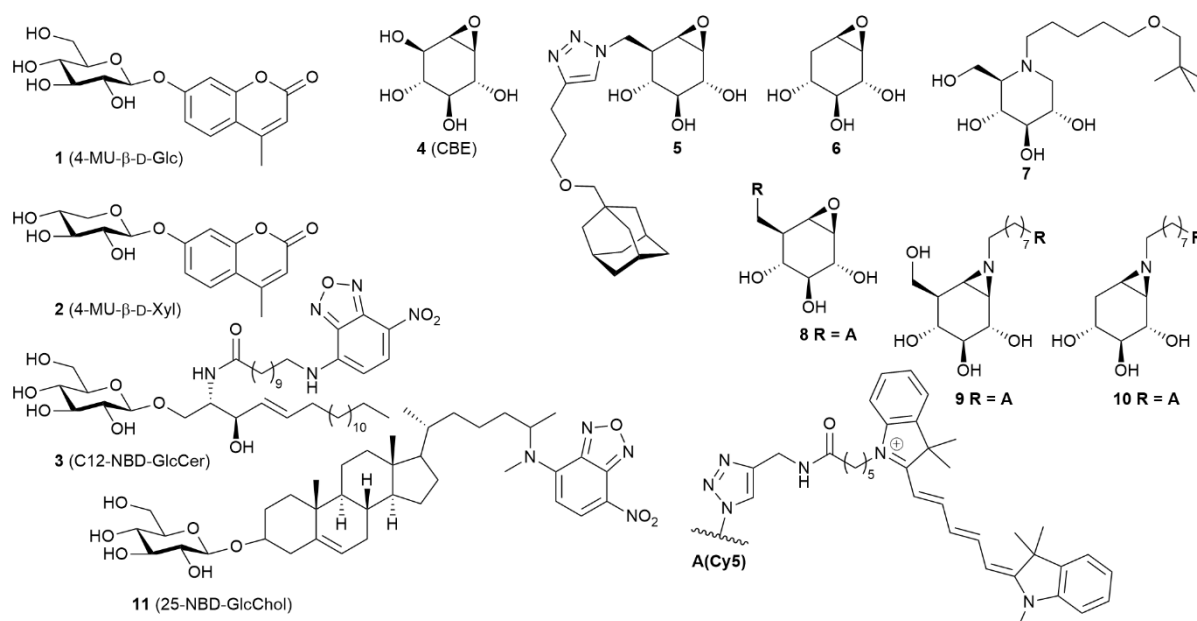


Figure 1. Substrates, inhibitors, and probes used in the here-presented studies.

Results

Chemical proteomics on *Nicotiana tabacum* extracts using a biotin-cyclophellitol aziridine activity-based probe (compound **16** in Chapter 5) in previous studies identified B56 as a retaining β-glucosidase with a pH activity optimum between 4 and 5, thereby indicating this enzyme to be a likely hGBA1 substitute, at least in terms of putative lysosomal activity.²² Rather than cloning and purifying the enzyme for subsequent exposure to human (Gaucher) cells, it was elected to stably express B56 in GBA1 knockout as well as GBA1/GBA2 double knockout cells as relevant Gaucher models. These cells, and extracts thereof, were interrogated on retaining β-glucosidase activity and on B56 intracellular trafficking and post-translational glycosylation. Selected reagents and probes that also featured in the preceding chapters and that were used to investigate hGBA1, hGBA2 and *C. elegans* GBA1-3 were used in these studies. These comprise (Figure 1) the artificial, fluorogenic substrates, 4-methylumbelliferyl (4-MU-) β-D-glucopyranoside (4-MU-β-D-Glc, **1**), 4-MU-β-D-xylopyranoside (4-MU-β-D-Xyl, **2**), the fluorescent synthetic GlcCer analogue, C12-NBD-GlcCer **3**, and GlcChol analogue, 25-NBD-GlcChol **11**, the hGBA1-selective inhibitors **4** (conduritol B epoxide, CBE),²³ cyclophellitol derivative **5**,²⁴ and β-D-xyl-o-cyclophellitol **6**,²⁵ the somewhat hGBA2-selective iminosugar competitive inhibitor **7**²⁶ as well as the hGBA1-selective (**8**)²⁴ and broad-spectrum retaining β-glucosidase (**9**²⁷, **10**²⁵) activity-based probes (ABPs).

Expression of active B56 enzymes in HEK293T cells

cDNAs encoding B56 (marked as B56 Wild-Type (WT)) or V5/His-tagged B56 (marked as B56 Tag) were transfected into human GBA1/GBA2 KO HEK293T cells. Lysate of HEK293T cells transfected with B56 cDNA showed a considerable increased β-glucosidase activity (40-50 nmol/h/mg) towards 4-MU-β-D-Glc **1** as compared to the non-transfected (mock) cells (< 2 nmol/h/mg) (Figure 2A). Recombinant B56 in cell lysate (both B56 WT and B56 Tag) also hydrolyzed 4-MU-β-D-Xyl **2**, but in an about two-fold lower rate than observed for **1** (Figure 2A). For comparison, hGBA1 activity towards **1** is about 20-fold higher than towards **2**. The transfected hGBA1/GBA2 KO HEK293T cells expressing recombinant B56 (WT or Tag) are for the remainder of this chapter termed as 'B56 (WT or Tag) cells'.

Characterization of B56 expressed in HEK293T cells by activity-based protein profiling (ABPP) and fluorogenic substrate assays

Lysates of B56 (WT or Tag) hGBA1/hGBA2 KO HEK293T cells were incubated with hGBA1-selective ABP **8** or broad-spectrum β -glucosidase ABP **9**. Compared with the absence of ABP-labelling in the non-transfected (mock) cells, ABPs **8** and **9** returned a clear signal in the fluorescence scan of the wet SDS-PAGE gel at around 57 kDa, which corresponds to the molecular weight of B56 (Figure 2B). The signal derived from the B56 Tag transfected cells is slightly higher at around 60 kDa, which would be expected due to the presence of the V5/His tag (Figure 2B). The pH optimum of B56 for ABP labelling and enzyme activity was next examined. To this end, the extracts were treated with 200 nM ABP **2** final concentrations, at a pH range varying from 3 to 8. As shown in Figure 2C, the emitted fluorescence intensity in the resultant SDS-PAGE gels is maximal at pH 5.0, with no signal for the samples incubated at the low and high end of the pH range. The pH-dependent fluorogenic substrate assay using 4-MU- β -D-Glc **1** also shows, both for B56 WT and B56 Tag, a maximal activity at pH 4.5-5. The optimum acidic pH of B56 for β -glucosidase activity thus reflects that of hGBA1, which has an activity maximum at pH 5.2. Next, lysates of B56 cells were incubated with 4-MU- β -D-Glc **1** under variable temperature conditions (20-70 °C) to investigate the optimum temperature in terms of enzyme activity. Intriguingly, B56 (WT or Tag) in HEK293T cell lysate showed maximal 4-MU- β -D-Glc **1** hydrolysis activity at 60 °C (Figure 2D). In sharp contrast, hGBA1 becomes inactive after exposure to 42 °C.

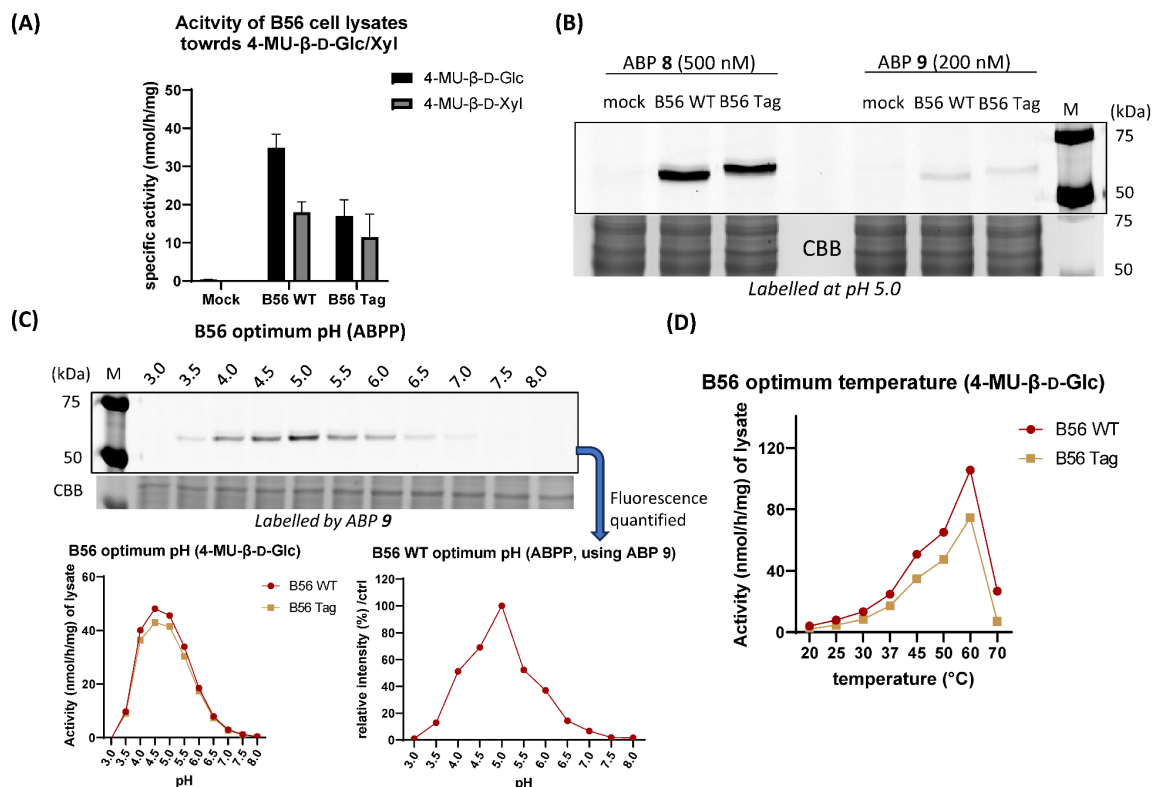


Figure 2. Characterization of B56 (WT and Tag) expressed in HEK293T hGBA1/GBA2 KO cells. Mock = lysate of hGBA1/GBA2 KO HEK293T cells. (A) Activity of B56 in cell lysates towards 4-MU- β -D-Glc **1** and 4-MU- β -D-Xyl **2**. Lysates of B56 cells were incubated with 4-MU substrate **1** or **2** at pH 5.0 for 30 min at 37 °C. (B) Reactivity of ABP **8** and **9** towards B56 (WT and Tag) in cell lysates. Lysates of B56 cells were incubated with 500 nM ABP **8** or 200 nM ABP **9** at pH 5.0 for 30 min at 37 °C and subjected to SDS-PAGE and fluorescence scanning of the wet gel slabs. (C) The optimum pH of B56 for labelling with ABP **9** and 4-MU- β -D-Glc hydrolysis activity, as determined by ABPP and fluorogenic substrate assays, respectively. For ABPP, lysates of B56 cells were incubated with 200 nM ABP **9** for 30 min at 37 °C at various pH values (3-8). For fluorogenic substrate assay, lysates of B56 cells were incubated with 4-MU- β -D-Glc for 30 min at 37 °C at various pH values (3-8). (D) Effect of temperature on enzyme activity of B56 in HEK293T cell lysates. Lysates of B56 cells were incubated with 4-MU- β -D-Glc for 30 min at pH 5.0 at various temperatures (20-70 °C).

Inhibition of B56 in hGBA1/GBA2 KO HEK293T cell extracts by classical hGBA1/hGBA2 inhibitors

In the next set of experiments, the sensitivity of B56 to the established hGBA1 and hGBA2 inhibitors **4-7** was assessed. Figure 3 lists the apparent IC_{50} values for inhibitors **4-7** as determined in a 4-MU- β -D-Glc **1** fluorogenic substrate assay, in a head-to-head comparison with recombinant hGBA1 (rhGBA1, Imiglucerase) and hGBA2. hGBA1-selective inhibitor **4-6** were found to potently inhibit B56 (WT and tagged) and rhGBA1. The hGBA2-selective inhibitor **7** in turn did not inhibit B56 (apparent IC_{50} value > 10 μ M). This result underscores that B56 may resemble in selectivity hGBA1, more so at least than it does hGBA2.

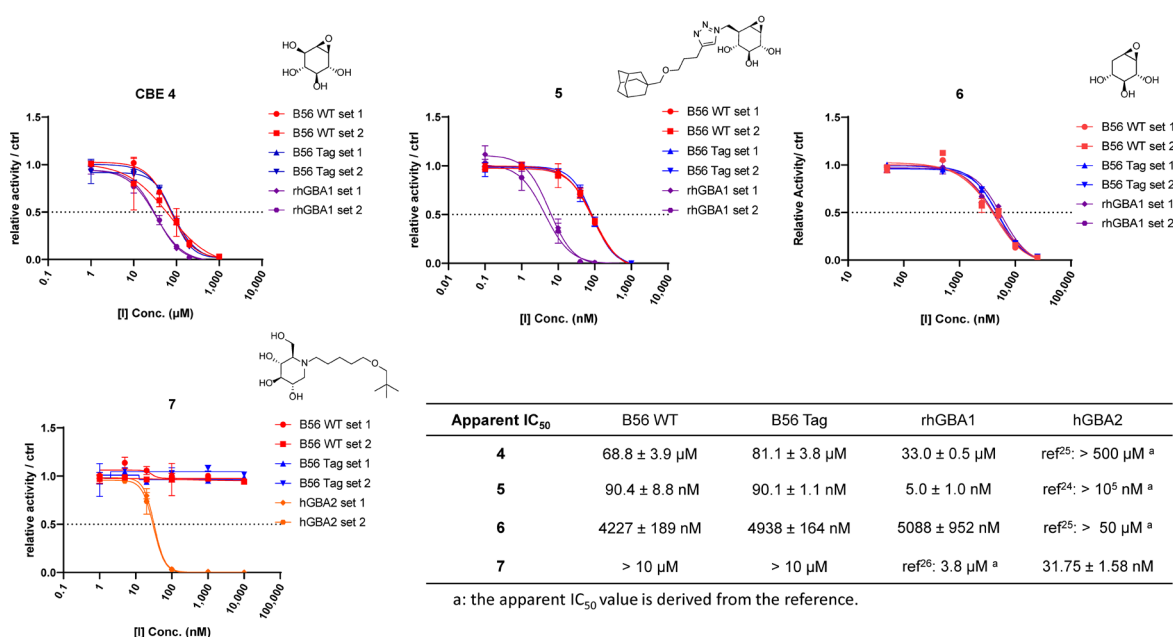


Figure 3. Inhibitory potency of β -glucosidase inhibitors **4-7** on B56. Lysates of B56 (WT and Tag) cells were incubated with inhibitor **4-6** or inhibitor **7** at pH 5.0 for 30 min at 37 °C, followed by incubation with 4-MU- β -D-Glc for 30 min. rhGBA1 = Imiglucerase. hGBA2 = lysate of hGBA1/GBA2 KO HEK293T cells overexpressing hGBA2. Errors range = \pm SD, n = 2 replicates.

B56 acquires high-mannose type N-glycans when expressed in hGBA1/hGBA2 KO HEK293T cells

To examine whether B56 undergoes N-glycosylation, extracts of B56 WT cells were treated with Sepharose beads modified with the α -D-mannosyl glycan receptor, Concanavalin A (ConA-beads).²⁸⁻³⁰ B56 WT was first incubated with ConA-beads, followed by several washing steps to remove unbound proteins. Following the final washing step, ConA beads were collected and are termed as the 'ConA beads' fraction. Then, the fractions from all washing steps as well as the ConA bead fraction were incubated with ABP **9**, the protein samples resolved by SDS-PAGE, and the resulting wet gel slabs scanned for in-gel fluorescence. As can be seen (Figure 4A) virtually all input signal (left lane) is retained in the ConA-beads fraction with little to no fluorescence in the lanes stemming from the washing steps, indicating that B56 binds ConA-beads and, therefore, contains (high mannose-type) N-linked glycans. To further study the type of N-glycans in B56, N-glycanase digestion experiments with the glycanases, PNGase F and Endo H, were conducted (Figure 4B). PNGase F can remove most N-glycans from glycoproteins whereas Endo H is only able to remove high-mannose-type N-glycans. Treating extracts from B56 WT as well as B56 Tag hGBA1/GBA2 KO HEK293T cells which were pretreated with ABP **9** with PNGase F, followed by SDS-PAGE and in-gel fluorescence scanning revealed several signals corresponding to a lower molecular weight compared to the non-PNGase F treated samples, suggesting partial de-N-glycosylation. Treatment with Endo H in turn returned a major and a minor band for the WT sample and two bands with similar intensity for the Tag one. The

near complete digestion with Endo H suggests that B56 protein predominantly acquired high-mannose type N-glycans.

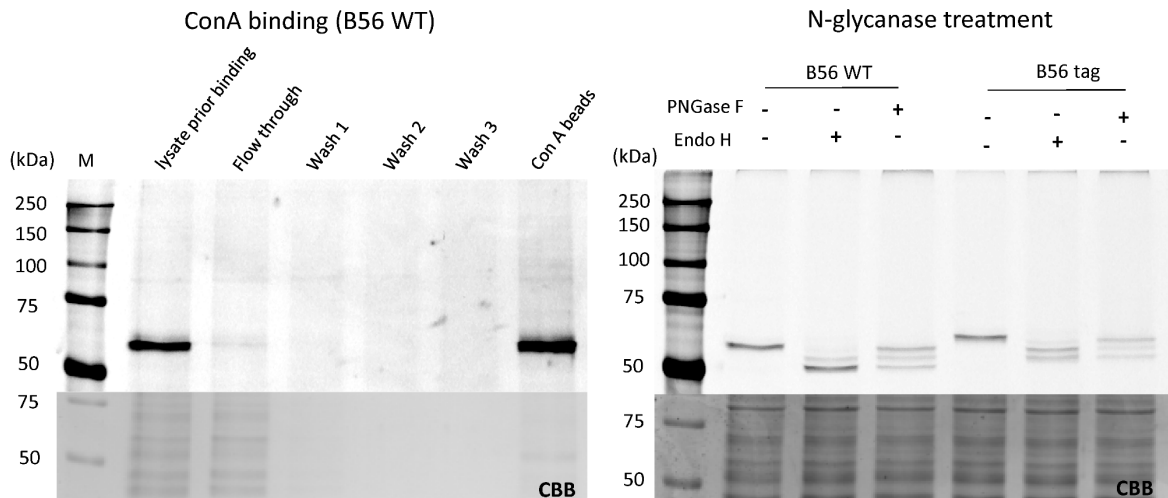


Figure 4. (A) ConA binding to B56 WT in hGBA1/GBA2 KO HEK293T cell extracts. Lysate of B56 WT ('Initial lysate' fraction) were incubated with ConA beads for 2 h at 4°C. After centrifugating, supernatant was collected as 'Flow through' fraction, the ConA beads were subsequently washed for three consecutive times and the washing solutions were collected as 'Wash 1-3' fractions. Following the final washing step, ConA beads were collected as 'ConA beads' fraction. All fractions were incubated with 500 nM ABP **9** for 30 min at pH 5.0 at 37 °C and subjected to SDS-PAGE and fluorescence scanning of the wet gel slabs. (B) PNGase F and Endo H digestion of extracts of B56 expressed hGBA1/GBA2 KO HEK293T cells. Lysates of B56 cells were first incubated with 500 nM ABP **9** for 30 min at 37°C at pH 5.0, followed by incubation with PNGase F or Endo H, and subjected to SDS-PAGE and fluorescence scanning.

Subcellular localization of B56 expressed in hGBA1/GBA2 KO HEK293T cells

To investigate the sub-cellular localization of B56 expressed in HEK293T cells, immunocytochemistry was employed. hGBA1/GBA2 KO HEK293T cells expressing V5-tagged B56 were fixed and stained with fluorescent anti-LAMP1 (lysosomal-associated membrane protein 1) antibody and fluorescent anti-V5 antibody. Subsequently, fluorescence of anti-LAMP1 antibody and anti-V5 antibody were visualized by confocal fluorescence microscopy. As shown in Figure 5, the fluorescence of anti-LAMP1 (indicating sub-cellular localization of lysosomes) and anti-V5 (indicating sub-cellular localization of B56) are overlapping, suggesting that the V5-tagged B56 is at least partly localized in LAMP1-positive lysosomes.

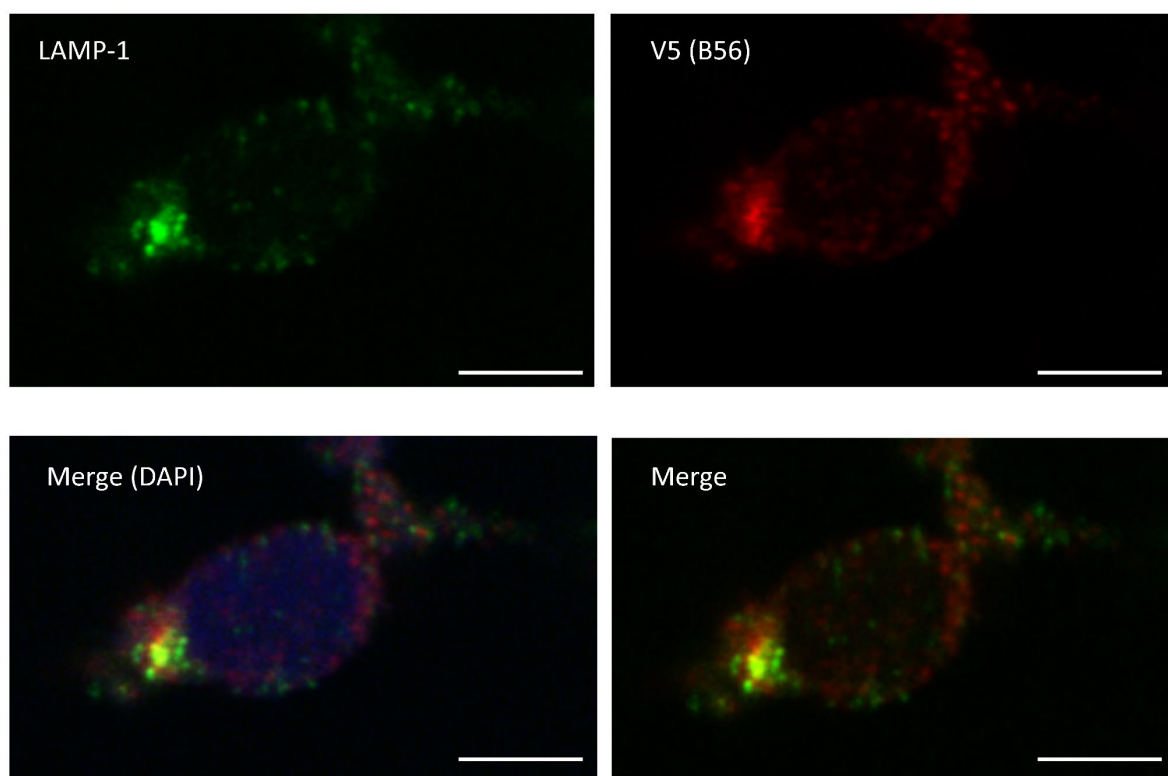


Figure 5. Sub-cellular localization of hGBA1/GBA2 KO HEK293T cells expressing V5-tagged B56. Alexa Fluor™ 488 (green)-tagged anti-LAMP1 antibody was used to visualize sub-cellular localization of lysosomes. Alexa Fluor™ 647 (red)-tagged Anti-V5 antibody was used to visualize sub-cellular localization of V5-tagged B56. Nuclei were stained with 10 µg/ml DAPI (shown as blue). Scale bar = 5 µm.

Processing of C12-NBD-GlcCer by B56-expressing hGBA1/GBA2 KO HEK293T cells and cell extracts

Next, the C12-NBD-GlcCer degradation capacity of B56 expressed in HEK293T cells was examined. Lysates of B56 cells were incubated with C12-NBD-GlcCer for the indicated time, after which lipids were extracted and subjected to high-performance thin layer chromatography (HPTLC) separation and fluorescence scanning of the TLC plates. rhGBA1 (Imiglucerase) was used as positive control to show the position of C12-NBD-Cer. No C12-NBD-Cer formation was observed after 2.5 h incubation *in vitro*, and neither upon prolonged incubation time up to 16 h or using ConA beads enriched B56 (Figure 6A/B). An assay was also conducted to assess whether NBD-GlcCer can be degraded by B56 *in situ*. To this end, 80% confluent hGBA1/GBA2 KO HEK293T cells expressing B56 (WT or Tag) were exposed to C12-NBD-GlcCer for 3 h *in situ*. Afterwards, cells were washed, collected, lysed, and subjected to HPTLC analysis (Figure 6C). Extracts of wild type (WT) HEK293T cells as positive control converted NBD-GlcCer to NBD-Cer *in situ*, while extracts of hGBA1/GBA2 KO HEK293T cells expressing B56 did not. Considering that BY2 cells may contain some components assisting B56 to hydrolyze GlcCer in tobacco, an attempt was conducted to examine whether a mixture of tobacco BY2 cell lysate and B56 expressing HEK293T cell lysate (in hGBA1/hGBA2 KO background) was able to degrade C12-NBD-GlcCer. BY2 cell lysates were treated or not with hGBA1-selective inhibitor **5** (with the aim to inhibit potential β -glucosidases in BY2 lysate), followed by washing with a desalting column to remove unbound inhibitor. Afterwards, the washed BY2 lysate was mixed with lysate of hGBA1/GBA2 KO HEK293T cells expressing B56 WT and incubated with C12-NBD-GlcCer for 3 h *in vitro*. The sample not treated with inhibitor **5** proved to be able to convert NBD-GlcCer, while the **5**-treated samples (including the sample using mixture of BY2 lysate and B56-expressing HEK293T lysate) did not.

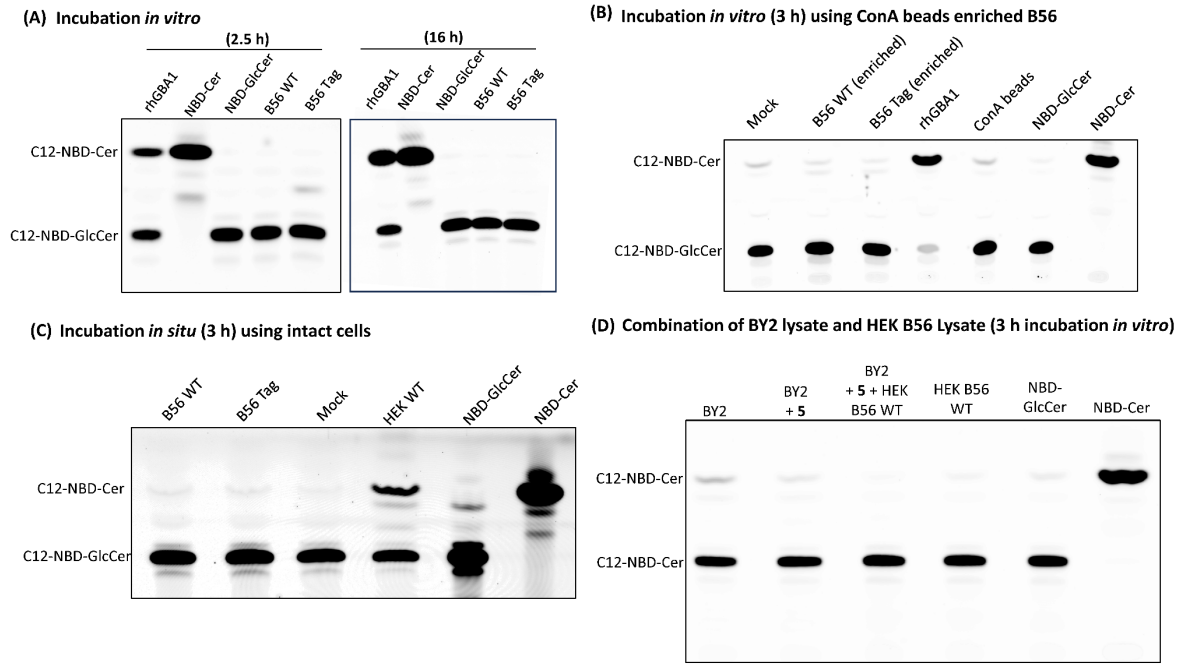


Figure 6. C12-NBD-GlcCer processing by hGBA1/hGBA2 KO HEK293T expressing B56 (WT or Tag) expression. ‘rhGBA1’ = sample using Imiglucerase. ‘B56 WT’ or ‘B56 Tag’ = sample of B56 (WT or Tag) cells or cell lysates. ‘Mock’ = HEK293T hGBA1/GBA2 KO cells or cell lysates. ‘HEK WT’ = intact living wild-type HEK293T cells. ‘ConA beads’ = sample containing ConA beads only. (A) Lysates of B56 cells incubated with 500 nM NBD-GlcCer for 2.5 h or 16 h at pH 5.0 *in vitro*. (B) ConA beads enriching B56 incubated with 500 nM NBD-GlcCer for 3 h at pH 5.0 *in vitro*. (C) Intact WT, hGBA1/GBA2 KO, or B56 expressed HEK293T cells incubated with 1 μ M C12-NBD-GlcCer for 3 h *in situ*. Subsequently, cells were washed, collected, lysed, and subjected to HPTLC separation and fluorescence scanning of the TLC plates. (D) BY2 lysate was preincubated with 200 nM inhibitor **5** for 1 h at 37 °C, then sample was washed by a desalting column. Afterwards, BY2 lysate was mixed with lysate of B56 WT cells and incubated with 500 nM NBD-GlcCer for 3 h at 37 °C at pH 4.5. ‘BY2’ = sample containing BY2 lysate without pre-treatment of **5**. ‘BY2 + **5**’ = sample of BY2 lysate with pre-treatment of **5** and washing step. ‘BY2 + **5** + HEK B56 WT’ = lysate of B56 WT cells mixed with BY2 lysate pre-treated with **5**. ‘HEK B56 WT’ = lysate of B56 WT cells. Lanes: ‘NBD-Cer’ or ‘NBD-GlcCer’ = sample containing NBD-Cer or NBD-GlcCer alone.

B56 expressing hGBA1/hGBA2 KO HEK293T cells do not process GlcCer and glucosylsphingosine

Characteristically, GlcCer is elevated in GD patients due to impaired lysosomal degradation, leading to a concomitant marked increase in glucosylsphingosine (GlcSph) through conversion of accumulating GlcCer by acid ceramidase.² To investigate whether B56 when expressed in human cells can process these storage glycolipids, LC-MS/MS was employed to detect the changes of glycosphingolipids in hGBA1 KO or hGBA1/GBA2 KO HEK293T cells expressing B56 (WT or Tag). As shown in Figure 7, GlcCer increased 3-fold in both non-B56-transfected hGBA1 KO HEK293T cells and hGBA1/GBA2 KO HEK293T cells, when compared to the wild-type cells. Expression of B56 in these cells did not lead to a decrease of GlcCer levels. GlcSph is present only in very low amounts in wild type HEK293T cells. In contrast, GlcSph levels are drastically increased both in hGBA1 KO HEK293T cells and in hGBA1/GBA2 KO HEK293T cells, resembling the situation of GD patients, and expression of B56 in these cells did not suppress these GlcSph levels. As well, β -glucosylcholesterol (GlcChol), a glycosphingolipid mainly degraded by hGBA1 and generated by hGBA2 via transglycosylation,³¹ was not considerably influenced by expression of B56 in hGBA1 KO or hGBA1/GBA2 KO HEK293T cells.

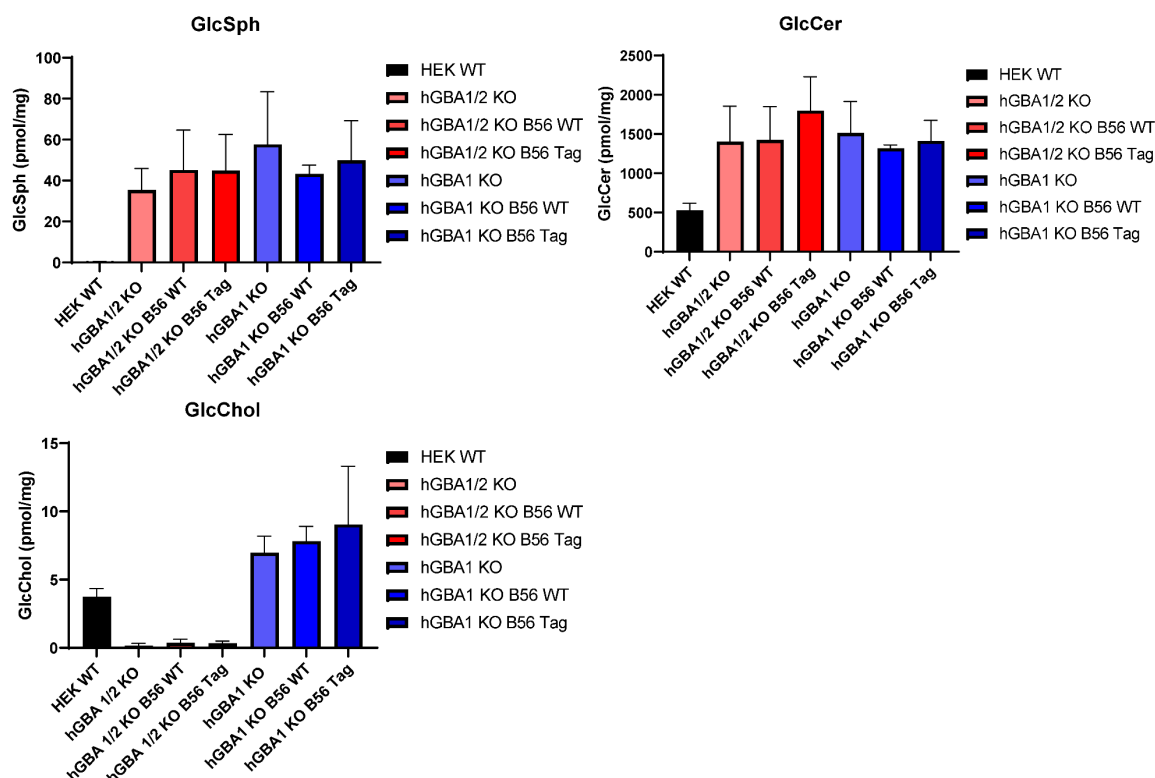


Figure 7. Glycosphingolipid levels in hGBA1 knockout (KO) or hGBA1/GBA2 KO HEK293T cells expressing B56 (WT or tagged), as detected by LC-MS/MS. *n* = 3 biological replicates. ‘HEK WT’ = HEK293T wild type cells; ‘hGBA1/2 KO’ = HEK293T hGBA1/GBA2 KO cells; ‘hGBA1 KO’ = HEK293T hGBA1 KO cells; ‘B56 WT or B56 Tag’ = wild type B56 or V5-tagged B56 expressed in HEK293T cells (in either hGBA1 KO or hGBA1/GBA2 KO background).

B56 expressing hGBA1/hGBA2 KO HEK293 cells do not produce GlcChol

Previous studies have revealed that hGBA1 catalyzes transglycosylation *in vitro*, generating β -GlcChol when incubated with cholesterol as an acceptor and 4-MU- β -D-Glc or GlcCer as sugar donors at appropriate conditions.³¹ *In vivo* hGBA1 is involved in degrading GlcChol into cholesterol and glucose. hGBA2 as well generates GlcChol via transglucosylation using GlcCer as sugar-donor.³¹ Additionally, hGBA1 also efficiently produces β -xylosylated cholesterol (XylChol) and even sequentially Xyl₂Chol *in vitro*. As the final experiment, B56 as produced by hGBA1/hGBA2 KO HEK293 cells studied on its transglycosylation capacity. Enriched B56 (by ConA beads) was incubated with 4-MU- β -D-Glc **1** or 4-MU- β -D-Xyl **2** as sugar donors and 25-NBD-Chol **11** as acceptor for 16 h at 37 °C. As shown in Figure 8, B56 did not generate GlcChol or XylChol. In sharp contrast, recombinant human GBA1 (rhGBA1, Imiglucerase) was able to generate GlcChol, XylChol and Xyl₂Chol as reported earlier.³²

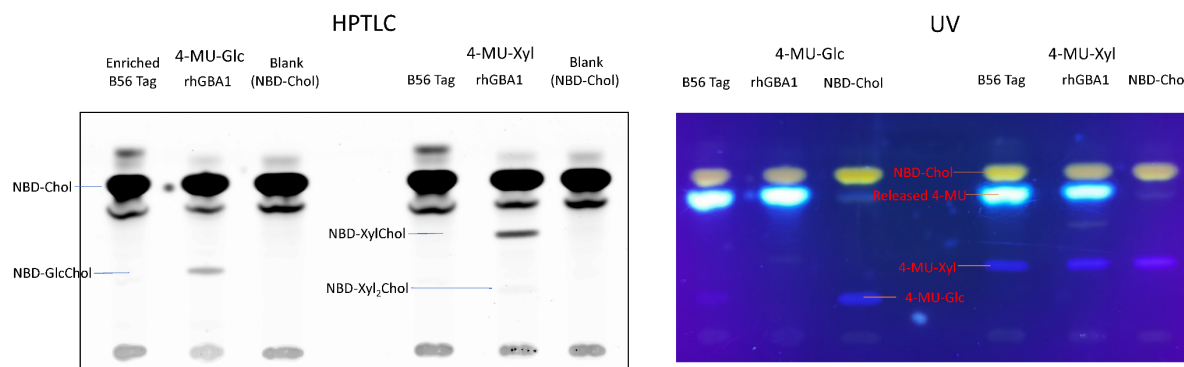


Figure 8. Transglycosylation capacity of HEK293T-produced B56. V5-tagged B56 enriched by ConA beads was incubated with either 4-MU- β -D-Glc or 4-MU- β -D-Xyl as sugar donor and 25-NBD-Chol as acceptor for 16 h at 37 °C at pH 5.0. Lanes: ‘B56 Tag’ = the enriched B56 (by ConA beads) expressed in hGBA1/GBA2 KO HEK293T cells was incubated with substrates (sugar donor and acceptor). ‘rhGBA1’ = isolated rhGBA1 (Imiglucerase) incubated with substrates at pH 5.2 (supplemented with 0.1% (v/v) Triton X-100, 0.2% (w/v) sodium taurocholate, and 0.1% (w/v) bovine serum albumin). ‘NBD-Chol’ = sample containing 25-NBD-Chol alone. Intensity of ‘released 4-MU’ reflects the amount of hydrolyzed 4-MU-glycoside, as detected under ultraviolet light (UV).

Discussion

The *Nicotiana tabacum* β -glucosidase B56 was previously identified as a potential analogue of the human lysosomal enzyme, deficient in GD, hGBA1. It has about the same molecular weight; it employs a retaining mechanism; and is active at lysosomal pH.²² At the onset of the studies described here, also some notable differences were apparent. It is a member of the GH5 CAZy family and therefore has a different fold compared to the GH1 family to which hGBA1 belongs, and indeed there is little to no sequence homology between the two enzymes (see SI Figure S1). As well, no GlcCer metabolizing activity has been ascribed to B56 for which no substrate is known, though B56 is listed as probable glucan 1,3- β -glucosidase A isoform X2 in UniProt. With this prior information available, a research campaign was started to investigate the possibility to express B56 in human cells, and to investigate its fate and catalytic activity in this foreign environment. The results, as described here, reveal that B56 is readily expressed in hGBA1 as well as hGBA1/hGBA2 KO HEK293 cells. It moreover acquires N-glycans and ends up in lysosomes, suggesting it is expressed and processed like hGBA1 (expression in the ER, where it is N-glycosylated and then routed to lysosomes). Once in lysosomes, it is active both towards fluorogenic substrates and retaining β -glucosidase ABPs, as well as susceptible to hGBA1-selective β -glucosidase inhibitors. It is, however, not able to process either natural or synthetic GlcCer derivatives and neither possesses transglycosylation activities. These last two features distinguishes B56, in this setting, from hGBA1 and also hGBA2. Functionally, B56 can therefore not be seen as a viable biological for new ERT strategies for treating GD patients. This important caveat aside, the work presented here does imply that true plant-origin hGBA1 homologues may be considered for this purpose. Obviously, such species need to be engineered in such way that the host immune system is not activated (this issue is not addressed in this chapter). Should such entities emerge, the workflow presented here including the *in vitro* and *in situ* assays reporting on enzyme activities as well as substrate turnover rates should be of help in evaluating their ability to repair, in Gaucher cells, impaired GlcCer turnover.

Experimental procedures

Materials

Recombinant human GBA1 (rhGBA1, Imiglucerase) was kindly provided by Genzyme (Genzyme Nederland, Naarden, The Netherlands). 4-MU- β -D-glucopyranoside (4-MU- β -D-Glc) and 4-MU- β -D-xylopyranoside (4-MU- β -D-Xyl) were purchased from Glycosynth (Warrington, UK). Wet gel slabs in the ABPP experiments were imaged using a Typhoon FLA 9500 scanner (GE Healthcare) at λ_{EX} 635 nm and $\lambda_{\text{EM}} \geq 665$ nm for Cy5 fluorescence. SDS-PAGE gels were stained for loading control of proteins with Coomassie G250 and scanned on a ChemiDoc MP imager (Bio-Rad, Hercules, CA, USA). Fluorescent NBD-lipids (C12-NBD-GlcCer, 25-NBD-Chol) were purchased from Avanti (Alabama, USA). Antibodies purchased from Abcam (Cambridge, MA, USA). PNGase F and Endo H were purchased from New England Biolabs (Ipswich, USA). Polytron PT 1300D sonicator (Kinematica, Luzern, Switzerland) and potassium phosphate buffer (25 mM KH_2PO_4 - K_2HPO_4 , pH 6.5, supplemented with protease inhibitor cocktail (EDTA-free, Roche, Basel, Switzerland) and 0.1% (v/v) Triton X-100) were used for lysing cells. Harvested cells (cell pellets) and cell lysates not used directly were stored at -80°C . The protein concentration of the lysates was determined using Pierce BCA Protein Assay Kit (Thermo Fisher Scientific; Waltham, USA). HEK293T cells were cultured and lysed as described in Chapter 2. CBE (condurotol B epoxide) was purchased from Enzo Life Sciences (Farmingdale, NY, USA). All other compounds were synthesized at the department of Bio-organic Synthesis of the Leiden Institute of Chemistry (LIC), Leiden University

Expression of B56 with or without V5-tag in HEK293T cells

The cDNA of B56 was purchased from GenScript. The B56 wild type gene and the wild type gene with C-terminal V5 epitope and a His tag (tagged B56) were amplified from pcDNA3.1+/C-(K)-DYK vectors in DH5 α *E. coli*. After amplification, a BP recombination reaction was conducted according to the Gateway® Technology with Clonase II (Invitrogen™). The produced donor vector pDONR221 -wild type and -tagged were transformed into DH5 α *E. coli* via heat shock. The plates with kanamycin were used to select the positive transformants and the plasmids were sequenced. Then a LR reaction was performed to clone both genes into the destination vector pDEST40. Then the pDEST40 wild type or V5-tagged plasmids were then transfected into the HEK293T cells (in either hGBA1 KO or hGBA1/GBA2 KO background) using polyethylenimine (PEI)³³ for B56 WT and B56 V5-tagged expression. Primers are shown in Table 1 below. hGBA1 KO and hGBA1/GBA2 KO HEK293T cell lines were generated as described in Chapter 2.

Table 1: Primers for the amplification and recombination of WT and tagged version.

Reaction	Forward	Reverse
Amplification	5'-GCACCAAAATCAA CGGGACT-3'	5'-TTGTCTTCCAAT CCTCCCC-3'
Recombination for WT	5'-GGGGACAAGTTTG TACAAAAAAGCAGGCT ACCACCATGGCAAGCT ACTCATGG-3'	5'-GGGGACCACTTTGT ACAAGAAAGCTGGGTC TTAAAGCTTGATATAGC CATTC-3'
Recombination for tagged	5'-GGGGACAAGTTTG TACAAAAAAGCAGGCT ACCACCATGGCAAGCT ACTCATGG-3'	5'-GGGGACCACTTTGT ACAAGAAAGCTGGGTC AAGCTTGATATAGCCAT TCTTG-3'

4-MU fluorogenic substrate assays

Enzyme activity and apparent IC_{50} of B56 in cell lysates were determined by 4-methylumbelliferyl-glycoside fluorogenic substrate assays as described in Chapter 2. To determine enzyme activity, lysate of B56 cells were prepared in 12.5 μ L potassium phosphate buffer, and mixed with 12.5 μ L McIlvaine buffer (150 mM, pH 5.0) and incubated with 100 μ L 3.75 mM 4-MU- β -D-Glc or 3 mM 4-MU- β -D-Xyl dissolved in McIlvaine buffer (150 mM, pH 5.0) for 30 min at 37 °C. To determine apparent IC_{50} , 12.5 μ L lysate of B56 cells were mixed with 12.5 μ L inhibitor (**4-7**) diluted in McIlvaine buffer (150 mM, pH 5.0) and incubated for 30 min at 37 °C, then the 25 μ L samples were incubated with 100 μ L 3.75 mM 4-MU- β -D-Glc dissolved in McIlvaine (150 mM, pH 5.0) at 37 °C for 30 min. After stopping the enzyme reaction with 200 μ L 1 M NaOH-glycine (pH 10.3), 4-Methylumbelliferone fluorescence was measured with a fluorimeter LS55 (Perkin Elmer, Waltham, MA, USA) with λ_{EX} 366 nm and λ_{EM} 445 nm. Where indicated, the pH of McIlvaine buffer, incubation temperatures, or the percentage of additives (Triton X-100, sodium taurocholate) in McIlvaine buffer was varied.

In vitro ABPP with SDS-PAGE

ABPP were conducted as described in Chapter 2. Lysates of B56 cells were incubated with a ABP (**8-10**) in McIlvaine buffer (150 mM, pH 5.0 or at indicated pH) at 37 °C for 30 minutes, and subjected to proteins denature, SDS-PAGE, and fluorescence scanning of the wet gel slabs.

Immunocytochemistry

HEK293T cells expressing B56 containing a V5-tag were used for immunochemistry using confocal fluorescence microscopy. Sterile coverslips were put into the wells of 6-well plates and 0.01% of poly-L-lysine (PLL) milliQ solution was applied on the coverslips for coating the coverslips aseptically. The cell homogenate was added on the coverslips and DMEM medium (Sigma-Aldrich) was added into wells for cell growing. When the confluency reached 80%-90%, cells were fixed on the coverslips with 4% (w/v) paraformaldehyde (PFA). After rinsing with phosphate-buffered saline (PBS), permeabilization buffer (0.1% Triton X-100 in Tris-buffered saline (TBS)) was applied on cells and cells were incubated in dark for 7 minutes. Then the blocking buffer (3% (w/v) BSA in PBS) was used and plate was kept in dark for 30 minutes or longer. Primary antibodies, mouse anti-V5 (Fisher) and rabbit anti-LAMP1 (SouthernBiotech) in blocking buffer (1% and 0.5%, respectively), were then applied on the coverslips. Incubation was performed in dark at room temperature for 2 hours. Secondary antibodies, donkey-anti-mouse-Alexa 647 antibody (Invitrogen) and donkey-anti-rabbit-Alexa 488 antibody (Invitrogen) in blocking buffer (0.1% and 0.1%, respectively), were applied on coverslips to bind with the primary antibodies and cells were incubated in dark at room temperature for 1 hour. Prolong gold with DAPI was applied then. Nail polish was used to seal the dried coverslips and the fluorescence of the coverslips was detected by Leica confocal SP8 microscope.

Binding of B56 to Concanavalin A-Sepharose 4B beads

A slurry of Concanavalin A-Sepharose 4B beads (GE healthcare Bio-Sciences) was prior washed with washing buffer (0.1 M sodium acetate, 0.1 M NaCl, 1 mM $MgCl_2$, 1 mM $CaCl_2$, 1 mM $MnCl_2$, (pH 6.0)) and then mixed with cell lysates. The mixture was incubated at 4 °C for 2 hours on a tumbling shaker. After centrifugation, supernatant was collected as flow-through and beads were washed for three time by washing buffer (collected as wash fractions). Eventually, beads were separated and collected as beads fraction.³⁴ Fractions were subjected to 500 nM ABP **9** labelling for 30 min at pH 5.0 at 37 °C, SDS-PAGE and fluorescence imaging of wet gel slabs. For experiments in Figure 6B using B56 enriched by ConA beads, beads were preincubated with B56 cell lysate for 2 h at 4 °C.

N-glycanases treatment

In total 20 µg proteins of B56 cell lysates in McIlvaine buffer (150 mM, pH 5.0) were incubated with 500 nM ABP **9** for 30 min at 37 °C. Afterwards, an aliquot of the samples were treated with PNGase F or Endo H according to the manufacturer's protocol (New England BioLabs). For samples as control (without N-glycanases treatment), samples with a normalized protein amount were incubated with 500 nM ABP **9** for 30 min at 37 °C in McIlvaine buffer (150 mM, pH 6.0). Subsequently, both the control and N-glycanase treated samples were subjected to ABPP as described above.

Assessment of NBD-lipid metabolism

C12-NBD-GlcCer degradation: lysate of hGBA1/GBA2 KO cells expressing B56 (100 µg) were incubated with NBD-GlcCer (500 nM) in McIlvaine buffer (150 mM, pH 5.0) for 2.5 h or 16 h at 37 °C. For rhGBA1, sample containing 10-20 ng rhGBA1 was incubated with NBD-GlcCer in McIlvaine buffer (150 mM, pH 5.2, supplemented with 0.2% (w/v) sodium taurocholate, 0.1% (v/v) Triton X-100, and 0.1% (w/v) bovine serum albumin). Afterwards, lipids were extracted by Blight and Dyer method³⁵ and subjected to HPTLC, using developing solvent (CHCl₃: methanol, 85:15 (v/v)), followed by fluorescence scanning at $\lambda_{\text{ex}} = 473$ nm and $\lambda_{\text{em}} \geq 510$ nm for detection of NBD fluorescence. For *in situ* assay, 80% confluent hGBA1/GBA2 KO HEK293T cells expressing B56 (WT or Tag) were exposed to 1 µM NBD-GlcCer for 3 h *in situ*, and subjected to lipid extraction and HPTLC. For assessment of NBD-GlcCer degradation by mixture of BY2 cell lysate and B56 WT cell lysate, BY2 cell lysate prepared in potassium phosphate buffer was preincubated with 200 nM inhibitor **5** or vehicle (DMSO, final concentration is 0.5%) for 1 h at 37 °C, then the sample was washed by passing through a ZebaTM spin desalting column with 7K molecular weight cutoff (MWCO). Afterwards, 35 µL BY2 lysate (around 50 µg) pre-inhibited by **5** was mixed with 50 µL lysate of B56 WT cells (70 µg) and incubated with 500 nM NBD-GlcCer in 150 µL McIlvaine buffer (150 mM, pH 4.5) for 3 h at 37 °C.

For the identification of newly formed fluorescent NBD-lipid, using 25-NBD-cholesterol as acceptor, ConA beads were pre-incubated with lysate of B56 (WT or Tag) cells for 2 h at 4 °C, followed by incubation with 400 µM 4-MU-β-D-Glc and 20 µM 25-NBD-cholesterol for 16 h at 37 °C at pH 5.0. For isolated rhGBA1 (Imiglucerase), samples were incubated in McIlvaine buffer (150 mM, pH 5.2, supplemented with 0.2% (w/v) sodium taurocholate, 0.1% (v/v) Triton X-100, and 0.1% (w/v) bovine serum albumin) for 16 h at 37 °C. Afterwards, samples were subjected to lipid extraction and HPTLC as described above. Hydrolysis of 4-MU-β-D-Glc or 4-MU-β-D-Xyl was indicated by the released 4-methylumbelliferone (released 4-MU) detected under ultraviolet light (UV).

References

1. T. Wennekes, R. J. van den Berg, R. G. Boot, G. A. van der Marel, H. S. Overkleeft, J. M. Aerts, Glycosphingolipids--nature, function, and pharmacological modulation, *Angew. Chem. Int. Ed.* 2009, **48**, 8848-8869.
2. J. M. Aerts, C. L. Kuo, L. T. Lelieveld, D. E. C. Boer, M. J. C. van der Lienden, H. S. Overkleeft, M. Artola, Glycosphingolipids and lysosomal storage disorders as illustrated by Gaucher disease, *Curr. Opin. Chem. Biol.* 2019, **53**, 204-215.
3. A. Massimo, S. Maura, L. Nicoletta, M. Giulia, M. Valentina, C. Elena, P. Alessandro, B. Rosaria, S. Sandro, Current and novel aspects on the non-lysosomal beta-glucosylceramidase GBA2, *Neurochem. Res.* 2016, **41**, 210-220.
4. K. S. Hruska, M. E. LaMarca, C. R. Scott, E. Sidransky, Gaucher disease: mutation and polymorphism spectrum in the glucocerebrosidase gene (GBA), *Hum. Mutat.* 2008, **29**, 567-583.
5. J. Stirnemann, N. Belmatoug, F. Camou, C. Serratrice, R. Froissart, C. Caillaud, T. Levade, L. Astudillo, J. Serratrice, A. Brassier, C. Rose, T. Billette de Villemeur, M. G. Berger, A review of Gaucher disease pathophysiology, clinical presentation and treatments, *Int. J. Mol. Sci.* 2017, **18**, 441.
6. R. Sam, E. Ryan, E. Daykin, E. Sidransky, Current and emerging pharmacotherapy for Gaucher disease in pediatric populations, *Expert Opin. Pharmacother.* 2021, **22**, 1489-1503.
7. T. Roshan Lal, E. Sidransky, The spectrum of neurological manifestations associated with Gaucher disease, *Diseases* 2017, **5**, 10.
8. J. Mitsui, I. Mizuta, A. Toyoda, R. Ashida, Y. Takahashi, J. Goto, Y. Fukuda, H. Date, A. Iwata, M. Yamamoto, N. Hattori, M. Murata, T. Toda, S. Tsuji, Mutations for Gaucher disease confer high susceptibility to Parkinson disease, *Arch. Neurol.* 2009, **66**, 571-576.
9. E. Sidransky, G. Lopez, The link between the GBA gene and parkinsonism, *Lancet Neurol.* 2012, **11**, 986-998.
10. G. A. Grabowski, N. W. Barton, G. Pastores, J. M. Dambrosia, T. K. Banerjee, M. A. McKee, C. Parker, R. Schiffmann, S. C. Hill, R. O. Brady, Enzyme therapy in type 1 Gaucher disease: comparative efficacy of mannose-terminated glucocerebrosidase from natural and recombinant sources, *Ann. Intern. Med.* 1995, **122**, 33-39.
11. Y. Sato, E. Beutler, Binding, internalization, and degradation of mannose-terminated glucocerebrosidase by macrophages, *J. Clin. Invest.* 1993, **91**, 1909-1917.
12. B. Friedman, K. Vaddi, C. Preston, E. Mahon, J. R. Cataldo, J. M. McPherson, A comparison of the pharmacological properties of carbohydrate remodeled recombinant and placental-derived β -glucocerebrosidase: implications for clinical efficacy in treatment of Gaucher disease, *Blood* 1999, **93**, 2807-2816.
13. L. van Dussen, M. Biegstraaten, C. E. Hollak, M. G. Dijkgraaf, Cost-effectiveness of enzyme replacement therapy for type 1 Gaucher disease, *Orphanet J. Rare Dis.* 2014, **9**, 51.
14. T. A. Burrow, G. A. Grabowski, Velaglucerase alfa in the treatment of Gaucher disease type 1, *Clin. Investig.* 2011, **1**, 285-293.
15. Y. Kacher, B. Brumshtein, S. Boldin-Adamsky, L. Toker, A. Shainskaya, I. Silman, J. L. Sussman, A. H. Futerman, Acid beta-glucosidase: insights from structural analysis and relevance to Gaucher disease therapy, *Biol. Chem.* 2008, **389**, 1361-1369.
16. L. van Dussen, A. Zimran, E. M. Akkerman, J. M. Aerts, M. Petakov, D. Elstein, H. Rosenbaum, D. Aviezer, E. Brill-Almon, R. Chertkoff, M. Maas, C. E. Hollak, Taliglucerase alfa leads to favorable bone marrow responses in patients with type I Gaucher disease, *Blood Cells Mol. Dis.* 2013, **50**, 206-211.
17. G. A. Grabowski, M. Golembo, Y. Shaaltiel, Taliglucerase alfa: an enzyme replacement therapy using plant cell expression technology, *Mol. Genet. Metab.* 2014, **112**, 1-8.

18. B. Shanmugaraj, I. B. C. J., W. Phoolcharoen, Plant Molecular Farming: A viable platform for recombinant biopharmaceutical production, *Plants* 2020, **9**, 842.
19. N. Uthailak, H. Kajiura, R. Misaki, K. Fujiyama, Transient production of human beta-glucocerebrosidase with mannosidic-type n-glycan structure in glycoengineered nicotiana benthamiana plants, *Front. Plant Sci.* 2021, **12**, 683762.
20. U. Naphatsamon, T. Ohashi, R. Misaki, K. Fujiyama, The production of human beta-glucocerebrosidase in nicotiana benthamiana root culture, *Int. J. Mol. Sci.* 2018, **19**, 1972.
21. M. J. B. Burnett, A. C. Burnett, Therapeutic recombinant protein production in plants: Challenges and opportunities, *Plants, People, Planet* 2019, **2**, 121-132.
22. K. Kytidou, Transfer of "goods" from plants to humans: fundamental and applied biochemical investigations on retaining glycosidases, Thesis, Leiden University, 2020, <https://hdl.handle.net/1887/123040>.
23. C. L. Kuo, W. W. Kallemijn, L. T. Lelieveld, M. Mirzaian, I. Zoutendijk, A. Vardi, A. H. Futerman, A. H. Meijer, H. P. Spaink, H. S. Overkleeft, J. M. Aerts, M. Artola, In vivo inactivation of glycosidases by conduritol B epoxide and cyclophellitol as revealed by activity-based protein profiling, *FEBS J.* 2019, **286**, 584-600.
24. M. Artola, C. L. Kuo, L. T. Lelieveld, R. J. Rowland, G. A. van der Marel, J. D. C. Codée, R. G. Boot, G. J. Davies, J. M. Aerts, H. S. Overkleeft, Functionalized cyclophellitols are selective glucocerebrosidase inhibitors and induce a bona fide neuropathic Gaucher model in zebrafish, *J. Am. Chem. Soc.* 2019, **141**, 4214-4218.
25. Q. Su, S. P. Schröder, L. T. Lelieveld, M. J. Ferraz, M. Verhoek, R. G. Boot, H. S. Overkleeft, J. M. Aerts, M. Artola, C. L. Kuo, Xylose-configured cyclophellitols as selective inhibitors for glucocerebrosidase, *ChemBioChem* 2021, **22**, 3090-3098.
26. D. Lahav, B. Liu, R. van den Berg, A. van den Nieuwendijk, T. Wennekes, A. T. Ghisaidoobe, I. Breen, M. J. Ferraz, C. L. Kuo, L. Wu, P. P. Geurink, H. Ovaa, G. A. van der Marel, M. van der Stelt, R. G. Boot, G. J. Davies, J. M. Aerts, H. S. Overkleeft, A fluorescence polarization activity-based protein profiling assay in the discovery of potent, selective inhibitors for human nonlysosomal glucosylceramidase, *J. Am. Chem. Soc.* 2017, **139**, 14192-14197.
27. S. P. Schröder, J. W. van de Sande, W. W. Kallemijn, C. L. Kuo, M. Artola, E. J. van Rooden, J. Jiang, T. J. M. Beenakker, B. I. Florea, W. A. Offen, G. J. Davies, A. J. Minnaard, J. M. Aerts, J. D. C. Codée, G. A. van der Marel, H. S. Overkleeft, Towards broad spectrum activity-based glycosidase probes: synthesis and evaluation of deoxygenated cyclophellitol aziridines, *Chem. Commun.* 2017, **53**, 12528-12531.
28. R. A. Bryce, I. H. Hillier, J. H. Naismith, Carbohydrate-protein recognition: molecular dynamics simulations and free energy analysis of oligosaccharide binding to concanavalin A, *Biophys. J.* 2001, **81**, 1373-1388.
29. J. H. Naismith, R. A. Field, Structural basis of trimannoside recognition by concanavalin A, *J. Biol. Chem.* 1996, **271**, 972-976.
30. L. Bhattacharyya, M. Haraldsson, C. F. Brewer, Concanavalin A interactions with asparagine-linked glycopeptides. Bivalency of bisected complex type oligosaccharides, *J. Biol. Chem.* 1987, **262**, 1294-1299.
31. A. R. Marques, M. Mirzaian, H. Akiyama, P. Wisse, M. J. Ferraz, P. Gaspar, K. Ghauharali-van der Vlugt, R. Meijer, P. Giraldo, P. Alfonso, P. Irun, M. Dahl, S. Karlsson, E. V. Pavlova, T. M. Cox, S. Scheij, M. Verhoek, R. Ottenhoff, C. P. van Roomen, N. S. Pannu, M. van Eijk, N. Dekker, R. G. Boot, H. S. Overkleeft, E. Blommaart, Y. Hirabayashi, J. M. Aerts, Glucosylated cholesterol in mammalian cells and tissues: formation and degradation by multiple cellular beta-glucosidases, *J. Lipid Res.* 2016, **57**, 451-463.
32. D. E. Boer, M. Mirzaian, M. J. Ferraz, K. C. Zwiers, M. V. Baks, M. D. Hazeu, R. Ottenhoff, A. R. Marques, R. Meijer, J. C. P. Roos, T. M. Cox, R. G. Boot, N. Pannu, H. S. Overkleeft, M. Artola, J. M. Aerts, Human glucocerebrosidase mediates formation of xylosyl-cholesterol by beta-xylosidase and transxylosidase reactions, *J. Lipid Res.* 2021, **62**, 100018.

33. P. A. Longo, J. M. Kavran, M. S. Kim, D. J. Leahy, Transient mammalian cell transfection with polyethylenimine (PEI), *Methods Enzymol.* 2013, **529**, 227-240.
34. K. Kytidou, T. J. M. Beenakker, L. B. Westerhof, C. H. Hokke, G. F. Moolenaar, N. Goosen, M. Mirzaian, M. J. Ferraz, M. de Geus, W. W. Kallemeijn, H. S. Overkleeft, R. G. Boot, A. Schots, D. Bosch, J. M. Aerts, Human alpha galactosidases transiently produced in nicotiana benthamiana leaves: new insights in substrate specificities with relevance for Fabry disease, *Front. Plant Sci.* 2017, **8**, 1026.
35. E. G. Bligh, W. J. Dyer, A rapid method of total lipid extraction and purification, *Can. J. Biochem. Physiol.* 1959, **37**, 911-917.

Appendix

	AA number
hGBA1 : MEFSSPSRECEPKPLSRVSIAGSLTGLLLQAVSWASCARPCIPKSGYSSVVCNATYCDSDPPTSPA-----LGTFSRYESTRSGR : 87	
B 5 6 : -----MASYSWARKLVV-----YFFIIFSCCIFSFSGRITPNKVRVAVNLGWLLEG---WI : 53	
hGBA1 : RMEI-SMGEIQANHTCTGILLTLQPEQRFQKVGFGGAMTDAAALNILALSPPAQNLLKSYFSEEGIGY---NIIIRVPMASCDIFSIRTY : 173	
B 5 6 : KPSIFDGIENKDFLDGTGLQFKSVTVGKYLCAELGGTIIVNR-----TAALCWETFKIWRINSTSFNERVFNK : 123	
hGBA1 : TYADT-----P-----DDEQLHNHNSLPEEDTKLTIPLIHRALQIAQRPVSILA-----SPWTS-----PTWLKTNCAVNGKGS LK : 238	
B 5 6 : EFVGVGDGSGNVVAVENKSGFSETDEIVRK--SDDPSRVRIKASN-GFFLEVKTETVTANNGGNGGAGDDDPVSFIMKTSCKLECEFO-- : 208	
hGBA1 : GQPGDIYHQTWARYFVKFLDAYAEHKLQFWAVTAENPSAGLLSGYPFQCLGFTPEHQRDFTIARDLGPTLANSTHHNVRLMLDDQRLLL : 328	
B 5 6 : -----ITNGYGPITIA-----PQVMR : 223	
hGBA1 : PHWAKVVLTDPEAA-----KYVHGIAVHWYLD-FLAPAKATLGETHRLFPNTMLFASACVGSKFWEQSVRLGSWDRGMQSHSITITNL : 412	
B 5 6 : EHWKTFIVEEDFKFIASNLNAVRIPVGWIASDPTTPPYVGGSLHALDNAFLWAKK-----YGLKVITIDH : 291	
hGBA1 : YHVVGWTDNIALNPEGGPNWVRNFV---DSPIIIVDITKDTFYKQPMFVHLGHFSKFI-PEGS-----QRVGLVASQNDLDAVALMH : 491	
B 5 6 : AAPGSQNPWEHSANRDCTIEWGKTDDTIQQTVAVIDFLTARYAKNESLMAVELINEPLAPEVSFEMVKYYEACYNVAVRKHSSDA----- : 376	
hGBA1 : PDGSVVVVLNRSSKDVLTIKDPAVGFLETI----- : 523	
B 5 6 : -----YVVMNRLGSADETELLPFASCLKGSVIDVHYYNLFSDMFNDMTVQONLDFVFTNRSQALNTVTQSNGLPLTLVGWVAEWQVRDA : 461	
hGBA1 : -----SPGYSIHTYLRRO----- : 537	
B 5 6 : TKEDYQKFAKAQLEVFGRATFGWAYWTLKNVNNHWSLEWMIKNGYIKL : 509	

Figure S1. Amino acid (AA) allignment of huaman GBA1 (hGBA1, UniProt code: P04062) and B56 (UniProt code: A0A1S4CL56) by BLAST, no significant similarity was found. Signal peptide (predicted by SignalP 5.0) is marked as blue. hGBA1 catalytic residues (without counting signal peptides), nucleophile E235 and acid/base E340, were marked as red.

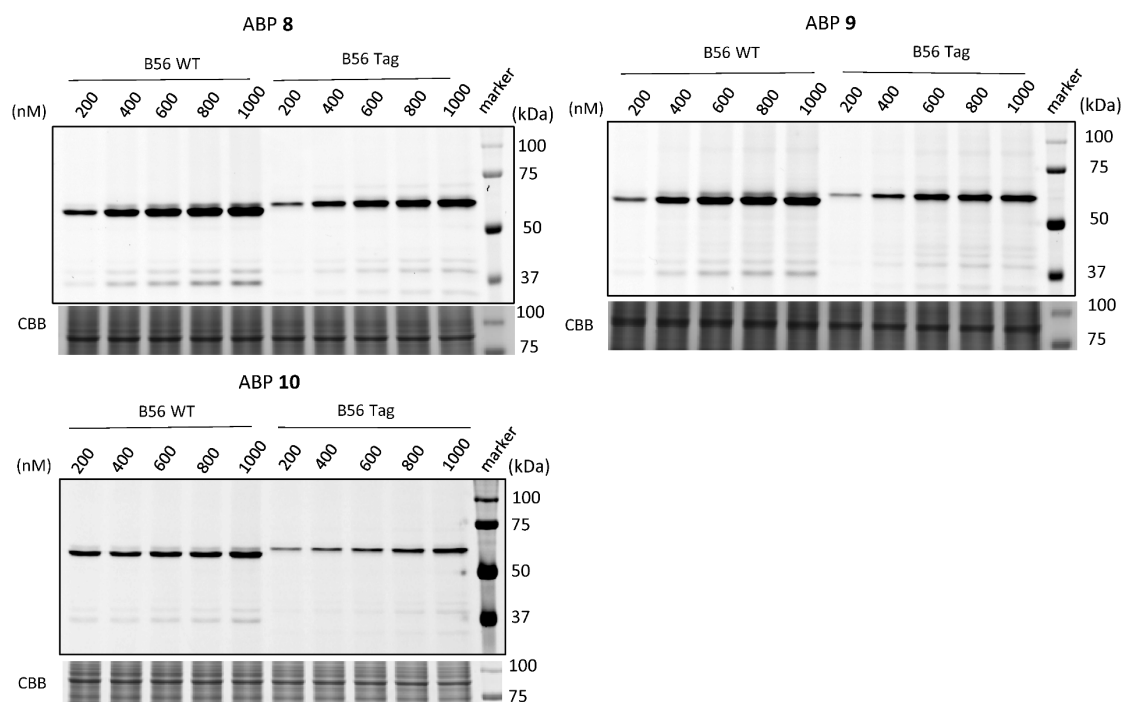


Figure S2. B56 (WT and Tag) reacted with varying concentrations of ABPs **8-10**. Lysates of B56 cells were incubated with indicated concentration of ABP **8-10** for 30 min at pH 5.0 at 37 °C and subjected to SDS-PAGE and fluorescence scanning of the wet gel slabs.

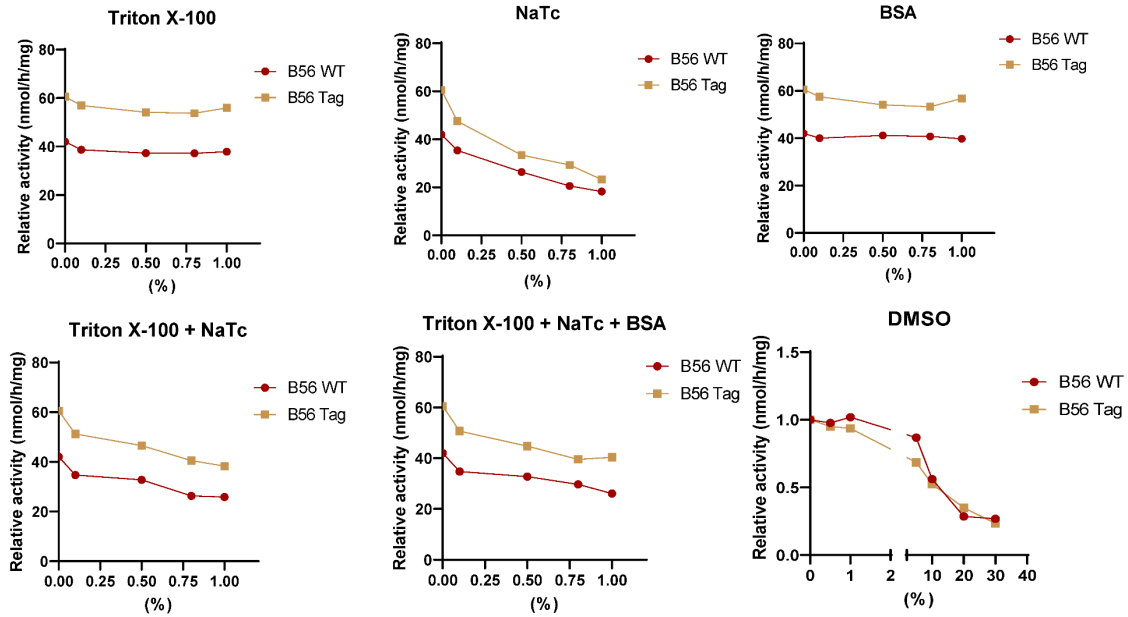


Figure S3. Influence of varying concentrations of various additives on B56 proteins activity, revealed by 4-MU fluorogenic substrate assay. B56 (WT and Tag) in hGBA1/GBA2 KO HEK293T cell lysate was incubated with 4-MU- β -D-Glc for 30 min at 37 °C at pH 5.0 in the presence of Triton X-100, sodium taurocholate (NaTc), bovine serum albumin (BSA), dimethyl sulfoxide (DMSO) alone, or a combination of these additives as indicated.

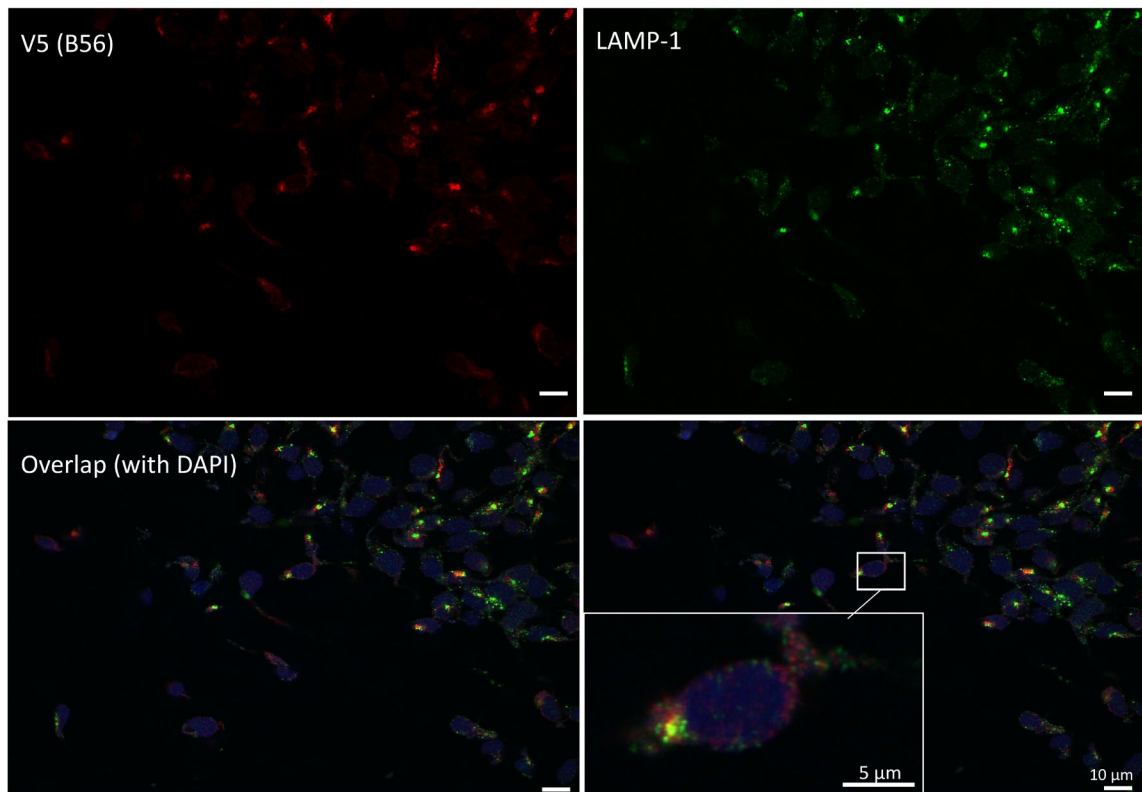


Figure S4. Zoom-out confocal microscopy of Figure 5, showing subcellular localization of V5-tagged B56 (shown as red) expressed in hGBA1/hGBA2 KO HEK293T cells, comparable to subcellular localization of LAMP1 (shown as green).

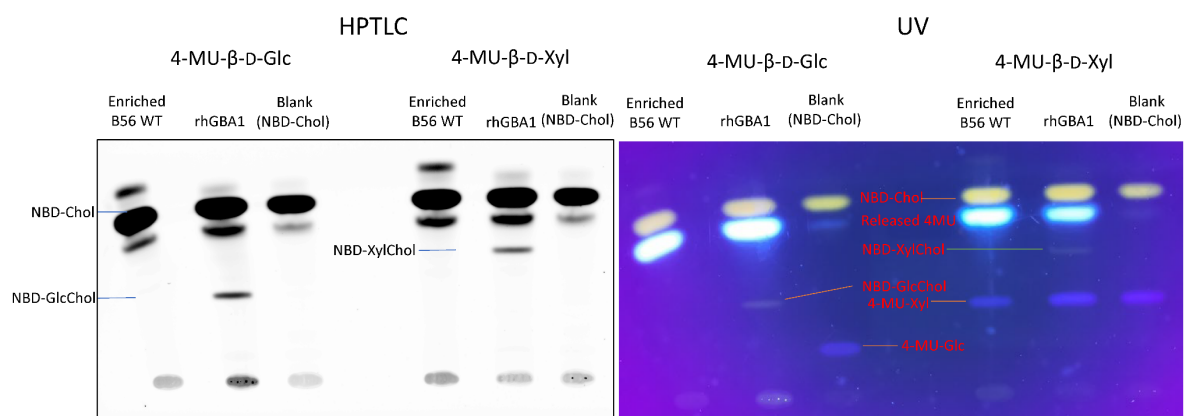


Figure S5. Transglycosylation assessment of B56 WT (enriched by ConA beads). B56 WT enriched by ConA beads was incubated with either 400 μ M 4-MU- β -D-Glc or 4-MU- β -D-Xyl as sugar donor and 20 μ M 25-NBD-Chol as acceptor for 16 h at 37 °C at pH 5.0. Assay was conducted as described in Figure 8.

Chapter 7

Summary and future prospects

The research described in this Thesis centered on retaining exo- β -glucosidases implicated in health and disease, in particular the human inherited lysosomal storage disorder, Gaucher disease (GD). Acid lysosomal β -glucosidase (GBA1), non-lysosomal β -glucosidase (GBA2), and cytosolic broad-specificity β -glucosidase (GBA3) all employ a Koshland double replacement mechanism in the hydrolysis of β -D-glucosides. Activity-based probes (ABPs) labelling retaining β -glucosidases are used throughout this Thesis to visualize human GBA1, GBA2 and GBA3, as well as analogous enzymes from other species. **Chapter 1** comprises a brief introduction on the human enzymes, their connection to human disease (Gaucher disease, Parkinson's disease) as well as on reagents and tools to study their activity. The first part of this thesis (**Chapters 2-4**) focus on the identification of selective inhibitors and activity-based probes (ABPs) for each of the three human retaining β -glucosidases, GBA1, GBA2 and GBA3. **Chapter 2** describes studies on the potency and selectivity of β -D-xylose-configured cyclophellitol aziridine ABPs towards the three human retaining β -glucosidases. In these studies, β -D-xylose-configured cyclophellitol, thus the compound lacking the hydroxymethylene as present in cyclophellitol, was found to be a GBA1 selective inhibitor, this in contrast to cyclophellitol itself which inhibits GBA2 and GBA3 as well. **Chapter 3** reports on the finding that β -D-arabinofuranose configured (β -D-Araf) cyclitol aziridines can be used to design GBA2-selective ABPs – compounds that did not exist prior to the in this Chapter described studies. **Chapter 4** describes the discovery of some relatively GBA3-selective mechanism-based inhibitors and ABPs. Their cross-reactivity towards GLB1 and GALC can be ameliorated by the inclusion of non-fluorescent inhibitors selective for these retaining β -galactosidases, enabling for monitoring of GBA3 activity in the presence of GBA1 and GBA2. The second part of this thesis centers on the identification of retaining β -glucosidase homologues in other species using established β -glucosidase ABPs and inhibitors. **Chapter 5** details studies on *Caenorhabditis elegans* (*C. elegans*) retaining β -glucosidases while **Chapter 6** characterizes a retaining β -glucosidase (termed B56) in *Nicotiana tabacum* and similarities and differences between these enzymes and human GBA1 and GBA2 are discussed in these chapters.

New GBA2-selective inhibitors and probes. GBA2 has attracted considerable attentions in last decade because of its involvement in human health and disease (see Chapter 3).¹⁻³ The discovery that β -D-Araf cyclitol aziridines equipped with fluorescent aziridine N-substituents are GBA2-selective ABPs may open new directions for medicinal chemistry. Inhibition of GBA2 ameliorates the phenotypes in GBA1-deficient type 1 GD and Niemann-Pick disease type C (NPC) mouse models, which highlights GBA2 as a potential therapeutic target.⁴⁻⁶ Conversely, GBA2 deficiency, such as homozygous mutant of GBA2, has been linked to hereditary spastic paraplegia and autosomal-recessive cerebellar ataxia.³ Miglustat **4** (N-butyl-deoxynojirimycin, NB-DNJ), an iminosugar inhibitor of glucosylceramide synthase (GCS), has been approved for treatment of mild type 1 GD and NPC.⁷⁻⁹ Besides inhibiting GCS, Miglustat **4** also potently inhibits GBA2.¹⁰ The clinical benefits of Miglustat **4** towards NPC may be partially attributed to this competitive inhibition of GBA2, which is relatively abundant in the brain and CNS.⁴ Therefore, the development of GBA2-selective inhibitors presents an attractive avenue for studying the enigmatic role of GBA2 in human (patho)physiology, for instance in central nervous system (CNS) motor coordination. Building upon the β -D-Araf aziridine scaffold, mechanism-based, covalent, and irreversible GBA2-selective inhibitors are thus proposed, as potential drug candidates and also to create bona fide GBA2-deficient models, complementing *GBA2* gene knockout approaches.¹¹⁻¹³ Ideally, GBA2 inhibitors insert well into cell membranes (where GBA2 acts) and are able to pass the blood-brain barrier (BBB). Therefore, modifications to enhance hydrophobicity, such as installing hydrophobic substitutions like adamantyl or biphenyl groups on the nitrogen of β -D-Araf aziridine, are suggested, also based on the precedent of cyclophellitol-C8-modified GBA1-selective inhibitors **5** and **6** in the generation of a GBA1-deficient zebrafish larvae model.¹⁴ Notably, the nature of the β -D-Araf aziridine tag impacts GBA2 selectivity over GBA1 and GBA3. For instance, Cy5-tagged and biotin-tagged β -D-Araf aziridine ABPs **3** and **7**, are much less selective for GBA2 than BODIPY-tagged derivatives **1** and **2**. At present, there is no crystal structure of human GBA2. The bacterial GBA2 homologue TxGH116,¹⁵ with an available crystal structure and a catalytic pocket comparable to that of human GBA2, may help in revealing the binding model of proposed GBA2-selective β -D-Araf aziridine

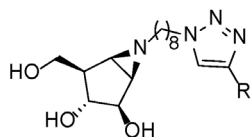
compounds (in Figure 1) and human GBA2. This, combined with structural studies on GBA1-complexed inhibitors may assist in the design of more active and more selective inhibitors.^{14,16,17}

In previous studies, overexpressed GBA2 constructs of different nature in cultured cells were found at different locations. GBA2-GFP was found at the plasma membrane¹⁸ while overexpressed, native GBA2 localized at the ER and Golgi.¹⁹ An earlier fractionation study of spleen identified endogenous GBA2 associated with an endosomal fraction.²⁰ The fluorescent β -D-Araf ABPs may provide a straightforward way to show the sub-cellular localization of endogenous GBA2 through directly binding to the catalytic active site of endogenous enzyme. The first attempt, as described in Chapter 3, to use β -D-Araf ABP **2** to reveal sub-cellular localization of native GBA2 in wild-type HEK293T cells did not present visible punctate labelling, possibly due to the dispersed distribution and low expression of GBA2 in these cells. To optimize the visualization of endogenous GBA2 by microscopy, several strategies could be employed, namely (1) the use of more advanced and sensitive fluorescence microscopy with higher quantum efficiency; (2) the use of other wild-type cell lines with more abundant GBA2; (3) substitution of the BODIPY group for a fluorescent group with higher quantum yield such as BODIPY-TMR to increase the fluorescence signal; or (4) the application of agents to amplify the labelled-GBA2 signal after initial labelling with tagged β -D-Araf ABP. With respect to the latter, one can envisage to first label GBA2 with BODIPY-tagged β -D-Araf ABP, then employ an anti-BODIPY primary antibody which is subsequently detected by a fluorescent secondary antibody for conjugating primary antibody to increase the fluorescence signal for microscope detection. The GBA2 selectivity window of β -D-Araf ABPs **1** and **2** proved already sufficient to selectively label GBA2 in different biological samples when used at appropriate concentrations, but also label GBA1 when high concentrations are used. Therefore, there is room for improvement in the GBA2 selectivity of these ABPs. In the future, new β -D-Araf ABPs with varying fluorescent substitutions at the aziridine might provide probes with even superior GBA2 selectivity.

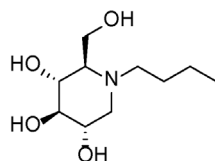
Recently, Shimokawa *et al.* identified a β -D-arabinofuranosidase in bacteria belonging to the same GH116 family as human GBA2.²¹ It may be speculated that β -D-Araf molecules are primary substrates for GH116 enzymes (including human GBA2) in nature, and that therefore β -D-Araf compounds fit the catalytic pocket of human GBA2 well. It is intriguing to explore whether the β -D-Araf cyclitol aziridine ABPs could react well with other GH116 enzymes, which may expand the utility of these β -D-Araf ABPs as the selective GH116 enzymes labelling probe. At present, a GBA2-selective fluorogenic substrate is not available, and it may be relevant to assess whether 4-methylumbelliferyl β -D-arabinofuranoside (4-MU- β -D-Araf) **8** (Figure 1) are hydrolyzed by human GBA2, and as well by other GH116 family glycoside hydrolases.

Compounds

β -D-Arabinofuranose configured
aziridine-based ABPs

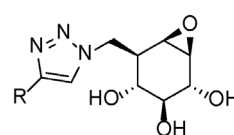


- 1 R = BODIPY green
- 2 R = BODIPY red
- 3 R = Cy5
- 7 R = biotin



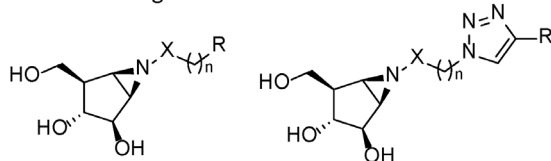
Miglustat 4
N-butyl-deoxynojirimycin
(NB-DNJ)

Cyclophellitol GBA1-
selective inhibitors



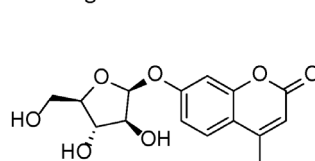
- 5 R = biphenyl
- 6 R = adamantyl

Proposed new β -D-arabinofuranose
configured aziridine-based inhibitors



X = CH₂ or CO R = biphenyl or adamantyl

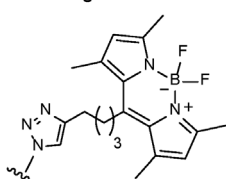
Proposed β -D-arabinofuranose
configured 4-MU substrate



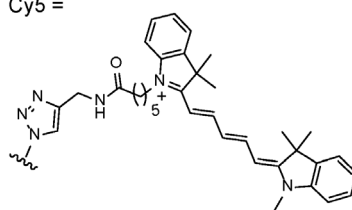
8

Tags

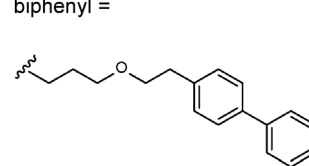
BODIPY green =



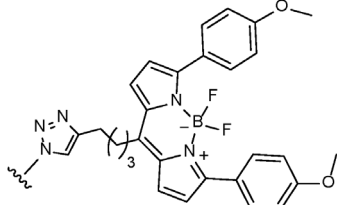
Cy5 =



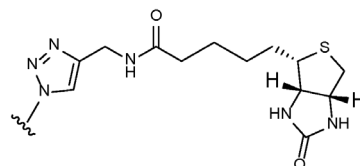
biphenyl =



BODIPY red =



biotin =



adamantyl =

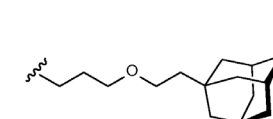


Figure 1. Compounds of (proposed) GBA2-selective inhibitors, ABPs, and fluorogenic substrates.

C. elegans as a model to study retaining β -glucosidases. The small round nematode *C. elegans*, the first multicellular organism whose genome was fully sequenced²², has been used as a model to study autophagy, neurobiology, and aging.²³⁻²⁷ As described in Chapter 5, enzymes identified by proteomic analysis are the hGBA1 resembling protein C-GBA1-3 (UniProt code: G5ECR8) encoded by *gba-3* gene and the hGBA2 resembling protein C-GBA2 (UniProt code: O01893) encoded by *R08F11.1* gene. The lack of detection of other putative β -glucosidases (encoded by *gba-1*, *2*, *4*, or *hpo-13*) may possibly be attributed to either low expression or lower reactivity towards the β -glucosidase ABPs used in Chapter 5. The *klo-1* and *klo-2* genes of *C. elegans* theoretically encode proteins that exhibit approximately 35% identity with human cytosolic broad-specificity β -glucosidase (hGBA3). These possible paralogues of hGBA3 in *C. elegans* merit characterization using existing β -glucosidase ABPs as well as new ones such as described in Chapter 4.

The pathways of carbohydrate and lipid metabolism in *C. elegans* are in general quite similar to those in mammals.²⁸ The occurrence of β -glucosidases in *C. elegans* implies that the nematode could be used as convenient organismal model to study β -glucosidases in relation to glycolipid metabolism. The glycosphingolipid d17iso-GlcCer of *C. elegans* is similar to mammalian GlcCer except for a slight difference in the sphingoid base (C17iso-sphingosine instead of C18-sphingosine). The lipid d17iso-GlcCer has been reported to play a vital role in growth of the nematode.^{29,30} The identified putative β -glucosidases C-GBA1-3 and/or C-GBA2 are hypothesized to be involved in metabolism of d17iso-GlcCer and future research, including lipid metabolism studies, may point out whether C-GBA1-3 degrades d17iso-GlcCer in *C. elegans*. One approach could involve using a *gba-3* knockout *C. elegans* strain, (available from the Caenorhabditis Genetics Center), to analyze changes in glycosphingolipid as compared to wild-type strains. Additional putative β -glucosidase KO nematode strains could be theoretically generated by genetic methods such as transgenesis, RNA interference (RNAi), and CRISPR-Cas9.³¹

Transglycosylation, another capacity of retaining β -glucosidases besides hydrolysis (see Chapter 1), presents an intriguing avenue for further study.³²⁻³⁵ GlcChol is a glycolipid formed in mammalian cells by transglycosylation, particularly by GBA2. The presence of GlcChol in *C. elegans* was observed (Chapter 5) and comprises the first report on the occurrence of the glycosylated sterol in the nematode. The physiological role of GlcChol in *C. elegans* is still unknown and this holds true also for the enzymes involved in GlcChol metabolism. Future studies should inform whether GlcChol in *C. elegans* is formed through transglycosylation and if so by which β -glucosidase.

In conclusion, the past decades have witnessed the design of inhibitors and ABPs designed for retaining exo- β -glucosidases have been successfully generated and established. The toolbox for glucosidase research provides powerful and diverse instruments to study aspects of particular glucosidases of interest. The work described in this thesis has further extended the toolbox, and those tools have been applied to shed light on retaining exo- β -glucosidases and their homologues in other species.

References

1. Y. Yildiz, P. Hoffmann, S. Vom Dahl, B. Breiden, R. Sandhoff, C. Niederau, M. Horwitz, S. Karlsson, M. Filocamo, D. Elstein, M. Beck, K. Sandhoff, E. Mengel, M. C. Gonzalez, M. M. Nothen, E. Sidransky, A. Zimran and M. Mattheisen, Functional and genetic characterization of the non-lysosomal glucosylceramidase 2 as a modifier for Gaucher disease, *Orphanet J. Rare Dis.*, 2013, **8**, 151.
2. A. Massimo, S. Maura, L. Nicoletta, M. Giulia, M. Valentina, C. Elena, P. Alessandro, B. Rosaria and S. Sandro, Current and novel aspects on the non-lysosomal beta-glucosylceramidase GBA2, *Neurochem. Res.*, 2016, **41**, 210-220.
3. M. A. Woeste and D. Wachten, The enigmatic role of gba2 in controlling locomotor function, *Front Mol. Neurosci.*, 2017, **10**, 386.
4. J. B. Nietupski, J. J. Pacheco, W. L. Chuang, K. Maratea, L. Li, J. Foley, K. M. Ashe, C. G. Cooper, J. M. Aerts, D. P. Copeland, R. K. Scheule, S. H. Cheng and J. Marshall, Iminosugar-based inhibitors of glucosylceramide synthase prolong survival but paradoxically increase brain glucosylceramide levels in Niemann-Pick C mice, *Mol. Genet. Metab.*, 2012, **105**, 621-628.
5. A. R. Marques, J. Aten, R. Ottenhoff, C. P. van Roomen, D. Herrera Moro, N. Claessen, M. F. Vinueza Veloz, K. Zhou, Z. Lin, M. Mirzaian, R. G. Boot, C. I. De Zeeuw, H. S. Overkleeft, Y. Yildiz and J. M. Aerts, Reducing GBA2 activity ameliorates neuropathology in Niemann-Pick type C mice, *PLoS One*, 2015, **10**, e0135889.
6. P. K. Mistry, J. Liu, L. Sun, W. L. Chuang, T. Yuen, R. Yang, P. Lu, K. Zhang, J. Li, J. Keutzer, A. Stachnik, A. Mennone, J. L. Boyer, D. Jain, R. O. Brady, M. I. New and M. Zaidi, Glucocerebrosidase 2 gene deletion rescues type 1 Gaucher disease, *Proc. Natl. Acad. Sci.*, 2014, **111**, 4934-4939.
7. K. A. Lyseng-Williamson, Miglustat: a review of its use in Niemann-Pick disease type C, *Drugs*, 2014, **74**, 61-74.
8. J. M. Aerts, C. E. Hollak, R. G. Boot, J. E. Groener and M. Maas, Substrate reduction therapy of glycosphingolipid storage disorders, *J. Inherit. Metab. Dis.*, 2006, **29**, 449-456.
9. N. J. Weinreb, J. A. Barranger, J. Charrow, G. A. Grabowski, H. J. Mankin and P. Mistry, Guidance on the use of miglustat for treating patients with type 1 Gaucher disease, *Am. J. Hematol.*, 2005, **80**, 223-229.
10. D. Lahav, B. Liu, R. van den Berg, A. van den Nieuwendijk, T. Wennekes, A. T. Ghisaidoobe, I. Breen, M. J. Ferraz, C. L. Kuo, L. Wu, P. P. Geurink, H. Ova, G. A. van der Marel, M. van der Stelt, R. G. Boot, G. J. Davies, J. M. Aerts and H. S. Overkleeft, A fluorescence polarization activity-based protein profiling assay in the discovery of potent, selective inhibitors for human nonlysosomal glucosylceramidase, *J. Am. Chem. Soc.*, 2017, **139**, 14192-14197.
11. Y. Yildiz, H. Matern, B. Thompson, J. C. Allegood, R. L. Warren, D. M. Ramirez, R. E. Hammer, F. K. Hamra, S. Matern and D. W. Russell, Mutation of beta-glucosidase 2 causes glycolipid storage disease and impaired male fertility, *J. Clin. Invest.*, 2006, **116**, 2985-2994.
12. L. T. Lelieveld, M. Mirzaian, C. L. Kuo, M. Artola, M. J. Ferraz, R. E. A. Peter, H. Akiyama, P. Greimel, R. van den Berg, H. S. Overkleeft, R. G. Boot, A. H. Meijer and J. M. Aerts, Role of beta-glucosidase 2 in aberrant glycosphingolipid metabolism: model of glucocerebrosidase deficiency in zebrafish, *J. Lipid. Res.*, 2019, **60**, 1851-1867.
13. E. Nakanishi, N. Uemura, H. Akiyama, M. Kinoshita, S. Masanori, Y. Taruno, H. Yamakado, S. I. Matsuzawa, S. Takeda, Y. Hirabayashi and R. Takahashi, Impact of Gba2 on neuronopathic Gaucher's disease and alpha-synuclein accumulation in medaka (*Oryzias latipes*), *Mol. Brain*, 2021, **14**, 80.
14. M. Artola, C. L. Kuo, L. T. Lelieveld, R. J. Rowland, G. A. van der Marel, J. D. C. Codée, R. G. Boot, G. J. Davies, J. M. Aerts and H. S. Overkleeft, Functionalized cyclophellitols are selective glucocerebrosidase inhibitors and induce a bona fide neuropathic Gaucher model in zebrafish, *J. Am. Chem. Soc.*, 2019, **141**, 4214-4218.

15. R. Charoenwattanasatien, S. Pengthaisong, I. Breen, R. Mutoh, S. Sansenya, Y. Hua, A. Tankrathok, L. Wu, C. Songsiriritthigul, H. Tanaka, S. J. Williams, G. J. Davies, G. Kurisu and J. R. Cairns, Bacterial beta-glucosidase reveals the structural and functional basis of genetic defects in human glucocerebrosidase 2 (GBA2), *ACS Chem. Biol.*, 2016, **11**, 1891-1900.
16. R. L. Lieberman, A guided tour of the structural biology of Gaucher disease: acid-beta-glucosidase and saposin C, *Enzyme Res.*, 2011, **2011**, 973231.
17. M. N. Offman, I. Silman, J. L. Sussman and A. H. Futerman, Crystal structure of the enzyme acid β -glucosidase, *Future Medicine*, 2013, DOI: <https://doi.org/10.2217/ebo.12.215>.
18. R. G. Boot, M. Verhoek, W. Donker-Koopman, A. Strijland, J. van Marle, H. S. Overkleeft, T. Wennekes and J. M. Aerts, Identification of the non-lysosomal glucosylceramidase as beta-glucosidase 2, *J. Biol. Chem.*, 2007, **282**, 1305-1312.
19. H. G. Korschen, Y. Yildiz, D. N. Raju, S. Schonauer, W. Bonigk, V. Jansen, E. Kremmer, U. B. Kaupp and D. Wachten, The non-lysosomal beta-glucosidase GBA2 is a non-integral membrane-associated protein at the endoplasmic reticulum (ER) and Golgi, *J. Biol. Chem.*, 2013, **288**, 3381-3393.
20. S. van Weely, M. Brandsma, A. Strijland, J. M. Tager and J. M. Aerts, Demonstration of the existence of a second, non-lysosomal glucocerebrosidase that is not deficient in Gaucher disease, *Biochim. Biophys. Acta*, 1993, **1181**, 55-62.
21. M. Shimokawa, A. Ishiwata, T. Kashima, C. Nakashima, J. Li, R. Fukushima, N. Sawai, M. Nakamori, Y. Tanaka, A. Kudo, S. Morikami, N. Iwanaga, G. Akai, N. Shimizu, T. Arakawa, C. Yamada, K. Kitahara, K. Tanaka, Y. Ito, S. Fushinobu and K. Fujita, Identification and characterization of endo-alpha-, exo-alpha-, and exo-beta-D-arabinofuranosidases degrading lipoarabinomannan and arabinogalactan of mycobacteria, *Nat. Commun.*, 2023, **14**, 5803.
22. C. e. S. Consortium, Genome sequence of the nematode *C. elegans*: a platform for investigating biology, *Science*, 1998, **282**, 2012-2018.
23. Y. Chen, V. Scarcelli and R. Legouis, Approaches for studying autophagy in *Caenorhabditis elegans*, *Cells*, 2017, **6**.
24. P. Shen, Y. Yue and Y. Park, A living model for obesity and aging research: *Caenorhabditis elegans*, *Crit. Rev. Food Sci. Nutr.*, 2018, **58**, 741-754.
25. N. Rani, M. M. Alam, A. Jamal, U. Bin Ghaffar and S. Parvez, *Caenorhabditis elegans*: A transgenic model for studying age-associated neurodegenerative diseases, *Ageing Res. Rev.*, 2023, **91**, 102036.
26. S. H. O. Zarroug, J. S. Bajaman, F. N. Hamza, R. A. Saleem and H. K. Abdalla, *Caenorhabditis elegans* as an in vivo model for the discovery and development of natural plant-based antimicrobial compounds, *Pharmaceuticals*, 2023, **16**.
27. V. M. Nigon and M. A. Felix, History of research on *C. elegans* and other free-living nematodes as model organisms, *WormBook*, 2017, **2017**, 1-84.
28. J. L. Watts and M. Ristow, Lipid and carbohydrate metabolism in *Caenorhabditis elegans*, *Genetics*, 2017, **207**, 413-446.
29. M. Zhu, F. Teng, N. Li, L. Zhang, S. Zhang, F. Xu, J. Shao, H. Sun and H. Zhu, Monomethyl branched-chain fatty acid mediates amino acid sensing upstream of mTORC1, *Dev. Cell*, 2021, **56**, 2692-2702 e2695.
30. A. F. C. Vieira, M. A. Xatse, H. Tifeki, C. Diot, A. J. M. Walhout and C. P. Olsen, Monomethyl branched-chain fatty acids are critical for *Caenorhabditis elegans* survival in elevated glucose conditions, *J. Biol. Chem.*, 2022, **298**, 101444.
31. A. Paix, A. Folkmann, D. Rasoloson and G. Seydoux, High efficiency, homology-directed genome editing in *Caenorhabditis elegans* using CRISPR-Cas9 ribonucleoprotein complexes, *Genetics*, 2015, **201**, 47-54.
32. A. R. Marques, M. Mirzaian, H. Akiyama, P. Wisse, M. J. Ferraz, P. Gaspar, K. Ghauharali-van der Vlugt, R. Meijer, P. Giraldo, P. Alfonso, P. Irun, M. Dahl, S. Karlsson, E. V. Pavlova, T. M. Cox, S. Scheij, M. Verhoek, R. Ottenhoff, C. P. van Roomen, N. S. Pannu, M. van Eijk, N. Dekker, R. G. Boot, H. S. Overkleeft, E. Blommaart, Y. Hirabayashi and J. M. Aerts, Glucosylated cholesterol

- in mammalian cells and tissues: formation and degradation by multiple cellular beta-glucosidases, *J. Lipid. Res.*, 2016, **57**, 451-463.
33. D. E. Boer, M. Mirzaian, M. J. Ferraz, K. C. Zwiers, M. V. Baks, M. D. Hazeu, R. Ottenhoff, A. R. A. Marques, R. Meijer, J. C. P. Roos, T. M. Cox, R. G. Boot, N. Pannu, H. S. Overkleeft, M. Artola and J. M. Aerts, Human glucocerebrosidase mediates formation of xylosyl-cholesterol by beta-xylosidase and transxylosidase reactions, *J. Lipid. Res.*, 2021, **62**, 100018.
 34. H. Akiyama, M. Ide, Y. Nagatsuka, T. Sayano, E. Nakanishi, N. Uemura, K. Yuyama, Y. Yamaguchi, H. Kamiguchi, R. Takahashi, J. M. Aerts, P. Greimel and Y. Hirabayashi, Glucocerebrosidases catalyze a transgalactosylation reaction that yields a newly-identified brain sterol metabolite, galactosylated cholesterol, *J. Biol. Chem.*, 2020, **295**, 5257-5277.
 35. H. Akiyama, S. Kobayashi, Y. Hirabayashi and K. Murakami-Murofushi, Cholesterol glucosylation is catalyzed by transglucosylation reaction of beta-glucosidase 1, *Biochem. Biophys. Res. Commun.*, 2013, **441**, 838-843.

Chemisch-biologische studies aan retaining exo- β -glucosidases

Dit proefschrift beschrijft chemisch-biologisch onderzoek aan retaining exo- β -glucosidases met behulp van activiteit-gebaseerde probes (ABP's). Retaining exo- β -glucosidases zijn enzymen die in organismen voorkomen en de hydrolyse van β -glucosides katalyseren: ze spelen een belangrijke rol in zowel gezondheid als ziekte. In menselijke cellen zijn drie β -glucosidases geïdentificeerd: lysosomale zure β -glucosidase GBA1 (ook bekend als glucosylceramidase, GCase), niet-lysosomale β -glucosidase GBA2, en cytosolische β -glucosidase GBA3. De eerste twee enzymen zijn betrokken bij de afbraak van glucosylceramide (GlcCer, ook wel glucocerebroside genoemd). Reduced glucosylceramide metabolisme is geassocieerd met de ziekte van Gaucher (GD), een lysosomale stapelingsziekte die het gevolg is van mutaties in het GBA1-gen die leiden tot enzym-deficiëntie. GD-patiënten vertonen doorgaans klinische symptomen als hepatosplenomegalie, en skelet-manifestaties, en in ernstige gevallen ook klachten in het centrale zenuwstelsel, als gevolg van de ophoping van glucosylceramide. Bovendien worden mutaties in GBA1 herkend als veelvoorkomende genetische risicofactor voor de ziekte van Parkinson. De rol van GBA2 en GBA3 in GD en hun functies in het menselijk metabolisme zijn nog niet volledig begrepen. Activiteitsgebaseerde eiwitprofieling (ABPP), een sleuteltechniek in de moderne chemische biologie, maakt gebruik van ABP's om de actieve doeleiwitten in complexe biologische monsters te detecteren. Op dit moment is een reeks ABP's specifiek voor glycosidases ontwikkeld, inclusief probes die gericht zijn tegen retaining exo- β -glucosidases.

Hoofdstuk 1 biedt een overzicht van de menselijke retaining exo- β -glucosidases, als ook fundamentele informatie over ABP's die selectief β -glucosidases kunnen labelen. Beschreven worden de biologische functies van β -glucosidases, ebeknopt de ziekte van Gaucher, het mechanisme van hydrolyse van β -glucosides, en de ontwikkeling en toepassing van β -glucosidase ABP's. Eerder onderzoek heeft geleid tot de ontwikkeling van ABP's die in staat zijn β -glucosidases selectief te labelen, waarbij cyclophellitol wordt gebruikt als een scaffold, een krachtige en actieve GBA1- en GBA2-remmer. Dit proefschrift beschrijft de ontwikkeling van nieuwe ABP's voor het selectief labelen van retaining β -glucosidases en de toepassing van bestaande ABP's en remmers in chemisch-biologische studies aan menselijke retaining exo- β -glucosidases en hun homologe enzymen in andere soorten.

Hoofdstuk 2 beschrijft het gebruik van ABPP en het fluorescente substraat 4-methylumbelliferyl- β -D-glucopyranoside om de activiteit en selectiviteit van β -D-xyloside verbindingen tegen menselijke retaining exo- β -glucosidases te onderzoeken. Eerdere studies wezen uit dat menselijk GBA1 chemische modificaties aan de C8-positie van cyclophellitol kan accommoderen, terwijl GBA2 dat niet kan. Bijvoorbeeld, een cyclophellitol met C8-verwijdering (bv. conduritol B epoxide, CBE) heeft een lagere affiniteit voor GBA2 dan voor GBA1. In vergelijking met cyclophellitol missen β -D-xyloside verbindingen de hydroxymethyl-zijketen op de C8-positie, waarvan werd verondersteld dat deze selectief voor GBA1 was. Hoofdstuk 2 bevestigt dat β -D-xyloside epoxide inderdaad meer selectief is voor GBA1 dan voor andere menselijke β -glucosidases (GBA2 en GBA3). β -D-xyloside aziridines vertonen ook selectiviteit voor GBA1. Echter, vergeleken met β -D-xyloside, vertonen β -D-xyloside aziridines een kleinere GBA1 selectiviteitsvenster vanwege hun betere affiniteit voor GBA2. β -D-xyloside aziridine ABP's kunnen breed menselijke β -glucosidases labelen (GBA1, GBA2, en GBA3), vergelijkbaar met cyclophellitol aziridine ABP's. Bovendien toonde lipide analyse van zebrafishlarven die met β -D-xyloside verbindingen werden behandeld verhoogde niveaus van glucosylsphingosine (GlcSph), een biomarker die kenmerkend is voor een GD-model veroorzaakt door GBA1-deficiëntie.

Hoofdstuk 3 onderzoekt de activiteit en selectiviteit van β -D-arabinofuranose-geconfigureerde aziridineverbindingen op menselijke retaining exo- β -glucosidases, in het bijzonder GBA2. De rol van GBA2 in de ziekte van Gaucher (GD) vereist verder onderzoek. Defecten in het GBA2-gen in verband gebracht met erfelijke spastische paraplegie. Anderzijds, remming van GBA2 activiteit is gemeld om symptomen te verlichten bij patiënten met type 1 GD en de ziekte van Niemann-Pick C (NPC), wat GBA2

tot een potentieel therapeutisch doelwit maakt. Voorafgaand aan het onderzoek dat in dit hoofdstuk wordt gepresenteerd, waren er geen covalente GBA2-selectieve remmers of ABP's geïdentificeerd. Dit hoofdstuk rapporteert de ontdekking van β -D-arabinofuranose aziridine ABP's die een goede selectiviteit vertonen voor GBA2, met lagere schijnbare IC₅₀-waarden voor GBA2 vergeleken met GBA1 en GBA3. Verdere ABPP-experimenten bevestigden de selectiviteit van β -D-arabinofuranose aziridine ABP's voor GBA2. Deze ABP's labelen GBA2 selectief, zowel *in vitro* als *in situ*, waarbij fluorescentiemicroscopie het selectieve labelen van GBA2 to overexpressie gebracht in cellen bevestigt. Een kristalstructuur studie toonde aan dat β -D-arabinofuranose aziridineverbindingen covalent binden aan een bacteriële GBA2-homoloog enzym met een vergelijkbaar actief centrum als dat van menselijk GBA2. Competitieve ABPP toonde aan dat de β -D-arabinofuranose aziridine ABP's GBA2 onomkeerbaar labelen. Bovendien blijken β -D-arabinofuranose aziridine ABP's selectief voor GBA2-homologen in zebravissen en muizen. De bevindingen in dit hoofdstuk wijzen op het potentieel van β -D-arabinofuranose aziridine scaffold voor de ontwikkeling van nieuwe GBA2-selectieve covalente remmers en ABP's.

Hoofdstuk 4 beschrijft een verkenning van fluorescente substraten en ABP's die door GBA3 gehydrolyseerd kunnen worden. GBA3 was eerder bekend tot hydrolyse van verschillende glycosidesubstraten (bijvoorbeeld β -D-glucosides, β -D-galactosides en α -L-arabinosides) en waargenomen was dat het gelabeld werd door cyclophellitol aziridine ABP's. De rol van GBA3 in het menselijke metabolisme blijft echter onduidelijk, en er waren voor deze studie geen fluorescente substraten of ABP's bekend die specifiek aan GBA3 konden binden. Dit hoofdstuk evalueert verschillende 4-methylumbelliferyl glycoside fluorescente substraten en ABP's voor hun activiteit tegen β -glucosidases. De studie leerde dat β -D-fucoside en α -L-arabinopyranoside substraten relatiefselectief worden gehydrolyseerd door GBA3 enzym vergeleken met andere retaining exo- β -glucosidases. Deze substraten kunnen echter ook worden gehydrolyseerd door andere enzymen (mogelijk β -D-galactosidases), wat hun toepassing voor selectieve GBA3-activiteitsdetectie beperkt. Daarnaast werden twee ABP's met relatief hoge selectiviteit voor GBA3 geïdentificeerd: α -L-arabinopyranoside aziridine ABP's en β -D-galactoside ABP's, die *in vitro* een grotere selectiviteit vertoonden voor GBA3 ten opzichte van andere β -glucosidases (GBA1, GBA2). Deze ABP's labelen echter ook β -galactosidases, waardoor ze geen ideale GBA3-selectieve ABP's zijn.

Hoofdstuk 5 onderzoekt β -glucosidases in het organisme *Caenorhabditis elegans* (*C. elegans*), dat vaak wordt gebruikt in biologisch onderzoek aan koolhydraat- en lipide metabolisme dat vrij overeenkomstig is met zoogdieren. Door sequentie-alignment met menselijke β -glucosidases werden verschillende potentiële β -glucosidase-kandidaten in *C. elegans* geïdentificeerd. Onderzoek toonde aan dat *C. elegans*-homogenaten in staat zijn 4-methylumbelliferyl- β -D-glucopyranoside-substraat en een kunstmatig GlcCer-analoog, C12-NBD-GlcCer, te hydrolyseren. Bovendien labelden de ontwikkelde β -glucosidase ABP's eiwitten binnen de homogenaten van *C. elegans*. Proteomics analyse gebruik makend van pull-down-experimenten met biotine-gelabelde ABP's voor pull-down-experimenten resulteerde in aanzienlijke verrijking van twee β -glucosidase-kandidaten uit de homogenaten van *C. elegans*. Deze β -glucosidase-kandidaten vertoonden kenmerken vergelijkbaar met respectievelijk menselijke GBA1 of GBA2, zoals binding aan specifieke remmers of ABP's en het hebben van vergelijkbare optimale pH-waarden, wat suggereert dat ze homoloog kunnen zijn aan het menselijke GBA1 en GBA2.

Hoofdstuk 6 onderzoekt een β -glucosidasekandidaat-eiwit (B56) dat in tabak werd geïdentificeerd. Eerdere studies hebben aangetoond dat B56 interactie vertoonde met een GBA1-selectieve ABP en verrijkt werd in pull-down assays met biotine-gelabelde β -glucosidase ABP's. In dit hoofdstuk werd B56 tot expressie gebracht in menselijke embryonale nier (HEK293T) cellen, waarin de endogene β -glucosidases waren uitgeschakeld, om de karakterisering ervan te onderzoeken. B56 vertoont verschillende overeenkomsten met menselijke GBA1, waaronder een zure optimale pH voor activiteit,

het vermogen om 4-methylumbelliferyl- β -D-glucopyranoside en 4-methylumbelliferyl- β -D-xylopyranoside te hydrolyseren, de binding van GBA1-selectieve ABP's en remmers, en de aanwezigheid van high-mannose N-glycanen. Fluorescentiemicroscopie toonde dat de subcellulaire locatie van B56 sterk overlapt met lysosomale geassocieerd membraanewit 1 (LIMP-1), wat wijst op een primaire locatie in lysosomen. B56 verschilt echter ook van menselijke GBA1 op verschillende punten, zoals een hogere thermische stabiliteit bij 60°C en een verminderde enzymactiviteit in de aanwezigheid van bepaalde toevoegingen. Het meest opmerkelijke is dat de experimentele gegevens in dit hoofdstuk aangeven dat B56 in HEK293T-cellen, glucosylceramide niet afbreekt zoals menselijke GBA1 doet en dus niet functioneel kan substitueren voor menselijke GBA1.

Hoofdstuk 7 biedt een samenvatting van de onderzoeksresultaten, bespreekt de vragen die zijn opgeworpen en beschrijft de vooruitzichten voor toekomstig gerelateerd onderzoek.

Deze dissertatie beschrijft de ontdekking van nieuwe tools voor β -glucosidase onderzoek, waaronder activiteit-gebaseerde probes (ABP's) en remmers, en de gerelateerde chemisch-biologische methoden die zijn gebruikt voor de identificatie en karakterisering van retaining β -glucosidases met behulp van deze bestaande ABP's en remmers. Het werk dat in deze dissertatie wordt gepresenteerd biedt nieuwe tools voor de studie van β -glucosidases en verkent potentiële homologe enzymen in andere soorten, waardoor nieuwe inzichten worden geboden voor onderzoek op het gebied van retaining β -glucosidases.

(Summary in Chinese 中文总结)

保留型外切- β -葡萄糖苷酶的化学生物学研究

本论文主要描述了应用活性分子探针 (activity-based probes, ABPs) 对保留型外切- β -葡萄糖苷酶(retaining exo- β -glucosidases)进行的化学生物学研究。保留型外切- β -葡萄糖苷酶是一类普遍存在于生物体中的可用于催化 β -葡萄糖苷水解的酶, 在健康和疾病中都扮演着重要角色。人体细胞中的 β -葡萄糖苷酶主要有三种: 溶酶体 (lysosomal) 酸性 β -葡萄糖苷酶 GBA1 (又称葡萄糖神经酰胺酶 glucosylceramidase, GCase), 非溶酶体 (non-lysosomal) β -葡萄糖苷酶 GBA2, 和胞质 (cytosolic) β -葡萄糖苷酶 GBA3。这三种酶均能降解葡萄糖神经酰胺 (glucosylceramide, GlcCer, 又称葡萄糖脑苷脂 glucocerebroside)。葡萄糖神经酰胺的代谢异常与戈谢病 (Gaucher Disease, GD) 相关。戈谢病, 是基因突变造成的 GBA1 酶缺陷所致的一种遗传性溶酶体贮积症 (lysosome storage disorder), 患者因体内葡萄糖神经酰胺降解障碍并导致其大量异常贮积, 从而出现肝脾肿大, 骨骼受侵及中枢神经系统受累等临床症状。另据报道, GBA1 的基因变异也属于常见的帕金森病 (Parkinson disease) 的遗传危险因素。而目前, 除 GBA1 外, GBA2 和 GBA3 在戈谢病中的作用与影响以及它们在人体代谢中所扮演的角色尚未完全探明。活性蛋白表达谱 (activity-based protein profiling, ABPP), 即应用活性分子探针对复杂生物样品中的靶标蛋白进行活性检测, 是化学生物学研究中的一种重要技术手段。经过不断的发展, 一系列用于特异性标记糖苷酶 (包括保留型外切 β -葡萄糖苷酶) 的 ABPs 已得到了开发。

在本论文中, 第 1 章简要介绍了人体保留型外切- β -葡萄糖苷酶, 以及能特异性标记 β -葡萄糖苷酶的 ABPs 的基本信息。主要包括: β -葡萄糖苷酶的生物学功能、戈谢病的概况、 β -葡萄糖苷的水解机制以及 β -葡萄糖苷酶 ABPs 的设计和应用。在本论文之前, 以能与 β -葡萄糖苷酶高效且特异性结合的活性分子六元环多醇 cyclophellitol 为骨架, 已经开发出了能够选择性标记 β -葡萄糖苷酶的 ABPs。本论文描述了关于新型选择性标记保留型 β -葡萄糖苷酶 ABPs 的研究开发工作, 以及利用已有的工具化合物 (ABPs 及抑制剂) 对人体中保留型外切 β -葡萄糖苷酶以及它们在其他物种中的同源基因酶所进行的化学生物学研究。

第 2 章介绍了利用 ABPP 及 4-甲基伞形酮- β -D-葡萄糖苷 (4-methylumbelliferyl- β -D-glucopyranoside) 荧光底物揭示 β -D-木糖类化合物对人体保留型外切 β -葡萄糖苷酶的活性和选择性的工作。早期有研究报道了人体 GBA1 可以适应 cyclophellitol 碳 8 位的化学结构修饰, 而 GBA2 则无法兼容在该位的修饰, 故 cyclophellitol 8 位碳的移除 (比如 conduritol B epoxide, CBE 结构) 会导致其对 GBA2 亲和作用的显著降低。与 cyclophellitol 相比, β -D-木糖型化合物缺失了位于碳 8 位 (或吡喃葡萄糖编号中的 碳 6 位) 的羟甲基支链, 因此被假定为具有 GBA1 选择性的化合物。本章的研究证实了 β -D-木糖类环氧化合物的确对 GBA1 显示出相对于其他人体 β -葡萄糖苷酶 (GBA2 和 GBA3) 更高的选择性。 β -D-木糖类氮丙啶 (aziridine) 化合物对 GBA1 也有较好的选择性, 但相对 β -D-木糖类环氧化合物而言, 因其同时对 GBA2 也表现出相对较好的亲和性, 所以显示了相对更小的 GBA1 选择性窗口。 β -D-木糖类氮丙啶 ABPs 可以如 cyclophellitol 氮丙啶 ABPs 一样广泛地标记人体的 β -葡萄糖苷酶 (GBA1, GBA2 及 GBA3)。此外, 当将斑马鱼幼苗置于包含 β -D-木糖类化合物 (GBA1 选择性抑制剂) 的环境中生长约五天后, 通过 LC-MS 对斑马鱼幼苗中的脂质组分进行定量分析, 结果表明 β -D-木糖类化合物处理后的斑马鱼幼苗显示出与 GBA1 缺陷导致的戈谢病模型相似的特征性的葡萄糖基鞘氨醇 (glucosyl sphingosine, GlcSph) 浓度水平上升。

第 3 章研究了 β -D-阿拉伯呋喃糖氮丙啶(β -D-arabinofuranose-configured aziridine)化合物对人体保留型外切 β -葡萄糖苷酶的活性和选择性。GBA2 在戈谢病中所起的作用尚未完全清楚。GBA2 的基因缺陷与遗传性痉挛截瘫 (小脑共济失调) 疾病相关。另有报道表明 GBA2 的抑制可

能有助于改善戈谢病 I 型和 Niemann-Pick C (NPC) 病人的临床症状。因此, GBA2 为这些疾病潜在的治疗靶点。在本章之前, 尚未发现能选择性地与 GBA2 相互作用的共价抑制剂和 ABPs。本章研究发现了 β -D-阿拉伯呋喃糖氮丙啶 ABPs 具有较为明显的 GBA2 选择性, 它们对 GBA2 显示出相对于 GBA1 及 GBA3 更低的表现半数抑制浓度 (apparent IC_{50})。后续通过 ABPP 进一步验证了 β -D-阿拉伯呋喃糖氮丙啶 ABPs 对于 GBA2 的选择性。 β -D-阿拉伯呋喃糖类氮丙啶 ABPs 可以在体外 (*in vitro*) 以及细胞原位 (*in situ*) 选择性地标记 GBA2, 并且荧光显微镜检测结果表明其还可以灵敏且特异性地标记细胞内过表达的 GBA2。三维晶体结构分析表明, β -D-阿拉伯呋喃糖氮丙啶化合物通过和 cyclophellitol 相似的结合模型, 与来源于细菌的具有和 GBA2 活性位点相似的同源酶 (TxGH116) 进行共价结合。竞争性 ABPP 也证明了 β -D-阿拉伯呋喃糖氮丙啶 ABPs 不可逆地标记 GBA2。另外, β -D-阿拉伯呋喃糖类氮丙啶 ABPs 对于斑马鱼和小鼠中的 GBA2 同源基因酶也表现出了相应的 GBA2 选择性。因此, 本章所发现的 β -D-阿拉伯呋喃糖氮丙啶结构有望用于开发更多新的 GBA2 选择性共价抑制剂及 ABPs。

第 4 章介绍了可被 GBA3 水解的 4-甲基伞形酮糖苷底物以及可以标记人体 GBA3 的 ABPs。GBA3 早前被报道可催化多种糖苷底物的水解 (如 β -D-葡萄糖苷、 β -D-半乳糖苷、 α -L-阿拉伯糖苷类底物等), 且可以被如 cyclophellitol 氮丙啶 ABPs (为广泛的保留型外切 β -葡萄糖苷酶 ABPs) 所标记。目前 GBA3 在人体代谢中所起的作用仍未完全探明, 且能够选择性检测 GBA3 酶活性的荧光底物以及选择性标记 GBA3 的 ABPs 尚未得到报道。为了寻找潜在的具有 GBA3 选择性的 4-甲基伞形酮糖苷荧光底物以及 ABPs, 本章评估了几种 4-甲基伞形酮糖苷荧光底物以及 ABPs 对于 β -葡萄糖苷酶的活性。研究发现 β -D-岩藻糖苷 (fucoside) 以及 α -L-阿拉伯吡喃糖苷 (arabinopyranoside) 类底物在保留型外切 β -葡萄糖苷酶中只能被 GBA3 水解, 但由于这两种荧光底物的糖苷键也可以被另外的酶 (推测为 β -D-半乳糖酶) 水解, 故不是理想的选择性检测 GBA3 酶活性的荧光底物。另外, 本章还介绍了两种对于 GBA3 具有相对较好选择性的 ABPs, 即 α -L-阿拉伯吡喃糖类氮丙啶 ABPs 和 β -D-半乳糖类 ABPs。他们能够在体外以优于其他 β -葡萄糖苷酶 (GBA1, GBA2) 的选择性对 GBA3 进行标记, 其中 β -D-半乳糖类环氧化物 ABPs 可以在细胞原位标记实验中保持其 GBA3 的选择性, 然而它们也同时标记 β -半乳糖苷酶, 因此不是理想的 GBA3 选择性 ABPs。

第 5 章研究了秀丽隐杆线虫 (*Caenorhabditis elegans*) 中存在的 β -葡萄糖苷酶。秀丽隐杆线虫是生物学研究中常用的生物模型, 该线虫具有与哺乳动物相似的碳水化合物和脂质代谢途径。与人体 β -葡萄糖神经酰胺酶进行的氨基酸序列比对揭示了几种秀丽隐杆线虫中可能的 β -葡萄糖苷酶候选蛋白。目前有关线虫中 β -葡萄糖苷酶的信息仍然有限, 因此将秀丽隐杆线虫作为 β -葡萄糖苷酶研究模型的可能性仍需进行更多验证。在本章实验中, 发现线虫匀浆可以使 4-甲基伞形酮 β -葡萄糖苷底物以及人工合成的 GlcCer 类似物 C12-NBD-GlcCer 水解, 且已有的 β -葡萄糖苷酶 ABPs 通过 ABPP 标记出了线虫体内的一些可相互作用的蛋白, 表明了线虫中存在 β -葡萄糖苷酶。蛋白组学 (Proteomics) 使用带有生物素 (biotin) 标记的 ABPs 进行钓靶 (Pull-down) 实验, 从线虫匀浆中显著富集到了两种 β -葡萄糖苷酶候选蛋白。这两种 β -葡萄糖苷酶分别表现出了与人体 GBA1 或 GBA2 相似的特征, 如可与特定选择性抑制剂或 ABPs 结合, 具有相近的最适 pH 值等。因此, 它们或许分别为秀丽隐杆线虫中的 GBA1 和 GBA2 同源基因酶。

第 6 章介绍了烟草中的一种 β -葡萄糖苷酶候选蛋白 (B56)。之前有研究发现 B56 可以与 GBA1 选择性 ABPs 发生反应, 并且可以被带有生物素标记的 β -葡萄糖苷酶 ABPs 通过钓靶实验富集。本章中, B56 被表达在人体胚胎肾细胞 (HEK293T) 中 (细胞中的人源 β -葡萄糖苷酶基因已被提前敲除) 用于表征实验。表达于 HEK293T 细胞中的 B56 与人体 GBA1 有许多相似之处。B56 拥有酸性的最佳活性 pH 值, 可以如人体 GBA1 一样水解 4-甲基伞形酮- β -D-葡萄糖苷和 4-甲基伞形酮- β -D-木糖苷, B56 可与 GBA1 选择性 ABPs 和抑制剂高效结合, 并且 B56 同样含有高甘

露糖型 N-聚糖。荧光显微镜检测显示 B56 与位于溶酶体的溶酶体相关膜蛋白 1 (LIMP-1) 的细胞内分布位置高度重合, 表明 B56 蛋白主要表达于细胞中的溶酶体。然而, B56 也在某些方面与人体 GBA1 不同, 比如 B56 可耐受 60°C 高温以及它的活性会受添加剂影响而降低, 最重要的不同之处在于: 目前的实验结果表明表达于 HEK293T 细胞内的 B56 无法像人体 GBA1 一样降解葡萄糖神经酰胺从而起到代替人体 GBA1 作用的功能。

第 7 章介绍了目前所取得的研究成果, 讨论了实验中发现的问题, 并描述了相关研究的未来前景。

本论文描述了新型 β -葡萄糖苷酶工具化合物 (ABPs 和抑制剂) 的发现, 并阐述了应用已有的 β -葡萄糖苷酶 ABPs 和抑制剂对保留型 β -葡萄糖苷酶进行鉴定和表征的化学生物学研究方法。本论文所述工作为研究 β -葡萄糖苷酶提供了新的工具化合物、以及探究了其他物种中可能的 β -葡萄糖苷酶同源基因酶, 为保留型 β -葡萄糖苷酶领域的相关研究思考提供了新的启示。

List of publications

1. **Su Q**, Louwerse M, Lammers RF, Maurits E, Janssen M, Boot RG, Borlandelli V, Offen WA, Linzel D, Schröder SP, Davies GJ, Overkleeft HS, Artola M, Aerts JMFG., Selective labelling of GBA2 in cells with fluorescent β -D-arabinofuranosyl cyclitol aziridines. *Chem. Sci.* doi.org/10.1039/D3SC06146A.
2. Kuo CL, **Su Q**, van den Nieuwendijk AMCH, Beenakker TJM, Offen WA, Willems LI, Boot RG, Sarris AJ, Marques ARA, Codée JDC, van der Marel GA, Florea BI, Davies GJ, Overkleeft HS, Aerts JMFG. The development of a broad-spectrum retaining β -exo-galactosidase activity-based probe. *Org. Biomol. Chem.* 2023 Oct 4;21(38):7813-7820.
3. **Su Q**, Schröder SP, Lelieveld LT, Ferraz MJ, Verhoek M, Boot RG, Overkleeft HS, Aerts JMFG, Artola M, Kuo CL. Xylose-configured cyclophellitols as selective inhibitors for glucocerebrosidase. *ChemBioChem.* 2021 Nov 3;22(21):3090-3098.
4. Rowland RJ, Chen Y, Breen I, Wu L, Offen WA, Beenakker TJ, **Su Q**, van den Nieuwendijk AMCH, Aerts JMFG, Artola M, Overkleeft HS, Davies GJ. Design, Synthesis and structural analysis of glucocerebrosidase imaging agents. *Chem. Eur. J.* 2021 Nov 25;27(66):16377-16388.

Curriculum vitae

Qin Su was born on 18th July 1993 in Laibin, Guangxi Zhuang Autonomous Region, China. In 2012 he graduated from Liuzhou Area Nationality Senior High School and commenced his bachelor's studies in Pharmaceutical Industry at School of Chemistry and Chemical Engineering, Chongqing University, Chongqing, China.

In June 2016, he obtained his BSc degree. Afterwards, he continued his master studies in Pharmacy at School of Pharmaceutical Sciences, Chongqing University, Chongqing, China in September 2016. Here he studied asymmetric catalysis and organic synthesis for construction of biologically active molecules under the supervision of Dr. Zhen Wang and Prof. Dr. Yun He. During this period, he generated great interest in chemical biology field and subsequently obtained his Master of Science degree in June 2019.

In September 2019, he was awarded a scholarship from the China Scholarship Council (CSC) and started his doctoral research in the department of Medical Biochemistry, Leiden University under the supervision of Prof. Dr. Hans Aerts from September 2019. His doctoral academic research focuses on studying retaining exo- β -glucosidases by chemical biology methods using of activity-based probes (ABPs) and exploring new inhibitors and ABPs for retaining exo- β -glucosidases.

Acknowledgements

Finally, it is almost to the end of my PhD career at Leiden University. There are so many people I want to acknowledge for assisting in the completion of this thesis.

First, I would like to express my sincere gratitude to my promotor, Prof. **Hans Aerts**. You are the best person I have worked with. It is my fortune that I had the chance to complete my PhD studies under your supervision. I greatly appreciate your patience and meticulous instruction to build up my academic sense and ability. Your passion and preciseness in science exemplify to me how to conduct academic research properly. I very enjoy the time we spent in Thorn. I also want to thank you for your care and comfort when I struggled with the stresses of the Covid-19 pandemic in my first two and a half years. Without your support, I would not have recovered so soon from the mental depression due to the pandemic. You are not only my supervisor in academics but also a very nice elder friend who is happy to share the wisdom in life with me. Thank you for all the help and support you have given to me.

I also want to thank my promoter Prof. **Hermen S. Overkleeft**. Thank you for giving me very professional and useful suggestions for my projects and the revision of manuscript and dissertation, as well as your generosity in providing precious compounds synthesized in BIOSYN department. Your meticulousness and patience greatly helped in my thesis writing. I am also very grateful for your help with my scholarship application to the China Scholarship Council when I was looking for an opportunity to start a PhD career in 2019. Without your help, I could not have achieved what I have now.

I would like to thank **Rolf G. Boot** and **Marta Artola** for your academic support. Rolf, thank you for being my co-promoter and teaching me much knowledge, as well as your kindness in helping me daily. Marta, you are always kind and happy to help me whenever I encountered issues. Thank you so much for your instruction on my research and manuscript. I would like to thank my colleagues at MEDBIO. I especially want to thank **Chi-Lin Kuo** (郭季霖), who enthusiastically guided me and systematically taught me many biological technologies related to my projects. You really helped me to adapt to the new circumstances in Leiden and build a solid foundation for my follow-up research. **Marco**, thanks for your advice on my projects and your daily help, as well as your humorous jokes that made us laugh. **Maria** and **Laura**, thank you for doing me numerous favors in technology support to promote my projects and taking care of daily issues in our lab. **Astrid**, I am very grateful that you dealt with many administrative affairs for me. I want to thank my nice and cool colleagues. **Remco, Rebecca, Lindsey, Max, Mats, Bas, Sophie, Martijn, Nicky, Rob, Steff, Kim, Kate, Lars, Daphne**—the time we spent together in and out of the lab was very enjoyable and memorable.

I sincerely thank all my collaborators and people who helped me during my PhD period. Prof. **Gideon Davies** and **Wendy**, thank you for assisting with crystallography. **Bobby Florea**, thank you for helping me with proteomics. **Ken, Valentina, Bing Liu, Yurong Chen**, thanks for helping me when I worked in DE3.14. I also want to thank my students who contributed to my projects: **Yang Lei, Tjebbe, Max Janssen**. I want to thank the China Scholarship Council (CSC) and Leiden Institute of Chemistry (LIC) for providing the financial support for my PhD career. I would like to thank all my friends accompanying me in Leiden: **Na Zhu, Tirong Guo, Jing Sun, Chenlin Feng, Tan Zhang, Dongdong Bi, Yunjiao Wu, Haoru Zhuang, Jianyun Guo, Qiang Ma, Pingping Zhu, Bingshu He, Liping Zhao, Lei Li, and Yangli Zhou**. It is my fortune to have met you and had fun together.

I want to specially thank my dear friends in Europe. **Zhimei Yu** (于治梅), **Qi Wu** (七爷), **Qing Tang** (唐庆), **Minghui Zhou** (慧姐), **Zirui Li** (睿哥). We spent 2-3 years together in the same laboratory in China when we were master students, it is very lucky that we can continue our journey together and support each other in Europe. I remember every happy moment we spent together in Europe. I wish you all the best in your ongoing career.

Finally, I would like to thank my parents. Thank you for your unconditional love, support, and encouragement, which helped me get through the difficult times.

Qin Su (苏秦),

Leiden, November 6, 2024